



UNIVERSITÀ
DEGLI STUDI
FIRENZE

UAB
Universitat Autònoma
de Barcelona

Towards an integrated removal of nitrogen and sulphur in biological treatments of tannery-like wastewaters

in candidacy for the

International Doctorate in Civil and Environmental Engineering (UNIFI).
Cycle XXXIII. Curriculum Environment, Resource and Security. S.S.D. ICAR/03.
Coordinator Prof. Claudio Borri

and

Doctoral Program in Environmental Science and Technology (UAB).
Coordinator Prof. Antoni Rosell Mele

PhD Candidate

Polizzi Cecilia

Supervisors

Professor Giulio Munz

Professor David Gabriel Buguña

Florence, 2021

*To all the students
that I had the pleasure to work with*

ABSTRACT

The emerging challenges in wastewater biological treatments are enclosed in the global debate on climate change, energy saving and circular economy. Energy autarchy, reduction in GHGs emissions and compact configurations are among the novel targets to be met by Wastewater Resource Recovery Facilities (WRRFs). In response of such an urgency, different innovative solutions have been proposed in the last decades, ranging from the adoption of novel technologies, such as granular sludge instead of floc-based activated sludge, to re-thinking of the conventional integration of Carbon (C), Nitrogen (N), Phosphorous (P) and Sulphur (S) cycles in the wastewater treatment line. Anaerobic (heterotrophic) treatments have emerged as valuable solutions for organic carbon valorization and autotrophic processes have gained attention for their role in waste sludge minimization. As a result, pioneering alternatives have been successfully adopted at real scale; among the most emblematic, there are the aerobic granular sludge (i.e. Nereda® technology) and the innovative SANI® process (Sulphate reduction Autotrophic denitrification and Nitrification Integrated). Nevertheless, further studies are needed for the application of advanced processes and technologies especially when dealing with industrial wastewaters, often characterised by potentially inhibitory substances that hamper long-term performance of biological systems.

The present work focuses on the integration of novel processes for the biological removal of Nitrogen (N) and Sulphur (S), specifically the anammox process and the sulphide-based autotrophic denitrification. In the recent years, partial denitrification (PD), i.e. the reduction of nitrate to the stage of nitrite typically over the oxidation of an organic electron donor, has emerged as a possible innovative process to act in synergy with anammox, as an alternative to partial nitrification whose long-term stability is reported to be critical in many applications. In case of sulphide-driven denitrification, partial autotrophic denitrification (PAD) is another valuable alternative. The novel integration of PAD with the anammox process (PAD/A) is of particular interest for the treatments of wastewaters highly rich in nitrogen and sulphur compounds, such as those derived from petroleum refineries, tanneries and fish processing. If anaerobic treatment is applied to these streams in order to exploit the carbonaceous content for methane production, the downward water stream would be particularly suitable for integrated N-S removal, providing the required reduced forms of sulphide and ammonia, low organic content (preventing competition with ordinary heterotrophs) and high temperatures. In the perspective of PAD/A implementation, S-driven denitrification should be operated in such a way to convert nitrate to nitrite only, in order to provide the nitrite supply required by the anammox biomass. Besides, biogas desulphurization could be accomplished in the same unit, as a sustainable alternative to the typically adopted chemical-physical treatments.

Within this framework, the present thesis aimed at gaining insight on the application of the novel PAD/A process, in high-strength wastewaters. The anammox and the PAD process have been studied in parallel lines of work, addressing different issues related to the two innovative treatments.

Industrial wastewater originated from vegetable tannery industry was selected as target stream for PAD/A implementation and the potential inhibitory drawbacks on the anammox granular biomass were studied. A fast start-up of an anammox gas-lift reactor was achieved with volumetric loads up to 0,48 gN-NO₂⁻/l/d, maximum specific nitrogen load of 0,28 gN-NO₂⁻/gVSS/d and stable nitrite removal higher than 95%. Mineral precipitation on the granules' surface was observed after 130 days of operation. An extensive study was conducted in order to characterise precipitate composition as well as its impact on reactor performance, biomass activity and microbial population. The results offer useful knowledge for the long-term stable operation of anammox granular systems, especially when treating wastewaters prone to precipitate formation. The possible inhibitory effect of bio-refractory compounds and high salinity of vegetable tannery wastewater was assessed through batch test experiments. The outcomes revealed that no evident inhibition could be ascribed to the organic tannins-related fraction of the industrial matrix, whereas a moderate disturbance was observed for the salinity content, that can be addressed through proper biomass acclimation. Thereby, it is concluded that there is no technical limitation for the application of anammox process on vegetable tannery wastewaters.

The PAD process was studied in a CSTR reactor, operated as an ideal chemostat and fed by nitrate and sulphide. The work aimed at evaluating the effect of influent S/N ratios and SRT conditions on the nitrite accumulation performance. Specifically, moderate to strict S-limiting conditions were studied and SRT was progressively decreased, from 40 to 23 to 13 hours. Successful nitrite accumulation was observed after one week of stable and strict S-limiting condition and maintained throughout the experimental work. Nitrite accumulation efficiency of 70-100% and nitrite conversion efficiency of 70% were observed at all the experimental phases, calculated over the converted and influent nitrate, respectively. Results indicate that S/N ratios as low as 0,6-0,8 gS/gN were a sufficient condition to ensure high nitrite accumulation efficiencies, whereas the SRT showed no significant impact on the process performance, at the studied values. Nevertheless, short SRT and the feeding conditions were crucial to obtain a highly selected sulphide-oxidizing biomass. A clear microbial population shift was observed: *Sulfurimonas* genus showed 90% relative abundance in the seeding sludge and, after 80 days of operation, was almost completely out-competed by *Thiobacillus*, exhibiting a relative abundance as high as 83%. It is speculated that microbial bioenergetics is a possible underlying reason of the clear population shift at the peculiar conditions applied, i.e. low SRT and stable electron donor deficiency. A discussion on the metabolic differences among the two genus is provided in support of such an assumption. A thermodynamic-based study was conducted in order to study the catabolic change observed in the experimental work, i.e. from full denitrification to partial denitrification (denitrification). Results indicate that even though denitrification is a highly favourable reaction, the sole denitrification could be a valuable energetic response in case of electron donor limitation, as it was the case of the experimental work.

Moreover, catabolic and full-metabolic stoichiometry have been solved according to theoretical models and a critical comparison of experimental and theoretically-derived biomass yields is provided. Aggregated information on process catabolic stoichiometry are presented as support tool for process design and optimization of the complex S-based denitrification process, over all the intermediate reactions and possible combinations of e-donor and e-acceptor. It is believed that the complexity of the S-driven denitrification due to the many possible intermediate reactions actually infers high flexibility to the combined PAD/A; indeed, a wide range of S and N loads can be successfully exploited according to the case-specific requirements.

RESUMEN

Los desafíos emergentes en los tratamientos biológicos de las aguas residuales se encierran en el debate global sobre el cambio climático, el ahorro de energía y la economía circular. La autarquía energética, la reducción de las emisiones de gases de efecto invernadero y las configuraciones compactas se encuentran entre los objetivos novedosos que deben cumplir las instalaciones de recuperación de recursos de aguas residuales (WRRF). En respuesta a tal urgencia, en las últimas décadas se han propuesto diferentes soluciones innovadoras, que van desde la adopción de tecnologías novedosas, como lodos granulares en lugar de lodos activados a base de flóculos, hasta repensar la integración convencional de los ciclos de Carbono (C), Nitrógeno (N), Fósforo (P) y Azufre (S) en la línea de tratamiento de aguas residuales. Los tratamientos anaeróbicos (heterótrofos) han emergido como soluciones valiosas para la valorización del carbono orgánico y los procesos autótrofos han ganado atención por su papel en la minimización de lodos residuales. Como resultado, se han adoptado con éxito alternativas pioneras a escala real; entre los más emblemáticos, se encuentran los lodos granulares aeróbicos (por ejemplo, la tecnología Nereda®) y el innovador proceso SANI® (Reducción de sulfatos, desnitrificación autotrófica y nitrificación integrada). No obstante, se necesitan más estudios para la aplicación de procesos y tecnologías avanzados, especialmente cuando se trata de aguas residuales industriales, a menudo caracterizadas por sustancias potencialmente inhibitorias que obstaculizan el rendimiento a largo plazo de los sistemas biológicos.

El presente trabajo se centra en la integración de procesos novedosos para la remoción biológica de Nitrógeno (N) y Azufre (S), específicamente en el proceso de anammox y la desnitrificación autotrófica a base de sulfuros. En los últimos años, la desnitrificación parcial (PD), es decir, la reducción de nitrato a la etapa de nitrito típicamente sobre la oxidación de donadores de electrones orgánicos, ha surgido como un posible proceso innovador para actuar en sinergia con el anammox, como una alternativa a la nitrificación parcial, cuya estabilidad a largo plazo es crítica en muchas aplicaciones. En el caso de la desnitrificación impulsada por sulfuros, la desnitrificación autotrófica parcial (PAD) es otra alternativa valiosa. La innovadora integración de la PAD con el proceso anammox (PAD/A) es de especial interés para los tratamientos de aguas residuales altamente ricas en compuestos de nitrógeno y azufre, como las derivadas de refinerías de petróleo, curtiembres y procesamiento de pescado. Si se aplica un tratamiento anaeróbico a estas aguas residuales con el fin de explotar el contenido carbonoso para la producción de metano, la corriente de agua residual sería particularmente adecuada para la eliminación integrada de N y S, proporcionando las formas reducidas de sulfuro y amoníaco requeridas, bajo contenido orgánico (evitando la competencia con heterótrofos) y altas temperaturas. En la perspectiva de la implementación del proceso PAD/A, la desnitrificación autotrófica debe operarse de tal manera que convierta el nitrato únicamente en nitrito, con el fin de proporcionar el suministro

de nitrito requerido por la biomasa anammox y la desulfuración del biogás podría lograrse en la misma unidad, como una alternativa sostenible a los tratamientos físico-químicos típicamente adoptados.

En este marco, la presente tesis tuvo como objetivo profundizar en la aplicación del novedoso proceso PAD/A, en aguas residuales de alta carga en N y S. El anammox y el proceso PAD se han estudiado en líneas de trabajo paralelas, abordando diferentes cuestiones relacionadas con los dos tratamientos innovadores.

Las aguas residuales industriales originadas en la industria de las curtidurías se seleccionaron como objetivo para la implementación del proceso PAD/A y se estudió la posible inhibición de la biomasa granular de anammox. Se logró una rápida puesta en marcha de un reactor gas-lift anammox con cargas volumétricas hasta 0,48 gN-NO₂⁻/l/d, carga máxima específica de nitrógeno de 0,28 gN-NO₂⁻/gVSS/d y eliminación estable de nitrito superior al 95%. Se observó la precipitación mineral en la superficie de los gránulos después de 130 días de operación. Se realizó un estudio extenso para caracterizar la composición del precipitado, así como su impacto en el rendimiento del reactor, la actividad de la biomasa y la población microbiana. Los resultados ofrecen conocimientos útiles para la estabilidad a largo plazo de los sistemas granulares de anammox, especialmente cuando se tratan aguas residuales propensas a la formación de precipitados. El posible efecto inhibitorio de los compuestos biorrefractarios y la alta salinidad de las aguas residuales de las curtidurías se evaluó mediante experimentos en batch. Los resultados revelaron que no se pudo atribuir una inhibición evidente a la fracción de la matriz industrial relacionada con los taninos orgánicos, mientras que se observó una influencia moderada debida al contenido de salinidad, que se puede abordar mediante una adecuada aclimatación de la biomasa. Por lo tanto, se concluye que no existe ninguna limitación técnica para la aplicación del proceso anammox en las aguas residuales de las curtidurías.

El proceso PAD se estudió en un reactor CSTR, operado como un quimiostato ideal y alimentado con nitrato y sulfuro. El trabajo tuvo como objetivo evaluar el efecto de los ratios S/N del influente y las condiciones de SRT sobre el rendimiento de la acumulación de nitritos. Específicamente, se estudiaron las condiciones limitantes de S de moderadas a estrictas y el SRT se redujo progresivamente de 40 a 23 y a 13 horas. Se observó una acumulación exitosa de nitrito después de una semana de condición estable de limitación de S y se alcanzaron altos niveles de nitrito durante todo el trabajo experimental. En todas las fases experimentales se observó una eficiencia de acumulación de nitrito del 70-100% y una eficiencia de conversión de nitrito del 70%, calculadas sobre el nitrato convertido y influente, respectivamente. Los resultados indican que ratios de S/N tan bajos como 0,6-0,8 gS/gN fueron una condición suficiente para asegurar altas eficiencias de acumulación de nitrito, mientras que el SRT no mostró un impacto significativo en el rendimiento del proceso, en los valores estudiados. Se observó un claro cambio de población microbiana: el género *Sulphurimonas* mostró una abundancia relativa del 90% en el inóculo y, después de 80 días de operación, fue superado casi por completo por el género *Thiobacillus*, que exhibió una abundancia relativa del 83%. Se especula que la eficiencia bioenergética microbiana es una posible razón subyacente del claro cambio de población en las condiciones peculiares aplicadas, es decir, un bajo SRT y una constante limitación de donador de electrones.

Se proporciona una discusión sobre las diferencias metabólicas entre los dos géneros en apoyo de tal suposición. Se realizó un estudio de base termodinámica para estudiar el cambio catabólico observado en el trabajo experimental, es decir, de la desnitrificación total a la desnitrificación parcial (desnitrificación). Los resultados indican que a pesar de que la desnitrificación es una reacción muy favorable, la desnitrificación podría ser una respuesta energética valiosa en caso de limitación del donador de electrones, como fue el caso del trabajo experimental. Además, la estequiometría catabólica y metabólica completa se ha resuelto de acuerdo con modelos teóricos y se proporciona una comparación crítica de los coeficientes de producción de biomasa derivados por vía experimental y teórica. La información sobre la estequiometría catabólica del proceso se presenta de forma agregada como herramienta de apoyo para el diseño del proceso y la optimización del complejo proceso de desnitrificación autotrófica, ya que ofrece todas las reacciones intermedias y las posibles combinaciones de e-donador y e-aceptor. Se cree que la complejidad de la desnitrificación autotrófica impulsada por el azufre en realidad infiere una alta flexibilidad al proceso combinado PAD/A; de hecho, una amplia gama de cargas S y N se pueden explotar con éxito de acuerdo con los requisitos específicos del caso.

RIASSUNTO

Le emergenti sfide nel trattamento biologico delle acque reflue si inseriscono nel dibattito globale sui cambiamenti climatici, il risparmio energetico e l'economia circolare. L'autarchia energetica, la riduzione delle emissioni di gas serra e la compattezza delle configurazioni impiantistiche sono tra i nuovi obiettivi che devono essere raggiunti dagli impianti di depurazione delle acque reflue. In risposta a tale urgenza, negli ultimi decenni sono state proposte diverse soluzioni innovative, che vanno dall'adozione di nuove tecnologie, come i fanghi granulari invece dei fanghi attivi in forma fioccosa, alla rivisitazione dell'integrazione convenzionale dei cicli di carbonio (C), azoto (N), fosforo (P) e zolfo (S) nei processi depurativi. I trattamenti anaerobici (eterotrofi) sono emersi come valide soluzioni per la valorizzazione del carbonio organico e i processi autotrofi hanno attirato l'attenzione per il loro ruolo nella minimizzazione dei fanghi di supero. Di conseguenza, alternative pionieristiche sono state adottate con successo su scala reale; tra le più emblematiche si menzionano i fanghi granulari aerobici (es. tecnologia Nereda®) e l'innovativo processo SANI® (sistema Integrato di Solfato riduzione, denitrificazione Autotrofa e Nitrificazione). Tuttavia, sono necessari ulteriori studi per l'applicazione di processi e tecnologie avanzate soprattutto quando si tratta di acque reflue industriali, spesso caratterizzate da sostanze potenzialmente inibitorie che compromettono le prestazioni a lungo termine dei sistemi biologici.

Il presente lavoro si concentra sull'integrazione di nuovi processi per la rimozione biologica di azoto (N) e zolfo (S), in particolare il processo anammox e la denitrificazione autotrofa a base di solfuro. Negli ultimi anni, la denitrificazione parziale (PD), ovvero la riduzione del nitrato allo stadio di nitrito tipicamente coniugata all'ossidazione di un donatore di elettroni organico, è emersa come un possibile processo innovativo per agire in sinergia con l'anammox, in alternativa alla nitrificazione parziale, la cui stabilità a lungo termine si è rivelata critica in molte applicazioni. Nel caso in cui si adotti la denitrificazione con solfuro, la denitrificazione autotrofa parziale (PAD) è un'altra valida alternativa. L'innovativa integrazione del processo PAD ed anammox (PAD/A) è di particolare interesse per i trattamenti di acque reflue altamente ricche di composti di azoto e zolfo, come quelle derivanti da raffinerie di petrolio, concerie e attività di lavorazione del pesce. Nella prospettiva di implementare filiere di trattamento innovative, tali flussi potrebbero essere sottoposti a un trattamento anaerobico per valorizzarne il contenuto carbonioso, attraverso la produzione di biometano, e il flusso risultante sarebbe particolarmente adatto per la rimozione integrata di N e S, fornendo le forme ridotte di solfuro e ammoniaca, un basso contenuto organico (limitando la concorrenza con biomasse eterotrofe) e alte temperature. Per un'efficace sinergia del processo combinato PAD/A, la denitrificazione con solfuro dovrebbe essere operata in modo tale da convertire i nitrati in nitriti (e non in azoto gassoso), al fine di fornire l'apporto di nitriti richiesto dalla biomassa anammox. Inoltre, la desolfurazione del biogas potrebbe essere realizzata nella stessa unità, come un'alternativa sostenibile ai trattamenti chimico-fisici convenzionalmente adottati.

In questo quadro, la presente tesi si è proposta di approfondire alcuni aspetti legati all'applicazione del nuovo processo PAD/A per acque reflue ad alta carica inquinante. I processi anammox e PAD sono stati studiati in linee di lavoro parallele, affrontando diverse problematiche legate ai due trattamenti innovativi.

Le acque reflue industriali provenienti dall'industria della pelle, da trattamento di concia al vegetale, sono state selezionate come potenziale target per l'implementazione del processo PAD/A e sono stati studiati i potenziali effetti inibenti sulla biomassa granulare anammox. Un reattore gas-lift anammox è stato avviato con brevi tempi di start-up, ottenendo carichi volumetrici fino a 0,48 gN-NO₂⁻/l/d, massimi carichi specifici di 0,28 gN-NO₂⁻/gVSS/d e rimozioni di nitrito stabilmente superiori al 95%. Dopo 130 giorni di operazione, si è osservata un'evidente precipitazione minerale sulla superficie dei granuli. È stato condotto uno studio approfondito per caratterizzare la composizione del precipitato e il suo impatto sulle prestazioni del reattore, sull'attività della biomassa e sulla popolazione microbica. I risultati offrono un ampio approfondimento utile come strumento di supporto per la gestione a lungo termine di sistemi granulari anammox, specialmente nel trattamento di acque reflue tendenti alla formazione di precipitati. Il possibile effetto inibente dei composti bio-refrattari e dell'elevata salinità delle acque reflue industriali da concia al vegetale è stato valutato attraverso esperimenti in batch. I risultati hanno rivelato che nessuna inibizione evidente può essere attribuita alla frazione organica della matrice industriale correlata ai tannini, mentre è stato osservato un moderato disturbo dovuto al contenuto di salinità, che può essere, tuttavia, controllato attraverso un'adeguata acclimatazione della biomassa. Si conclude quindi che non sono emerse limitazioni tecniche per l'applicazione del processo anammox alle acque reflue dell'industria della concia al vegetale.

Il processo PAD è stato studiato in un reattore CSTR, operato come un chemostato ideale ed alimentato con nitrato e solfuro. Il lavoro si è proposto di valutare l'effetto del rapporto S/N nell'influente e di diversi SRT sull'efficienza di accumulo di nitrito. In particolare, sono state studiate condizioni da moderate a strettamente limitanti per il solfuro e l'SRT è stato progressivamente ridotto, da 40 a 23 a 13 ore. L'accumulo di nitriti è stato osservato dopo una settimana di condizioni strettamente e stabilmente limitanti di S e alte efficienze di accumulo sono state mantenute per tutto il lavoro sperimentale. In tutte le fasi sperimentali sono state osservate efficienze di accumulo di nitriti del 70-100% e un'efficienza di conversione di nitriti del 70%, calcolate rispetto al nitrato rimosso ed influente, rispettivamente. I risultati indicano che il mantenimento di bassi rapporti S/N (0,6-0,8 gS/gN) è stata una condizione sufficiente per garantire elevate efficienze di accumulo di nitriti, mentre l'SRT non ha mostrato un impatto significativo sulle prestazioni del processo, ai valori studiati. Tuttavia, i bassi valori di SRT e le condizioni di alimentazione hanno permesso di ottenere una biomassa solfuro-ossidante altamente selezionata. È stato osservato un chiaro shift nella composizione della popolazione microbica: il genere *Sulfurimonas*, che mostrava un'abbondanza relativa del 90% nel fango di inoculo, è stato quasi completamente surclassato dal genere *Thiobacillus* dopo 80 giorni di funzionamento, momento in cui quest'ultimo ha mostrato un'abbondanza relativa fino all'83%. Si ipotizza che la differenza nell'efficienza bioenergetica dei due generi sia una possibile spiegazione alla base del chiaro shift di popolazione osservato alle condizioni applicate, ovvero basso SRT e deficit stabile di donatore di elettroni. A sostegno di tale ipotesi

viene fornita una discussione sulle differenze metaboliche tra i due generi di batteri. È stato condotto uno studio basato sulla termodinamica del processo di denitrificazione con solfuro, per studiare il cambiamento catabolico osservato nel lavoro sperimentale, ovvero il chiaro cambio dalla denitrificazione completa alla denitrificazione parziale (denitratazione). I risultati indicano che anche se la denitrificazione è di per sé una reazione energeticamente molto favorevole, la sola denitratazione potrebbe essere una risposta energetica in caso di costante limitazione del donatore di elettroni, ovvero costante limitazione di energia disponibile, come nel caso del lavoro sperimentale. Inoltre, la stechiometria delle reazioni cataboliche e del metabolismo completo sono state risolte secondo modelli teorici; viene fornito un confronto critico tra i fattori di resa della biomassa disponibili in letteratura con quelli derivati su base sperimentale e teorica. I risultati stechiometrici sono presentati come informazioni aggregate di tutte le possibili combinazioni di e-donatore e e-accettore, con l'intenzione di fornire uno strumento di supporto per la progettazione e l'ottimizzazione del complesso processo di denitrificazione con solfuro. Si ritiene che la complessità della denitrificazione con solfuro dovuta alle numerose reazioni intermedie inferisca in realtà un'elevata flessibilità all'innovativo processo PAD/A, che si propone come trattamento altamente adattabile a diverse combinazioni di carichi di S e N, secondo le richieste specifiche del caso.

ACKNOWLEDGMENTS

I want to express my deep gratitude to my supervisors Professors Giulio Munz and David Gabriel Buguña, for their continuous support during my PhD work. Thank you both for allowing me to work in autonomy, learning through my errors and achievements, while always being present with your vigilant and delicate guidance. I would like to thank you for sharing your knowledge and experience while caring for building an empathic and professional relationship. I am deeply grateful for all the tools and opportunities that you offered me throughout these years. Thank you a lot for that.

I would like to thank Consorzio Cuoioedepur S.p.a for the financial support to my project and for the resources and spaces made available for the experimental work. Special thanks go to Gualtiero Mori; it is greatly inspiring to see your love for biology and research combined with the demanding daily work of running a complex plant like Cuoioedepur. Thanks to Francesco and Andrea for always being so responsive to the needs of the staff working at the Cer2co laboratory. Thanks to Salvatore for his ingenious artworks that were fundamental for troubleshooting the problems of the gas-lift reactor.

Thanks to the research group at Unifi that I have the pleasure to be part of. Thanks to Tommaso, for the help in assembling my reactor as well as for the fundamental suggestions and enlightening discussions on the anammox world, thermodynamics and much more. To me you are a role model due to your passionate and brilliant scientific mind combined with a genuine spirit; it was a pleasure to work in collaboration with you during my PhD. Thanks to Alberto for your help, your cheerful attitude and the good synergy that we had, we will miss you a lot but I am confident that our collaboration will go on. Thanks to Riccardo for the granulometric analysis on the granular sludge and for your nice and quick replies every time I asked for help. Thanks to all the group members, to the professors and the new research fellows and PhD students for their nice and collaborative attitude.

Thanks to the UAB Genocov group, I was delighted to be part of your team. The year I spent in Barcelona was likely the best of my PhD. My gratitude goes to all the professors and the technicians that have helped me in my work and to my PhD colleagues and new friends. Despite the pandemic impeded many of our plans, from mountain hiking to social cooking, I felt your warm hospitality anyway. I really think that you are a great team, leading high quality research with the rigour and the relaxed attitude that are combined so well in Catalonia.

A special thanks go to Professor Claudia Vannini from the Biology Department of the University of Pisa for her kind availability and for conducting the TEM analysis on the granular biomass.

Thanks to Professor Matteo Ramazzotti and Dr. Lorenzo Mazzoli, from the Biology Department of the University of Florence, for their work on the bioinformatics study on the granular biomass and for their patience in answering my questions as a neophyte in molecular biology.

Part of the work detailed in the present thesis was supported by the European project RECYCLES (Marie Skłodowska-Curie Rise, 872053) that offered me the opportunity to work at Aeris Technologias Ambientales SL. Thanks to Oscar Prado and all the Aeris' staff for welcoming me in their team in such a difficult moment like the one that we experienced right after the Covid-19 outbreak. Working with you and visiting your pioneering installations have enabled me to complete my studies with a practical approach to system control and installation.

A sincere thanks to all the master students and interns that I had the honour to work with and that helped me in conducting the experimental work. Thank you for your dedication, passion and curiosity, for all your questions and doubts that challenged my knowledge and renovated my passion for research. Thanks to Alessandra for her perseverance and work during the tough start-up of the experimental work. Thanks to Alex and Federica for their essential contribution on the operation of the anammox reactor. The impressive devotion and enthusiasm of Alex inspired me and made it possible to realise the part of the study focusing on the anammox granular biomass. Thanks to Serena and Andrea for their work during the experimental activity related to the SOB reactor. We really worked as a team and I believe that we experienced how productive and pleasant a teamwork could be. Thanks a lot, to all of you I dedicate my thesis work.

Last but definitely not least, very special and heartfelt thanks to my family and all the beloved people that gave me their support time after time throughout these years. Thank you for being there when I hardly admitted to be living tough moments. I strongly believe that a PhD work requires passion and good mentors as much as strong emotional support. Lucky me that I found them all.

LIST OF ABBREVIATIONS

ADP	Adenosine Diphosphate
ATP	Adenosine Triphosphate
AD	Anaerobic Digestion
AMX	Anammox
COD	Chemical Oxygen Demand
CANON	Completely Autotrophic Nitrogen removal Over Nitrite
CSTR	Continuous Stirred Tank Reactor
DEAMOX	DEnitrifying AMonium Oxidation
DNA	Deoxyribonucleic acid
Dnpe	diNitrogen gas Production Efficiency
ED	Electron Donor
EDX	Energy Dispersive X-Ray
EPS	Extracellular Polymeric Substances
FNA	Free Nitrous Acid
GHG	Greenhouse Gas
HRT	Hydraulic Retention Time
ICP	Inductively Coupled Plasma
MSAA	Maximum Specific Anammox Activity
NRE	Nitrate Removal Efficiency
NUR	Nitrate Uptake Rate
NiAE	Nitrite Accumulation Efficiency
NiCE	Nitrite Conversion Efficiency
NiUR	Nitrite Uptake Rate
NLR	Nitrogen Loading Rate
NRR	Nitrogen Removal Rate
OTU	Operational Taxonomic Unit
NAD	Oxidized Nicotinamide adenine dinucleotide
PD	Partial Denitrification
PAD	Partial Autotrophic Denitrification
PAD/A P	Partial Autotrophic Denitrification/Anammox
PN	Partial Denitrification
PN/A	Partial Nitritation/Anammox

PCR	Polymerase Chain Reaction
FAD	Reduced Flavin Adenine Dinucleotide
FADH ₂	Reduced Flavin Adenine Dinucleotide
NADH	Reduced Nicotinamide adenine dinucleotide
RET	Reverse Electron Transport
rRNA	Ribosomal Ribonucleic Acid
SI	Saturation Index
SEM	Scanning Electron Microscope
SRT	Sludge Retention Time
SAA	Specific Anammox Activity
SLNLR	Specific Nitrogen Loading Rate
SRB	Sulfate Reducing Bacteria
SANI	Sulfate reduction Autotrophic denitrification Nitrification Integrated
SOB	Sulfur Oxidizing Bacteria
SLR	Sulphur Loading Rate
SO-NR	Sulphur Oxidizing-Nitrate Reducing
TEM	Tansmission Electron Microscope
TEA	Terminal Electron Acceptro
TDS	Total Dissolved Sulphide
TN	Total Nitrogen
TS	Total Solids
TSS	Total Suspended Solids
UASB	Upflow Anaerobic Sludge Blanket reactor
VS	Volatile Solids
VSS	Volatile Suspended Solids
WRRF	Wastewater Resource Recovery Facility
WWTP	Wastewater Treatment Plant

LIST OF CONTENTS

ABSTRACT	i
ACKNOWLEDGMENTS	xiii
LIST OF ABBREVIATIONS	xv
LIST OF CONTENTS	xvii
CHAPTER 1. General introduction.....	1
1.1 The nitrogen network.....	4
1.1.1 Denitrification.....	7
1.1.2 Anammox	10
1.2 The Sulphur cycle.....	14
1.2.1 Sulphur biochemistry.....	14
1.2.2 Denitrifying Sulphur Oxidizing Bacteria, metabolic pathways and variety	18
1.3 Integrating S-based denitrification and anammox: state of the art	22
1.4 Objective of the thesis	26
1.5 Thesis outline.....	26
CHAPTER 2. General materials and methods	29
2.1 Continuous reactors	30
2.1.1 Anammox gas-lift reactor	30
2.1.2 SOB CSTR reactor	32
2.2 Activity tests	34
2.2.1 Manometric test – AMX activity.....	34
2.2.2 In-situ batch test – AMX activity	36
2.2.3 Respirometric and titrimetric test – SOB activity.....	37
2.3 Analytical methods	38
2.4 Molecular analysis.....	39

2.5	SEM and TEM analysis and sample preparation.....	39
CHAPTER 3. Coping with mineral precipitation during the start-up of an anammox gas-lift reactor		41
3.1	Introduction	42
3.1.1	Mineral precipitation in granular sludge systems	42
3.2	Materials and methods.....	43
3.2.1	Gas-lift reactor.....	43
3.2.2	Experimental phases	45
3.2.3	Activity batch tests	46
3.2.4	Analytical methods.....	47
3.2.5	Metabarcoding study, granular size distribution and analyses with electron microscopy	47
3.3	Results	48
3.3.1	Reactor operation.....	48
3.3.2	Activity tests.....	53
3.3.3	Granular size distribution and microbial community	54
3.3.4	Carbonate-minerals precipitation.....	56
3.3.5	TEM and SEM-EDX analyses.....	59
3.4	Conclusions	65
CHAPTER 4. Tannery wastewater as target stream for PAD/A process: assessing potential inhibition on anammox biomass		67
4.1	Introduction	68
4.1.1	Tannery wastewaters and Cuoiodepur WWTP.....	68
4.2	Material and methods	72
4.2.1	First inhibition experiment on stored biomass.....	72
4.2.2	Second inhibition experiment.....	75
4.2.3	Fast biomass acclimation procedure to saline conditions	76
4.2.4	Analytical measurements and microbial analysis.....	77
4.3	Results	78
4.3.1	Preliminary reactivation experiment.....	78
4.3.2	First inhibition experiment	79

4.3.3	Second inhibition experiment.....	81
4.3.4	Molecular analysis.....	85
4.3.5	Discussion.....	86
4.4	Conclusions	88
CHAPTER 5. Successful nitrite accumulation over sulphide oxidation in a SRT-controlled CSTR.....		89
5.1	Introduction	90
5.2	Material and methods	91
5.2.1	Reactor operation.....	91
5.2.2	Experimental conditions	93
5.2.3	Process performance assessment	95
5.2.4	Respirometric tests	96
5.2.5	Analytical methods.....	98
5.2.6	Microbial community analysis	99
5.3	Results	99
5.3.1	Successful NO ₂ ⁻ accumulation.....	99
5.3.2	N ₂ O emission.....	104
5.3.3	Microbial diversity	106
5.3.4	Respirometric test.....	108
5.3.5	Discussion on nitrite accumulation strategies.....	112
5.4	Conclusions	114
CHAPTER 6. A thermodynamics insight on S-driven denitrification. Focus on partial denitrification		117
6.1	Introduction	118
6.1.1	Basics of Gibbs energy dissipation methods for overall growth estimation.....	119
6.2	6 Materials and Methods	124
6.2.1	Catabolic reaction stoichiometry	124
6.2.2	Application of the free Gibbs energy method to study SOB biomass yield: hypotheses and simplifications	125
6.2.3	Partial autotrophic denitrification: a thermodynamic insight on experimental outcomes	127
6.3	Results	128

6.3.1	Study on the catabolic intermediate reactions	128
6.3.2	Biomass yield: sensitivity study and literature review	135
6.3.3	Thermodynamic study of experimental results on Partial Denitrification.....	140
6.4	Conclusions	143
CHAPTER 7. General conclusions		145
7.1	Future work	148
REFERENCES		151
APPENDIX		165

CHAPTER 1.

General introduction

The global debate on climate change and circular economy calls for innovation also in the field of wastewater treatments. A shift in the paradigm of wastewater treatment plant (WWTP) towards a more comprehensive concept of wastewater resource recovery facility (WRRF) has emerged with the objective of upgrading the current technological asset. The new targeted standards go far behind the basic need for wastewater depuration (whose quality requirements become always more demanding). The new challenges to be addressed can be synthesized as follows: (i) resource recovery or valorisation, i.e. P recovery, bio-methane production and water reuse; (ii) waste sludge minimization; (iii) energy autarchy of WWTFs; (iv) low carbon footprint through the reduction/control of typically diffuse emissions of greenhouse gas such as CO₂, CH₄ and N₂O; (v) reduction in land use, through compact and highly loaded configurations (Guest et al., 2009; Song et al., 2018; Villarin and Merel, 2020).

In this context, anaerobic and autotrophic processes are of pivotal importance due to their lower energy requirement, sludge production and CO₂ emissions, compared to the conventional heterotrophic/aerobic processes applied in activated sludge systems. Innovative processes and new synergies in microbial consortium have inspired alternative treatment line configurations, implementing a renewed integration of biological removal of carbon, nitrogen, sulphur and phosphorus. The combined anammox and partial nitrification process and the emerging aerobic granular sludge process are among the main examples of successful innovative advances.

From the technological point of view, granular sludge and attached/immobilized sludge showed to be a successful solution for compact and highly loaded configuration, behind the advantage for the selection of diversified biomass consortium. The microbial consortia distribution within the biofilm provides optimized biomass stratification, according to the different environmental conditions along the biofilm width (Lotti et al., 2014). Beside the stronger microbial structure of biofilm compared to suspended flocs in conventional activated sludge systems, the excellent settling properties of granular and carrier-attached sludge allow for compact settling units and high hydraulic loads, preventing biomass washout.

Some industrial wastewaters deriving from leather production petroleum refineries, fish processing, as well as landfill leachate are highly rich in nitrogen and sulphur compounds. Representative compositions of some of the mentioned streams are reported in table 1.1. Currently, the removal of these two pollutants is mainly achieved separately. Biological nitrogen removal is a consolidated and robust treatment conventionally accomplished by the coupled system of nitrification-denitrification.

In the last decades anammox proved to be an effective environmental-friendly alternative to conventional biological processes, typically very energy-requiring and not devoted to resource (e.g. C and N) valorisation. Nevertheless, anammox spreading worldwide has been hindered by problems such as: (i) long start-up periods, (ii) long-term instability of the coupled process of partial nitrification (PN); (iii) inhibition of anammox biomass or out-competition by other microbial population, in case of possible inhibitory compounds or (residual) COD.

On the other hand, sulphur is a very peculiar pollutant found in limited types of (industrial) wastewaters, where it can be present in its oxidized and reduced forms of sulfate and sulphide, respectively. When sulfate is present it can be reduced in case anaerobic treatments are present (such as side-stream anaerobic digestion) and it returns to the treatment line as sulphide. When sulphide is present, either in the liquid or gaseous stream, its removal is fundamental due to the highly corrosive and toxic nature of the compound. Since it can easily volatilize and thereby be transferred from the liquid to the gaseous phase, non-aerated tanks are typically closed and equipped with aspiration systems, in order to divert gaseous emissions to further treatments. Residual sulphide concentration in liquid streams are usually addressed through chemical or biochemical aerobic oxidation, whereas physical-chemical treatments such as adsorption and chemical scrubbers have been conventionally adopted for the treatment of the gaseous fluxes. Biological sulphide oxidation has emerged as a cost-effective sustainable alternative, since it mediates aerobic sulphide oxidation to the less reactive forms of sulfate and elemental sulphur, with no need of chemical additions. Biotrickling filters and bioscrubbers are among the most common and effective installations of aerobic biological desulphurization in biogas treatments (Lens, 2020). A less implemented solution implies the use of nitrate as oxidative agent instead of oxygen, the first pilot-scale applications of denitrifying sulphide oxidation dating back to the late 90's (Mulder et al., 1995).

Table 1.1 Average concentration of some industrial streams, targeted as feasible stream for PAD/A. Note that TKN measurements are not easily available in literature, but ammonia content would increase in case of anaerobic treatment for COD removal.

	COD mg/l	N mg/l	S mg/l
Fish processing ^{1, 2, 3}	2000-20000	30-200 as N-NH ₄ ⁺ 112-350 as TKN	100-1200 as S-SO ₄ ²⁻
Petroleum refineries ⁴	200-800	<50	20-700 as S-HS ⁻ 30-130 as S-SO ₄ ²⁻
Tannery industry ⁵	12000-23000	100-250	30-400 as S-SO ₄ ²⁻

1 Queiroz et al., 2013; Cristovao et al., 2015; 3 Marin-Leal et al., 2015.

4 Jain et al., 2020.

5 Mannucci et al., 2010.

A successful implementation of novel Carbon (C), Nitrogen (N) and Sulphur (S) cycles integration in a wastewater treatment line is represented by the SANI® process, the acronyms standing for Sulfate reduction Autotrophic denitrification Nitrification Integrated process, implemented in the Hong Kong area (China). Saline wastewater has been used in the city since the late 50's for toilet flushing with a straightforward 22% saving of freshwater utilization (Wang et al., 2009; Lu et al., 2012). The novelty of the SANI® process lays in the reforming way of integrating organic source valorisation through anaerobic treatment and autotrophic processes, acknowledging a primarily role to sulfate reduction and sulphide-based denitrification. The results

are 35% reduction in waste sludge, 35% reduction in energy consumption and 36% reduction in fossil CO₂ emissions, compared to conventional biological nitrogen removal systems (Lu et al., 2012).

In this chapter, a general introduction on the nitrogen and sulphur cycles is provided, with a special focus on the microbial process of interest of the present thesis, i.e. anammox, denitrification and sulphur oxidation. The state of the art on the current applications and perspective of the system coupling anammox and sulphur-driven denitrification is provided in order to complete the general framework in which the thesis finds its place.

Moreover, particular attention is posed on the metabolic pathways adopted by the different microbial populations, in order to introduce some of the crucial notions addressed in Chapters 3 and 5 as well as the thermodynamic considerations in Chapter 6. Indeed, it is believed that the technical implementation of complex processes like S-driven denitrification cannot overlook the diverse and versatile physiology of the implicated bacterial population.

1.1 The nitrogen network

Nitrogen is one of the essential macro elements for all kinds of living being on earth and is involved in the synthesis of fundamental molecules and structural units, such as proteins, of all the domains of life. In many prokaryotes and archaea, it plays a fundamental role also in their bioenergetics, since they are able to harvest energy from redox reactions transforming inorganic N compounds from one oxidation state to another. In nature, nitrogen cycle is one of the main bio-geo-chemical cycles together with the Carbon, Sulphur and Phosphorous cycles and the vast majority of nitrogen transformations are biologically mediated.

Multiple studies on the microbial metabolic versatility in nitrogen utilization as well as recently discovered processes (such as Anammox) consolidate the complexity of the nitrogen cycles, considered in fact, as an interconnected network more than a balanced cycle of input and output transformations (Sparacino-Watkins et al., 2014; Kuypers et al., 2018). Moreover, the extensive use of molecular biology techniques such as environmental genomics (metagenomics) gave an important insight in the highly diverse microbial populations mediating nitrogen transformation for a variety of metabolic functions (Cabello et al., 2009; Kuypers et al., 2018).

In figure 1.1 the schematic of the main processes of the nitrogen network presented in Kuypers et al. (2018) is shown as a comprehensive representation of the current knowledge on the inorganic nitrogen transformation in its five main forms of (from the most oxidized to the most reduced): NO₃⁻, NO₂⁻, NO, N₂O, N₂, NH₃¹. Apart from N₂, all the other forms are usually referred to as reactive Nitrogen (N_r) due to their involvement in bio-

¹ Hydrazine (N₂H₄) and hydroxylamine (NH₂OH) are also important players in the N biochemical cycle, though as intermediate metabolites and their role is not clearly addressed in many biochemical processes, especially for hydroxylamine (Soler-Jofra et al., 2021).

chemical reactions (from biomass synthesis to light-driven reactions). The unfixated form of N_2 is considered the non-reactive form of nitrogen. Organic nitrogen is another main form of nitrogen on earth. Six main processes are known so far, all mediated by enzymatic activities of eukaryotes (mainly plants and fungi), prokaryotes and archaea, even though prokaryotes play the prominent role (Cabello et al., 2009). Two main purposes for N utilization can be distinguished: (1) assimilatory, in case N is directly utilized for biomass/functional unit synthesis (anabolism) and (2) dissimilatory, in case N is not involved in biomass synthesis. Dissimilation, in turn, may be run for energy production, usually referred to as nitrate respiration (catabolism), or for detoxing or electron sink/energy dissipation (Cabello et al., 2009). Even though dissimilatory and respiration are not overlapping concepts, they are often used as equivalent notions in literature².

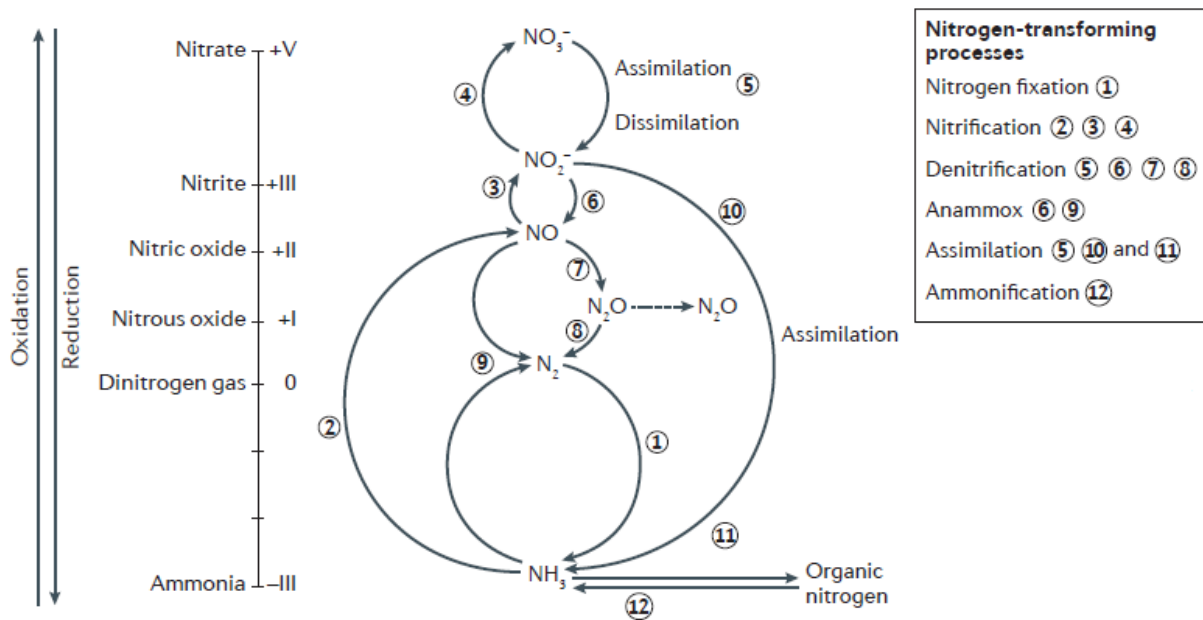


Figure 1.1 Biological processes involved in the Nitrogen network (modified from Kuypers et al., 2018).

² To be rigorous, *dissimilation* strictly refers to a non-assimilatory process involved in processes other than proton motive force generation, e.g. detoxification. On the contrary, *respiration* strictly refers to non-assimilatory electron transferring mechanisms involving a reduced compound (electron donor) and a terminal electron acceptor coupled with proton motive force generation (Cabello et al., 2009).

Atmospheric dinitrogen gas represents the main sink of available nitrogen³ (Kuypers et al., 2018). Natural nitrogen fixation to ammonia is a process mediated by few types of bacteria and archaea and transforms N₂ to the highly bio-available form of ammonia (NH₃). Through assimilation, bio-available nitrogen is used to synthesize new organic matter, i.e. organic nitrogen. Ammonia is the form that actually enters biomass synthesis mechanisms and, consequently, it is generally the preferred nitrogen source. Ammonification refers to the returning of ammonia back in the environment, after organic matter degradation (mineralization carried out by saprophyte bacteria and fungi, Cabello et al., 2009). The two-step nitrification oxidizes ammonia to nitrite and nitrate. Nitrate can be either reduced to organic matter (prior to its reduction to nitrite and then to ammonia) in the assimilatory nitrate reduction or to dinitrogen gas in case of dissimilatory nitrate reduction. In both cases, nitrite is the main intermediate of the reaction and the process is usually referred to as denitrification (in wastewater engineering, denitrification mainly refers to the dissimilatory energy-producing pathway). The reduction of nitrate to the most reduced state of ammonia is also mediated in nature for dissimilatory energy-yielding purposes and it is named after its acronym DNRA (Dissimilatory Nitrate Reduction to Ammonia). In a cycle-type approach, denitrification, i.e. nitrate reduction to dinitrogen gas used to be the sealing process returning reactive nitrogen to the inert atmospheric sink of N₂. The discovery of the anammox process have significantly reformed the thereto knowledge on the nitrogen cycle, adding the novel process to the flux from reactive nitrogen to N₂ sink. After its discovery, anammox contribution to N turnover from marine environments was estimated around 40-50% of the total N₂ production whereas denitrification is still considered the prevailing mechanism for N₂ turnover in soils and freshwaters (Cabello et al., 2009; Kuenen, 2020). Incomplete reactions in the nitrification and denitrification pathways may give rise to diffuse emissions of undesired intermediates, mainly NO and N₂O. NO is a highly toxic strongly oxidative compound, that can be easily degraded to the less toxic N₂O (either biologically or chemically), which in turn is a potent greenhouse gas and ozone-depleting agent. Significant N₂O emissions are estimated to derive from fertilizers' decomposition in soil systems (Davidson, 2009).

Beside the natural network, the anthropogenic contribution to nitrogen fluxes has become of prominent importance since additional and typically fast transformations are inferred to the natural equilibrium. The sources and the consequences of human impacts on nitrogen cycle are multiple: (i) massive combustion of fossil fuels yields to the release of gaseous nitrogen oxides (NO_x) and N₂O, with adverse impact on global warming and ozonosphere depletion; (ii) extensive and inefficient use of fertilizers and animal manure provoke direct leakage and run-off of ammonia and nitrate in groundwater and surface waters, impacting freshwater supply quality and causing eutrophication, probably the most severe environmental impact of N-cycle unbalances; (iii) industrial activity and high anthropic pressure in urbanized areas produce massive amounts of wastewaters, and, in many regions of the world, sewage systems and subsequent wastewater treatments are poorly efficient when not missing at all.

³ Mineral-bonded ammonia present in the lithosphere is actually a bigger reservoir, but its availability in natural systems is much less relevant since it is limited to erosions events (Kuypers et al., 2018).

An astonishing impact in the anthropogenic nitrogen flux has been caused by the discovery of the Haber-Bosh process and its massive use in the last seventy years. Such a process allows for synthetic industrial nitrogen fixation from inert atmospheric N_2 to the reactive and versatile form of ammonia. The analogue flux in natural environments is mediated by few types of N-fixing bacteria and is the ultimate limiting (and regulating) process for N availability in the biosphere. Through industrial nitrogen fixation, such a constraint for nitrogen availability has fallen and the influx of anthropogenic fixed form of nitrogen in the environment has increased steadily over the years. The ammonia synthesized through the Haber-Bosh process is applied for multiple production activities, such as those related to fertilizers, animal feed additives, plastics, explosives, etc. A further not well defined flux of reactive nitrogen towards the environment derives from such productive activities in terms of by products, waste and wastewater (Galloway et al., 2008). Agricultural production has increased enormously and allowed population growth worldwide at the level observed today. Galloway et al. (2008) report that perhaps 40% of protein dietary comes from synthetic nitrogen; an analogue concept is warned by Chen and Strous (2013) reporting studies in which half of the nitrogen atoms present in the biosphere is currently generated from fertilizers and use of fossil fuels, i.e. from human activities. Estimates on the current industrial nitrogen fixation has reached annual yields comparable to those produced by natural microbial fixation in the terrestrial environment, and some studies estimated that the industrial flux would even overcome the one produced in natural environment by 2030 (Vitousek, 1997; Kuypers et al., 2018).

In this context, the urgency to limit the adverse effect of irrational use and release of reactive nitrogen has become clear and regulations have been adopted in the last decades in order to limit indiscriminate discharge of reactive nitrogen in natural environments. At the European level, the so called Nitrate Directive (91/676/CEE) and the Water Framework Directive (2000/60/EC) have been among the main communitarian actions towards a more rational use of fertilizers and greater attention on surface water quality. Several national and/or regional regulations have followed in order to define ever-more stringent limits for water discharge.

Wastewater collection and treatment are strategical for intercepting reactive nitrogen emissions and returning them into the inert gaseous state of N_2 . The conventional activated sludge systems widely implemented worldwide, have accomplished such a scope by coupling nitrification and denitrification processes. The novel anammox process boosted further innovation in biological nitrogen removal treatments, due to its lower energy requirement and GHG emissions.

1.1.1 Denitrification

Denitrification refers to the biologically mediated process of nitrate reduction. In engineered systems for wastewater treatment, it is usually considered as a one-step process leading to the final production of dinitrogen gas. Indeed, in conventional activated sludge process, nitrite is rarely detected after denitrification, even though intermediate by-products such as volatile N_2O started to be monitored in the recent years due to the high global

warming potential (GWP) embedded by this strong greenhouse gas⁴. The actual pathway of complete nitrate reduction comprises four steps according to the following reduction chain: $\text{NO}_3^- \rightarrow \text{NO}_2^- \rightarrow \text{NO} \rightarrow \text{N}_2\text{O} \rightarrow \text{N}_2$. Each step is mediated by different enzymes, in turns differentiated for their functionality in the cellular metabolism. Denitrification can be mediated by bacteria, archaea and eukaryotes (such as plant and fungi); facultative anaerobic (proto)bacteria are by-far the most relevant players (Zumft, 1997; Kraft et al., 2011; Kampschreur et al., 2012). A schematic of the denitrification pathway in Gram-negative bacteria is reported in figure 1.2.

The first step of nitrate reduction to nitrite, denitrification, is mediated by the Nitrate Reductase enzymes (NR). In prokaryotes, different NR are used for assimilatory or dissimilatory functions. In the assimilatory pathway nitrate is reduced into biomass components (same oxidation state as ammonia) and the assimilatory nitrate reductase, Nas, is involved; dissimilatory denitrification is generally linked to the catabolic activity (i.e. nitrate respiration), mediated by the respiratory nitrate reductase, Nar, and the periplasmic nitrate reductase, Nap. In contrast to the assimilatory route, in dissimilatory nitrate reduction, the reduced nitrogen end-products are ultimately released in the bulk liquid (Sparacino-Watkins et al., 2014). A fourth type of NR is found in Eukaryotes (mainly plants and fungi), euk-Nar, used for assimilatory purposes.

In wastewater treatment, denitrification is carried out mainly by bacteria. Both Nar and Nap contains Molybdenum-based units but contradictory conclusions on their importance in the denitrifying microbial community are encountered in literature. Nar is generally considered the main NR involved in catabolic reactions using nitrate as terminal electron acceptor (TEA). Even though the role of Nap on denitrification in natural system seems to be limited, Nap is often encountered in many denitrifiers (Bell et al., 1990; Tavares et al., 2006; Kraft et al., 2011; Sparacino-Watkins et al., 2014).

⁴ GWP of N₂O is almost 300 times higher than that of CO₂. N₂O emissions remain in the atmosphere for 100 years, on average (Source: www.epa.gov, on GHG emissions).

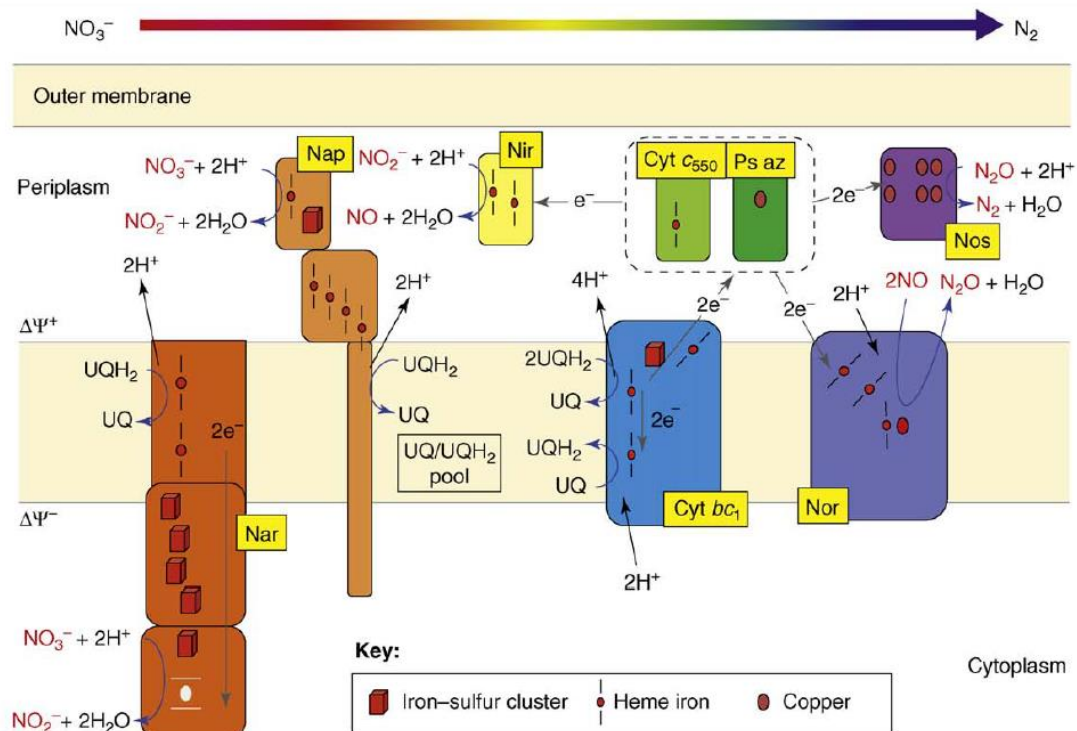


Figure 1.2 Chained reduction pathway in denitrification and related enzymology; modified from Richardson et al., 2009.

Nar is a membrane-bound complex whose active site faces the cytoplasm (fig. 1.2). When nitrate is detected in the periplasm by Nitrate sensors, they activate the expression of nitrate transporters (belonging to the Nark family) that translocate NO_3^- ion to the cytoplasm where its reduction to nitrite takes place (Kraft et al., 2011). Oxygen inhibits Nark transporters and, in turn, the whole reduction chain. Two electrons are required for nitrate reduction and are acquired in the electron chain across the membrane and two protons are released across the membrane, ultimately contributing to the generation of proton motive force. On the contrary, Nap is a membrane-bound complex whose active site is located on the periplasm; thereby no proton gradients are generally produced by periplasmic nitrate reduction and, as a consequence, no energy is directly harvested (Sparacino-Watkins et al., 2014). Genes encoding for Nar and Nap expression as well as enzyme isolation techniques can be used to assess which one of the two nitrate reductases is used in a given organism. Though, their co-presence has been observed in many bacteria (Tavares et al., 2006; Cabello et al., 2009; Kraft et al., 2011; Kuypers et al., 2018).

Nitrite reduction to nitric oxide (NO) is mediated by two types of Nitrite Reductase (Nir), differing from their cofactors units: the *cb-1* nitrite reductase and the copper-base nitrite reductase, expressed by NirS and NirK genes, respectively (Cabello et al., 2009; Chen and Strous, 2013). Usually, their co-presence is not observed, so it seems that bacteria express exclusively one or the other (Zumft 1997, Tavares et al., 2006). Both types are periplasmic enzymes and thereby, the enzymatic activity is not directly linked to the generation of proton motive force.

Nitric oxide reduction to N_2O is mediated by the membrane-bound Nitric Oxide reductase, Nor, with the active site on the periplasmic side. The best studied Nor is the one depending on the cytochrome *c* (Richardson et al., 2009). NO is a very reactive radical whose accumulation may pose severe harm to the cell; for this reason, studies have proposed a co-regulation of the Nir and Nor in order to prevent nitrite reduction to NO in case of undesired NO accumulation (Kraft et al., 2011; Chen and Strous, 2013). Studies on the *Thiobacillus* genus, found that in case of excess of reductant, periplasmic nitrite reductase may be inhibited by complexation with Nor, in order to limit NO accumulation in the periplasm (Tavares et al., 2006 and references therein). The final step of N_2O reduction to N_2 is mediated by the periplasmic Nitrous Oxide Reductase (N_2O_r). A highly specific Copper-sulphur core enzyme is used in this step due to the poorly metal-bonding attitude of N_2O . N_2O_r is a soluble enzyme located in the bacterial periplasm.

As a general observation, enzymes operating in the periplasm are more affected by environmental pH (their activity been usually favoured at neutral pH), compared to those operating in the cytoplasm (Richardson et al., 2009). In gram-positive bacteria, it is suggested that all the enzymes involved in denitrification are membrane-bound, since periplasm is not present (Kraft et al., 2011).

Unbalance in electron donor supply is one of the main factor that causes a partial functioning of the highly branched reduction chain of denitrification and possible intermediate release; signalling and regulatory mechanism are in place in order to limit highly cytotoxic intermediates (such as NO) accumulation (Chen and Strous, 2013; Kampshcreur et al., 2012). In the vast category of denitrifying bacteria, some are capable of mediating only some of the denitrification steps such as *E. coli*, *P. denitrificans* and *T. denitrificans*, whereas others encode only some of the genes necessary for the transcription of the required enzymes and thereby, they are able to mediate only some of the three denitrification steps. For instance, *Thiobacillus thioparus* only mediates the denitratation step, whereas *A. Tumefaciens* can drive the denitrification until N_2O but lack of N_2O reductase (Beller et al., 2006; Madigan et al., 2019; Kampschreur et al., 2012; Lin et al., 2019).

1.1.2 Anammox

The discovery of anammox in the late 90's had an astonishing impact in the fields of microbiology, geochemistry and environmental engineering. The unique physiology and morphology of the thereto unknown bacteria have intrigued microbiologists worldwide and an impressive number of studies has been published in the last 30 years with the aim of delineate such a unique microbial functioning. From the geochemistry perspective, it turned out that up to 40- 50% of the biologically formed N_2 is mediated by anammox bacteria and their presence has been found almost ubiquitously in anoxic niches, either in freshwaters, marine and terrestrial environments and wastewater treatment plants, even under extreme conditions such as saline and hypersaline waters, alkaline lakes and oceanic deep thermal vents (Kartal et al., 2012; Oshiki et al., 2016). The famous discovery in the pilot plant of Gist-Brocades treating yeast industry wastewater arose from the unexpected loss of ammonia in a sulphur-oxidizing denitrifying reactor (Mulder et al., 1995). Kuenen (2020)

refers that *a posteriori* analysis of previous studies revealed that unexplained depletions of ammonia in activated sludge systems were reported back in the first decades of the IX centuries.

So far, five genera and nine species have been identified but the wide distribution in diverse natural systems suggest a broader community still to be defined (Kuenen, 2020). The five genera are: *Ca. Kuenenia*, *Ca. Brocadia*, *Ca. Anammoxoglobus* and *Ca. Jettenia*, all belonging to the order *Brocadiales*, phylum of *Planctomycetes*. Conventional cultivation techniques have failed in reaching a pure anammox culture and continuous or semi-continuous cultivation systems, typically sequencing batch reactors (SBR) and membrane biological reactors (MBR), have shown to be the most feasible way to achieve enrichment levels as high as 75% and 90%, in a floc-aggregate and planktonic state, respectively in the two systems⁵ (Peeters and van Niftrik, 2019). For this reason, all the genera hold the status of *Candidatus*.

The unique metabolism of anammox bacteria is strictly related with their unique ultrastructure. Yet, many aspects of cellular biology and metabolism are still unclear. Planctomycetes represent some of the exceptions to the classical notion of cellular simplicity in bacteria, since they present an internal organized structure usually based on two compartments. Still, among planctomycetes, anammox exhibits a peculiar three compartment-structure, divided in anammoxosome, cytoplasm and periplasm⁶. Each compartment is lined by a specific membrane. In figure 1.3a, the ultrastructure scheme in a typical anammox is presented. In the highly folded lipidic membrane surrounding the anammoxosome, ATP synthetase is present suggesting that this organelle is directly involved in energy production, in strict analogy with eukaryotic mitochondrion (Fuerst et al., 2017). The interaction mechanism between anammoxosome metabolic activity and the ATP-generation through its membrane in the cytoplasm still requires further studies (Peeters and van Niftrik, 2019). Another singularity is the composition of the anammoxosome membrane: compared to normal membranes, exclusive lipids called “ladderanes” (cyclo-butane rings in linear concatenation) confer to the membrane a normal permeability to hydrazine and low permeability to protons. These characteristics are in line with the evidence of hydrazine concentration in the bulk (diffusion through the cell membranes) and with the hypothesis of bioenergetics efficiency increase through the limitation of proton motive force dissipation, further confirming the energy-related role of the organelle (Kartal et al., 2012; Peeters and van Niftrik, 2019). The outer layer of the anammox cell is a S-protein layer probably bonded to the outer periplasmic membrane (Peeters and van Niftrik, 2019).

⁵ Very high enrichment levels of 95% and 97% in MBR systems are reported by Hu et al. (2019) and Lotti et al. (2014b).

⁶ Recent studies have confirmed that Anammox contains a periplasm as gram-negative bacteria, unlike reported in previous works (see the review from Peeters and van Niftrik, 2019).

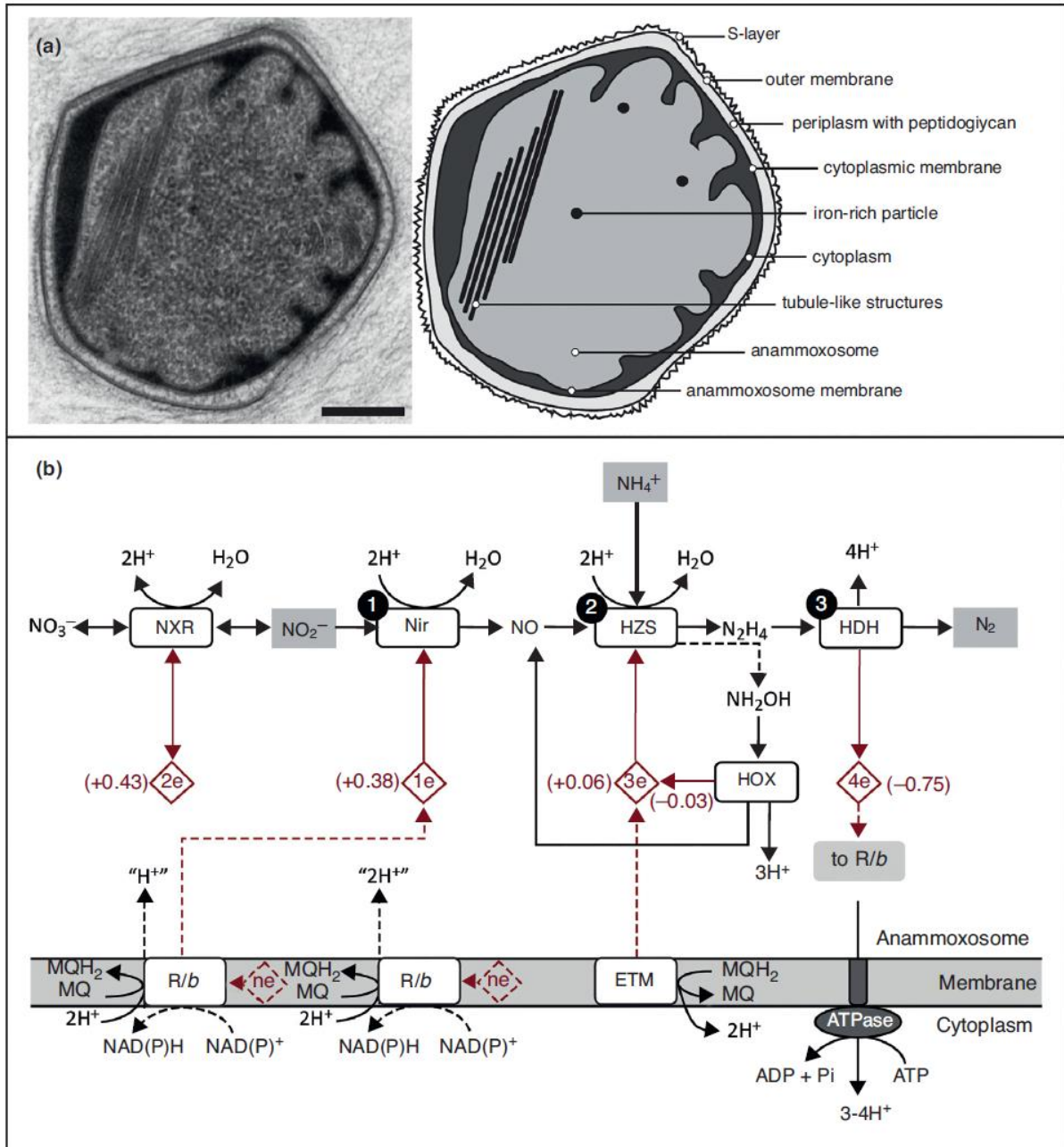


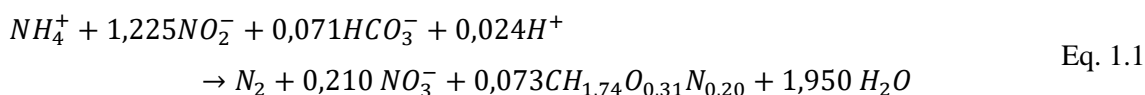
Figure 1.3 Anammox ultrastructure (a) and currently accepted catabolic pathway (b); from Peeters and van Niftrik, 2019.

Concerning their catabolic activity, anammox bacteria have the unique capacity of mediating ammonium oxidation, using nitrite as electron donor. At the same time, nitrite is used as electron donor in the autotrophic anabolism with a consequent production of nitrate. Indeed, in the conduction of anammox reactors, nitrate presence is generally linked to biomass growth⁷. Acetyl-CoA is reported to be the Carbon fixation pathway, based on genomic evidences in *Kuenenia stuttgartiensis* (Strous et al., 2006).

⁷ A recent study from Hu et al. (2019) confutes such a generally accepted notion. In their work authors observed no nitrate formation when anammox bacteria were fed with NO instead of nitrite.

In figure 1.3b, the currently accepted metabolic pathway is presented, provided that metabolic routes may differ in the different species and that the knowledge on anammox metabolic versatility is still not exhaustive. The general redox chain begins with nitrite reduction to nitric oxide. Nitrite reductase NirS and NirK are encoded in the genome of *Ca. Scalindula* and *Ca. Jettenia*, whereas none of the two are encoded in *Ca. Brocadia*, suggesting that an unknown nitrite reductase is expressed and currently missing (Peeters and van Niftrik, 2019) or that hydroxylamine rather than nitrite is used for the subsequent hydrazine synthesis (Oshiki et al., 2016b). Nitric oxide further reacts with ammonium to form the rocket fuel compound of hydrazine, N_2H_4 , through the catalytic activity of the hydrazine synthetase (HZS). The units forming the HZS also differ among the studied genera. The slow activity of HZS is speculated to be a possible cause of the slow cellular growth (Kartal et al., 2012). Hydroxylamine is thought to be formed as (undesired/occasional) by-product of hydrazine synthesis and converted back to nitric oxide by the hydroxylamine oxidase (HOX). The final oxidation of hydrazine to dinitrogen gas delivers 4 electrons and is mediated by the hydrazine dehydrogenase (HDH). A recent publication from Soler-Jofra et al. (2021) highlights that the role of hydroxylamine in anammox (and other N-related biochemical processes) is object of discussion. Specifically, among the proposed alternative pathways, some authors envisage that hydroxylamine more than NO is reacting with hydrazine for the formation of N_2 , thereby explaining the role of HOX enzymes highly expressed in anammox bacteria but not clearly related to specific metabolic mechanisms yet. It is interesting to note that the strong greenhouse gas N_2O is not produced in the proposed anammox metabolism, unlike denitrification (and nitrification), adding further environmental advantages to the innovative process. Still, enzymes for N_2O production are encoded in the genomes but apparently NO detoxification towards N_2O production is not adopted and literature works seem to agree in acknowledging a very minor release of N_2O in anammox reactions (Jia et al., 2018; Hu et al., 2019). The characteristically red colour of anammox enriched cultures directly derives from the very high content in cytochromes (up to 20-30% of their total proteins according to Jetten et al., 2009 and Kartal et al., 2012), in fact Iron-based heme-proteins.

The full metabolic stoichiometry has been first published by Strous et al. (1998). A more recent publication from Lotti et al. (2014b) questioned the widely adopted stoichiometry and proposed an updated statistically validated stoichiometric reaction, derived from a long-term MBR operation, with planktonic anammox cells. In their work, the authors complete the study by integrating the experimentally-derived stoichiometry with data reconciliation analyses and offer the derived stoichiometry under three different scenarios: (i) no constraints for N source, (ii) $N-NH_4^+$ as N source and (iii) $N-NO_3^-$ as nitrogen source. In the present thesis, the stoichiometry of the no-constraint scenario for the N source is considered for stoichiometry considerations and is presented in equation 1.1.



Anammox are generally considered as slow-growing bacteria with maximum growth rate (μ_{\max}) of 0,06-0,1 d^{-1} , and consequent doubling time of 7-11 days (Kartal et al., 2012). Higher growth rates have been observed for free-living cell compared to aggregated states; still, the high tendency to form aggregates of anammox bacteria suggest a net advantage underlying such a behaviour (Kartal et al., 2012). Lotti et al. (2015) obtained growth rate as high as 0,3 d^{-1} (in fact, the highest ever reported) in a MBR reactor operated under stepwise reduction of sludge retention time (SRT), suggesting that the slow growth generally reported might be related to the growing conditions applied instead of being an intrinsic physiologic feature of the microorganisms. High substrate affinity for ammonia and nitrite are generally reported with half saturation constants (K_s) below 0,07 mgN/l for both ammonia and nitrite (Kartal et al., 2012; Lotti et al., 2015). Significant variations can be observed among genus (and species within the same genus) regarding the main kinetic parameters (namely μ_{\max} and K_s), distinguishing anammox bacteria among k-strategist, such as *Ca. Kuenenia* and r-strategist, such as *Ca. Brocadia* (Oshiki et al., 2016; Yu et al., 2020).

In 2014, around 100 full-scale installations worldwide were detailed by Lackner et al. (2014). All of them rely on the synergistic cooperation of the Partial Nitritation (PN) process carried out by Ammonium Oxidizing Bacteria (AOB) and anammox. The technological solutions vary from one-stage to two-stage configurations, SBR and MBR operations, suspended or aggregated biomass. Anammox activity can be disrupted by a variety of inhibiting conditions such as those related to the presence of: heavy metals, sulphide, phosphates, salinity, nitrogen and dissolved oxygen, whose inhibiting concentrations and consequent adverse effect varies depending on the applied biomass and operational conditions (see reviews from Jin et al., 2012 and Dapena-Mora et al., 2007).

1.2 The Sulphur cycle

1.2.1 Sulphur biochemistry

Compared to the N cycles, the natural Sulphur (S) cycle is even more complex due to high chemical reactivity of many sulphurous compounds. Thereby the main biological processes involved in S transformations coexist with a complex system of chemical transformations. Eight reduction states are possible for S, but three are the most relevant in natural systems, where inorganic S exists mainly in the forms of: (i) Sulfate, the most oxidized form (reduction state of +6), (ii) elemental sulphur (zero-valent solid form) and (iii) sulphide, its most reduced and reactive form (reduction state of -2). Sulphur is another fundamental element for all living beings, whose presence is linked with fundamental functioning components such as protein prosthetic units or enzymatic co-factors. This is also the reason why the combustion of fossil fuels (in fact, among the ultimate products of organic decomposition) yields the release of sulphur compounds, mainly in the form of SO_2 .

The main S sink on earth is the lithosphere (sediments and rocks), where S is present in form of gypsum (CaSO_4 , the most abundant) or other minerals (such as pyrite FeS_2), but the oceans constitutes the main inventory for biologically available S, mainly as SO_4^{2-} ; indeed, the average sulfate concentration in oceanic waters is as high as $2,7 \text{ gSO}_4^{2-}/\text{l}$ (Madigan et al., 2019; Lens, 2020). Natural environments such as active volcanic zones and sulphide springs contribute to the natural release of hydrogen sulphide and sulphur oxides into the atmosphere.

The main processes involved in the biological sulphur cycles are depicted in figure 1.4.

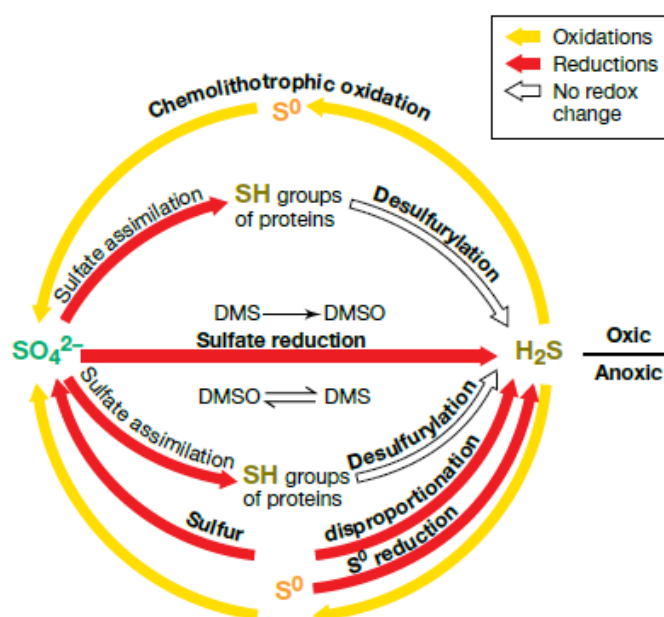


Figure 1.4 Main process in biological Sulphur cycle (from Madigan et al., 2019).
DMS: dimetil sulphide; DMSO: dimetil sulphoxide.

As for the N biological cycles, processes can be mediated for assimilatory or dissimilatory purposes. While prokaryotes are the major players in S dissimilation, S assimilation is mediated by a wider spectrum of organisms, from bacteria to eukaryotes such as plants, fungi and algae (Lens, 2020). Sulfate is the form typically adopted for synthesis of organic compounds through sulfate assimilation (in fact, a reduction step). Sulfate reduction usually refers to the dissimilatory energy-producing process carried out by a variety of bacteria, capable of using SO_4^{2-} as terminal electron acceptor for the oxidation of organic carbon or hydrogen. Sulfate reducing bacteria (SRB) are widespread in marine anoxic environments and their activity yields to the direct production of biogenic hydrogen sulphide that easily reacts with Fe^{2+} precipitating as FeS_2 . The so-called *sulphur* reducing bacteria are able to carry out dissimilatory reduction of elemental sulphur or sulfite to sulphide, but are not able to reduce sulfate. Sulphide oxidation is a dissimilative reaction carried out by a wide and diverse group of Sulphur Oxidizing Bacteria (SOB), whose vast majority are aerobic and facultative

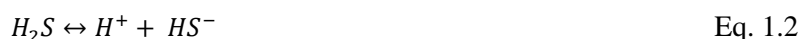
anaerobic, i.e. they use oxygen as preferred electron acceptor but are able to mediate nitrate respiration in oxygen-depleted conditions. SOB are usually split into two main categories: phototrophic (coloured) bacteria, namely purple and green SOB⁸ and chemolithotrophic (or colourless) SOB. A separate paragraph is dedicated to chemolithotrophic denitrifying SOB in section 1.1.4.

Another important biological process involves the oxidation of the dimethyl sulphide (DMS, formula $\text{CH}_3\text{-S-CH}_3$), to dimethyl sulphoxide (DMSO) and its reduction back to DMS. DMS is the most abundant organic sulphur compound in nature and is released in marine environment by phytoplankton and from algae degradation; in microbial metabolism, it can be used as electron donor, or as electron acceptor, in its oxidized form of DMSO, as well as for methane production (Madigan et al., 2019).

The complex pool of chemical reactions involved in Sulphur transformations imply different type of reactions, from abiotic redox to concatenation (of elemental sulphur) to protonation/deprotonation to photochemical decomposition, whose extent and reaction rates are highly dependent on the environmental conditions such as species concentration, temperature, pH, light presence and redox potential. In this paragraph only the reactions of interest for the thesis work are described, i.e. elemental sulphur concatenation and sulphide chemical oxidation. Extensive reviews on the chemistry of sulphur are available in literature (Steudel, 1996; Kleinjan et al., 2005; Lens, 2020).

Elemental sulphur (S^0) is present in nature as rings or polymeric chains of sulphur atoms, the orthorhombic $\alpha\text{-S}_8$ being the most common and stable one at temperatures of 20°C and atmospheric pressure (Lens, 2020). It shows a high tendency in developing long chains of concatenated S atoms, with no theoretical limitation on the chain length. This feature increases the complexity of the available S^0 forms in nature. In general, all its allosteric forms are insoluble in almost all solvents but its solubility increases in alkaline sulphide solutions (Lens, 2020).

Hydrogen sulphide speciation follows the following equilibrium reactions:



At 20°C, the acid constant of the first dissociation (eq. 1.2) is $k_{a1} = 10^{-7}$; the second acid dissociation has an average value of $K_{a2} = 10^{-14}$, but its value can range up to 10^{-17} depending on the ionic strength of the solution (Lens, 2020). The resulted speciation diagram at 20°C is reported in figure 1.5.

⁸ Purple and green sulphur oxidizing bacteria utilize sulfide as electron donor to drive photosynthesis. The photoreactive pigment involved in their metabolism and determining their colour are betacarotenoids and chlorosome (a complex of cytochromes), respectively for purple and green bacteria (Ghosh and Dam, 2009; Madigan et al., 2019).

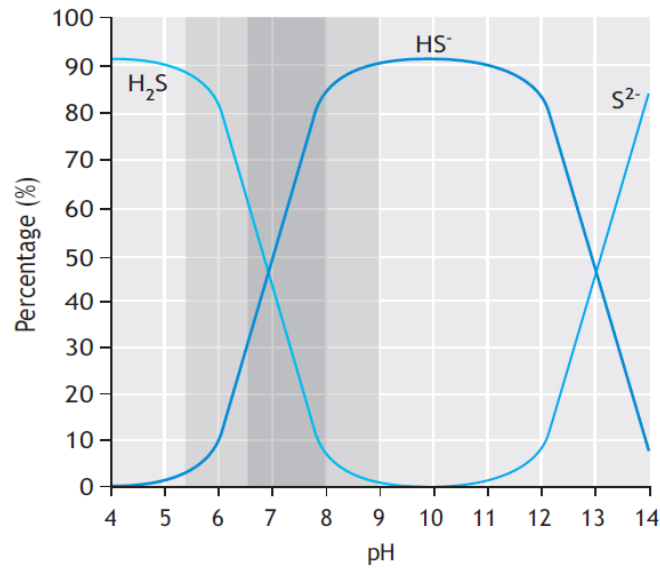
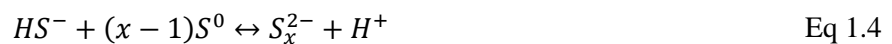


Figure 1.5 Sulphide speciation over pH, at 25°C (from van Loosdrecht et al., 2016).

Thereby, only at $\text{pH} > 12$ S^{2-} concentration becomes significant (at 20°C and atmospheric pressure). The expression of Total Dissolved Sulphide (TDS) is often used to account for the three species that might be present in aqueous solutions.

Due to its high tendency to be oxidized, abiotic oxidation of sulphide may occur spontaneously in presence of oxidants, such as oxygen, leading to the formation of polysulphides, thiosulfate and sulfate. Such chemically formed intermediates are undesired by-products both in laboratory and full-scale installations of the biological sulphide oxidation process. Indeed, their presence interfere with the biologically induced oxidation, by altering the e-donor/e-acceptor availability or creating undesired end-products, such as sulfate in case of applications aiming at sulphur-recovery (van de Bosch et al., 2007). Polysulphides S_x^{2-} are chained aggregates of sulphur atoms and a sulphide ion, whose formation is promoted in presence of oxygen in alkaline solutions containing biogenic elemental sulphur (more hydrophilic than the synthetic analogue), according to the following reaction (Steudel, 1996; Kleinjan et al., 2005):



Their further oxidation leads to the production of thiosulfate (eq. 1.5) and, ultimately, sulfate.



For instance, in laboratory scale applications, the salt $\text{Na}_2\text{S}\cdot 9\text{H}_2\text{O}$ is commonly used for the preparation of sulphide concentrated solutions, often kept at alkaline conditions in order to limit the formation of H_2S and its consequent volatilization (eq. 1.2). Nevertheless, in case of even low concentrations of oxygen and elemental sulphur, such alkaline conditions favour cascade sulphide oxidation to polysulphides, thiosulfate or sulfate. As a matter of fact, such impurities can be present even in commercial concentrated sulphide solutions (Lens, 2020).

On the general debate on environment quality and climate change, less attention has been paid on the mitigation of human alterations of the S cycles, compared to the huge effort dedicated to C, N and P cycles (Lens, 2020). The primary source of anthropogenic S release in the environment, in the form of SO_2 , is the combustions of fossil fuels; SO_2 emissions derives also by the combustion of non-fossil biomass such as wood. Petroleum refineries and some industrial activities produce significant amounts of gaseous sulphur compounds, often treated through chemical scrubbers and alkaline solutions of calcium carbonate or hydroxide for the final production of gypsum (Lens, 2020). Another source of SO_2 is the chemical industry, for the production of sulphuric acid and its various by-products. SO_2 is among the primary responsible for the phenomena of acid rains. In the last decades, effective regulations have been adopted in Europe and USA in order to mitigate SO_2 anthropogenic emissions and consequent drawbacks, but the problem of acid rain remains significant in emerging countries, especially in Asia (Lens, 2020). Environmental technologies and regulations have been adopted in order to mitigate anthropogenic sulphur emission and their drawbacks. Collection and treatment of S-polluted gaseous and liquid streams have been a successful solution for limiting the impacts originated by industrial activities and biological desulphurization of gaseous streams has been the core and novel process of applied environmental biotechnologies for S removal, in the last twenty years.

1.2.2 Denitrifying Sulphur Oxidizing Bacteria, metabolic pathways and variety

Sulphur Oxidizing Bacteria (SOB) have been discovered at the end of the XIX century by Sergei Winogradsky as the first group of chemolithotrophic bacteria; the category of chemolithotrophic bacteria has been created, in fact, after their discovery. Moreover, chemolithotrophic Sulphur-based metabolism is acknowledged as the first self-sustained metabolism experienced at the origin of life on Earth (Ghosh and Dam, 2009; Bao et al., 2020).

SOB are a wide and phylogenetically diverse group of bacteria, capable of thriving in a broad variety of natural and artificial ecosystems. SOB have been found in almost all environmental conditions in terms of pH, i.e. acidophilic, neutrophilic and alkalophilic conditions, and temperature, i.e. psychrophilic, mesophilic and thermophilic (Lin et al., 2018). Many SOB showed to be highly versatile; morphological and physiological characteristics showed to be dependent on the environmental conditions more than being intrinsic features of specific bacterial species (Ghosh and Dam, 2009). SOB have been described to be able of remarkably diverse metabolisms in terms of energy and C source: from strict chemolithotrophic to mixotrophic to heterotrophic

and from autotrophic to heterotrophic, and all the derived combinations (Robertson and Kuenen, 2006); they can be found as cocci, concatenated cocci, or filamentous, and their size may vary from few to hundreds μm^9 (Madigan et al., 2019; Kuenen, 2020).

Considering only strict chemolithoautotrophic denitrifying SOB, different metabolic pathways are displayed for electron donor oxidation, Carbon fixation and terminal electron acceptor (TEA) reduction. Moreover, according to genomic analysis, some species appear to be able to drive more than one mechanism for electron donor reduction, further increasing the metabolic complexity. The basics of nitrate/nitrite reduction mechanisms and enzymology of denitrifying SOB are the same described in section 1.1.1. In the following paragraph a brief description of the C-fixation and S-oxidation pathways is provided.

C-fixation and S oxidation pathways

Denitrifying SOB are reported to adopt both the Calvin cycle or the reverse tricarboxylic acid (rTCA) pathway for inorganic carbon fixation (Klatt and Polerecky, 2015; Madigan et al., 2019).

Concerning sulphur-compound oxidation, three pathways have been described so far. The most established sulphur oxidation pathway is the periplasmic Sox enzymatic system (also known as TOMES system, from Thiosulfate-oxidizing multi enzyme), based on four main proteins SoxA, SoxYD, SoxCD and SoxB. As described in Madigan et al. (2019) and presented in figure 1.6, the basic mechanism starts with the action of SoxA which bonds the sulphur atom of the reduced S compound (either sulphide, thiosulfate or elemental sulphur) to the carrier protein SoxYD; SoxB is responsible for electron transfer to the electron transport chain, in case of intermediate of sulphur globules or final state of sulfate, whose formation is mediated by the action of protein SoxCD. Some bacteria lack of the latter protein, leading either to the formation of sulphur globules or to alternative sulphur-utilizing mechanisms.

⁹The genus *Thiomargarita* is considered the biggest bacteria on earth, as it can reach 750 μm in size. Due to the alternated exposure to aerobic and anoxic conditions it is able to accumulate nitrate in specific vacuoles inside the cell (responsible for the cellular dimension increase) and use its reservoir for the oxidation of sulfide, being able to survive at long anoxic periods (Madigan et al., 2019).

related to sulfate reduction metabolism) and adenosine phosphosulfate (APS) enzymes is deemed responsible for the latter oxidation steps (Ghosh and Dam, 2009).

Relevant denitrifying SOB species in environmental biotechnology

Thiobacillus denitrificans and *Sulfurimonas denitrificans* (previously classified as *Thiomicrospira denitrificans*) are the main denitrifying SOB, in autotrophic denitrification applications. Both have been extensively studied through pure cultivations in chemostats (Justin and Kelly, 1978; Timmer-ten Hoor, 1981; Visser et al., 1997).

The genus *Thiobacillus* (gram-negative β -proteobacteria), encompasses a wide range of physiologically heterogeneous bacteria, whose main common characteristic is to mediate inorganic reduced sulphur compound oxidation. Over the last forty years, reclassifications of the species belonging to this genus have been proposed as the observed metabolic variety brought to misclassification of new species (Kelly and Wood, 2000). Molecular biological techniques based on 16s rRNA sequencing have finally lead to the currently approved classification, according to which six accepted strains are recognized, namely: *T. thioparus*, *T. denitrificans*, *T. aquaesulis*, *T. thiophilus*, *T. plumbophilus*, and *T. sajanensis* (Kumar et al., 2020). *T. denitrificans* is by far the most studied SOB species able to carry out both aerobic and nitrate-dependent respiration (Beller et al., 2006). Many environmental solutions have exploited *T. denitrificans* for aquifers or soil remediation, due to its denitrifying as well as metal-oxidizing ability (Beller et al., 2006). Also, it turned out to be the only obligate autotrophic species able to carry out Uranium oxidation, opening rooms for its application in remediation of uranium-contaminated aquifers (Beller et al., 2006). Sequencing of its entire genome have revealed that it is able of multiple sulphur oxidizing pathways (Sox-related genes are present as well as those responsible for the branched pathway); moreover, the genomic information for driving Calvin cycle for C-fixation are fully present (Beller et al., 2006). *T. denitrificans* also displays the full enzymatic system necessary to carry out complete denitrification, compared to other *Thiobacillus* species encoding only nitrate reductase-related genes (Lin et al., 2018).

Up to the early 2000's, many studies described the activity and physiology of denitrifying SOB *Thiomicrospira denitrificans* (Timmer-ten Hoor, 1981). Since 2006 and based on 16s rRNA genomics, *Thiomicrospira denitrificans* has been reclassified as *Sulfurimonas denitrificans*, a gram-negative ϵ -proteobacteria, strictly anaerobic (Takai et al., 2006). Complete genome sequencing confirmed some of the observed characteristics: *Sulfurimonas denitrificans* are strictly anaerobic, adopt rTCA cycle for C-fixation and encodes genes for the Sox-pathways and complete nitrate reduction to N_2 (Sievert et al., 2007).

1.3 Integrating S-based denitrification and anammox: state of the art

The extensive studies on the natural niches suitable for anammox bacteria have recently brought to light the role of sulphide-driven denitrification in contributing to shape anammox geographical distribution in marine environments. The synergic interaction of anammox and denitrifying SOB has been reported in marine and estuary sediments (Prokopenko et al., 2006, Lisa et al., 2014, Oshiki et al., 2016).

In real-scale anammox implementation, ensuring long-term stability of partial nitrification remains so far one of the main challenges in full-scale anammox implementations. Especially in mainstream applications, the stable suppression of NOB activity is even more challenging than in side-stream conditions, since the usually lower temperatures and ammonia concentrations alter the kinetic advantage of AOB over NOB, accomplished in successful PN operations in side-streams. As a consequence of such technical problems, an emerging research topic is the so-called partial denitrification (PD), referring to the reduction of nitrate to the state of nitrite (denitratation), with the objective to provide an alternative path fulfilling the nitrite requirement for the anammox process (Zhang et al., 2020).

Partial autotrophic denitrification (PAD), based on reduced sulfur compounds oxidation, covers a narrow niche of the mentioned studies, likely due to the fact that sulphide-rich streams are a limited category of those generated by industrial activities and municipal wastewaters are usually poor in sulphur-components.

Different possible treatment solutions have been proposed oriented towards the general advantages that could be achieved in terms of Oxygen supply reduction, fast kinetics also at mainstream loading and temperature conditions, high total nitrogen (TN) removal. Indeed, partial denitrification could also be conceived as post-treatment of highly loaded PN/A in order to increase TN removal in case of high nitrogen concentration of the PN/A system and consequent significant nitrate concentrations in the effluent (figure 1.7a). In such a case, the effluent of the PD treatment could be fed back to the deammonification unit incrementing NO_2^- supply and further reducing the O_2 requirement in PN/A.

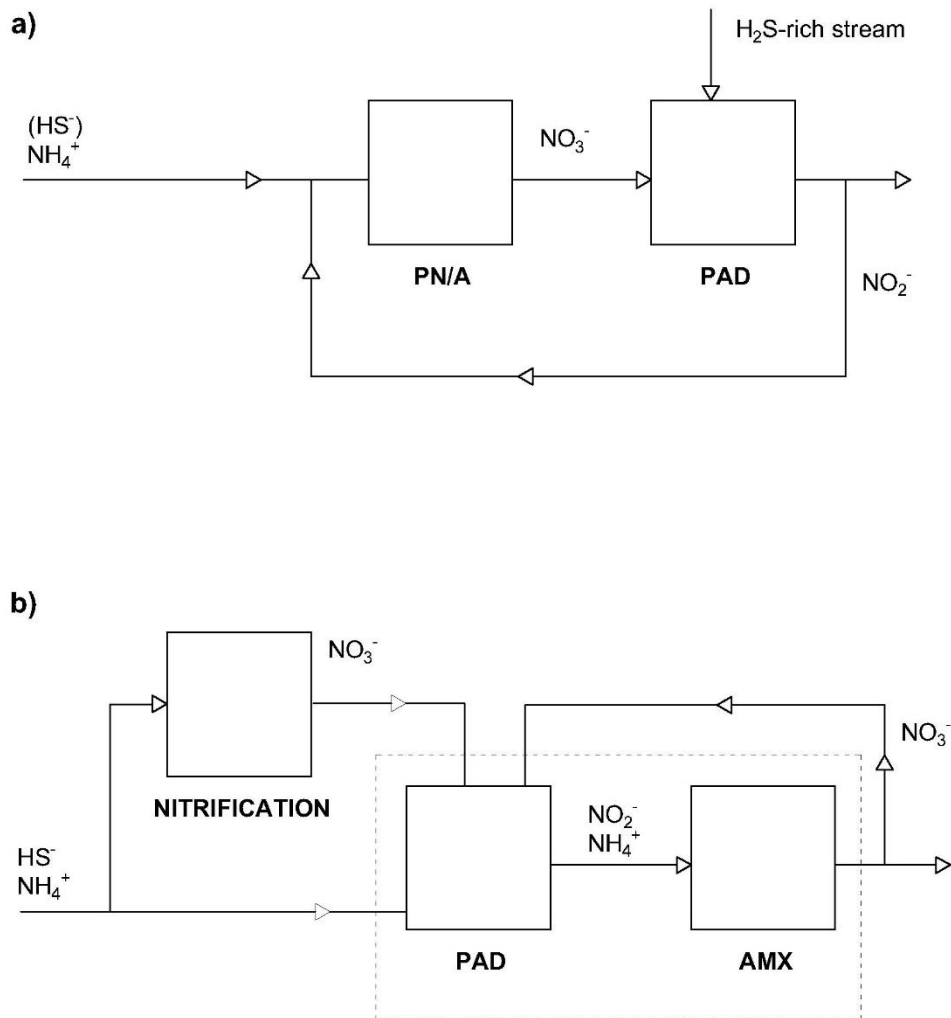


Figure 1.7 Possible treatment configuration for the integration of PAD and AMX process, exploiting PAD as post-treatment of PN/A units (a) or in a DEAMOX-like configuration (b).

In 2006, Kalyuzhnyi and colleagues published the first successful lab-scale operation of a simultaneous autotrophic denitrifying and anammox reactor, called DEAMOX (DENitrifying AMonium OXidation), patented a couple of years before by Mulder (EP 1 630 139 A1), co-author of the publication as well as of the famous work on the anammox discovery in the S-denitrifying unit in the pilot plant in Gist Brocades (Mulder et al., 1995). The DEAMOX process has been explored by this research groups (based in Delft and Moscow) and promising results were obtained, adopting either inorganic sulphide or organic matter as electron donor for denitrification, named S-DEAMOX and O-DEAMOX, respectively (Kalyuzhnyi et al., 2008; Kalyuzhnyi and Gladchenko, 2009; Trukhina et al., 2011). A schematic of the DEAMOX configuration is presented in figure 1.7b. In the present thesis the acronym PAD/A, standing for Partial Autotrophic Denitrification/Anammox, is adopted and refers to the process coupling S-driven denitrification and anammox. Other acronyms have been proposed such as SDAD-Anammox (Sulphur Driven Autotrophic Denitrification-

Anammox by Qin et al., 2019) and SADN-Anammox (Sulphur autotrophic denitrification-Anammox by Chen et al., 2018).

At the beginning of the present PhD work (2017/2018), other few studies were available on PAD or the combined PAD/A process, reporting interesting results on continuous reactor operations (Kalyuzhnyi et al., 2006, Russ et al., 2014; Liu et al., 2017; Qian et al., 2018, among the others) or batch assays (Rios-Del Toro and Cervantes, 2016). The number of PAD/A publications have noticeably raised in the very last years (2019/2020) confirming the increasing interest of the international community on the emerging topic. In figure 1.8, a simple bibliometric analysis of the published documents is provided. The analysis has been conducted on November 2020, using the key words “Partial Denitrification” or “Deamox”.

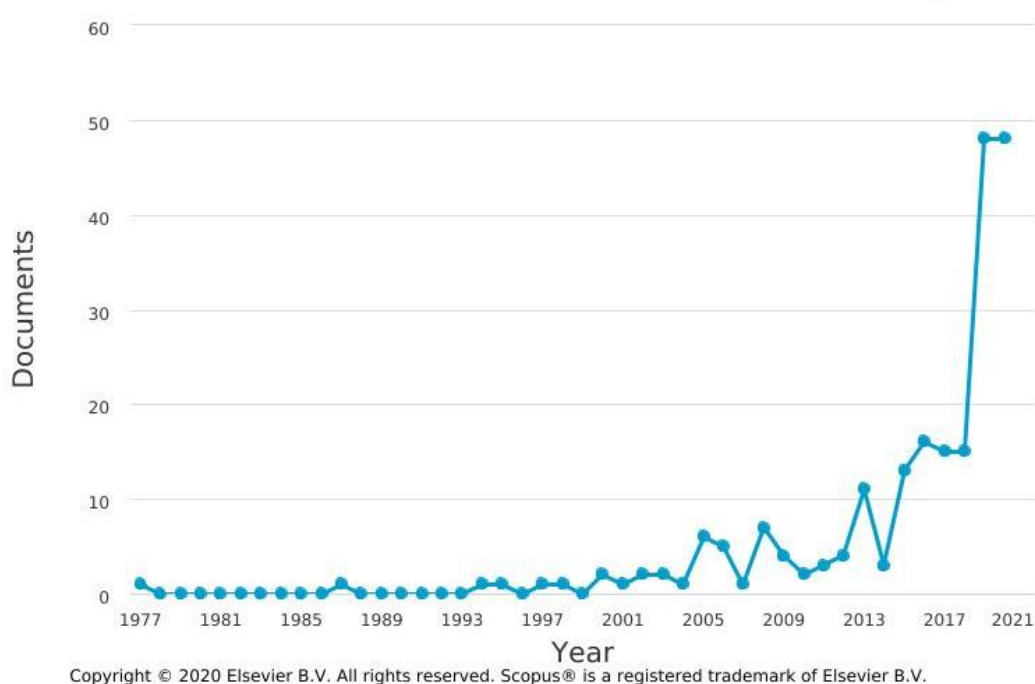


Figure 1.8 Bibliometric analysis of the available studies on “Partial Denitrification” and “Deamox”, conducted on November 2020 on Scopus Elsevier database.

As for the PN/A systems, one-stage or two-stage configurations can be conceived for PAD/A implementation. Among the mentioned studies, successful results have been presented on simultaneous (one-stage) PAD/A in lab-scale reactors, typically UASB-like. Compared to PN/A, the two biomasses involved in PAD/A (SOB and AMX) are potentially competitors for the nitrite as electron acceptor. It is clear that the key point is to maintain process conditions in such a way to favour anammox over SOB for nitrite uptake, while ensuring complete sulphide oxidation and maximum nitrate-to-nitrite conversion. Less studies have focused on the maximization of nitrite accumulation over nitrate, in the scenario of a two-stage system, whose advantages would probably be easier operation and no biomass competition, compared to the one-stage solution. On the other hand, the benefits should be considered together with possible drawbacks rising from accumulation of high nitrite levels,

namely possible biomass inhibition and release of undesired intermediates such as NO and N₂O. Another important focus should be the potential inhibition of anammox biomass by sulphide. Sulphide is acknowledged as a highly toxic compound and results from batch tests have revealed IC₅₀ concentrations as low as 0,1-5 mgS/l, in case of short-term exposure (Dapena-Mora et al., 2007; Russ et al., 2014, Jin et al., 2012; Carvajal-Arroyo et al., 2013), the entity of the inhibition being related also to the aggregated state of the biomass (i.e. free-living cells showed higher inhibition at lower sulphide levels). On the contrary, stimulatory effect on anammox activity have been observed by Van de Graaf et al. (1996) at concentration over 5 mgS/l and presence of nitrate, but it is quite accepted that it was likely related to the favourable contribution of simultaneous partial denitrification (Dapena-Mora et al., 2007; Carvajal-Arroyo et al., 2013). Toxicity is usually ascribed to the non-ionic sulphide form, the gaseous H₂S (usually limited at pH>7,5 and TDS concentrations around few ppm), able to enter the cell and irreversibly interfere with its metabolism. Russ et al. (2014) detail that, even though the exact disturbing mechanism of sulphide is not clear, sulphide is likely to reversibly interfere with cytochrome activities (fundamental units in anammox metabolism) and that the high abundance of cytochrome proteins in anammox help in restoring cellular functionality. In case of a two-step configuration, the risk of anammox inhibition by sulphide would be avoided by its full oxidation in a preliminary denitrifying unit, whereas an effective control strategy would be required in order to prevent high-sulphide exposure in a one-stage system.

The literature studies on the combined PAD and Anammox process, also differ for the electron donor used in S-driven denitrification (sulphide, thiosulfate and elemental sulphur) as well as for the targeted end-product of its oxidation (elemental sulphur or sulfate).

Some operational parameters are recognized to be crucial for successful PAD or PAD/A, such as influent S/N ratio, HRT, pH and loading rates. Nevertheless, some results lead to contradictory conclusions and many evidences and underlying mechanisms still need to be clarified. For instance, slightly alkaline pH has been observed to discourage denitrification coupled with S⁰-uptakes (Chen et al., 2018; Qian et al., 2018) whereas almost an opposite evidence is presented in Yan et al. (2020). S-limiting conditions, i.e. low influent S/N values, has proved effective for PAD achievement in Deng et al. (2019), but it showed not necessary in other successful operations (Chen et al., 2018). Moreover, almost no attention has been paid on the SRT effect on the nitrite accumulation efficiency and the relevance acknowledged to the HRT is questionable since it is often linked to loading rate variations, possibly the actual responsible of the observed impacts rather than the HRT itself.

In chapter 5 and 6 of the present thesis, the work on PAD is presented. PAD instead of simultaneous PAD/A has been selected as a study target in order to gain insight on the operational strategies and underlying mechanism leading to stable nitrite accumulation, even though results are deemed useful also in the perspective of simultaneous PAD/A.

1.4 Objective of the thesis

The main objective of the present thesis was to gain insight in the novel process combining partial autotrophic denitrification in synergy with the anammox process for the treatment of high strength wastewaters. Specifically, the novel integration of innovative biological treatments for N and S removal is proposed as an alternative solution towards newly conceived WRRFs for the treatment of industrial wastewaters. In order to accomplish with such a general objective, two parallel lines of work have been developed in order to address specific issues related to the two innovative processes.

Tannery wastewater was selected as targeted stream for possible PAD/A implementation. The application of advanced technologies, especially in industrial wastewaters, often requires case-specific studies due to potentially inhibitory substances that might hamper long-term performance of biological systems. Thereby, one line of the research aimed at assessing the feasibility of the anammox process to the vegetable tannery wastewater. A granular anammox gas-lift reactor was operated with the aim of assessing the long-term performance and stability of the granular systems whereas the potential inhibitory effect of the industrial matrix was assessed through batch test experiments. The second research line focussed on the achievement of stable nitrite accumulation over nitrate reduction and sulphide oxidation, i.e. stable PAD. A CSTR reactor was operated with the aim of studying the S/N and SRT effect on the process performance, challenging to untangle the underlying mechanisms promoting stable denitrification while completely preventing the subsequent step of denitrification. Due to complexity of the Sulphur Oxidizing and Nitrate Reducing (SO-NR) process, the work was also intended to offer a critical discussion on some open or not fully addressed issues found in literature, such as the role of SRT, the competition among nitrite and nitrate as electron acceptors and sulphur oxidizing biomass yields. In order to complete the analysis, experimental data were integrated with a thermodynamic-based study.

1.5 Thesis outline

Chapter 1 offers a general introduction to the environmental issues related to the contaminants of interest of the present thesis, i.e. Nitrogen and Sulphur. A wide picture on the N and S cycles, the related biochemical processes, as well as the human impact on the natural equilibrium, is presented. Particular attention is devoted to the microbial diversity and metabolic pathways of the microbial population of interest.

In Chapter 2, the general material and methods adopted in the experimental work are reported. Information on continuous reactors' operation, batch activity tests and analytical methods are detailed.

Chapter 3 presents an extensive work on the long-term operation (ca 270 days) of an anammox granular gas-lift reactor. The operational conditions and process performance are presented together with a broad study on the mineral formation faced after ca 130 days of operation. The comprehensive study provides useful insights in the mineral formation morphology and composition; the gathered knowledge can be directly transferred to facilitate real-scale granular sludge implementation when treating wastewaters prone to precipitation.

In Chapter 4, two inhibitory experiments on anammox granular biomass were conducted in order to assess potential drawbacks due to the exposure of vegetable tannery wastewaters. Specifically, the possible adverse effect of high salinity and bio-recalcitrant organic content, typical of the industrial stream, were addressed either in their combined or separate effect.

Chapter 5 presents the promising results obtained from a Sulphide Oxidizing-Nitrate Reducing chemostat, successfully operated in order to achieve high and stable nitrite accumulation over nitrate reduction and sulphide oxidation. The effects of influent S/N ratio and SRT on the process performance were studied. Beside an accurate monitoring of the continuous reactor, respirometric tests were conducted in order to study the biomass activity under different electron acceptor conditions; moreover, molecular biology techniques were used to profile the microbial community over the different experimental phases.

The evidence on the experimental work on PAD, i.e. catabolic change from full denitrification to partial denitrification and the clear population shift, inspired the study presented in Chapter 6, where a thermodynamic-based analysis was conducted in order to better characterise the process of PAD. Moreover, catabolic and full-metabolic stoichiometry of all the intermediate reactions occurring in the complex SO-NR process were solved and critically discussed.



CHAPTER 2.

General materials and methods

2.1 Continuous reactors

2.1.1 Anammox gas-lift reactor

A 7-liter jacketed gas-lift reactor was used for the continuous experiment with anammox biomass. The reactor comprised three main parts: mixed reactive zone (6,5 l), three-phase separator (0,5 l), comprising the settling zone for the solid separation and the gas collector, and headspace. Internal gas recirculation was accomplished by a micro diaphragm pump (NMP 830 KTDCB 12, KNF) providing a flowrate of around 1 l/min. Influent was provided by a peristaltic pump (502S, Watson-Marlow). Inlet port was placed at the bottom side-part of the reactor column, while the overflow exited through an open side at the upper part of the settling zone. Process gas, extracted from the gas collector, was continuously recirculated in order to allow internal mixing in the reactive zone through convective motion. More details on reactor dimensions are available in previous studies (D’Aniello, 2010), where also results from checks on the optimal recirculation efficiency with nonreactive compounds are presented. A detailed description of the experimental set-up and results on reactor operation are presented in Chapter 3.

General composition of the synthetic medium is reported in tables 2.1 to 2.3 according to Van de Graaf et al. (1996).



Figure 2.1 Pictures of the anammox gas-lift reactor and experimental set-up.

Table 2.1 Synthetic medium composition in the anammox reactor.

Compound	Concentration g/l
NaHCO ₃	1
KH ₂ PO ₄	0,025
MgSO ₄ · 7H ₂ O	0,1
CaCl ₂ · 2H ₂ O	0,15
Solution A (ml/l)	1,25
Solution B (ml/l)	1,25

Table 2.2 Composition of solution A.

Compound	Concentration g/l
EDTA	1
FeSO ₄ · 7H ₂ O	9,14

Table 2.3 Composition of solution B.

Compound	Concentration g/l
EDTA	15
ZnSO ₄ · 7H ₂ O	0,43
CoCl ₂ · 6H ₂ O	0,24
MnCl ₂ · 4H ₂ O	0,99
CuSO ₄ · 5H ₂ O	0,25
Na ₂ MoO ₄ · 2H ₂ O	0,22
NiCl ₂ · 6H ₂ O	0,19
NaSeO ₄ · 10H ₂ O	0,21
H ₃ BO ₃	0,014

2.1.2 SOB CSTR reactor

A 2,5-liter CSTR reactor (reactor R1) was used for the experimental work in Chapter 5 for the experimental work on the Sulphur Oxidizing Biomass (SOB). The reactor was covered with a steel lid, equipped with inlet/outlet and sensor ports and a mechanical stirrer and it was operated as an ideal chemostat. Continuous influent flow was ensured by a continuously operated pump (Gylson Minipuls 3), dosing the sulphide concentrated solution and the mineral medium on two different channels. Sulphide solutions were prepared with $\text{Na}_2\text{S}\cdot 9\text{H}_2\text{O}$ salt, whereas synthetic medium was prepared as a modified ATCC 1255 medium, according to Mora et al. (2014a). Mineral medium composition is reported in tables 2.4. Outflow was regulated by a temporized peristaltic pump (Masterflex L/S Easy-Load II), in such a way that volume variations within the reactor never exceeded 1%. Temperature was maintained at $30\pm 1^\circ\text{C}$ by recirculating tempered distilled water on the bottom the reactor. pH was controlled through the automatic addition of concentrated acid and base solutions. Temperature and pH monitoring was ensured by a Crison 5333 probe. Automatic controls and data acquisition were controlled through the software AdD (Advanced Digital control), developed within the UAB-Genocov group.

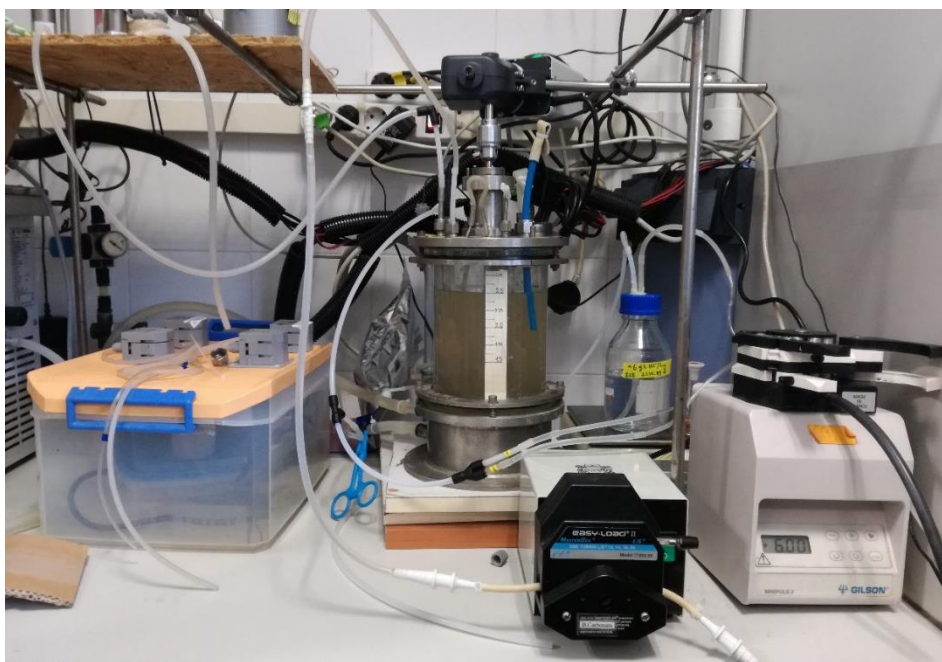


Figure 2.2 SOB CSTR reactor and experimental set-up.

Table 2.4 Synthetic medium composition of the CSTR reactor.

Compound	ATCC 1255	ATCC 1255
	(g/l)	modified (g/l)
NH ₄ Cl	1	0,2
KH ₂ PO ₄	2	0,2
MgSO ₄ *7H ₂ O	0,8	0,8
MgSO ₄	0	0,39
CaCl ₂ *2H ₂ O	0	0,075
NaHCO ₃	1	1
FeSO ₄ *7H ₂ O	0,002	0,002
KNO ₃	2	1,44
Na ₂ S ₂ O ₃ *5H ₂ O	5	0
Trace Element Solution SL-4 (ml/l)	2	2

Table 2.5 Trace element solution SL-4.

Compound	Concentration (g/l)
EDTA	0,5
FeSO ₄ *7H ₂ O	0,2
Trace Elements Solution SL-6 (ml/l)	100

Table 2.6 Trace Element solution SL-6.

Compound (g/l)	Concentration (g/l)
ZnSO ₄ *7H ₂ O	0,1
MnCl ₂ *4H ₂ O	0,3
H ₃ BO ₃	0,3
CoCl ₂ *6H ₂ O	0,2
CuCl ₂ *2H ₂ O	0,01
NiCl ₂ *6H ₂ O	0,02
Na ₂ MoO ₄ *2H ₂ O	0,03

2.2 Activity tests

2.2.1 Manometric test – AMX activity

Manometric tests are used to assess biomass activity in processes involving the production of gaseous compounds with a very low solubility, i.e. nitrogen production in denitrification and anammox processes or methane production in anaerobic digestion. In case of concomitant production of CO₂ (heterotrophic denitrification and anaerobic digestion), CO₂ NaOH-based trapper can be inserted in the system headspace in order to absorb CO₂ and limit pressure interference. In the present thesis, manometric tests were conducted on granular anammox biomass to assess specific anammox activity (SAA). The commercial OxiTop system (WTW, Germany) was adopted. OxiTop system comprises tempered glass bottles with two sampling ports, manometric heads and remote controller. The procedure was implemented according to van Loosdrecht et al. (2016), widely applied by Dapena-Mora (2007), Scaglione et al. (2009), Lotti et al. (2012). Manometric bottles with a total volume of 1 litre and 350 ml were used. If not specified otherwise, granular biomass was re-suspended in nutrient-free synthetic medium (van de Graaf, 1996) or real wastewater, depending on the experimental activity. When a rough estimation of the SAA was available from preliminary analysis, the amount of biomass in each bottle was set as such to provide a full nutrient consumption profile in a time laps of 4 to 12 hour, so that overnight experiments were easily conducted, if needed. In general, biomass concentration ranged between 0,7 and 2 gVSS/l. The exact amount of solid was estimated either at the end (more frequently) or beginning of each test. Analysis of VSS at the end of the manometric test were conducted by filtering and incinerating the entire amount of biomass present in each bottle (0,45µ glass-fibre filters were used). When solids were analysed at the beginning of the manometric test, an aliquot of wet granular biomass was used for VS analysis and, concomitantly, an aliquot of wet biomass (at the same moisture level than the one used to characterize VS content) was weighted. Solid amount in each bottle test was thereby calculated as the product of the wet weight and the specific VS content (expressed as gVS/g_{ww}¹⁰). VS and VSS analysis were performed according to standard methods (APHA, 2005). Once biomass was re-suspended in the liquid medium, bottles were equipped with the manometric heads and closed air-tightly. A mixture of N₂/CO₂ (95% and 5%, respectively) was sparged in the headspace for 5 to 10 minutes, in order to create anoxic conditions. Bottles were then placed in a pre-heated incubator at 30°C. Continuous mixing was provided by an orbital shaker set at 150-180 rpm. After 30 minutes, the headspace pressure was re-equilibrated to atmospheric pressure, in order to avoid overpressure errors due to air expansion and water vapour production. After that, the manometric test was started and pressure recorded through the pressure logger. Concentrated pulses of

¹⁰ gVS content per gram of wet weight.

ammonia and nitrite were provided by 1 M solutions of $(\text{NH}_4)_2\text{SO}_4$ or NH_4HCO_3 and 1 M NaNO_2 , respectively. Concentrated solutions were dosed by mean of 1-3 ml disposable syringes. Liquid samples were withdrawn right after or right before the pulse injection. Samples were filtered through 0,45 disposable syringe filters and analysed for nitrogen compounds (ammonia, nitrite and nitrate), according to section 2.3. Since manometric tests allow for dinitrogen production estimation through pressure measurements, the exact estimation of actual headspace volume is of prominent importance. Injected and withdrawn volumes were meticulously registered in order to calculate the exact liquid and headspace volumes at each spike and, therefore, minimize related errors.

The OxiTop remote controller allows for continuous overpressure monitoring. A typical overpressure profile following a nutrient pulse is presented in figure 2.3. As it can be observed, after the nutrient injection, pressure grows exponentially until it slows down and levels off to a constant value, reaching a plateau. Preliminary tests showed that reliable and clear pressure profile were obtained when N_2 production was as high as to produce a minimum pressure increase of 30 hPa, at 30°C (data not shown). Thereby, nutrient concentrations were always set in order to achieve such a minimum threshold in the expected N_2 production.

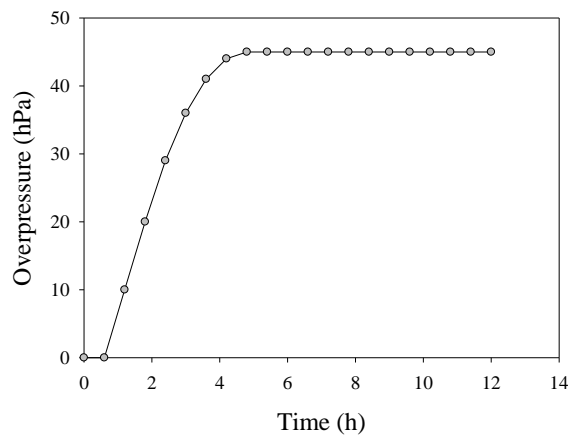


Figure 2.3 Typical overpressure profile following nutrient pulse (data from Inhibition test 2, Chapter 4)

The maximum slope observed in the exponential phase is calculated by linear regression. Overpressure gap as well as maximum overpressure rate can be transformed in N_2 production and maximum N_2 production rate, through the ideal gas law, according to the following equation (Van Loosdrecht et al., 2016):

$$n_{\text{N}_2} = \frac{\Delta P \cdot V_{hs}}{RT}$$

Where n_{N_2} are the moles of N_2 , $\Delta P(t)$ is the overpressure, R is the universal constant ($0,082057 \text{ L atm K}^{-1} \text{ mol}^{-1}$) and T is the temperature (K). Maximum N_2 production rate normalised to the total VSS content in the bottles result in the specific anammox activity, SAA, expressed as $\text{gN}_2/\text{gVSS}/\text{d}$. In the present work, all the activity tests and the anammox continuous reactor were conducted in nitrite-limiting conditions. As a consequence, it

was decided to express all the SAA values as $\text{gN-NO}_2^-/\text{gVSS}/\text{d}$, in order to ease value comparison throughout the chapters.

In order to confirm test reliability, nitrogen mass balance was performed during the first manometric tests as well as randomly in the following ones. N_2 production estimated through overpressure measurements was compared with N_2 production estimated through nitrite and ammonia removal from the liquid phase. Initial concentration of NO_2^- and NH_4^+ were either estimated by knowing the exact concentration of the concentrated solutions used and the volume dosed or measured by sampling the liquid phase right after the pulse. The former method was used in the first inhibition test (Chapter 4). The latter method was considered more precise and was used in the second inhibition test and in the activity tests performed during the gas-lift operation (Chapter 3 and Chapter 4). Nitrogen balance errors below 15% were deemed satisfactory considering error propagation in sampling procedure, analytical measurement and pressure transducer.

2.2.2 In-situ batch test – AMX activity

In-situ batch tests were only conducted during the operation of the anammox gas-lift reactor, typically during the events of significant nitrite accumulation ($> 80 \text{ mgN-NO}_2^-/\text{l}$), provided that also the ammonia concentration was not limiting. In order to perform the test, the reactor was operated in batch mode, by stopping the influent flow and monitoring nutrient concentration. Samples were withdrawn from the mixed zone of the reactor at regular interval with the aim of assessing the nutrient uptake rates ($\text{mgN}/\text{l}/\text{h}$), calculated by linear regression of nutrient concentration profiles. A typical nutrient profile during in-situ batch test is presented in figure 2.4.

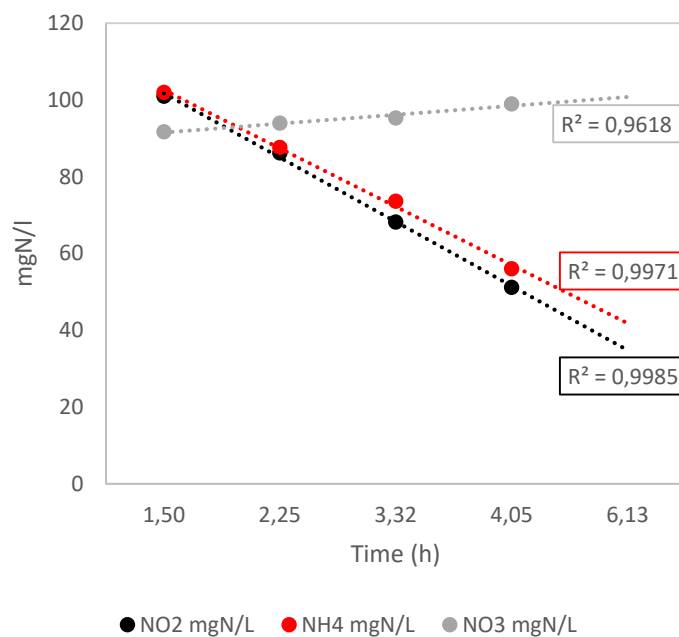


Figure 2.4 Typical nutrient profile during in-situ batch tests for anammox biomass activity assessment.

2.2.3 Respirometric and titrimetric test – SOB activity

Respirometric tests were conducted in a 350 ml glass vessel, sealed with a steel lid equipped with sensor and sampling ports. The vessel was placed in a thermostatic bath ensuring constant temperature of 30 ± 0.5 °C. DO, pH and temperature were measured by WTW sensors (CellOx 235 and SenTix 81) connected to a WTW InoLab multimeter. The software used in this study for pH and DO control and data acquisition was the same used in former works (Mora et al., 2014a). Thanks to continuous pH control and data acquisition, titrimetric data were also available. In figure 2.5, a schematic of the respirometric set-up is presented. Acid solution (1M HCl) and base solution (1M NaOH) dosing was provided through Multi-Burette 2S-D (Crisson Instruments).

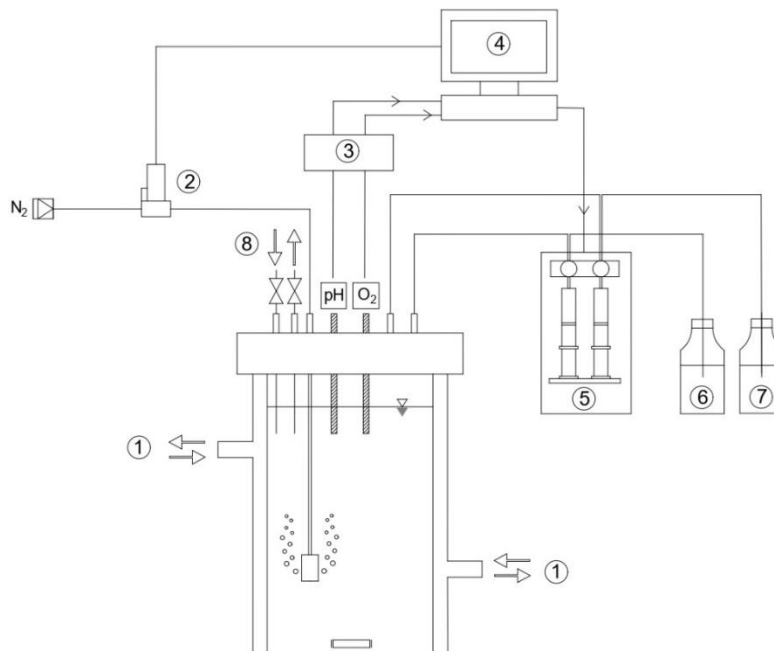


Figure 2.5 Respirometer set-up.. Legend: to the thermostatic water bath (1); mass flow meter (2); multimeter (3); PLC (4) automatic dispensing burette (5); HCl solution (6); NAOH solution (7); sampling and spike points (8); from Falcioni, 2020.

2.3 Analytical methods

In Chapter 3 and 4, the following methods were applied for off-line measurements¹¹:

- N-NH_4^+ , N-NO_2^- , N-NO_3^- and COD were analysed spectrophotometrically, through commercial kits (Hach Lange, Germany). For nitrate analysis, few μg of sulfamic acid were added in order to avoid nitrite interference. For COD analysis, results were corrected in order to account for the contribution of nitrite and sulphide, when present.
- Chloride and sulfate ion were measured through Ionic Chromatography, IC (Dionex ICS-1100, ThermoScientific). Prior to the analysis, samples were filtered with $0,45\mu$ disposable syringe filters (MiniSart, Sartorius) and diluted, if necessary.
- Total Phosphorous and metals concentrations were analysed through Inductively Coupled Plasma Optical Emission Spectrometry ICP-OES (Optima 2100 DV ICP-OES, PerkinElmer), after sample digestion with nitric acid.
- pH was analysed through bench pH-meter (Hanna instrument, Series Edge, sensor HN/010430) and conductivity (at 25°C) through the portable electrical conductivity meter CM 35 (Crison instrument), equipped with a temperature sensor (Pt 1000). Both instruments were regularly calibrated.
- VSS, TSS, VS and TS were measured according to standard measurements (APHA, 2005)

In chapter 5, the following methods were applied for off-line measurement¹²:

- Anions of N-NO_2^- , N-NO_3^- , $\text{S-S}_2\text{O}_3^-$ were analysed through ionic chromatography (Dionex ICS-2000, ThermoScientific). Prior to the analysis, samples were filtered at $0,22\ \mu\text{m}$ through disposable syringe filter and diluted with unionised water, if necessary.
- Ammonia and COD were analysed spectrophotometrically, through commercial kits (Dr. Hach Lange, Germany).
- TOC was analysed through Multi N/C analyser (2100s, Analytik Jena AG).
- Sulphide was analysed through Silver/Sulphide ion selective electrode method. Sample preparation required the use of a sulphide antioxidant buffer (SAOB), rising the sample pH over 12 and thereby shifting the total dissolved sulphide (TDS) in the form of S^{2-} . Fresh SAOB solutions were prepared every 10-14 days and calibration curves repeated every week. Sulphide concentrated solutions ($>5\ \text{gS/l}$) were used as standard solutions for calibration. Before their use, sulphide concentrated solutions were characterized in order to define their exact concentration through titration with Pb^{2+} commercial solutions (1 M).

¹¹ If not specified otherwise, all the analyses were conducted in the Cer2co laboratory and the laboratory operating at Cuoiolepur wastewater treatment plant (Pisa, Italy).

¹² If not specified otherwise, all the analyses were conducted at the UAB-Genocov laboratories

- VSS and TSS analyses were conducted according to standard methods (APHA, 2005). As discussed in chapter 5, two main types of 0,7- μm glass-fibre filters were used: Millipore AP4004705 and the and highly retaining filter Millipore APFF04700. Filters were ignited at 550°C, prior to their use.

2.4 Molecular analysis

In chapter 4 and 5, fresh samples of anammox biomass were delivered to the Biology department of the University of Florence for DNA extraction and PCR amplification of the V3 and V4 variable regions of the 16s rRNA gene. Primers couple from Takahshi et al., (2014) were used, with a slightly modified forward primer, optimised for anammox bacteria (Mazzoli et al., 2020). Amplicons were then sent to BMR Genomics (Padova, Italy) and high throughput sequencing was performed through Illumina MiSeq, achieving 2x300 bp sequencing. Bioinformatics elaboration was performed with the MICCA software. Briefly, reads were merged with a minimum overlapping length of 100 bp; primers and bad-quality reads were trimmed away; Paired-End (PE) reads with less than 350 bp or with quality rate lower than 0,5 as well as chimeras were removed. After data filtering, OTU classification was based on the 97% similarity criterion. Taxonomic classification until the genus level was conducted through Bayesian classification with Ribosomal Database Project (RDP). More information on the procedure and bioinformatics are available in Niccolai et al. (2020).

In chapter 5, fresh samples of sulphur oxidizing biomass were concentrated and centrifuged. Concentrated pellets were kept in Eppendorf vials, after removing the supernatant; in case DNA extraction was not performed immediately after sample collection, concentrated biomass pellets were kept at -20°C until extraction. DNA was extracted with commercial kit (Biofilm-kit, Norgen), according to the manufacturer's instructions. DNA quality and concentration were checked by analyses on NanoDrop 1000 Spectrophotometer (Thermo Fisher Scientific). Extracted DNA samples were delivered to the UAB Genomics and Bioinformatic Service. PCR amplification targeted the V3 and V4 region of 16s gene and amplicon sequencing was conducted on Illumina MiSeq according to the Illumina MiSeq protocol for library preparation (available at https://support.illumina.com/content/dam/illumina/support/documents/documentation/chemistry_documentation/16s/16s-metagenomic-library-prep-guide-15044223-b.pdf). Taxonomic classification was based on Greengenes database.

2.5 SEM and TEM analysis and sample preparation

SEM and TEM analysis were performed on anammox granular sludge. SEM-EDX analyses were conducted at the UAB-Microscopy Service (Spain). Samples were fixed with 2,5% glutaraldehyde and 0,1 M BPS overnight. Repeated rinse with the same BPS were performed prior to dehydration at increasing ethanol

concentrations (50%, 70%, 90%, 96% and 100%) and, finally, at hexamethyldisilazane (HMDS). Dried samples were coated with Gold and Platinum, prior to their analysis. TEM analysis were conducted at the Biology department of the University of Pisa (Italy). For sample preparation, a glutaraldehyde-based fixation was conducted according to the procedure presented in Lin et al. (2017). Basically, samples were let overnight at 4°C in glutaraldehyde (3%); then they were repeated rinsed with BPS and fixed in osmic acid (1%) for around 3 h. Eventual dehydration was achieved through exposure to ethanol solutions at increasing concentrations (50%, 60%, 70%). Transversal granules' sections of 70-90 nm were obtained through PowerTomeXL ultramicrotome.

CHAPTER 3.

Coping with mineral precipitation during the start-up of an anammox gas-lift reactor

3.1 Introduction

Behind the astonishing impact on the research field, AMX-based full-scale installations have been successfully implemented in Europe, USA and China (Lackner et al., 2014; Nsenga et al., 2020). When granular sludge technology is applied for autotrophic processes such as AMX and PN/A, the advantages are multiple: (i) effective retention of the slow-growing biomass, with the ultimate result of high specific reactor removal capacity; (ii) superior sludge settleability properties; (iii) synergy optimization between microbial consortium, due to optimal substrate and redox gradients within the granule. Still, among the obstacles hindering the widespread implementation of the PN/A process there is the long start-up time required by the slow-growing biomass (Ali et al., 2014). Active sludge seeding is a successful solution to achieve rapid start-up or reactor rescue in case of unexpected failures and long-term biomass storage is a key issue to ensure biomass availability when needed. Thereby, effective storage strategies for keeping an active seed sludge are crucial.

In this chapter, the start-up of a gas-lift reactor is presented. The reactor was inoculated with anammox biomass restored after more than one-year storage and remarkable specific anammox activities (SAA) and Nitrogen Loading Rate (NLR) were achieved rapidly. The experimental work was originally planned in such a way to reach stable NLR of 1 gN/l/d (N as ammonia and nitrite) with synthetic wastewater and then switch to real tannery wastewater in order to assess long-term performance of the process. Process deterioration was faced due to unexpected mineral precipitation mainly affecting the granule surface. Substrate diffusion limitation from the bulk to the inner layers, insufficient mixing due to higher granule density and shear stress increase due to hard-particle collision were acknowledged as the main mechanisms that lead to progressive process disruption. A successful rescue strategy was implemented, and process restoration was achieved after that. Throughout the experimental work, anammox process was monitored in detail in terms of nitrogen removal rate, solid concentration, biomass activity, microbial community and granular sludge size and morphology. An extensive study on the mineral precipitation is also presented as a warning in case of anammox process implementation in wastewaters prone to mineral precipitate formations.

3.1.1 Mineral precipitation in granular sludge systems

Mineral precipitation has been reported to occur in granular biomass systems, either in anaerobic, PN/A and AMX and aerobic granular sludge (AGS), in lab-scale as real-scale applications. Precipitate composition strongly depends on influent composition and operational/process conditions (such as pH and process effect on pH). Yet two types of minerals are mainly reported: carbonated minerals and PO₄-bonded minerals.

In granular systems applied in anaerobic digestion (AD) treating Ca and Mg rich streams, Ca-Mg carbonate minerals are very likely to occur, since the process results in carbonate-related alkalinity increase (CO₂ is a

final product), favouring carbonates precipitation (van Langerak et al., 2000; Batstone et al., 2002). PO₄-bonded mineral precipitation also occur in such AD sludge, though it is strongly affected by the proportion of Ca²⁺, Mg²⁺, CO₃²⁻ and PO₄³⁻, since high carbonate alkalinity negatively affects precipitation of PO₄-minerals competing for Ca or Mg, such in struvite (MgNH₄PO₄·6H₂O) or Calcium-phosphate (Ca-P) minerals (Haroon-Hakimi et al., 2019, Chen et al., 2020).

Ca-P minerals have been mainly reported in PN/A or AMX granular sludge, ranging from amorphous forms to crystalline apatite (mainly as hydroxyapatite, HAP, or its precursors, being the more stable form at neutral pH), in accordance to the fact that PN/A processes have been vastly implemented in side stream treatment of digestate where phosphorus concentrations ranges 20-300 mgP/l (Lin et al., 2013; Ma et al., 2020).

From the one hand, mineral precipitation allows for better settleability, higher density and improved mechanical strength properties of granules, avoiding biomass washout and increasing granules' structure strength. From the other hand, excessive mineralization would be detrimental due to possible substrate diffusion limitation and, ultimately, to granule or granular bed mineralization (Chen et al., 2010; Lin et al., 2013, van Langerak 2000). Recently, enhanced Ca-P mineral precipitations in granular biomass has received growing attention as a valuable alternative for simultaneous N removal and P recovery in anammox granular sludge, e.g. the coupled anammox-HAP crystallization granules (Lin et al., 2019; Johansson et al., 2017; Ma et al., 2020; Xue et al., 2020), in AGS (Mañas et al., 2011; Pishgar et al., 2020) and in AD sludge (Tervahauta et al., 2014; Cunha et al., 2019), the latter case limited to P recovery.

3.2 Materials and methods

3.2.1 Gas-lift reactor

A 7-liter reactor was run for more than 270 days. Figure 3.1 shows a schematic of the reactor; more details are presented in section 2.1. In order to avoid undesired inlet of air from the outside, reactor headspace was maintained at a slight overpressure of 0,05 bar, visually checked by a pressure-control water lock. A mixture of N₂ and CO₂ (95% and 5%, respectively) was provided manually every day (except during weekends), at a flowrate of 0,1 l/min for 20 minutes, in order to reintegrate internal recirculation gas as well as to ensure CO₂ availability to the system. A U-shape tube was placed prior to the effluent collection tank and acted as a further settling unit; apart from exceptional events, outflow collected in the effluent tanks was, in fact, free from granules and solids. A black coat was placed on the reactor to protect it from light. Temperature, pH and ORP were monitored by two probes (5336T Hach Lange for pH and T and 5361 Hach Lange for ORP). No control of pH was performed. Temperature was maintained at 30±1 °C, by mean of continuous tempered water recirculation in reactor's jacket. HRT was maintained at 1,1 d for the first 40 days, and then increased to 1,6 d

from day 41 on. The experimental set-up and the consequent laboratory activities were carried out in the laboratory facilities of the tannery WWTP (Consorzio Cuoioedepur S.p.a, Pisa, Italy).

A synthetic influent (Van de Graaf et al., 1996) was prepared regularly and nutrient concentrations, in terms of nitrite and ammonia, were set according to the experimental phases and added as NaNO_2 and NH_4HCO_3 ($(\text{NH}_4)_2\text{SO}_4$ was used in phase 4, instead). Distilled water was used for the preparation of the mineral medium, except for the period from day 55 to 135, during which tap water was used instead (well water used in Cuoioedepur WWTP for process operations), due to technical problems to the reverse osmosis unit. Influent characterization was performed every time a new mineral medium was prepared and intermediates checks were performed, if deemed necessary. Monitoring of reactor performance was conducted by withdrawing samples from the mixed zone, by mean of a sampling tube located at middle height of the reactor column. Concentrations of ammonia, nitrite and nitrate as well as pH and conductivity were monitored almost daily. Monitoring and mass balances were done over the volume of the mixed zone and the reactor was assumed to be an ideal CSTR.

Total and volatile suspended solids (TSS and VSS) were characterized every other week to follow reactor biomass concentration, by withdrawing a sample from the mixed zone. Also, concomitant TSS and VSS characterization of solids retained in the U-shaped effluent tube was performed in order to assess biomass washout extent. Solids retained in the U-tube were removed from the system, apart from specific cases of intense granule flotation, during which granules were re-introduced in the system as detailed in the following paragraphs. No other active SRT control was performed, apart from solid washout monitoring (SRT was estimated around 200-300 days).

The reactor was inoculated with 500 ml of settled granular biomass from the CANON plant in Olburgen WWTP, the Netherlands (Abma et al., 2010). Initial VSS concentration in the reactor was about 2.5 gVSS/l. Prior to seeding, the inoculum biomass was kept at 4°C for almost one year, ensuring a minimum supernatant concentration of 100 mgN- NO_3^- /l, with regular check on pH and conductivity. Almost 10-20% of the supernatant was replaced with freshwater or mineral medium on average once a month or when deemed necessary.

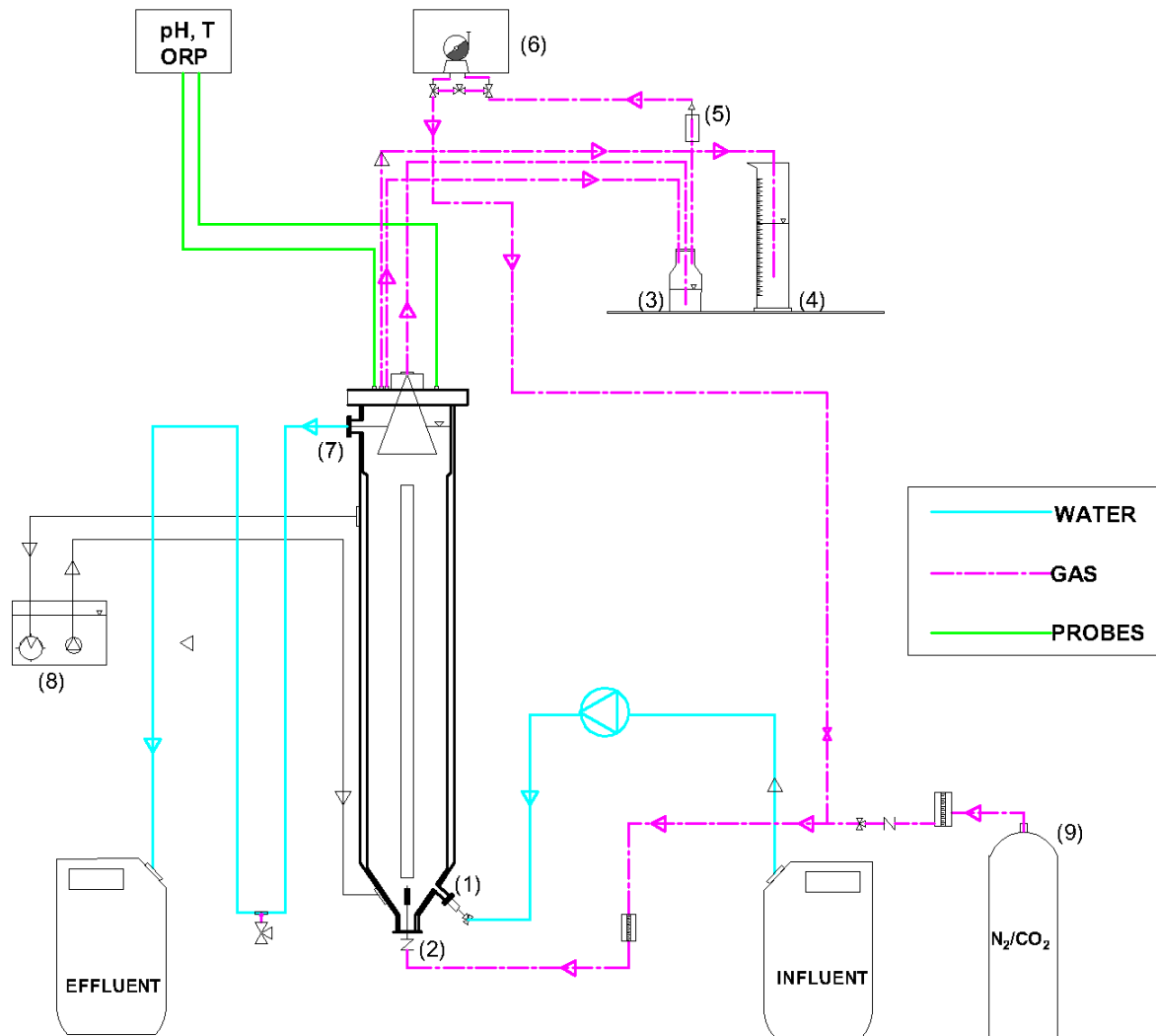


Figure 3.1 Experimental set-up. Water line (cyan), gas line (dotted pink) and sensors (green). Influent port (1); gas recirculation inlet (2); disconnection (3); water-lock and overpressure control (4); condensate trap (5); vacuum pump (6); outlet port and U-shape outlet tube (7); thermostatic unit (8); N_2 - CO_2 mixture cylinder (9).

3.2.2 Experimental phases

Four experimental phases are presented and described in table 3.1. Throughout the experiment, influent ammonia/nitrite ratio was maintained at least at the stoichiometric value, more frequently slightly above, operating under nitrite-limiting conditions. Phase 1 (P1, days 1-15) aimed at biomass reactivation and reactor start-up; ammonia and nitrite inlet concentration were 100 to 200 mgN- NH_4^+ /l and 45 to 200 mgN- NO_2^- /l, respectively, with a weekly-base stepwise increase of 50 mgN/l for the nitrite. As a general rule, influent concentration increase was applied when effluent nitrite concentration showed a decreasing trend for at least three consecutive days or when it kept stably below 10 mgN- NO_2^- /l. An inlet concentration of 150

mgN-NO₃⁻/l was dosed as redox buffer. Also, 10 mgCOD/l as acetate were added to restore glycogen storage that might have been consumed due to one-year starvation¹³. The aim of Phase 2 (P2, days 16-130), was to maximise the reactor removal capacity by progressively increase inlet concentration, i.e. inlet load. In a few cases, nitrite accumulation raised up to 100 mgN-NO₂⁻/l. At the occurrence of these events, the feeding was paused and the reactor was operated in batch condition until nitrite concentration decreased to less than 40 mgN-NO₂⁻/l, often performing an in-situ activity tests (see sec. 3.2). Phase 3 (P3, days 131-154), was characterized by uncontrolled process instability and deterioration. Severe increase of nitrite concentration and pH inside the reactor was observed together with a change in granules appearance. After few weeks, mineral precipitation on the granules' surface was deemed responsible for process instability. An off-site rescue procedure was implemented during days 155-177; this break in reactor operation is not reported in process performance graphs in section 3.3.1. Process stability was restored in phase 4 (P4, days 178-270) at a NLR of 0,22 gN-NO₂⁻ /l/d.

Table 3.1 Experimental phases, duration and applied conditions.

<i>Phase</i>	Days	HRT [d]	NLR [gN-NO ₂ ⁻ /l/d]
<i>P1-start up</i>	1-15	1,1±0,3	0,02-0,09
<i>P2- NLR increase</i>	15-130	1,1 to 1,6	0,09-0,50
<i>P3 – Process disruption</i>	131-154	1,6±0,2	0,50±0,05*
<i>Off-site biomass rescue</i>	155-177	-	-
<i>P4- Process restoration</i>	178-270	1,6±0,2	0,22±0,02

Process operations and performance were expressed in terms of Nitrogen Loading Rate, NLR, and Nitrogen Removal Rate, NRR, as applied and removed daily loads over the active volume of the reactor (i.e. gN/l/d) and Specific Nitrogen Loading Rate (SNLR), expressed as gN/gVSS/d. As ammonia was often intentionally dosed in excess, resulting in nitrite as the limiting substrate, NLR, NRR and SNLR were referred to the sole nitrogen-nitrite. General stoichiometry was checked by means of mass balances on the removed compounds.

3.2.3 Activity batch tests

Two types of activity batch tests were regularly performed throughout the reactor operation: in-situ batch activity tests and manometric batch activity tests (see section 2.2). In-situ batch activity tests were conducted

¹³All anammox genera are reported to have glycogen storage and evidences suggest that its function is to serve as an energy and carbon reservoir, in case of stress or starvation, and glycogenolysis and glycogenogenesis are found completely encoded in anammox genome (van Niftrik et al., 2008).

by operating the reactor in batch-mode. When nitrite accumulation was higher than 80 mgN-NO₂⁻/l or in case of an unexpected nitrite accumulation, the inlet was paused, the reactor was operated in a batch-mode and samples were collected every 45 or 120 minutes to assess the maximum removal capacity of the reactor (NRR_{max}, gN/l/d). Manometric tests were conducted in 300-ml Oxitop® bottles, allowing continuous monitoring and recording of headspace overpressure. A detailed procedure is presented in section 2.2.1. Biomass was withdrawn from the mixed zone of the reactor and re-suspended in nutrient-free mineral medium. On average, biomass concentration ranged from 0,6 to 1,2 gVSS/l. After flushing a mixture of N₂/CO₂ (95% and 5%, respectively) in the headspace, the bottles were placed in a pre-heated incubator at 30°C. Continuous mixing was provided by an orbital shaker set at 180 rpm. Concentrated pulses of 1 M (NH₄)₂SO₄ and 1M NaNO₂ solutions were spiked in order to provide 30 to 80 mgN/l, as nitrite and ammonia, in the liquid phase. A minimum input NH₄⁺/ NO₂⁻ ratio of 1 was ensured. When N₂ exponential production phase was followed by stable pressure plateau, a further pulse of concentrated solutions was provided. In each test, a minimum of two and a maximum of five consecutive spikes were provided in order to have a more robust estimation of the maximum activity. After each test, the total amount of biomass was incinerated for VSS assessment.

Manometric tests allowed to assess the maximum specific anammox activity (MSAA), expressed as gN/gVSS/d, whereas the in-situ batch tests allowed the estimation of the maximum removal capacity of the reactor (NRR_{max}, gN/l/d), according to Dapena-Mora et al. (2010). These two measurements were matched with the reactor VSS concentration in order to be straightforwardly comparable. A total of 10 activity tests were performed.

3.2.4 Analytical methods

Samples from the mixed zone were filtered at 0,45-micron syringe-filter and characterized in terms of ammonia, nitrite and nitrate, using commercial kits (section 2.3). VSS and TSS were assessed according to standard methods (APHA, 2005). The following parameters were analysed on tap water: (i) Ca²⁺, K⁺, Mg²⁺, Na⁺ by ionic chromatography (UNI EN ISO 14911:200, from an external laboratory); (ii) total alkalinity according to Italian standard regulations (method APAT CNR IRSA 2010 B, from an external laboratory) and metals and total Phosphorous by Inductively Coupled Plasma Optical Emission Spectrometry, ICP-OES. Also, qualitative assessment of total and carbonate-related alkalinity was obtained through commercial Quantofix® test strips.

3.2.5 Metabarcoding study, granular size distribution and analyses with electron microscopy

Biomass samples were collected almost every 30-45 days for Next Generation Sequencing (NGS) analyses. When possible, DNA extraction was performed on the fresh sample; otherwise, sludge samples were

concentrated by mean of high-spin centrifugation (10000 rpm), supernatant was removed and the concentrated sample stored at -20°C. Information on 16s rRNA amplicon sequencing are reported in section 2.4. Granular size analyses were performed on the inoculum and on days 50 and 260, by mean of image elaboration in order to assess granules' size distribution over time. The granules dimensions were determined in order to evaluate the average diameter and size distribution profiles. For digital image analysis the programme Image ProPlus® was used according to Tjihuis and Loosdrecht (1994). SEM-EDX and TEM analyses were performed on a dozens of granules in order to study their superficial appearance and composition as well as the internal structure; sample preparation procedures are reported in section 2.5.

3.3 Results

3.3.1 Reactor operation

Reactivation phase P1 was relatively fast as noticeable nitrite and ammonia removal was observed after the first week of operation (figure 3.2a)¹⁴. Nitrite effluent concentration stayed below 10 mgN-NO₂⁻/l, and a proportional nitrate increase was shown as well, indicating active growth of anammox bacteria (Lotti et al., 2014b). During P2, influent concentrations were step-wise increased up to 350 mgN-NO₂⁻/l and 350 mgN-NH₄⁺/l at a relatively high pace, since a 75% NLR increase was applied in less than 10 days (fig. 3.2b). On day 37, a progressive accumulation of nitrite was observed up to 80 mgN-NO₂⁻/l. On this day, the inflow was paused and an in-situ activity test performed (see section 3.2). Results showed that the applied NLR was above the maximum removal capacity of the system (0,30 vs 0,23 mgN-NO₂⁻/l/d, applied NLR vs maximum capacity, respectively). Moreover, granules flotation was observed in those days and biomass washout was likely to contribute to process instability. Consequently, NLR was decreased by decreasing the flowrate from 7 to 4 l/d. The resulting 1,6-day HRT was kept from this day on. Significant granule flotation was observed also on days 93-103, 120-128. In these periods, bulk NO₂⁻ concentration ranged 80-100 mgN/l (peak value of 130 mgN/l, on day 150). Granules flotation has been reported by many authors (Dapena-Mora, 2004; Trigo et al., 2006; Chen et al., 2014; Li et al., 2014) and authors agree in acknowledging system overloading as one of the major causes. According to the proposed floatation mechanisms and causes, there is the role of phenomena of sudden increase in substrate concentration in the bulk liquid: when the nutrient concentration in the bulk medium is high, substrates can diffuse to inner layers of the granule, usually less active than the external layers and thriving on low residual concentrations, thereby increasing their uptake rate and N₂ production, that in turn hardly diffuses out and creates gas accumulation inside the granules.

¹⁴ Trukhina et al. (2011) report reactivation periods of 126 and 73 days for S-DEAMOX sludge stored for 16 and 5 months, respectively. However, the concept of *reactivation* is not absolute. In the present work, reactivation refers to the positive response of the biomass to the applied nutrient load, i.e. no nutrients were accumulated in the effluent.

When severe granular floatation was observed, floating granules exiting the system were recollected from the U-shape effluent tube to avoid excessive biomass washout. A practical and effective procedure was applied to favour nitrogen gas release from the granules and was operated as follow: floating granules were poured into 2 to 4 litres beaker equipped with a vertical stirrer to provide controlled agitation. Ranging from gentle to strong agitation (20 to 150 rpm) an increasing centrifugal force was applied to squeeze out the entrapped gas. In case such a procedure was not effective, resistant floating granules were squeezed against the glass wall of the beaker, by exercising gentle pressure with a spoon. These procedures are similar to those reported by Chen et al. (2010) and Li et al. (2014). Floating granules were observed to be those characterized by higher diameter (see section 3.3), in agreement with other works (Dapena-Mora et al., 2004; Chen et al., 2010; Chen et al., 2014) also reporting that diffusion from the inside to the outside of the granule can be further hindered in granules with higher diameter, as in small granules gas release is favoured. It is worth mentioning that the granules used for inoculating the reactor were formed under specific hydro-dynamic conditions and wastewater characteristics and that dimensional changes and gas-pocket formation are likely to occur when this operational conditions change or when sludge seeding is used for fast reactor start-up (Xing et al., 2015; Chen et al., 2014). From day 35 to 70 stable operation was maintained to promote granule re-adaptation and process stability. After this period, nitrite removal efficiency was constantly higher than 95% (fig. 3.2b) while the biomass appeared with a bright carmine colour (fig. 3.4a), smaller in size and with a more uniform granular dimension (see section 3.3). NLR increase strategy was started again on day 71, targeting a final NLR of 1 gN/l/d (N as sum of nitrite and ammonia).

Since day 90 to day 120, a slight but progressive process disruption was observed together with an unexpected increase in pH and decrease in VSS/TSS ratio. Regular episodes of nitrite (and ammonia) accumulation occurred and resulted in concentrations up to 80 and 102 mgN-NO₂⁻/l on day 103 and 117, respectively (fig. 3.2a). In those cases, influent was stopped for a few hours and nitrite removal rate was assessed prior to resumption. As a contingency measure, influent nitrite concentration was temporary reduced by almost 100 mgN/l and then increased again to restore the applied NLR. Nevertheless, nitrite accumulation showed chronic after day 130.

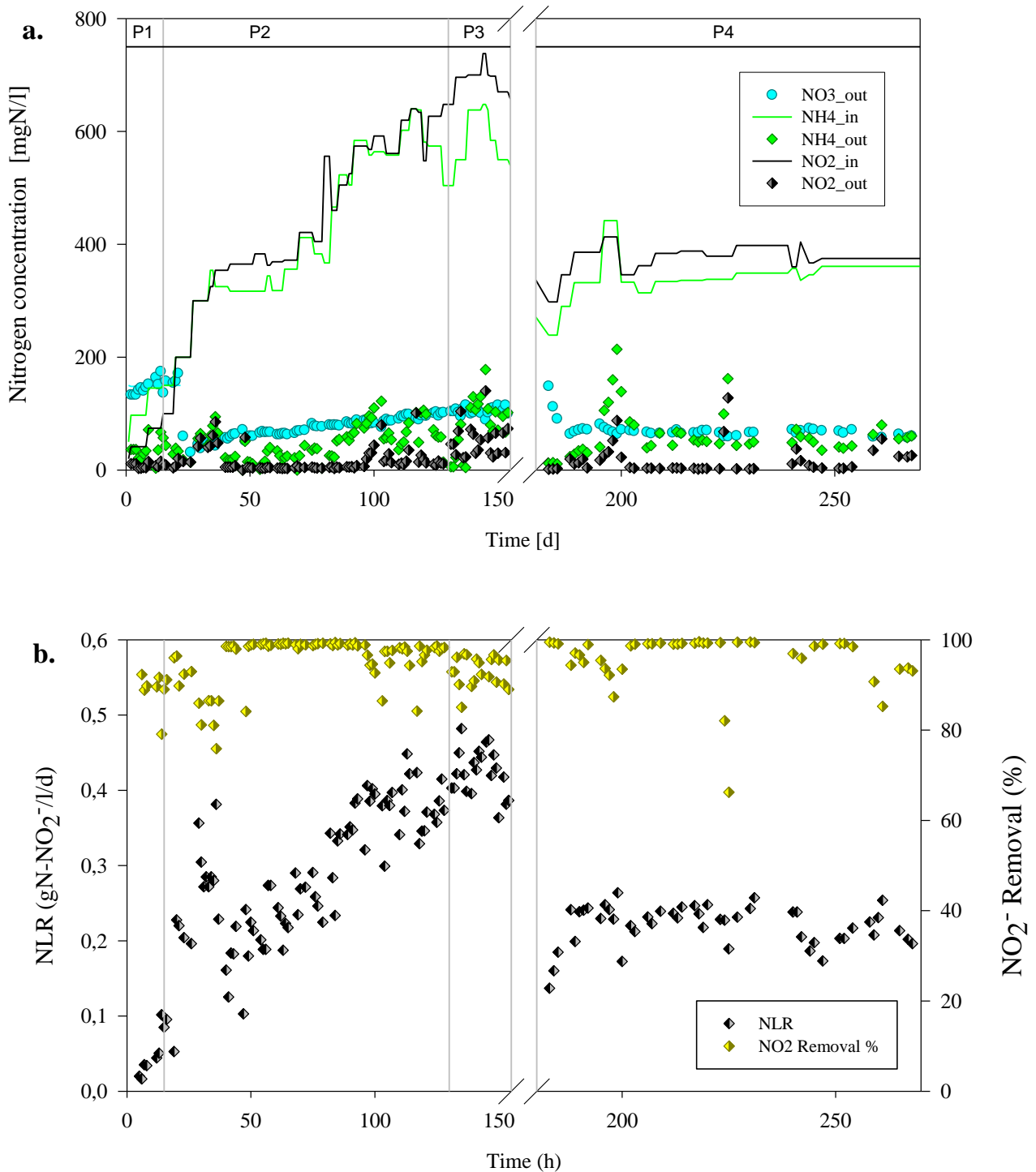


Figure 3.2 Influent and effluent nitrogen concentration (a); NLR and NO₂⁻ removal efficiency (b). Nitrate was dosed in phase 1 only, at influent concentration of 150 mgN-NO₃⁻/l.

As shown in figure 3.3, beside a gradual increase in the overall VSS concentration, a dramatic decrease in VSS/TSS ratio was observed from day 60 to day 140, down to the lowest observed values of 39% on day 140. Concomitant changes in granule appearance and density were observed: granules progressively turned from bright red to white-rosy and their density increased notably, since usual agitation provided by gas flow

recirculation was not sufficient to suspend the biomass, which started to settle at the bottom of the reactor. Further evidences, discussed in section 3.4, showed that it was mainly due to an unexpected deposition of minerals on the surface of the granules (fig. 3.4). It was concluded, that from day 130 to day 155 biomass experienced severe limitation of substrate diffusion due to the physical barrier of mineral shell, explaining the progressive decrease in removal capacity. Acid test was performed on the granules' mineral ash by applying drops of 1M HCl and the result indicated that the minerals had a high carbonate content as the characteristic fizzing was observed¹⁵.

Moreover, contrary to the stable pH observed throughout the period ranging from day 1 to day 120 (pH stable at $8,1 \pm 0,2$), from day 140 to 155 a pH increase was observed, with values of $8,5 \pm 0,2$ and peaks of 8,9. As a countermeasure, influent pH was lowered from 7,6-7,8 to 6,9-7,2 from day 130, without any positive result on the reactor pH. This alkaline increase was not justified by the acidity consumption due to the anammox process itself, as the NLR was not significantly higher than during the last weeks of the previous period. Considering that from day 137 on, synthetic influent was prepared with distilled water rather than tap water, it is reasonable to ascribe such a pH raise to the progressive release of carbonate ions from the carbonates deposition (i.e. carbonates dissolution), promoted by the shift from hard tap water to distilled water.

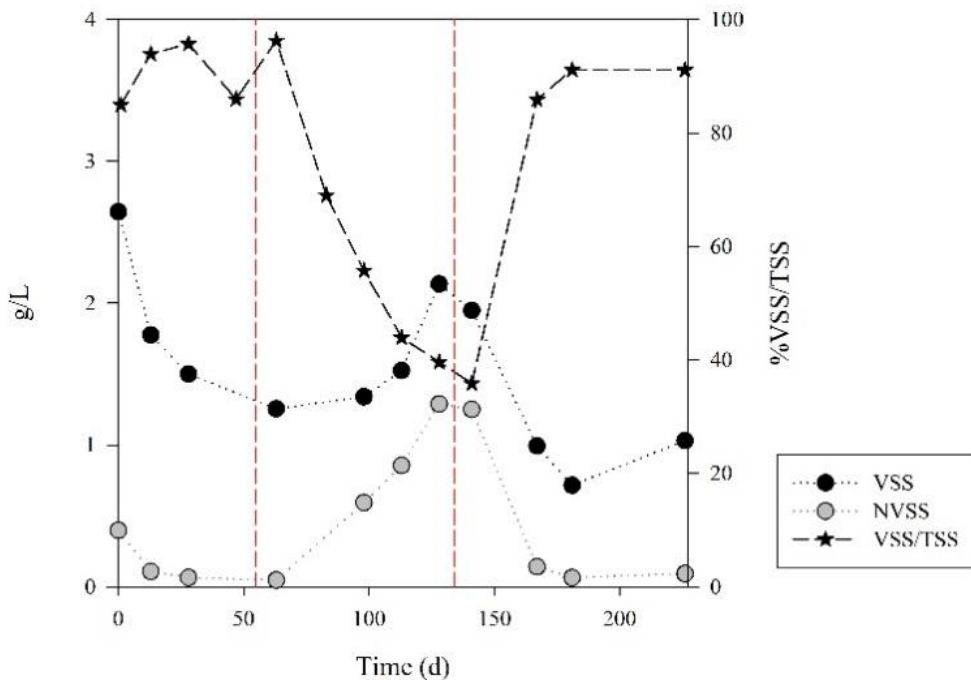


Figure 3.3 VSS concentration in the reactor and VSS/TSS ratio. Dotted vertical lines define the hard-water feeding period.

On day 155, the reactor was emptied in order to rescue as much biomass as possible. In light of all these evidences, an off-site rescue strategy was implemented with the aim of removing those granules severely

¹⁵ Acid test is commonly used in geology to identify carbonates minerals, comprising mineral compounds of CO_3^- ions with metals. Acid addition dissolves the minerals by turning carbonates into gaseous CO_2 (Tiessen, 1983).

affected by mineral precipitation; in fact, precipitation did not affect all the granules with the same extent so that some appeared completely covered of a whitish shell whereas others appeared almost free from any deposition (fig 3.4b). The rescue procedure was as follow: (i) gravimetric selection was applied exploiting the high density of mineral-covered granules; (ii) selected biomass was re-suspended in HEPES-buffered medium at pH 6,5 for five consecutive days, replacing the slightly acid medium almost every day, in order to dissolve residual carbonate minerals as much as possible.

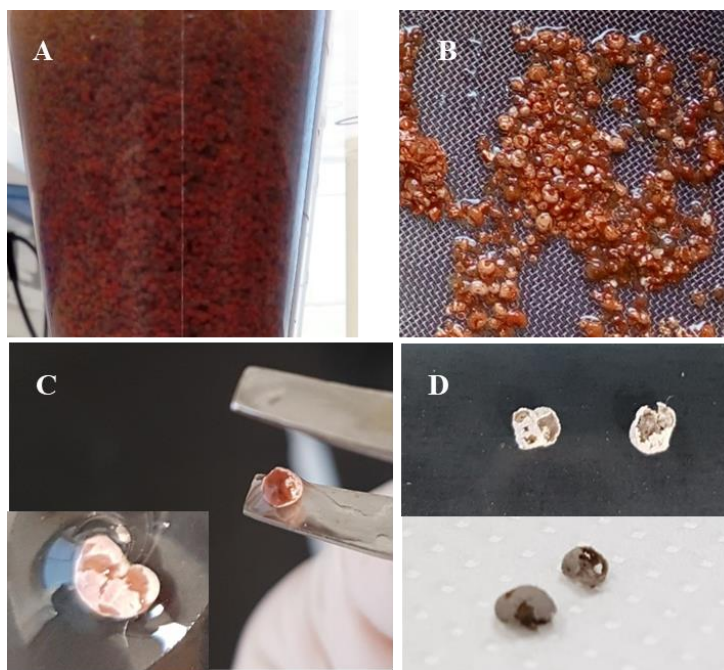


Figure 3.4 Pictures of biomass at day 83 (A) and day 155, on a 0,5-mm sieve (B); granules with external mineral deposition (C); mineral shells, after granules incineration (D).

The rescued biomass, which was almost half of the total biomass present in the reactor in the reference period of days 130-150, did not show severe mineral deposition and was inoculated back in the reactor (day 160). For almost two weeks, the reactor was operated at HRT much lower than the one applied in phase 2, i.e. from 1,6 d down to few hours (2 to 6 h, on average). In order to promote the residual carbonates dissolution, a synthetic medium free from (bi)carbonates and calcium was used and influent pH was lowered to 6,5. Taking into account that the biomass was halved and underwent starving and stressful conditions, a 60% reduced NLR was applied. Days 155-160 are not reported in figure 3.2 and neither are the applied nutrient concentration and removal efficiencies referred to days 160-177, since the reactor was operated under exceptional conditions due to the contingency measures required.

On day 178, an in-situ activity test was performed in order to set the proper NLR according to the system capacity and the restoring phase, P4, started. From day 200 on, stable NLR of 0,22 gN-NO₂⁻/l/d was applied at HRT of 1,6 d, and a stable 95% nitrite removal efficiency was established from that day on. An episode of

temporary nitrite accumulation occurred on day 223, due to inorganic carbon limitation. Indeed, the synthetic medium was prepared with low bicarbonate concentrations (<100 mg/l); NaHCO₃ was dosed at 400 mg/l from that day on.

Table 3.2 shows the removal stoichiometry observed throughout the experimental phases as $\text{gN-NO}_2^-_{\text{removed}}/\text{gN-NH}_4^+_{\text{removed}}$ and $\text{gN-NO}_3^-_{\text{produced}}/\text{gN-NH}_4^+_{\text{removed}}$. Values were in agreement with the stoichiometry reported by Lotti et al. (2014b). Interestingly, a slight increase in both N ratios were observed during the most critical periods (P3 and first days of P4). It can be speculated that an additional ammonia release could be derived from cellular lysis (ammonification) thereby affecting the measured ratios.

Table 3.2 Observed stoichiometry during the operational phases

<i>Phase</i>	Days	NO₂⁻/ NH₄⁺ [gN/gN]	NO₃⁻/ NH₄⁺ [gN/gN]
<i>P1-start up</i>	1-15	-	-
<i>P2- NLR increase</i>	15-130	1,146 ±0,080	0,167±0,063
<i>P3 – Process disruption</i>	131-155	1,271±0,045	0,165±0,008
<i>Off-site biomass rescue</i>	155-177	-	-
<i>P4- Process restoration</i>	178-225	1,322± 0,092	0,211±0,072
	226-270	1,182± 0,091	0,164±0,058

3.3.2 Activity tests

Manometric and in-situ batch tests showed comparable results when both types of tests were performed within few days, corroborating the applied stoichiometry as well as the validity of the adopted methods. In fig. 3.5 MSAA value from manometric tests are presented as mean value and standard deviation of the multiple rates observed in each test (multiple spikes were provided in each test), whereas for in-situ batch tests, MSAA value and its error are calculated as the average and standard deviation values of the removal rates observed during the test (three to six hours, sampling interval from 0,75 to 2 h)¹⁶. Since reactor operation was conducted under nitrite limiting condition, MSAA and SNLR values are referred to the sole nitrogen-nitrite (Dapena-Mora et al., 2004). On day 36 and 47 the MSAA was 0,155±0,004 gN-NO₂⁻/gVSS/d, considering results from both types of test, and it more than doubled after one month, reaching 0,349±0,034 gN-NO₂⁻/gVSS/d, at day 83. This result was in agreement with the very high anammox efficiency observed (>95% nitrite removal), confirming the successful biomass reactivation and reactor start-up. The progressive process disruption observed in the reactor was reflected in a decline in MSAA on days 117 and 135, with a decrease of the 21% and 59%, respectively, compared to the maximum value observed on day 83. Successful process restoration

¹⁶ Further data on activity tests are presented available in figures A.1 and A.2, in the appendix section.

after biomass rescue and segregation, was proven by subsequent increase of MSAA value on day 178 (after re-inoculation) up to its maximum value of $0,387 \pm 0,027$ gN-NO₂⁻/gVSS/d observed on day 218, maintained quite stable also on day 245. The highest MSAA achieved at the end of the experimental period is in line with literature results of well performing anammox granular sludge (Dapena-Mora et al., 2007). The calculated SNLRs are also plotted in fig. 3.5. SNLR (gN-NO₂⁻/gVSS/d) has been calculated as the applied NLR (N-NO₂⁻) specific for the VSS content of the reactor. On days 35, 47 and 135 SNLR was higher than the MSAA of the biomass, pointing that the imposed nitrogen load was above the system capacity (Dapena-Mora et al., 2014). Indeed, significant nitrite accumulation was observed in those days, causing severe episodes of granule flotation. On day 178, SNLR equal MSAA since the batch test was intentionally performed to define the proper NLR to apply after the critical period of phase 3. In phase 4 (days 218 and 245), as the MSAA raised again to the highest values observed in day 83, the constant SNLR applied ranged 60-65% of reactor's maximum capacity.

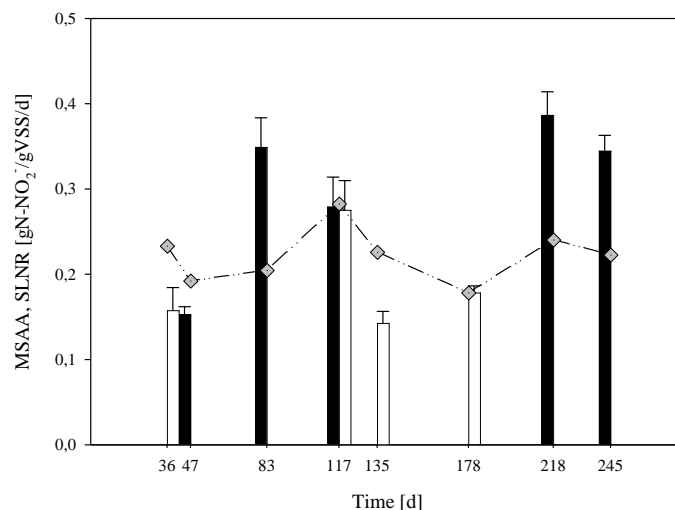


Figure 3.5 Results on activity tests versus the applied SNLR: MSAA from manometric assays (black columns) and from in-situ batch tests (white column); SNLR (--o--).

3.3.3 Granular size distribution and microbial community

Size distribution analyses were performed on the inoculum biomass and on day 40 and 260. Floating granules were also collected during the severe floating events during days 40-50 and analysed as well. Results are reported in table 3.3. As it can be observed, after 40 days of operation, granules' average diameter was lower than the one presented by the seeding sludge, i.e. 1,55 and 1,11 mm, respectively. A higher value of 1,82 mm was observed on day 260 (phase 4, after process restoration), when the diameter values falling in the 10th, 50th and 100th percentile were much closer between each other and the average value in comparison with values of inoculum and day 40, witnessing higher homogeneity in granular size distribution, compared to the previous

samples. Floating granules exhibited by far the highest average diameter of ca 3 mm, in accordance with what described in section 3.1.

Table 3.3 Granular size distribution, average diameter and diameters corresponding to the 10th, 50th and 100th percentiles

Day	Average diameter [mm]	D10 [mm]	D50 [mm]	D100 [mm]
0 (Inoculum)	1,55	0,22	1,31	2,88
40	1,11	0,16	0,97	2,12
260	1,82	1,17	1,78	2,37
Floating granules	3,12	2,21	3,22	3,76

In figure 3.6 the microbial distribution in terms of relative abundance is presented at class (a) and genus level (b). *Planctomycetia* was the class showing the highest relative abundance in all the samples, whose percentage remained almost constant throughout the experimental phases, namely $38 \pm 3\%$. An undefined bacterium, whose taxonomic classification could not go further than the domain level, resulted the second highest relative abundance of 10%, 22%, 22% and 16% for samples withdrawn on days 49, 105, 190 and 232, respectively; a similar abundance was observed at genus level. At genus level, anammox bacteria were related to *Ca. Brocadia* and *Ca. Kuenenia* and an interesting population change within them was observed. *Ca. Brocadia* was the predominant planctomycetes on day 49, 105 and 232 with relative abundance of 38%, 35% and 25%. Only the sample on day 190 showed a significantly lower (15%) relative abundance in *Ca. Brocadia*. A complementary behaviour was observed for *Ca. Kuenenia* which was almost absent on day 49, but its relative abundance achieved 5% and 19% on day 105 and 190 and decreased to 8% on day 232. At day 49, the reactor was responding very well to the fast increase in NLR. As process disruption started to be evident due to the mineral precipitation, the relative abundance of *Ca. Kuenenia* started to increase up to its maximum value on day 190, i.e. at the end of the critical period. *Ca. Brocadia* is reported to be a r-strategist organism and *Ca. Kuenenia* a k-strategist instead (Kartal et al., 2012; Oshiki et al., 2016). Then, the former is favoured at high nutrient concentration due to its higher maximum growth rate (high μ_{\max}), whereas the latter is favoured in substrate-limiting conditions due to its higher substrate affinity (low K_s). Under the assumption that severe precipitation hindered substrate diffusion within the granule, nutrient-limiting conditions might have resulted in the internal layers where anammox used to thrive on higher nutrient concentrations, promoting a (temporary) advantage of *Ca. Kuenenia* over *Ca. Brocadia*. In line with such an assumption, the evidence that *Ca. Brocadia* returned to be the predominant anammox genus as the process stability was restored and the most damaged biomass removed.

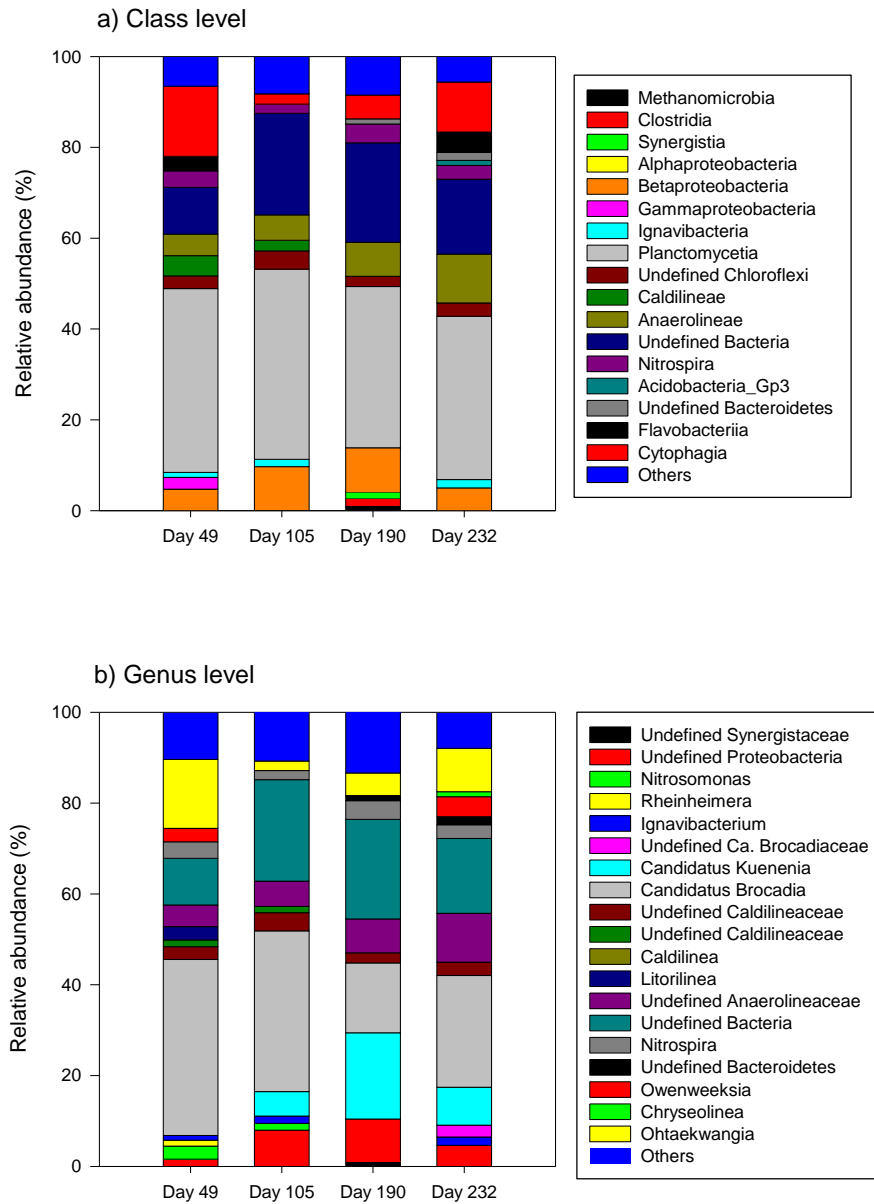


Figure 3.6 Microbial diversity profiles over the experimental work, at class (a) and genus level (b).

3.3.4 Carbonate-minerals precipitation

Despite a progressive increase in the VSS concentration in the system, the VSS/TSS ratio decreased dramatically from day 60 to 150, dropping from 95% to 39% (fig. 3.3). Figure 3.4 (b to d) shows the macroscopic appearance of the granules affected by severe mineral deposition and their inorganic shell after incineration at 550°C. Interestingly, granules ash produced during VSS analysis, looked like whitish mineral shell around the granules (fig. 3.4d) and no mineral precipitation affected the reactor internal surfaces nor the

tubes submersed in the reactor, neither in the mixed zone nor in the three-phase separator; the latter evidence suggesting for a biologically-induced precipitation (Johansson et al., 2017).

Analysis on tap water alkalinity revealed values as high as $8,8 \pm 0,082$ m_eq/l and the composition of the main alkalinity-related components is presented in table 3.4. Due to the mineral and nutrient addition, the final concentration of Ca, Mg, Na, K, P and bicarbonates in the influent medium was further increased. Values corresponding to the mineral medium prepared with distilled water (days 36-50 as reference period) and tap water (days 60-120) are also reported in table 3.4.

Table 3.4 Tap water and mineral medium during phase 2: characterization for alkalinity, total (filtered) phosphorous and hardness related components.

Parameter	Tap water*	Influent on days 36-50** (distilled water and nutrient addition)	Influent on days 60-120** (tap water and nutrient addition)
Ca ²⁺ [mg/l]	133±18	54	187
Mg ²⁺ [mg/l]	45,5±6	10	55,4
Na ⁺ [mg/l]	129±18	849	970-1422
K ⁺ [mg/l]	2,41±0,38	7,1	9,6
C-HCO ₃ ⁻ [mg/l]		440	495-730
Total P [mgP/l]	0,067±0,003	5	5

*Analysed

**Estimated from nutrient addition and tap water analysis

Analyses showed that the tap water used was remarkably hard, very rich in Ca²⁺ and Mg²⁺, mainly as bicarbonate salts (carbonate-related hardness was around 50°f). The software Visual MINTEQ 3.1 (Gustafsson, 2014) was used to calculate the saturation index of each possible compound, according to the concentration of table 3.4, pH and temperature values. Saturation Index is expressed as:

$$SI = \log \frac{IAP}{K_{ps}}$$

where IAP is the Ionic Activity Product and K_{ps} is the solubility product of a given compound (Ma et al., 2020). SI values higher than 0 indicate super saturation conditions, i.e. possible precipitation. The condition with the highest nitrogen load was considered (upper limits of C-HCO₃⁻ and Na⁺ concentration ranges), as a worst-case scenario. The list of minerals with positive SI is presented in table 3.5. Software prediction on mineral precipitation regards: (i) calcite, around 2 mM; (ii) dolomite, around 2 mM and, in a little extent (iii) hydroxyapatite, around 10⁻² mM. As already discussed, PO₄-bonded minerals, are reported as common precipitates in anammox granules. In this study, phosphorous in the influent was added as KH₂PO₄ in order to provide 5 mg P-PO₄³⁻/l; ICP-MS analysis carried out on tap water and effluent samples¹⁷, shows values of

¹⁷ Samples from reactor effluent were withdrawn on days 140 and 180.

0,07±0,01 and 3,77±1,1 mgP_{tot}/l, respectively. Since influent P- PO₄³⁻ was around 5 mg/l, the total P concentration in reactor effluent witnesses that the majority of P-PO₄³⁻ was exiting the system, net of biomass uptake and possible marginal precipitation, confirming the hypothesis that the visible mineral precipitate was not belonging to any of the Ca-PO₄ bonded minerals. As a qualitative speculation, according to the software calculation, the amount of calcite and dolomite would increase system TSS concentration with around 500 mgNVSS/l, determining a significant decrease in VSS/TSS ratio in a system with 1,5-2 gVSS/l, being in line with the progressive decline in VSS/TSS ratio experienced in the present study.

Table 3.5 Saturation indexes, outcomes from Visual MINTEQ®.

MINERAL	SATURATION INDEX	MOLAR COMPOSITION
ARAGONITE	1,631	1 Ca ²⁺ 1 CO ₃ ²⁻
CA ₃ (PO ₄) ₂ (AM1)	0,736	3 Ca ²⁺ 2 PO ₄ ³⁻
CA ₃ (PO ₄) ₂ (AM2)	3,466	3 Ca ²⁺ 2 PO ₄ ³⁻
CA ₃ (PO ₄) ₂ (BETA)	3,728	3 Ca ²⁺ 2 PO ₄ ³⁻
CA ₄ H(PO ₄) ₃ :3H ₂ O(S)	3,816	4 Ca ²⁺ 1 H+1 3 PO ₄ ³⁻ 3 H ₂ O
CACO ₃ XH ₂ O(S)	0,448	1 Ca ²⁺ 1 CO ₃ ²⁻ 1 H ₂ O
CALCITE	1,771	1 Ca ²⁺ 1 CO ₃ ²⁻
DOLOMITE (DISORDERED)	2,903	1 Ca ²⁺ 1 Mg+2 2 CO ₃ ²⁻
DOLOMITE (ORDERED)	3,433	1 Ca ²⁺ 1 Mg+2 2 CO ₃ ²⁻
HUNTITE	2,442	3 Mg ²⁺ 1 Ca+2 4 CO ₃ ²⁻
HYDROXYAPATITE	13,663	5 Ca ²⁺ 3 PO ₄ ³⁻ 1 H ₂ O -1 H ⁺
MAGNESITE	0,369	1 Mg ²⁺ 1 CO ₃ ²⁻
VATERITE	1,218	1 Ca ²⁺ 1 CO ₃ ²⁻

For the sole calcite, also the Langelier saturation index, LSI, can be calculated and expressed as follows (Langelier, 1936):

$$LSI = pH - pH_s$$

where pH_s is defined as saturation pH. Such an index is usually used to characterize waters for their tendency to be aggressive (LSI<0) or scale-forming (LSI>0) and the saturation pH is calculated as a function of carbonate-bicarbonate equilibrium constant, calcite solubility constant, calcium ion concentration and alkalinity. Specifically, the higher the Ca²⁺ concentration and alkalinity, the lower the pH_s. LSI was calculated with the aid of Aqion® software and confirmed the scale-forming tendency of the water (LSI = 0,57).

The location of mineral precipitation is also of interest. The vast majority of works report the main precipitation to occur in the core of the granule and many reasons have been proposed to support this evidence. First, mineral precipitate nuclei can form in the bulk liquid and may act as supporting material for granule formation; then,

the inner region of the granule is typically less active and more abundant in inert cellular-lysis product and minerals, compared to the external layers; also, mineral core precipitation, in turn, may progressively involve more external layers in case of favourable local conditions in terms of pH and concentrations. Carbonates precipitation *into* AMX granules has been reported recently by Ma et al. (2020). In their study, enhanced precipitation of hydroxyapatite was targeted and concomitant, though undesired, carbonate precipitation was observed when bulk pH raised to values of 8,5 or above, whereas it was successfully controlled at lower pH values. In this study, carbonate precipitation occurred at lower pH, around 8,1, but the saturation pH, as defined by Langelier (1936), strongly depends on the level of calcium and alkalinity, very high in the present study: the influent concentration $C\text{-HCO}_3^-$, as sole salt addition, in the present study was up to 730 mgC/l against the 90 mgC/l reported in Ma et al. (2020).

Precipitation on the surface of AMX granular biomass seems far more unusual and it has been experienced by Trigo et al., (2006) and Zhang et al. (2018), both operating AMX systems with synthetic influent. Similar to the present study, Trigo et al. (2006) observed concomitant VSS/TSS reduction (down to a minimum of 45%), colour shift from red to whitish and nitrogen removal deterioration, due to mineral formation *onto* the granule surface; minerals were apatite-like. A significant decrease in influent phosphate and calcium concentration, allowed the authors to restore process efficiency and notably increase VSS/TSS ratio, within five weeks. Zhang et al. (2018) operated an AMX ESGB reactor, filled with granules of activated carbon. While studying the effect of inorganic carbon (IC) addition (as NaHCO_3) on process performance, the authors report on diffusion limitation due to mineral deposition on the surface of the granule at IC concentration of 130 mg/l, much lower than the one applied in the present study (see tab.3.4); X-ray analyses pointed at calcite, CaCO_3 , as the main precipitate formation.

3.3.5 TEM and SEM-EDX analyses

TEM analyses were performed in order to gain insight in biomass organization within the granule as well as to assess possible differences between granules affected by severe precipitation (discarded during the off-site rescue period) and those without any evident precipitation (withdrawn in phase 4). Figure 3.7 displays the most significant pictures obtained from the TEM analysis¹⁸. Granules not affected by precipitation (fig. 3.7a to d) showed a dense presence of the typically round shaped anammox, with the usual concavity on the cellular wall. The unique anammoxosome organelle is clearly distinguishable in some cells (fig. 3.7a). Lin et al. (2017) have proposed a tertiary organization in AMX granules' structure, based on TEM and SEM observations as well as EPS characterization. Specifically, the authors suggest a first level of aggregation among few cells (clusters or zoogloae), a secondary aggregation embedded by EPS and a tertiary cementation of aggregates. A similar structure in clusters of few cells, subunits (aggregates of clusters) and the ultimate granular structure has been also supported by other authors (Lu et al., 2012; Kang et al., 2019). In figure 3.7 (a to d), such a structure based

¹⁸ Courtesy of Professor Claudia Vannini, Biology Department, University of Pisa.

on sub-unit aggregates is clearly represented. Anammox zoogloae of few to tens of sole anammox bacteria are contoured by EPS, in turn aggregated to other units. The number of cells forming a single zoogloea has been suggested to be possibly linked to loading rate conditions: the higher the loading rate, the higher the number of cells in the cluster (Kang et al., 2019). Moreover, in “healthy” granules, microorganisms other than anammox were detected in the interspaces among (and not within) bacteria agglomerates as also reported by Lin et al. (2017). Regarding samples affected by significant precipitations, less observations can be done. A lower resolution was obtained, probably due to a lower efficiency in the preliminary fixation procedure as deep diffusion of reactants might have been hindered by the mineral structures. As a general consideration, anammox cells in figure 3.7e-f appear more dispersed and non-anammox microorganism are encountered more randomly over the analysed areas. Similar evidences are reported by Hu et al. (2017), comparing anammox granules grown under nutrient abundance (dense cell agglomeration) vs nutrient limitation (dispersed cell distribution). In the present work, it is, in fact, assumed that mineral precipitation lead to nutrient diffusion limitation along the granule section.

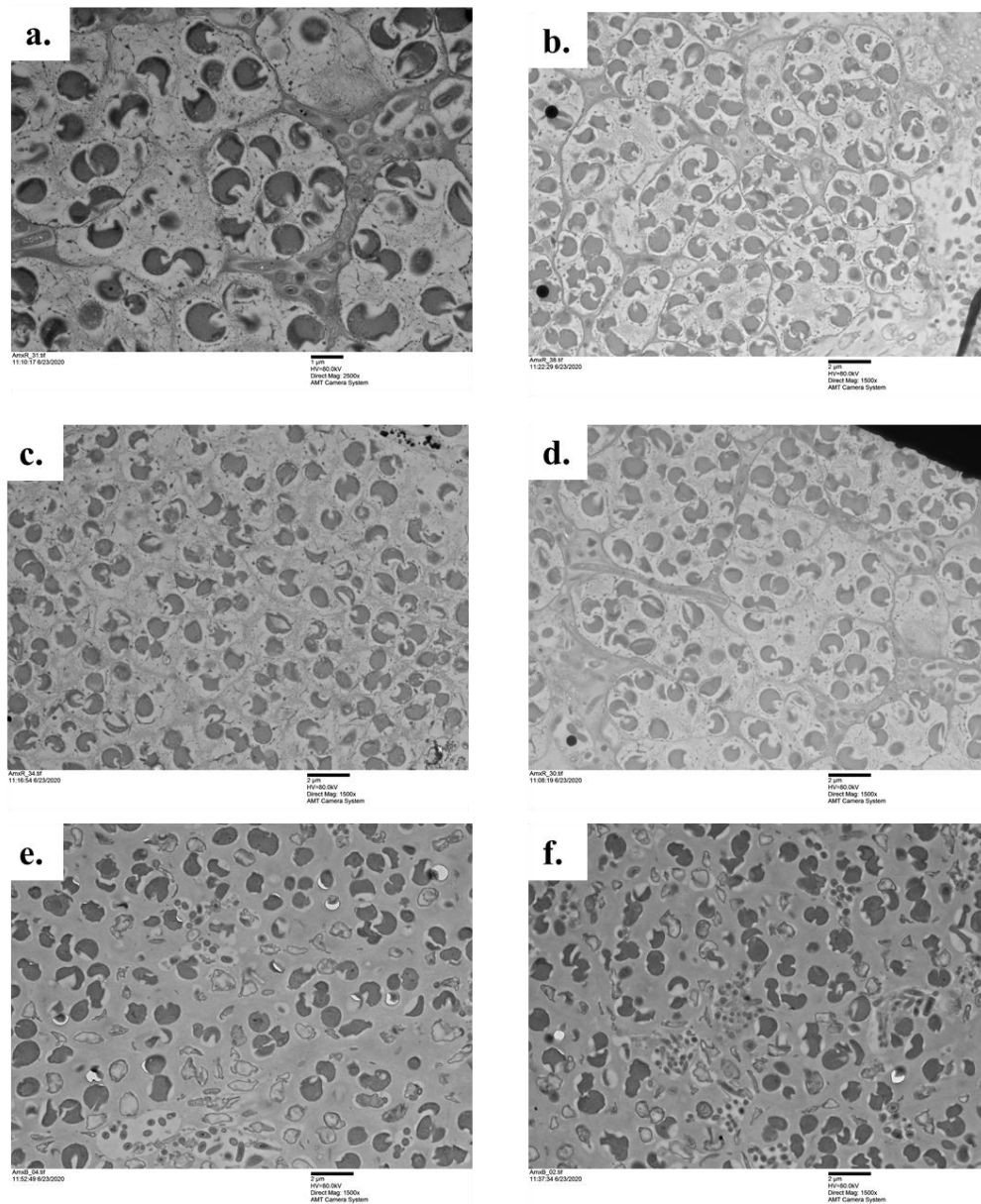


Figure 3.7 TEM observations on internal sections of granules not affected by mineral precipitation (a to d) and with evident precipitation (e and f). Black bars represent 1 μm (a) or 2 μm (b to f).

SEM and EDX analysis were conducted in order to gather information on granules' morphology and composition. As a general consideration, the morphological appearance of the granules exhibited the typical cauliflower-like aspect with concavities and irregular pattern (fig 3.8, fig. 3.9a-b-c and fig. 3.10a), similar to what reported by many authors (Arrojo et al., 2006; Trigo et al., 2006; Kang et al., 2019). When more than one point was considered for EDX analysis, spectrum and composition are reported in the figures as representative example of the replicates. In the spectrum graphs, the peaks related to Pt and Au (2,050 and 2.123 keV, respectively) must be neglected since they are related to the preliminary sample coating. In figure 3.8, the results analysis on a precipitate-free granule are presented. The granule was halved after fixation, before drying. Average O/C molar ratio was calculated over the spectrum analyses in 8 internal (fig. 3.8a) and three external (fig. 3.8b) points and resulted in a value of $0,56 \pm 0,19$, slightly higher than the value of anammox

biomass composition of $\text{CH}_{1.74}\text{O}_{0.31}\text{N}_{0.20}$ (Lotti et al., 2014b), more in line with the O fraction in the general formulation of biomass $\text{CH}_{1.8}\text{O}_{0.5}\text{N}_{0.2}$ (Heijnen et al., 1992). Biomass composition from Lotti et al. (2014b) was estimated from an almost pure culture of free-living anammox cells, a condition far different from the one in the present study with granular sludge (EPS-rich VSS) with an almost complete sludge retention (enriched conditions but wide microbial diversity). Calcium fraction results in negligible concentration (below 5% in weight, in fact the sensitivity threshold of the instrument), either along the internal section and on the external surface. In figures 3.9 to 3.12, the results on granules with evident mineral precipitation are reported. According to SEM observations, it is possible to distinguish a thin uniform surface reminding to biofilm aggregates and a more irregular and rough surface reminding inorganic structures. EDX analysis were performed on the two type of surfaces revealing that Ca^{2+} was abundant in the irregular surface whereas it was almost absent in the biofilm-like one (fig. 3.10). Ca-rich surfaces seemed to be colonised by bacteria either on the very external layer and on the internal-facing concavities. As a matter of fact, the problem of mineral precipitation lasted few months before being addressed, allowing for bacterial colonies to develop along with the precipitate formation. Phosphorus was not detected in any of the analysed areas, confirming that the inert precipitation was not related to phosphate-bond minerals. EDX analyses over several points and areas of the surfaces with precipitate-like appearance returned a Ca/C molar ratio ranging from 0,9 to 2,5. A highest value of 3,7 was observed in points illustrated in fig. 3.10. Calcite mineral was among the most likely compound to precipitate according to the known synthetic water composition (section 3.4), whose Ca/C molar ratio is 1. The higher values observed suggest either that others Ca-based minerals were present or that the results on the analysed areas were affected from interference from (not-clearly distinguishable) biofilm aggregates.

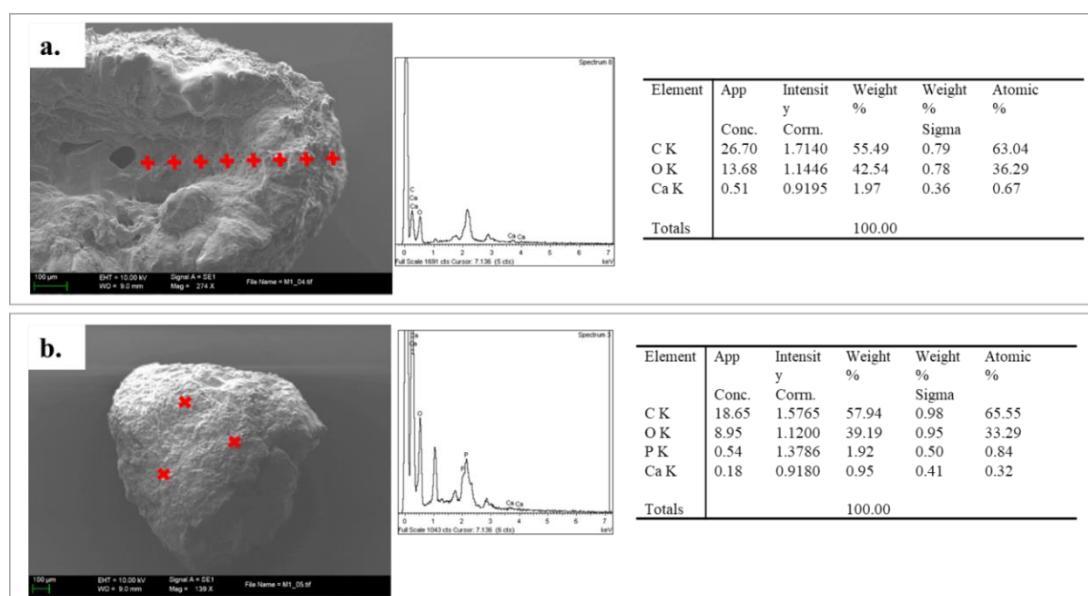


Figure 3.8 SEM images and EDX analysis of one AMX granule without any evident precipitation. EDX spectrum were analysed on the points displayed in cyan along the internal section (a) and on the external surface (b). Red cross indicates the points analysed with EDX.

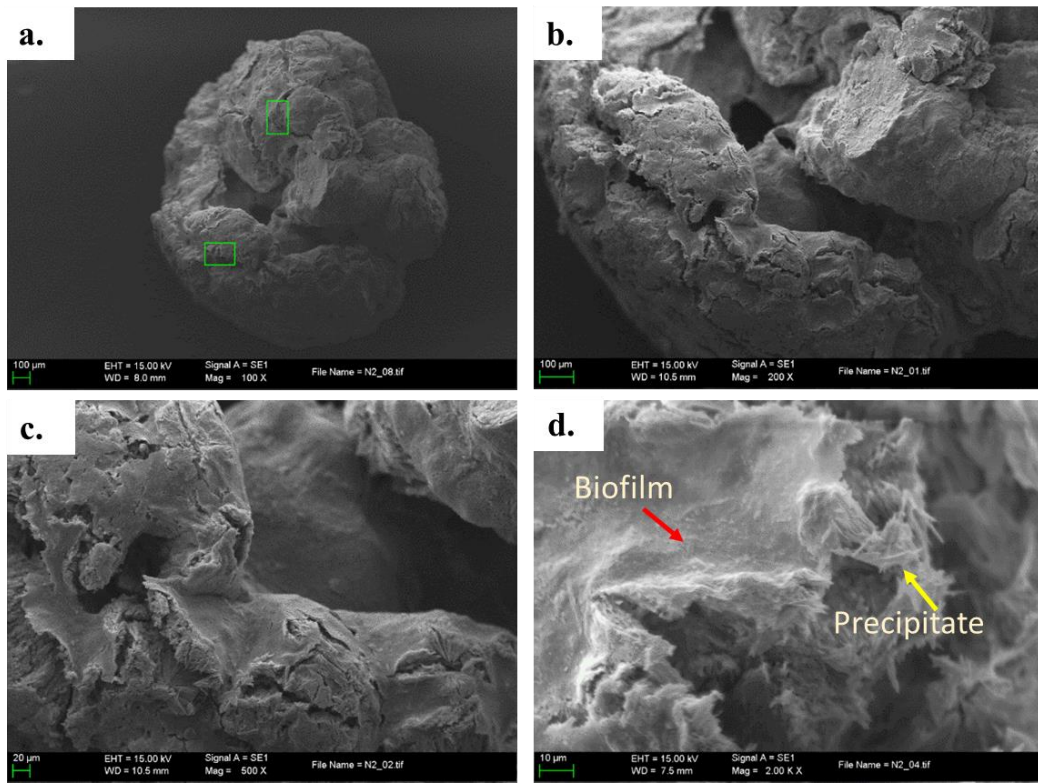


Figure 3.9 Morphological appearance at SEM of a granule showing evident mineral precipitation (a, b and c). particular of an area exhibiting two surfaces with a clear different texture, a biofilm-like uniform layer over a rough irregular surface with crystal precipitates (d)

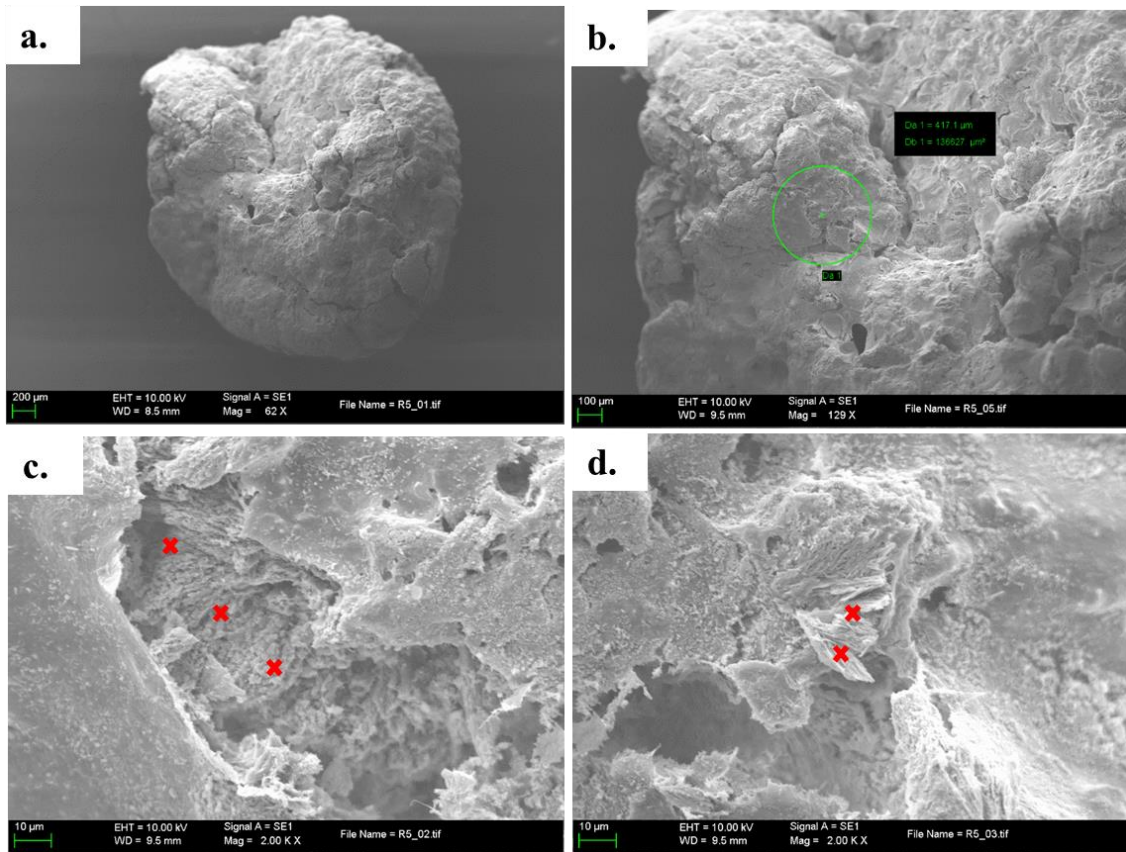
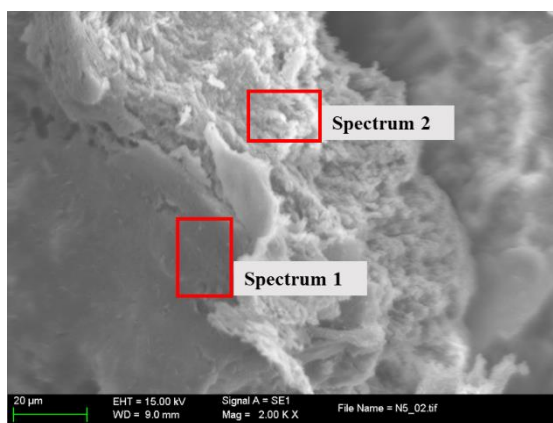


Figure 3.10 Morphological appearance of the surface of an AMX granule showing evident precipitation (a and b). EDX analysis were conducted on points (red crosses) of irregular rough areas (c) and crystals (d). Red cross indicates the points analysed with EDX.



Spectrum 1

Element	App Conc.	Intensity Corr.	Weight%	Weight% Sigma	Atomic%
C K	6.43	0.9768	39.79	3.33	51.71
O K	4.18	0.6484	38.92	3.42	37.97
Na K	0.80	1.0458	4.65	0.90	3.15
Si K	0.66	0.9668	4.14	0.78	2.30
Ca K	2.01	0.9731	12.50	1.32	4.87
Totals			100.00		

Spectrum 2

Element	App Conc.	Intensity Corr.	Weight%	Weight% Sigma	Atomic%
C K	1.14	1.1813	10.60	2.39	21.35
O K	0.91	0.3695	27.15	5.01	41.07
Ca K	5.97	1.0539	62.25	4.59	37.58
Totals			100.00		

Figure 3.11 Particular of an AMX granule showing evident precipitation, SEM image. EDX areal analyses showed Ca:C molar ratio of 1,7 in spectrum 2, whereas Ca²⁺ shows insignificant in spectrum 1 (biofilm-like area).

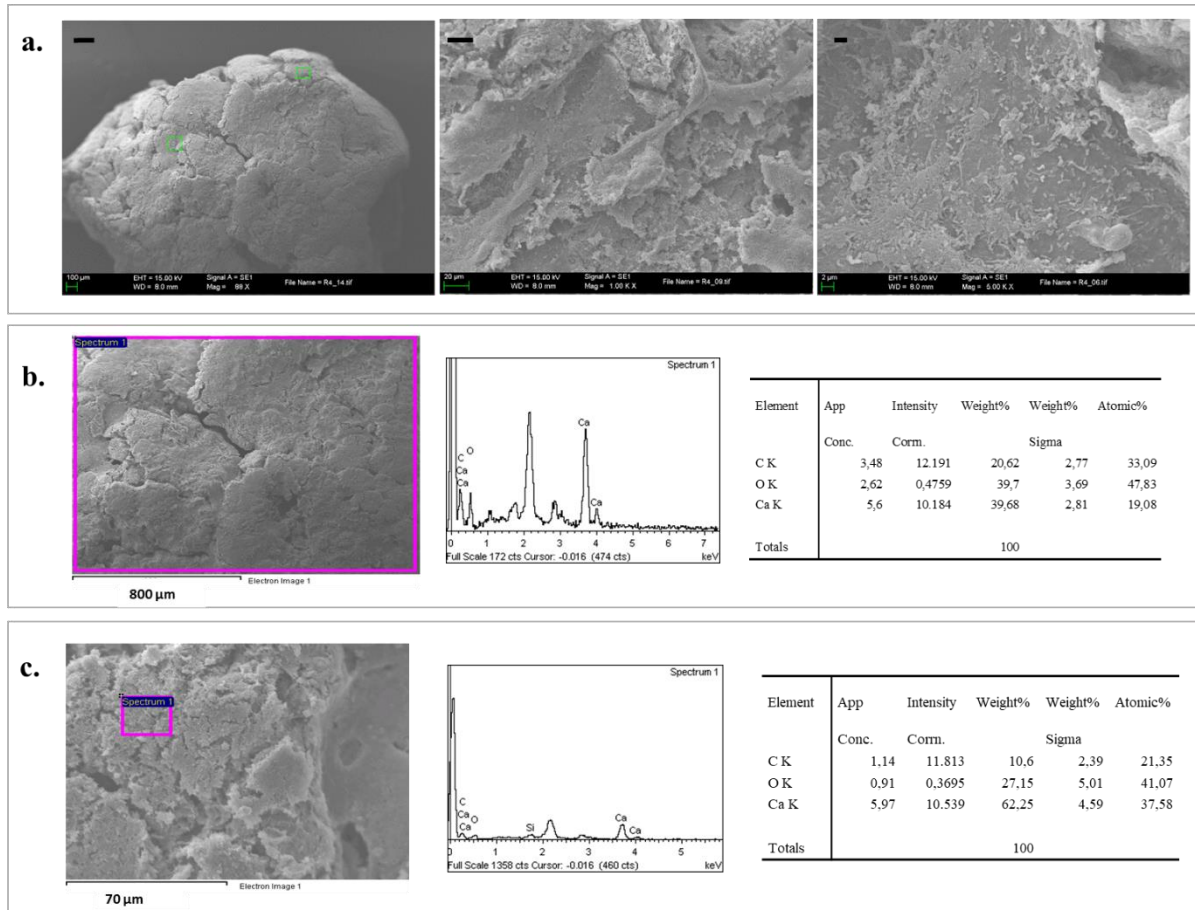


Figure 3.12 Progressive magnification of a granule with evident precipitation (black bars represent 200, 20 and 2 μm, reading left to right). Bacterial colonies are visible on the surface of the granule (a). EDX areal analysis on two different areas Average Ca:C molar ratio is around 1,1±0,8 (b and c).

3.4 Conclusions

In this chapter, a fast reactivation of the restored biomass was achieved, confirming that the storing conditions adopted over more than one-year were effective for long-term storage of active anammox biomass. The reactor responded every well to NLR increase achieving volumetric loads up to 0,48 gN-NO₂⁻/l/d, with a maximum specific nitrogen load of 0,28 gN-NO₂⁻/gVSS/d and stable nitrite removal higher than 95%. The mineral precipitation faced at the end of the NLR-increase phase, lead to a gradual process disruption. The evidence that the precipitation occurred on the surface of the granules and did not affect other surfaces on the bulk liquid (such as submersed probes or tubes) suggested that the precipitation reaction was somehow biologically mediated. Local pH gradients at the granule surface, due to the proton-consuming AMX activity, are likely to be the major drivers to promote local precipitation offering a favourable surface for incipient calcite

precipitation and the consequent severe deposition. The phenomenon observed in this work appears to be uncommon among the reported studies on mineral precipitation in AMX granular systems, both for the type of mineral compounds involved (CO_3 instead of PO_4 -bonded minerals) and for the region of the granule mainly affected by precipitation (the surface instead of the inner core).

To address the problem, the reactor was emptied and an effective procedure was implemented with the aim of selecting those granules not affected by severe precipitation. Gravimetric selection and repeated rinsing in slightly acid solutions proved crucial during the rescue phase. The reactor was inoculated back with the selected biomass, almost half of the one present in the reactor in the precedent operational phase, but exhibiting the highest SAA observed in the whole experimental period. NLR of $0,23 \text{ gN-NO}_2^-/\text{l/d}$ were applied and SLNR were $0,22 \text{ gN-NO}_2^-/\text{gVSS/d}$, around 60% of the reactor maximum capacity with a consequent average nitrite removal exceeding 95%.

It is believed that the extended study provided by the present work delivers useful warnings for anammox implementations, either at pilot or full scale, in case of wastewaters prone to precipitate formation.

CHAPTER 4.

Tannery wastewater as target stream for PAD/A process: assessing potential inhibition on anammox biomass

4.1 Introduction

Tannery wastewaters are considered a feasible target for the implementation of the innovative treatment object of the present thesis, i.e. the combined PAD and AMX process, due to two main characteristics: high N and S content and almost constant temperature of 25-32°C throughout the year¹⁹. In the perspective of WWTP rethinking towards energy self-sustainability and resource valorisation, the present chapter aims at evaluating possible inhibitory effects of vegetable tannery wastewaters on the anammox biomass, considered more sensitive than the sulphur-oxidizing one. Recalcitrant tannin-related organic matters and salinity are selected as the two potential inhibitory factors and studied either for their separate and combined effect. Indeed, in the suggested PAD/A implementation, other disturbing factors to the anammox process, such as organic COD and sulphide, are intended to be removed prior to the anammox unit.

4.1.1 Tannery wastewaters and Cuoiodepur WWTP

Tannery industry produces highly polluted wastewaters with high content in nitrogen (as ammonia and organic nitrogen), organic compounds, sulphur (as sulphide and sulphate), salts and chemicals (Mannucci et al., 2010; Saxena et al., 2017). Two types of tanning process are usually adopted: Chromium(III)-based and vegetable tannin-based, the former covering the vast majority of leather processing worldwide. The high salinity of these industrial wastewaters is a crucial aspect that needs to be considered when biological treatments are adopted. The high content in chlorides (and sodium) is due to the fact that salted flesh remains the most cost-effective manner to preserve the raw material prior to its processing. Leather processing comprises multiple steps during which raw leather undergoes several chemical-physical treatments in order to stabilize the organic matter and confer the required physical properties to the final product. Rinsing is the first phase of the process and high loads of chlorine and sodium are released during this step. Sulphate salts are used in the subsequent phase whereas sulphuric acid is added during the de-hairing step, when no hair-recovery system is implemented. Thereby, the most important sulphide load is produced in this phase, in fact prior to the real tanning step. When vegetable or synthetic tannins are used in the production process, further drawbacks may rise in the biological treatment unit, due to their bio-recalcitrant and potentially inhibitory nature. Tannins inhibition on bacterial activities has been reported by Nelson et al. (1997) and Munz et al. (2010), among others.

The tannery district located in the Italian region of Tuscany is the second district in Italy for leather annual production and among the biggest in Europe. Wastewaters produced by tannin-based and chromium-based tanneries are collected by two different sewage systems and treated separately. Cuoiodepur WWTP (Pisa, IT) treats industrial wastewater generated by the vegetable-tannery sub-district and municipal wastewater from the

¹⁹ Average yearly values observed in the aerobic tank at Cuoiodepur WWTP (courtesy of Consorzio Cuoiodepur S.p.a).

surrounding area. The majority of the polluted load in terms of nitrogen, organic carbon, sulphur and salts is related to the industrial stream; in terms of flowrate, the municipal stream accounts for around 40% of the total incoming flowrate. The almost 1:1 dilution is, in fact, a practical way to attenuate the potential inhibitory effect of high salinity and tannins levels. Over the years, plant operation issues and laboratory-scale studies pointed at nitrifying bacteria as the most sensitive microbial population to high salinity and tannins gradients as confirmed by other studies reported in literature (Moussa et al., 2003; Szpyrkowicz and Kaul, 2004; Munz et al., 2009). Munz et al. (2009) found a very slow nitrifying biomass at Cuoiodepur WWTP, probably as a result of several factors such as inhibitory compounds (either organic and inorganic) as well as temperature and salinity fluctuations. Szpyrkowicz and Kaul (2004) reported a similar conclusion, i.e. low maximum growth rate for nitrifying biomass treating tannery wastewater as an aggregate result of temperature conditions and inhibitory effect of compounds related to the tanning process. As a consequence, very high SRT are required for ensuring proper N removal. Another peculiar aspect is the slow biodegradability of a significant fraction of the COD. Indeed, high SRT are also conducive for high COD removal efficiency. Carucci et al. (1999) reports that COD/N ratios higher than those usually required by conventional applications are required for tannery wastewaters in order to satisfy the e-donor supply for denitrification.

The current treatment layout of Cuoiodepur WWTP is presented in figure 4.1.

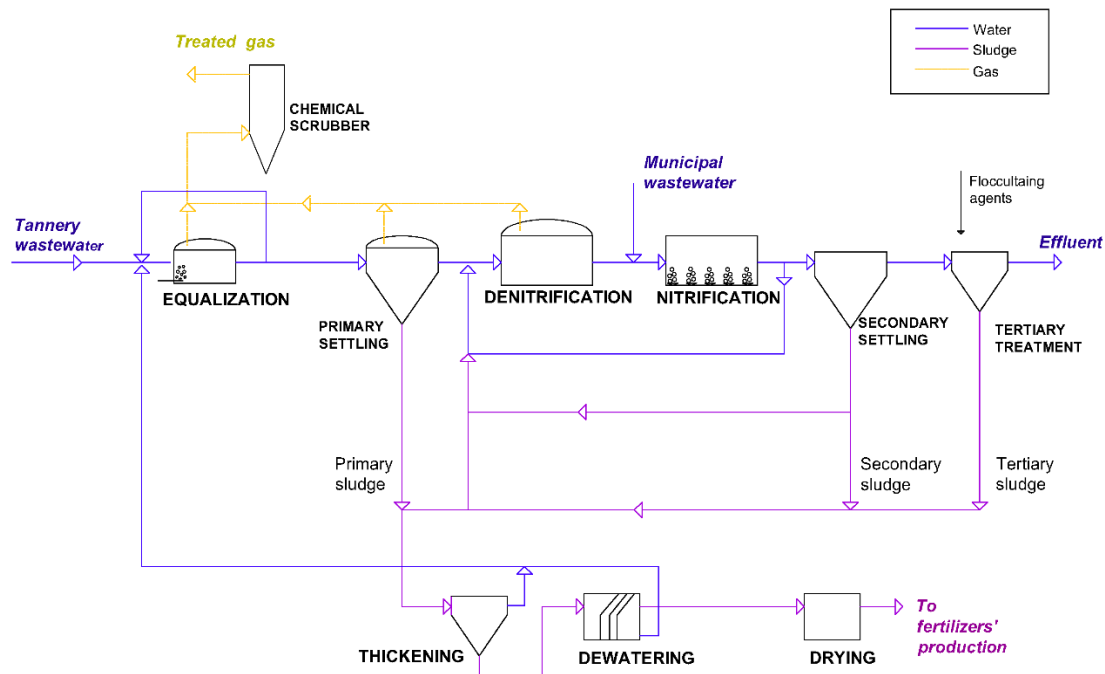


Figure 4.1 Treatment line at Cuoiodepur WWTP.

Speculating on possible future and innovative plant configurations, figure 4.2 depicts a possible alternative scenario in which the PAD/A process could be implemented. Such an integrated solution for C, S and N removal would meet many of the emerging challenges in wastewater treatment: (i) resource valorisation through methane production in the anaerobic unit (ii) energy saving thanks to limited use of aeration (iv) low sludge production and low GHG emission resulting from the adoption of autotrophic processes for S and N removal. Depending on operational constraints (e.g. actual N and S loads, effluent quality requirements, fate of stabilized sludge, investment costs), the solution presented in figure 4.2, could be implemented either in the sludge line of the current layout of Cuoiodepur WWTP or in the mainstream. In the former case, the PAD/A process and the preliminary nitrification unit would be applied to the returned water after sludge thickening and dewatering. In the latter case, the possibility of a separate collection system for sulphide-rich and COD-rich streams originated from the de-haring and the tanning phases, respectively, could be considered in order to optimize S and C removal. Such a solution is already implemented in other tannery districts in Europe. In either case, the option of elemental sulphur recovery could be implemented if deemed suitable; a solid separator unit could be in fact planned between the PAD and Anammox unit.

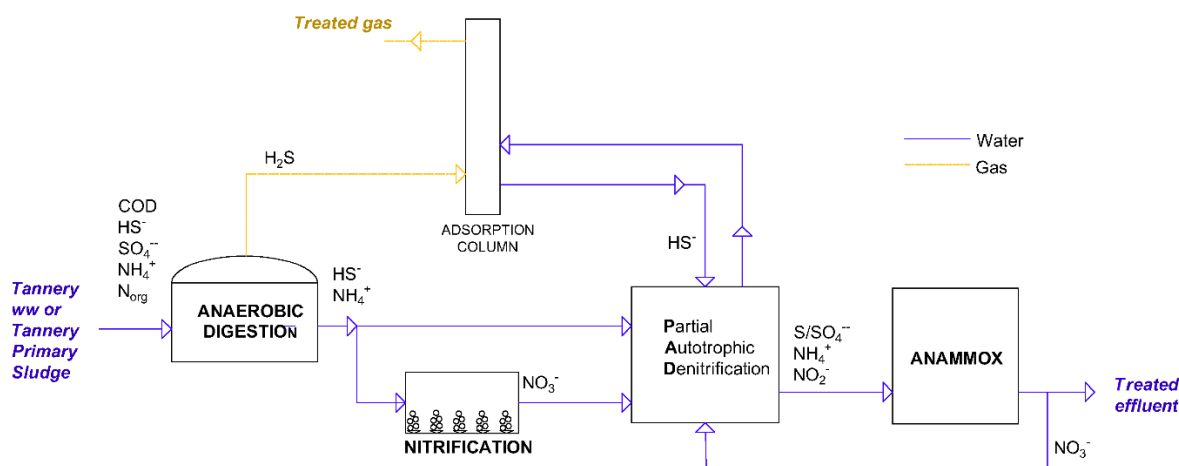


Figure 4.2 Alternative lay-out scenario implementing a PAD/A and gas desulphurization.

In the presented scenario anammox biomass would be exposed to the salt-and-tannin rich pre-treated wastewater, either in the main or side-stream line of the plant. Currently, the actual salinity content of water entering the biological unit is 2-3 gCl/l and 1-1,5 mgSO₄²⁻/l, with an average electrical conductivity of 10-12 mS/cm (at 25°C). It owns to be mentioned that the salinity level of the sole industrial stream is almost twice, due to the dilution achieved by mixing it with the municipal inflow. Salinity may vary significantly over the year according to the industrial activity (e.g. vacation periods and market fluctuations). As a consequence, activated sludge biomass is exposed to salinity and load gradients.

The effect of salinity on anammox biomass has been studied in the last decades, in order to study its feasibility with saline N-rich wastewaters such as those generated by seafood, leather and textile dyeing industries as well as leachate. Two main factors are reported to be crucial for stable treatment of saline wastewaters: (i) microbial population shift towards halophilic or more saline-tolerant species, such as *Ca. Scalindula* and *Ca. Kuenenia*; (ii) proper biomass acclimation to saline conditions. High salt concentrations may have severe detrimental effect on biological activity due to cascade mechanisms related to osmotic pressure on the cell wall, enzymatic inhibition and, ultimately, cellular lysis (Zhang et al., 2019). Stable anammox activity at saline conditions has been reported after biomass acclimation and 30 gNaCl/l is pointed out by many authors as the salinity threshold for stable process performance (Kartal et al., 2006; Dapena-Mora et al., 2010; Ma et al., 2012; Li et al., 2018). In some cases, a conducive effect on SAA have been shown in case of gradual increase in salinity concentration until 20 gNaCl/l (Dapena-Mora et al., 2010; Jin et al., 2011) or moderate salinity shock (Ma et al., 2012). On the contrary, in case of intense salinity shock events, a transient (and typically reversible) inhibition in anammox activity has been observed together with a progressive process recover, the recovery period being related to the saline gradient.

A successful implementation of PN/A process on Chromium-based tannery wastewater was presented by Frijters et al. (2007), reporting the pioneering treatment line (figure 4.3) implemented in the Lichtenvoorde wastewater facility. Specifically, in the mentioned plant, an anaerobic IC® reactor allows for COD removal, sulfate reduction and biogas production; an aerobic sulphide oxidation reactor provides sulphide removal coupled with elemental sulphur recovery and last, a PN CIRCOX® reactor is coupled with an Anammox reactor for autotrophic N removal²⁰. An important milestone of their work was the achievement of stable operation in the anaerobic treatment unit, since the effectively treatment of the complex COD mixture present in tannery wastewater was not obvious. The innovative treatment plant is currently managed by Waterstromen and treats wastewater from Rompa Tanneries (former Hulshof Royal Dutch Tanneries)²¹.

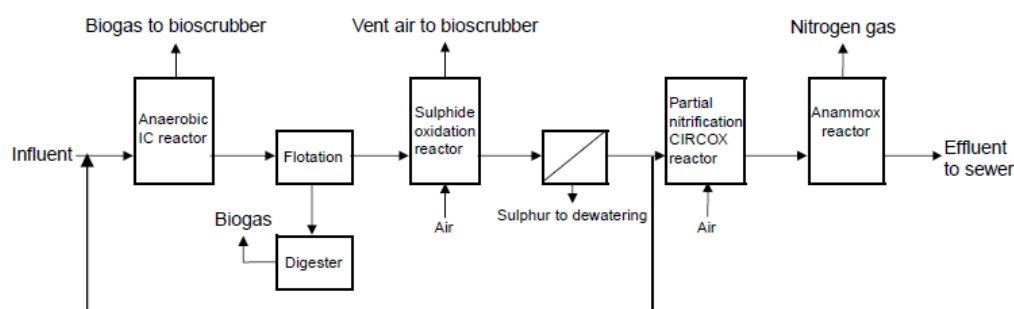


Figure 4.3 Treatment line at Lichtenvoorde WWTP, treating chromium-based wastewater (from Frijters et al., 2007).

²⁰ In their installation, chromium was removed through chemical precipitation prior to the anaerobic IC® unit.

²¹ Few more information are available at <https://www.waterstromen.nl>.

In this work, vegetable tannery wastewater is targeted instead, with the perspective of implementing an adopted version of the treatment layout from the Lichtenvoorde plant, as depicted in fig. 4.2.

Specifically, this chapter presents the results from two batch test experiments aimed at assessing the inhibitory effect of pre-treated tannery wastewater on anammox biomass. The first experiment was conducted on stored biomass, prior to its reactivation, and a gradual exposure to the pre-treated tannery wastewater was implemented. In the second inhibition experiment, fresh active biomass was used and exposed to the pre-treated tannery wastewater after biomass acclimation, in order to avoid transient saline shock effect in the assessment of biomass activity. To the best of our knowledge, this is the first study on anammox activity with vegetable tannery wastewaters.

4.2 Material and methods

4.2.1 First inhibition experiment on stored biomass

The first inhibition experiment was conducted on stored biomass. Prior to the inhibition test, a two-week reactivation experiment was conducted in batch conditions on stored biomass until a stable SAA was observed. PN/A granular biomass from Olburgen WWTP (The Netherlands) was stored at 4 °C for ten months, according to the storage procedure described in chapter 3. Figure 4.4 offers a schematic of the experimental activity, in order to ease the description of the work.

Briefly, during the 10-month storage, biomass was kept in three different bottles (herein B1, B2 and B3), regularly monitored for pH, conductivity and nitrate levels (used as redox buffer). Biomass from B1, B2 and B3 was used to inoculate three 1-L manometric reactors for the reactivation experiment: R1, R2 and R3, respectively. The manometric batch test was conducted according to the procedure described in section 2.2.1, except for the temperature: during the first 8 days, reactivation test was conducted at room temperature (20-26 °C); from day 9 to day 16 the batch reactors were placed in an incubator, at constant temperature 30°C. Synthetic wastewater was used as liquid medium and prepared according to Van de Graaf (1996). The liquid volume was 700 ml and the headspace was flushed with a mixture of N₂/CO₂ (95% and 5%, respectively), prior to start the test. Manometric bottles were placed in an orbital shaker and agitation was kept at 120-150 rpm throughout the test. Nutrients pulses were provided through injection of few ml of concentrated solutions: 1M of (NH₄)SO₄ and 1M NaNO₂ for ammonia and nitrite, respectively. A ratio of NH₄⁺/NO₂⁻ of 2:1 was provided in order to operate in nitrite-limiting conditions. Nitrite concentration at every spike, was maintained around 20 mgN/l, in order to avoid toxic effects in case of accumulation or slow uptake rates. Once SAA biomass shown a constant SAA, the reactivation experiment was ended.

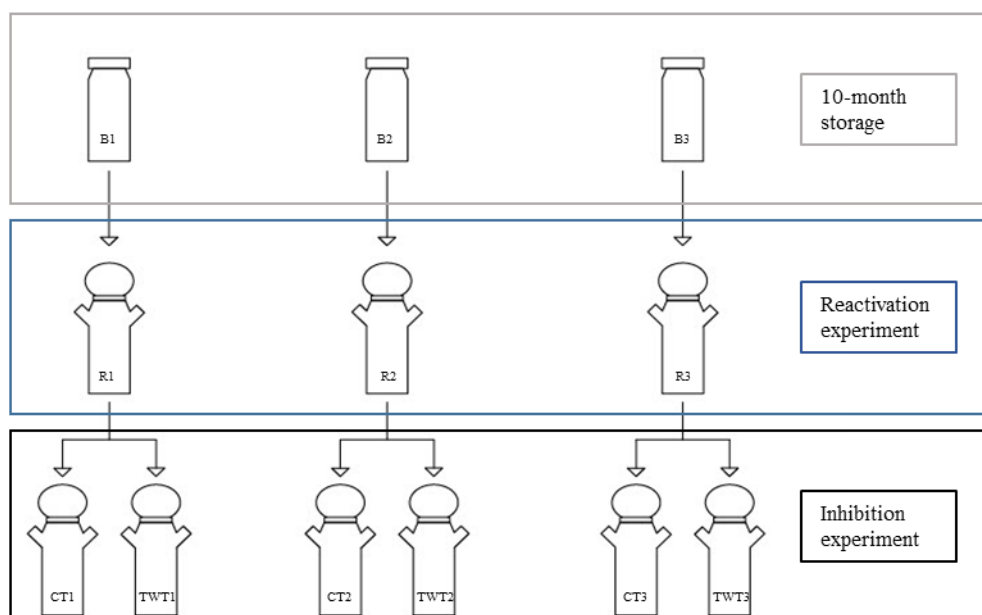


Figure 4.4 Schematic of the experimental work comprising the Reactivation test and the 1st inhibition test.

The subsequent inhibition experiment lasted from day 16 to day 54. A total of six OxiTop bottles were run and placed in a thermostatic incubator at 30°C. Part of the reactivated biomass from R1, R2 and R3 was used to inoculate the control test (CT) triplicate: CT1, CT2 and CT3, respectively, holding a liquid volume of 700 ml (1 litre of total volume). Another part of the biomass was used to inoculate other three 300-ml OxiTop bottles for the tannery wastewater test (TWT), named TWT1, TWT2, TWT3. The remaining biomass was used to characterize VS content (as gVS/g_{ww}), of the granules from each of the three reactivation bottles. The aliquot of biomass used to inoculate each bottle was weighted (as wet weight); data on wet weight and VS content were then used to know the exact amount of VS in each bottle.

Biomass in CT bottles was re-suspended in fresh synthetic medium. Fresh tannery pre-treated wastewater, herein tannery WW, was withdrawn at the exit of the secondary effluent and used in TWT. Such a pre-treated wastewater was deemed the most suitable stream to study potential inhibitory effect on anammox biomass since the salt and tannin content is the same of the stream entering the biological unit and no easily biodegradable COD is present. In TWT, a gradual shift from synthetic to real tannery WW was operated during four operational phases, according to the dilution steps described in table 4.1. On a weekly base, TWT supernatant was removed and replaced with a mixture of synthetic medium and increasing fractions of tannery WW. In the last operational phase (phase 4), TWT triplicate was run with sole tannery WW. At each phase, fresh tannery WW was analysed for the following parameters: pH, conductivity, ammonia, nitrite, nitrate, COD, chloride and sulphate. Operational conditions of reactivation and inhibition experiments are summarized in table 4.1. Prior to be used in the test, tannery WW was filtered with paper filters in order to remove residual activated sludge in suspension. At every change of supernatant mixture, headspace was flushed with a mixture of N₂/CO₂ (95% and 5%, respectively); a concomitant headspace flushing was provided in CT bottles. From

day 26 on, headspace flushing was done with sole N₂ gas, since the N₂/CO₂ mixture was temporarily unavailable. Pulses of nitrite and ammonium concentrated solutions were provided in order to achieve a NH₄⁺/NO₂⁻ ratio of 1-1,5 and a nitrite concentration of 40-70 mgN/l.

Table 4.1 Operational conditions in the reactivation and 1st inhibition experiment.

	Condition tested	Days/ Operational phase	Liquid medium	Liquid Volume (ml)	Temperature
Reactivation experiment	Reactivation	0-8	Synthetic	700	20-26°C*
		9-16			30°C
1st inhibition experiment	Control test, CT	17-54	Synthetic	700	30°C
	Tannery WW test, TWT	17-26 Phase 1	¾ Synthetic + ¼ Tannery WW	200	30°C
		27-34 Phase 2	½ Synthetic + ½ Tannery WW	200	
		35-47 Phase 3	¼ Synthetic + ¾ Tannery WW	200	
		48-54 Phase 4	Tannery WW	200	

*Room temperature

Both in reactivation and inhibition experiments, liquid samples were taken after each spike, once a pressure plateau was observed and analyses on nitrate, nitrite and ammonia concentration performed. COD_{filtered} was analysed on the TWT bottles (phase 4) as well. Both the reactivation and the inhibition experiments were run over several consecutive days, thereby results are available for those days in which nutrient pulses were provided (almost daily or 3/4 days per week, not during weekends).

In order to favour the comparison with values obtained in chapter 3, all the SAA values are expressed as gN-NO₂/gVSS/h instead of gN₂/gVSS/d (as estimated by manometric results). The conversion factor is directly derived by applying the stoichiometry from Lotti et al (2014b).



Figure 4.5 First inhibition test: front-line bottles, tannery WW test during phase 4; back-line bottles, control test.

4.2.2 Second inhibition experiment

Six OxiTop® bottles (each with a total volume of 350 ml) were run for a total of 8 days. The manometric batch test was implemented according to the general procedure reported in chapter 2 (section 2.2.1). Fresh biomass was withdrawn from the gas-lift reactor described in Chapter 3, at day 245 of the experimental work. In this experiment, some of the biomass was acclimated to salinity levels as high as the tannery WW and exposed either to saline synthetic medium or to tannery WW (see sec. 4.2.2). The objective was to assess the effect of salinity and of (possible) inhibitory organic compounds, such as tannins, separately. Two thirds of the withdrawn biomass were acclimated to saline conditions as explained below; one third was let in non-saline sythetic medium. Each bottle was filled with the required amount of biomass and 150 ml of liquid medium, either non-saline and saline synthetic medium or tannery WW. Three conditions were tested in duplicates: (i) fresh biomass suspended in synthetic medium, herein Control Test, CT; (ii) fresh biomass acclimated to saline conditions suspended in synthetic saline medium, herein Saline Control Test, SCT; (iii) fresh biomass acclimated to saline conditions suspended in pre-treated tannery wastewater, herein TWT.

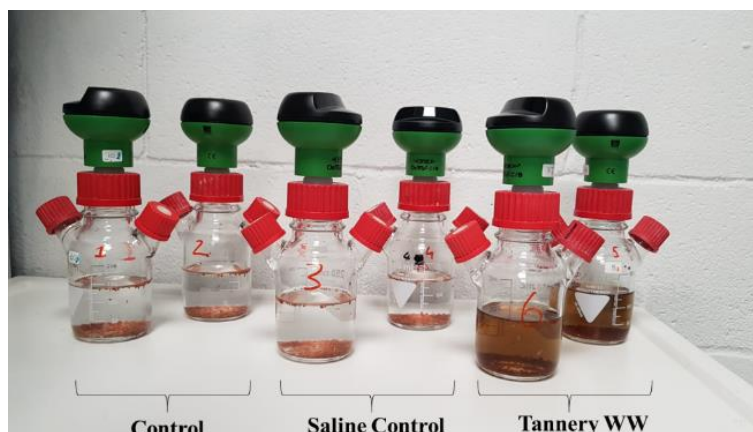


Figure 4.6 Second inhibition experiment.

Tannery WW was filtered with paper filters in order to remove residual activated sludge in suspension. The amount of biomass placed in each bottles was decided in order to achieve a complete nutrient removal within 7-12 hours. Pulses were provided early in the morning or late in the afternoon; in the latter case, test was let run overnight²². Concentrated pulses of ammonia and nitrite were provided through addition of 1M $(\text{NH}_4)_2\text{SO}_4$ and 1 M NaNO_2 , in order to achieve 30-60 mgN/l, as ammonia and nitrite. A minimum of 1:1 ratio of ammonia and nitrite was ensured in order to obtain nitrite-limiting conditions. A total of 7 consecutive pulses were provided. Between spike 4 and spike 5, a mixture of N_2 and CO_2 (95% and 5%, respectively) was sparged in the headspace in order to avoid CO_2 limitation drawbacks. Intermediate supernatant samples were taken between one spike and the subsequent in order to analyse ammonia, nitrite and nitrate concentration as well as pH. COD was also analysed in TWT. Analysis on the nitrogen components were used to perform nitrogen balance check by comparing removed nitrogen (as N-NO_2^-) and N_2 estimated by pressure increase. For this purpose, during spikes 2, 4 and 6, additional samples were withdrawn right after the injection of the stock solutions in order to assess the exact initial concentration of ammonia and nitrite²³. VSS analysis were done at the end of the test. The entire liquid content was filtered and incinerated.

4.2.3 Fast biomass acclimation procedure to saline conditions

The procedure described here was adopted in order to avoid saline shock effect on the biomass activity. Tannery wastewater was withdrawn from the outflow of the biological unit (figure 4.1) and characterized in terms of conductivity, chlorine, sulphates, metals, COD, ammonia, nitrite and nitrate. The conductivity observed in tannery WW was as high as 10 mS/cm and mainly related to chlorine and sulphate ions. Synthetic mineral medium used to feed the gas-lift reactor hold a background conductivity of 4,3 mS/cm and was

²² Data on SAA activity were available from previous activity tests, see chapter 3.

²³ Analysis on stock solutions were also performed. Nevertheless, since their concentration was very high and the added volume very small (1 to 3 ml), it was decided to analyse the initial concentration in the bulk liquid, in each bottle, after the pulse injection. Such a procedure was deemed more accurate for the nitrogen balance, compared to the concentration estimation from the added volume.

prepared according to van der Graaf (1996), except for the sodium bicarbonate that was dosed to 0,4 g/l. A saline synthetic medium was prepared by adding chlorine (as NaCl and KCl, in a 1:1 ratio) and sulphate (as Na₂SO₄) to the synthetic mineral medium in order to achieve the same conductivity of tannery WW. The ratio Cl:SO₄ ions was kept as close as possible to the one observed in the real WW. A total of 10 saline solutions (around 300 ml each) were prepared by diluting the saline synthetic medium with different ratio of distilled water. The saline solutions had increasing conductivity levels starting from 5 mS/cm to 10 mS/cm (targeted conductivity, i.e. real wastewater conductivity), with a progressive increase of 0,5 mS/cm. All the solutions were kept at room temperature (21-24 °C). Fresh granular biomass was withdrawn from the anammox reactor and acclimated to room temperature in a 300 ml, with (non-saline) synthetic medium. A step-wise exposure procedure towards increasing saline conditions was implemented. At each step, supernatant was removed and granular biomass poured into the saline solutions at increasing conductivity. The maximum conductivity increase at each step was around 0,5 mS/cm and biomass was left to acclimate for a minimum of 20 minutes prior to be poured in the saline solution with higher conductivity. Once the biomass was exposed for more than 20 minutes to the last saline solution (10 mS/cm) the acclimation procedure was considered concluded. The overall acclimation procedure lasted around 5 and half hours.

The aliquot of the withdrawn biomass used to seed the non-saline control test was left at room temperature in non-saline synthetic medium during the duration of the acclimation procedure, in order to avoid activity discrepancies due to temperature gradients, between the acclimated and the not-acclimated biomass.

4.2.4 Analytical measurements and microbial analysis

Ammonia, nitrite, nitrate and COD were analysed spectrophotometrically, through commercial kits. Further analysis on Chlorine, Sulphate and Phosphate ions were conducted through Ionic Chromatography (IC). Inductively coupled plasma optical emission spectrometry (ICP-OES) analyses on tannery WW were performed during the second inhibition test to characterize possible inhibitory metal elements. TS-VS and TSS-VSS analysis were performed according to standard methods (APHA, 2005).

At the end of the first inhibition experiment, biomass from the six bottles was sampled and processed for molecular analysis, according to the procedure described in section 2.4.

4.3 Results

4.3.1 Preliminary reactivation experiment

Overpressure production and nitrogen consumption were observed since the very first days of the experiment. Nevertheless, heterotrophic denitrification and biological processes other than anammox were deemed the main responsible for the observed overpressure in the first 4 days (data not shown). From day 5 on, the ratio on the consumed nitrite and ammonia, started to level off to values close to anammox stoichiometry. In figure 4.7, the SAA activity registered from day 5 to day 16 is reported. Average values are reported together with the standard deviation (calculated over the triplicate values). It owns to be mentioned that one of the three bottles (namely, bottle R3) showed to be generally more active than the other two and this is the reason why standard deviation depicts a wide variation over the triplicate. Such a higher activity remained so also in the subsequent inhibition experiment²⁴. It can be observed that SAA increase gradually over the days and that a significant increase in SAA was observed from day 9 to 13, during which a stable temperature of 30°C was ensured. The high SAA registered after incubation at 30°C showed a $\text{NO}_2^-_{\text{rem}}/\text{NH}_4^+_{\text{rem}}$ higher than 1,5 mgN/mgN, suggesting a possible concomitant increase of heterotrophic denitrifiers activity. In day 14 and 15, a sharp decrease in temperature was caused by a temporary failure of the heating system (experiment were conducted in January). Excluding such high stoichiometric values, on average, during the reactivation experiment the observed $\text{NO}_2^-_{\text{rem}}/\text{NH}_4^+_{\text{rem}}$ $\text{NO}_3^-_{\text{prod}}/\text{NH}_4^+_{\text{rem}}$ ratios were $1,4\pm 0,7$ and $0,1\pm 0,3$ mgN/mgN, confirming the prevalence of the anammox process. The value registered on days 14 and 16 were in line with those observed on day 6-9 and an average SAA of $0,04\pm 1$ gN- NO_2^- /gVSS/d was considered as reference value for the reactivated biomass. Indeed, it was confirmed in the subsequent inhibition experiment.

A remarkable result of the reactivation experiment was the very fast reactivation of the biomass after 10 months of storage. Reactivation experiment confirmed that the storing procedure adopted in the present work was successful since it allows a fast biomass reactivation within two weeks. This result was further validated during the fast start-up of the anammox gas lift reactor described in chapter 3.

²⁴ During the 10-month storage, the biomass stored in bottle B3 (used to inoculate the manometric bottle R3 first, and CT3 and TWT3 in the inhibition experiment) was the only one that never showed low nitrate levels nor bad odour or colour and probably kept more active than the one stored in the other two bottles.

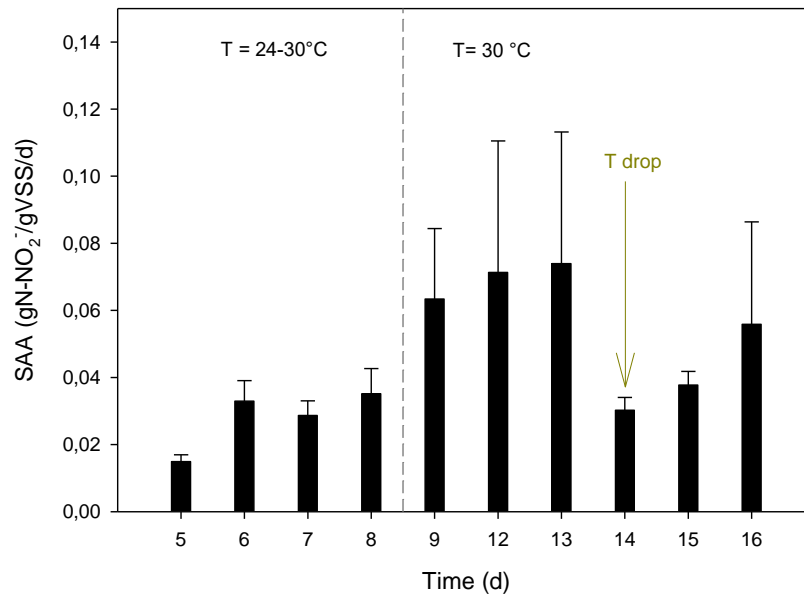


Figure 4.7 SAA values observed in the reactivation experiment.

4.3.2 First inhibition experiment

On day 18th, the first inhibition experiment started. In phase 1, biomass in TWT bottles was re-suspended in a mixture of synthetic medium and real WW, $\frac{3}{4}$ and $\frac{1}{4}$ of the total liquid volume, respectively. Table 4.2 reports the composition of tannery WW used in the four phases.

Table 4.2 Pre-treated tannery wastewater used in the inhibition test, during phases 1 to 4.

Parameter	Phase 1	Phase 2	Phase 3	Phase 4
pH	7,86	7,24	7,6	7,6
Conductivity (mS/cm, at 25°C)	11,1	11,1	11,3	11,7
COD _{filt}	442	468	450	420
NH ₄ ⁺ (mgN/l)	<1	<1	<1	<1
NO ₂ ⁻ (mgN/l)	<1	<1	<1	<1
NO ₃ ⁻ (mgN/l)	3,7	5,9	9	6,8
Cl ⁻ (mg/l)	2750	2950	3630	3326
SO ₄ ⁻ (mg/l)	1580	1660	2060	1780

Figure 4.8 shows the SAA observed in the CT and in the TWT, over the four experimental phases. The lower values observed in the control test, on days 23, 26 and 27 are due to the fact that the manometric data on bottle 3 (the one with the highest SAA) were accidentally lost; as a consequence, the average values result in a lower values compared to values in the previous and following days. It can be clearly observed that SAA from CT and TWT remains comparable in phase 1 and phase 2 of the experiment, suggesting that tannery WW did not show any detrimental effect, at dilution ratios of 1:4 and 1:2. From day 34 on, a gradual and continuous decrease in SAA activity was shown either by the CT and the TWT triplicate until a dramatic decline registered on day 64, with a 90% SAA decrease compared to values observed on days 30-34. Since biomass activity deterioration was observed equally in the CT and TWT tests, inhibition effects related to tannery WW were excluded. CO₂ limitation was deemed responsible for such a dramatic SAA drop. From day 26 on, atmosphere change in the bottles' headspace was conducted by mean of pure N₂ gas, instead of a mixture of N₂/CO₂, as in the previous days of the experiments. Severe CO₂ stripping is ascribed to repeated N₂ flushing. A posteriori analysis on pH trend confirmed such a hypothesis, since pH in the bottles gradually increased from 7,7±1 on days 33-34 to 8,2±1 on days 60-64. According to the equilibrium reactions of carbonates, CO₂ stripping causes a direct consumption of H⁺, and, ultimately pH increase. From day 64 on, the mixture of N₂/CO₂ was restored and a gradual though slow SAA improvement was observed (data not showed).

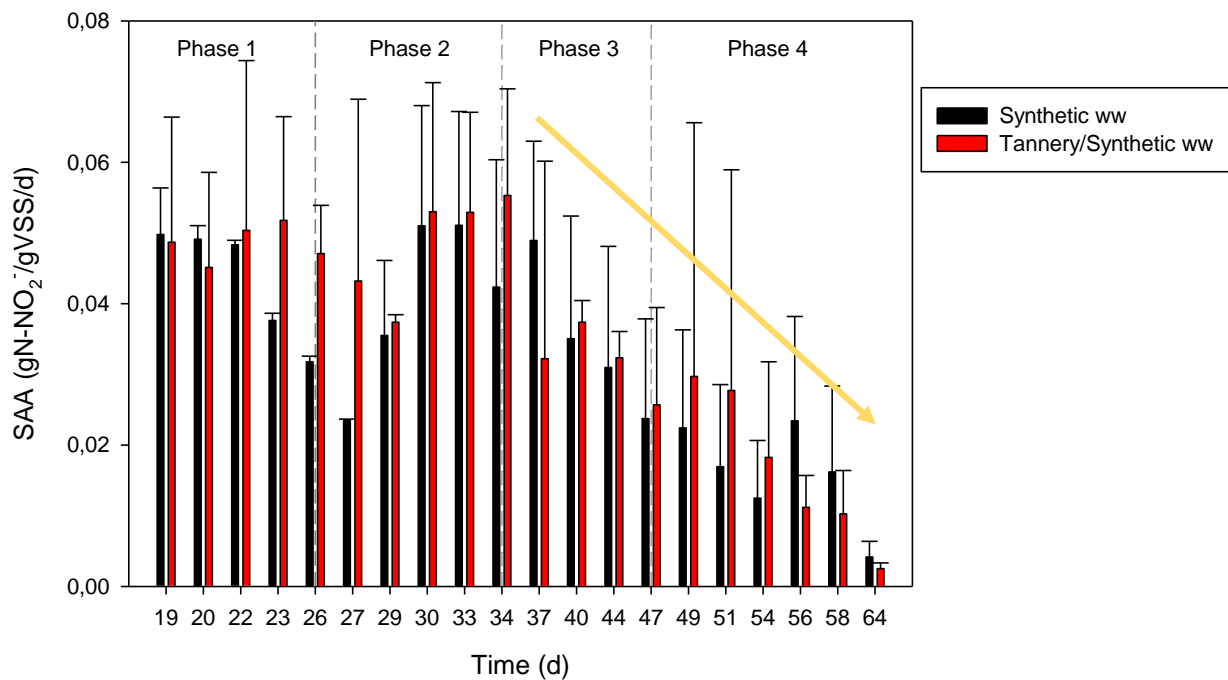


Figure 4.8 SAA values from the first inhibition test.

Even though the last part of the experiment suffered from inorganic carbon limitation, some general conclusions can be drawn. Table 4.3 presents the observed SAA values during each phases; values are presented in such a way to compare each TWT bottles with the corresponding CT (CT1 vs TWT1, CT2 vs TWT2, CT3 vs TWT3). It can be clearly observed that in phase 1 and phase 2, SAA registered in the CT and the corresponding TWT bottle is totally comparable and as high as 0,04-0,06 gN-NO₂⁻/gVSS/d. Each couple of CT and TWT continues to show a comparable behaviour also during phase 3 and phase 4. The extent of the observed SAA decline is, in fact, the same in each CT and TWT couple. Thereby, it can be concluded that the cause of biomass activity reduction is not related to the tannery WW. Stated in other words, no clear inhibition due to tannery WW was observed, after 40 days of (gradual) exposure.

Table 4.3 Comparison of SAA values in CT and the corresponding TWT, at each phase of the 1st inhibition samples.

SAA gN-NO ₂ ⁻ /gVSS/d									
		P1		P2		P3		P4**	
CT1	TWT1	0,04±0,01	0,04±0,01	0,03±0,01	0,04±0,01	0,03±0,01	0,04±0,01	0,01	0,01
CT2	TWT2	0,04±0,01	0,04±0,01	0,03±0,01	0,04±0,01	0,02±0,01	0,03±0,01	0,01	0,01
CT3	TWT3	NA *	0,06±0,01	0,06±0,01	0,06±0,01	0,05±0,01	NA*	0,03	0,03

* Not Available: manometric data from CT3 (phase1) and TWT (phase 3) were accidentally lost

** Standard deviation values < 0,01

4.3.3 Second inhibition experiment

Table 4.4 reports the analytical composition of the pre-treated wastewater; pH was 7,5 and conductivity 10 mS/cm. The saline synthetic solution achieved a Chloride and Sulphate concentration of 2100 mgCl⁻/l and 1400 mgSO₄⁻/l, respectively. Chloride concentration was slightly lower than the one of the tannery WW, but were sufficient to achieve a conductivity of 10 mS/cm since the background conductivity of the synthetic medium was as high as 4 mS/cm. Analysis on metals concentration showed that none of the element presented inhibitory levels.

Table 4.4 Tannery (pre-treated) wastewater used in the 2nd inhibition experiment.

Parameter	Concentration [mg/l]
COD _{tot}	451
COD _{filtered}	400
N-NH ₄ ⁺	0,6
N-NO ₂ ⁻	<0,1
N-NO ₃ ⁻	2,2
Cl ⁻	2750
SO ₄ ⁻	1370
Cu	0,02
Cr	0,31
Ni	<DL*
Pb	0,5
B	0,5
Cd	<DL*
Al	0,11
Zn	0,17
Fe	1,51
P	0,47

*lower than the Detection Limit (DL)

Figure 4.9 shows the results of the SAA values observed in the three tests, at each of the 6 consecutive spikes. Average values and standard deviation are reported for each duplicate. Nitrogen balance closed within a 10% error²⁵. Thereby the manometric procedure implemented confirmed to be reliable and robust. It can be observed that the control test (CT) keeps the highest activity throughout the experiment. SAA in CT showed its maximum values after spikes 3, 4 and 6, during which nitrite and ammonium concentrations were around 75 mgN/l, higher than in the other spikes where reached around 40 mgN/l²⁶.

²⁵ The amount of N₂ (mgN) estimated from manometric data was compared with the expected N₂ estimated from NO₂⁻ (mgN) removed in the liquid phase, according to the stoichiometry from Lotti et al. (2014b).

²⁶ When measurement on the initial concentration were not performed, values were estimated according to the added volumes of the stock solutions.

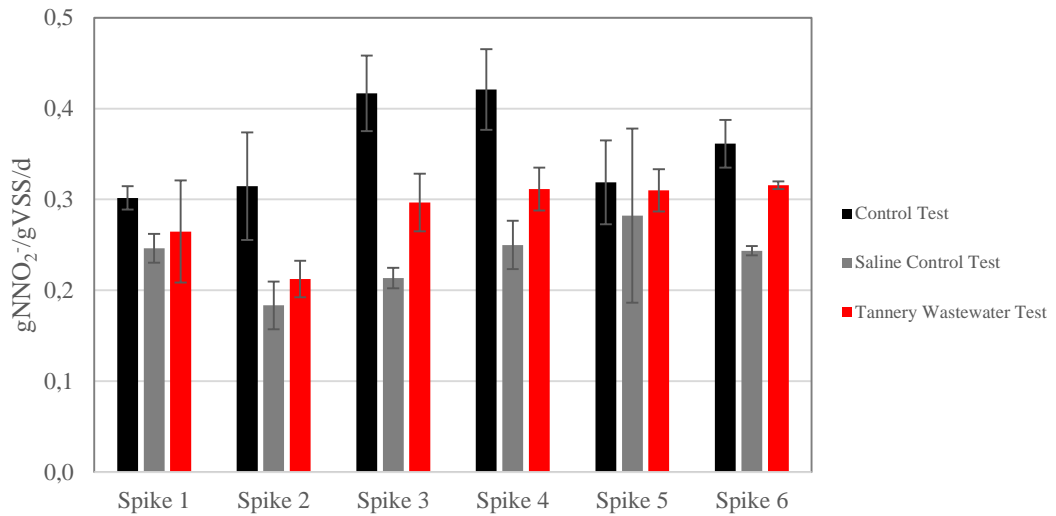


Figure 4.9 SAA results from 6 consecutive spikes of nutrients.

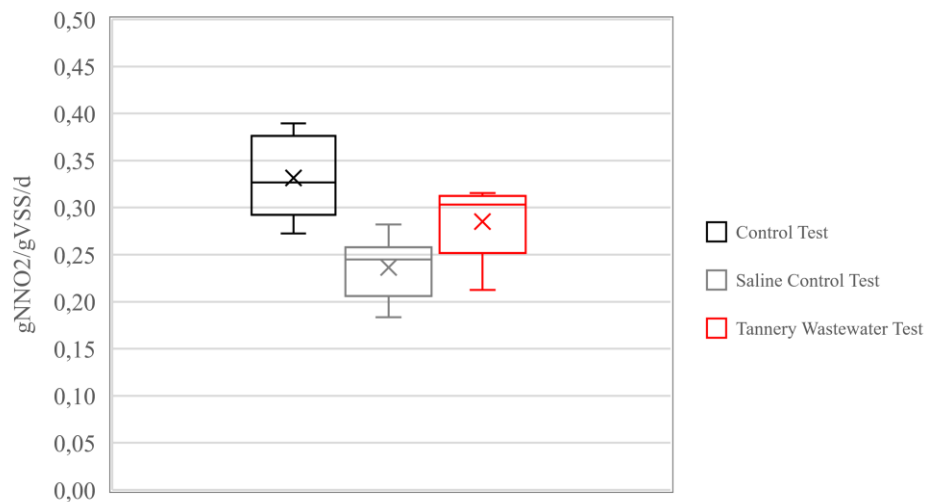


Figure 4.10 Box-and-whisker plot of SAA activities for the three tested conditions (median, internal line; mean, internal cross).

In figure 4.10, box-and-whisker plot of the SAA values obtained in each of the three series of data is reported. Considering average values and comparing to control test, SAA in saline control test and tannery WW test showed a decrease of 28% and 14%, respectively. The stoichiometry observed in each test is reported in table 4.5 (values estimated for spike 2, 4 and 6). As it can be observed, TWT is the one presenting a higher variation

either in $\text{NO}_3^-/\text{NH}_4^+$ ratio and in the $\text{NO}_2^-/\text{NH}_4^+$ one. COD analysis were performed prior to the 5th pulse and at the end of the test in order to assess possible heterotrophic denitrification. COD_{filt} resulted in 372 ± 4 and 364 mg/l in the intermediate and final analysis, respectively. Thereby ca 30 mg/l of COD_{filt} were removed (COD_{filt} at initial value was 400 mg/l) from the initial and the intermediate time, whereas COD remained quite stable from the 5th spike until the end of the test. The average value of $\text{NO}_2^-/\text{NH}_4^+$ ratio for test TWT was higher than the one observed in test CT and SCT, suggesting a possible impact of heterotrophic denitrification, due to a higher NO_2^- removal than the stoichiometric one. In case of concomitant heterotrophic denitrification, SAA activity would be overestimated since a fraction of the N_2 would be produced by denitrifying rather than anammox biomass. Nevertheless, N_2 balance closed with a 10% error, suggesting that such an impact was likely to be of minor extent.

Table 4.5 Observed stoichiometry in the 2nd inhibition experiment.

Test	$\text{NO}_3^-_{\text{prod}}/\text{NH}_4^+_{\text{rem}}$ mgN/mgN	$\text{NO}_2^-_{\text{rem}}/\text{NH}_4^+_{\text{rem}}$ mgN/mgN
CT	$0,15 \pm 0,06$	$1,44 \pm 0,32$
SCT	$0,13 \pm 0,02$	$1,42 \pm 0,31$
TWT	$0,21 \pm 0,13$	$1,61 \pm 0,47$

Filtered COD of pre-treated tannery WW is mainly due to dispersed or colloidal organic fractions, mainly tannins, a recalcitrant fraction that exits the biological unit, even under extensive aeration conditions (high SRT). In the Cuoidepur WWTP, such a high content in filtered COD is removed through chemical precipitation prior to effluent discharge. According with personal communication with plant process manager and the UNIFI research group working since many years with tannery wastewater at Cuoidepur WWTP, sudden COD depletion has been observed in several occasions when pre-treated WW was dosed in activated sludge lab-scale reactors. Such a fast depletion has been ascribed to adsorption phenomena more than to fast biodegradation due to the recalcitrant nature of the suspended organic matter as well as the physical properties of colloidal particles. The evidence that COD_{filt} remains almost constant in the last two days of the test, confirms such an assumption. As a conclusion, it cannot be excluded that heterotrophic denitrification partially contributed to the observed N_2 production, but it is reasonable to think that its contribution was of minor extent. Indeed, this might be an explanation to the fact the TWT showed a slightly higher SAA than the SCT.

Results from the second inhibition experiments confirmed the general conclusion drawn from the first inhibition experiment: tannery wastewater does not show any clear inhibition effect on anammox granular biomass.

4.3.4 Molecular analysis

Figure 4.11 shows the result of molecular analysis performed on biomass withdrawn at the end of the first inhibition test, in terms of relative abundance at class and genus level. The three biomass samples withdrawn from the control test bottles (CT1, CT2, CT3) showed almost the same composition at both taxonomic levels. A similar correspondence can be observed for the TWT triplicate even though sample TWT3 differed for a much higher relative abundance of *Nitrospira* (17% at class and genus level) compared to TW1 and TW2 (around 2-3%), this higher *Nitrospira* relative abundance in TWT3 is outbalanced by a lower relative abundance of an Undefined Bacteria (12% in TWT3 and 30% in TWT1 and TWT3). The values of the relative abundance of the other species were comparable among the triplicate. Apart from this discrepancy, the results in the two triplicates are consistent and comparable. This evidence suggests that reliable qualitative information can be derived from molecular analysis even when technical or sample replicates are not conducted. In the following paragraphs, results are discussed as triplicate average values.

At class level (fig. 4.11a), both CT and TWT showed Undefined bacteria as the most abundant one, with a relative abundance of $26\pm 2\%$ and $24\pm 10\%$, respectively; unfortunately, no further classification was possible apart from the domain. Planctomycetes showed a relative abundance of $24\pm 3\%$ and $9\pm 1\%$, in the CT and TWT, respectively. The reduction of Planctomycetes abundance in TWT compared to CT can be partially ascribed to the increase in relative abundance of other classes.

The same is observed at genus level, consistently. The Undefined Bacteria showed the highest relative abundance both in CT and TWT, with a $26\pm 2\%$ and $24\pm 10\%$, respectively, also at genus level. *Ca. Brocadia* was the second most abundant genus in the CT, with a relative abundance of $22\pm 3\%$, whereas the relative abundance in TWT was $7\pm 1\%$. The decrease in *Ca. Brocadia* relative abundance must be read together with the increase of the relative abundance of other genera. Specifically, compared to CT values, Poribacteria_genera_incertae_sedis, Rhodocyclaceae (undefined genus) and *Nitrospira* showed an increase in the corresponding relative abundance of 3, 4 and 3%, respectively. Tannery wastewater used for the TWT was withdrawn at the exit of the secondary settler of Cuoiodepur WWTP, whose biological unit is operated at very high SRT (ca. 100 d), promoting a high microbial diversity. Exogenous population as well as different composition in the liquid medium (especially in terms of COD) are likely to be the causes of the moderately different profile in genus distribution between CT and TWT. *Ca. Brocadia* has been reported to be outcompeted by *Ca. Kuenenia*, under extended salinity conditions (Huang et al., 2021). *Ca. Kuenenia* and *Ca. Scalindula* are the genus reported to have higher tolerance to high salinity (Oshiki et al., 2016; Li et al., 2018). In the present work, *Ca. Brocadia* remains the far predominant anammox genera after around 40-day exposure to moderate saline conditions.

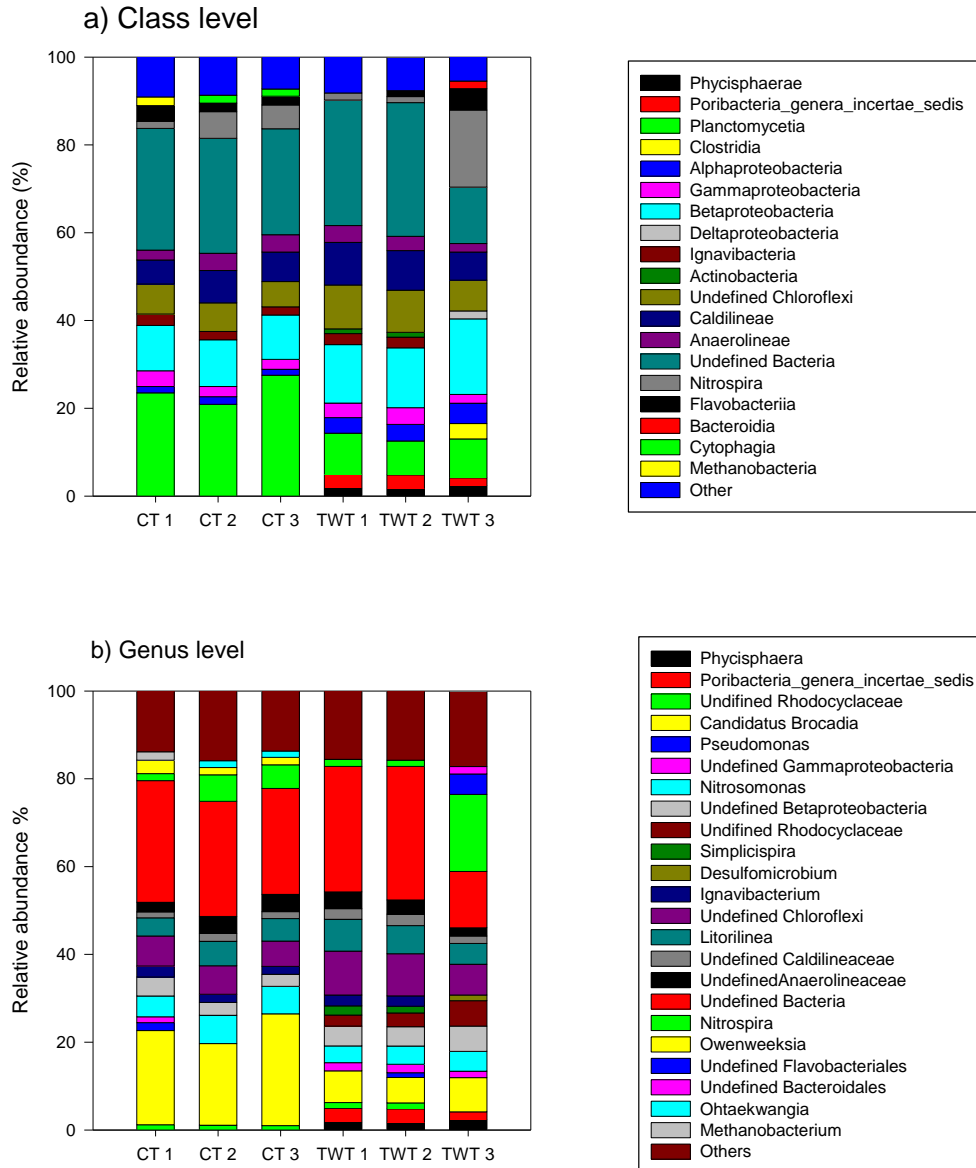


Figure 4.11 Microbial analysis results on biomass withdrawn at the end of the 1st inhibition experiment. CT, Control Test triplicate; TWT, Tannery Wastewater Test triplicate.

4.3.5 Discussion

The results from both the inhibition experiments suggest that the application of the anammox process to vegetable tannery wastewater has no technical limitation. According to the outcomes from the 2nd inhibition experiment, salinity more than tannins seems to show a potential inhibitory effect. Tannery wastewater considered in the present study presented a chloride concentration of around 3 gCl⁻/l, corresponding to an equivalent NaCl concentration of ca 5 gNaCl/l. In the scenario in which anammox process would be applied to treat only the industrial wastewater collected to Cuioidepur WWTP, chloride concentration would be around

6 gCl/l, equivalent to 8 gNaCl/l. Such threshold concentrations, as gNaCl/l, are considered in the present discussion. Dapena-Mora et al. (2010) and Kartal et al. (2006) reported a conducive effect of moderate salt concentrations (5-6 gNaCl/l) on not acclimated biomass, whereas Jin et al. (2011) reported the same positive effect on acclimated biomass and around 70% SAA reduction in not acclimated biomass after shock exposure of few days to the saline condition. In the present work, a 30% SAA reduction was observed in the SCT (2nd inhibition experiment), holding a comparable saline concentration as the mentioned studies. It is believed that the acclimation procedure adopted in the present work was effective to prevent severe and transient SAA reduction due to saline shocks and that the observed reduction is likely to be further attenuated in case of long-term exposure to the moderate saline level of pre-treated tannery wastewater as reported by several works in literature (Kartal et al., 2006; Dapena-Mora et al., 2010; Ma et al., 2012). Also, a longer adaptation period would have been conducive for a better biomass activity response in the inhibition experiment, since the acclimation time was much shorter than the one reported in similar studies (5,5 hours versus 12h to few days). Since the shock effect of sharp gradients in salinity concentration was not the objective of the present work, the fast acclimation procedure proved to be an effective solution to avoid transient responses to saline shocks.

Another interesting aspect of long-term salinity exposure is the impact on granules morphology and composition. Fang et al. (2018) and Zang et al. (2019) recently published two comprehensive studies aimed at untangling mechanisms of anammox granulation response to high salinity levels. Specifically, the long-term effect of saline exposure on anammox granular biomass have been studied in terms of granule dimensions, EPS content and composition, metal ions distribution on the anammox granular biomass exposed to 0, 15 and 30 gNaCl/l. Fang et al. (2018) did not observe changes in granule dimension with the increasing salinity levels (compared to the freshwater control reactor), opposite to what observed by Zang et al. (2019) where a clear dimension reduction was observed at the same saline gradients. Both studies agreed in the general conclusion that high salinity levels (15 and 30 gNaCl/l) are not beneficial to granulation, due to many factors that can be synthesized as follows:

- The total EPS content of granular biomass did not vary with salinity, whereas EPS composition changed remarkably. As the salinity increased, polysaccharides (PS) content increased and the protein content (PN) decreased. As reported by the authors, PS are hydrophilic water-retaining polar molecules whose higher production is an effective response to high osmotic pressure to prevent water loss whereas PN exhibits hydrophobic properties. The decrease in PN content lead to an overall decrease in granule hydrophobicity, hindering granulation mechanisms.
- Ionic strength due to metal cations is usually reported as conducive to biomass aggregation into granules up to 0,1-0,2 M since it reduces electrostatic repulsion due to the free energy layer on the granule surface; at higher values, led by massive Na⁺ addition in their studies, authors observed the opposite effect. A possible explanation would be that Na⁺ substitute to Ca²⁺ ion, which is involved in

bridging mechanism within PS molecules. Similarly, hydrogen bonds, that are important player in EPS aggregation, lowered with increasing salinity.

The salinity levels considered by Fang et al. (2018) and Zang et al. (2019) are much higher than the one considered in the tannery WW in Cuoiodepur WWTP, either pre-treated (and diluted) or not. Nevertheless, such evidences and possible mechanisms should be considered in case of real-scale implementation in order to ensure stable process performance.

4.4 Conclusions

Results from batch tests on stored and fresh biomass as well on biomass acclimate and not-acclimated to saline conditions consistently indicate that there is no evident inhibition of anammox biomass due to exposure to vegetable tannery wastewater.

Despite the fact that the first inhibition test suffered from CO₂ limitation, the comparison between the control test and the one conducted with tannery wastewater indicate that no further adverse effect could be ascribed to the industrial matrix. Also, in line with the results reported in Chapter 3, another remarkable result is related to the very fast biomass reactivation obtained in the preliminary test, confirming that the applied storage procedure successfully kept a significant residual anammox activity, even after almost one year of storage. This finding is deemed relevant as proper biomass storage can be a practical and effective solution for fast reactors' start-up or rescue in case of system failure, at real-scale conditions.

Results from the second inhibition test indicated that salinity more than the mix of bio-refractory organic compounds is likely to be the disturbing factor of anammox biomass activity, since a 28% and 14% decrease in biomass activity was observed in the saline test and tannery ww test, compared to the non-saline control test. Nevertheless, biomass acclimation is widely reported to be sufficient to increase anammox activity under saline conditions and high anammox activities are likely to be achieved.

Further study on long-term exposure, through continuous pilot-reactor operations are suggested as future developments. Analyses on microbial population as well as on granule's morphology and EPS composition are recommended in order to produce comprehensive studies conducive for the real-scale implementation of the anammox process.

CHAPTER 5.

Successful nitrite accumulation over sulphide oxidation in a SRT-controlled CSTR

5.1 Introduction

The link between sulphur-based autotrophic denitrification and anammox processes lays at the very beginning of the anammox story, since the discovery of the most important process in biological nitrogen removal of the past 30 years comes from a theretofore unclear nitrogen consumption in a denitrification reactor treating a sulphide rich stream. Nitrite necessary for the anammox process was, indeed, provided by the nitrate reduction through sulphur-based denitrification. Despite that evidence on the actual feasibility of a combined process, little attention has been paid on the potential of coupling sulphide-driven partial autotrophic denitrification (PAD) and anammox (AMX or A) and, even less, on the feasibility of achieving stable nitrite accumulation over sulphide oxidation as a possible pre-treatment for anammox (Liu et al., 2017; Chen et al., 2018). The reason is probably the combination of multiple factors: (i) sulphide is present mainly in few types of industrial wastewaters, and in a narrower range of them, both high nitrogen and sulphide loads are encountered; (ii) autotrophic denitrification is still not widely applied for biogas desulphurization and (iii) nitrite competition between denitrifying sulphide oxidizing bacteria (SOB) and AMX together with high sulphide toxicity for AMX biomass are possibly among the main problems hampering a combined process implementation. In the perspective of PAD/A implementation, a two-stage configuration could provide stable and controlled nitrite accumulation through partial autotrophic denitrification or more precisely, sulphur-driven complete denitratation, for a subsequent anammox treatment, avoiding the risk of (irreversible) sulphide toxicity. Among the few works that explicitly challenged a stable nitrite accumulation over S-oxidation (either as sulphide, sulphur or thiosulfate), S/N ratio is recognised as a crucial parameter to achieve nitrite accumulation, together with HRT and sulphur loading rate (the latter two being often related). In systems where HRT is uncoupled from SRT (like biofilm systems, either granular or biofilm-based), system breakpoint has been reported at decreasing HRT. This failure might be either appointed to overload conditions (i.e. rate limitation) or sludge washout in case of upward flows, this latter case suggesting a SRT influence instead. Much more attention has been paid on combining heterotrophic denitrification (HDN) and anammox processes, and successful works have achieved one-stage processes combination, with the main aim of removing the residual nitrate produced by the anammox process by HDN, thereby increasing the total nitrogen removal efficiency (Chen et al., 2018; Qian et al., 2018). Though, high substrate competition and possible heterotrophic denitrifiers overgrowth over AMX biomass as well as possible residual COD in the effluent seem to be the main drawbacks of such a system. Kinetics of denitrifying SOB biomass are generally known to be very fast, thanks to the high energy yield of sulphide as e- donor (ED). Maximum growth rates are reported to be 1-3 d⁻¹ (Campos et al., 2008) in fact comparable with heterotrophic denitrifiers rate. Moreover, the autotrophic nature of SOB allows for low biomass productions, holding biomass yields of 0,3-0,6 gVSS/gN, rather than 0,8-1,3 gVSS/gN typical of heterotrophic denitrifiers (Campos et al., 2008; Cui et al., 2019). Lower biomass yields would result in a more balanced competition between the two microbial communities while the high sulphide oxidation rate, would

promote a complete sulphide oxidation, preventing toxicity. Nitrite accumulation is often reported in continuous or batch operations as a temporary and undesired consequence of e-donor limitation or overload conditions (Manconi et al., 2007; Campos et al., 2008).

In the present chapter, the result on the operation of a SRT-controlled CSTR reactor fed by nitrite and sulphide is presented. The experimental work was intended to challenge a stable nitrite accumulation over nitrate reduction and complete sulphide oxidation to sulfate. The study focussed on the effect of influent S/N ratio and SRT on achieving stable partial autotrophic denitrification. Monitoring of microbial population, N₂O emissions and biomass specific activities was carried out for a more comprehensive understanding of the system performance.

5.2 Material and methods

5.2.1 Reactor operation

A 2,5-liter glass CSTR reactor was operated for 115 days (reactor 1, R1, figure 5.1). A detailed description of the instrumental set-up is provided in section 2.1.2. As inoculum, a SOB-enriched sludge was withdrawn from a pilot-scale CSTR treating sulphide gas stream together with nitrate/nitrite rich stream (SLR up to 2,4 gS/l/d, ca 2000-3000 ppmv of S-sulphide in the gas and 1000-3000 mgN/l in the influent). The biomass was kept at 4°C for two weeks before inoculation. A gentle agitation of 100-120 rpm was provided in order to accomplish with ideal completely mixing condition as well as with limitation of sulphide stripping. Temperature was maintained at 30±1°C, by continuously recirculating tempered water in the steel bottom jacket of the reactor. Synthetic wastewater was prepared as a modified ATCC 1255 medium (see section 2.1.2). A concentrate sulphide solution (0,06-0,18 M) was fed separately in order to avoid sulphide metal precipitation in the mineral medium tank. The sulphide solution was kept in an air-tight 2-liter browned bottle, connected to a N₂ gas pocket, in order to prevent air inlet and compensate inner depression caused by pump suction. A moderate flow of 0,1 l/min of a mixture of N₂-CO₂ (95% and 5%, respectively) was regulated by mass flow controllers and bubbled at the bottom of the reactor in order to strip away any residual/undesired dissolved oxygen and to ensure CO₂ availability to the autotrophic biomass. Influent tank and sulphide solution bottle were placed on electronic balances (with 0,1 g and 0,01 kg of sensitivity, respectively); weights were monitored daily (and even more frequently, with intermediate checks within the day) in order to assess the actual flowrates provided. Special attention was put on flowrate accuracy, since one of the main aim of the study was to assess influent S/N effect on the process. It is worth mentioning that working with sulphide concentrated solution is not a trivial exercise, due to the extreme reactivity of sulphide to chemical oxidations and its high volatility. pH was constantly monitored and set at 7,3 for the first 15 days of operation and then increased to 7,6, controlled by

adding 1 M NaOH or 1M HCl. Pumps operation, temperature, pH monitoring/control as well gas flowmeters were controlled by a centralised PLC, operating the AdD-Control software.

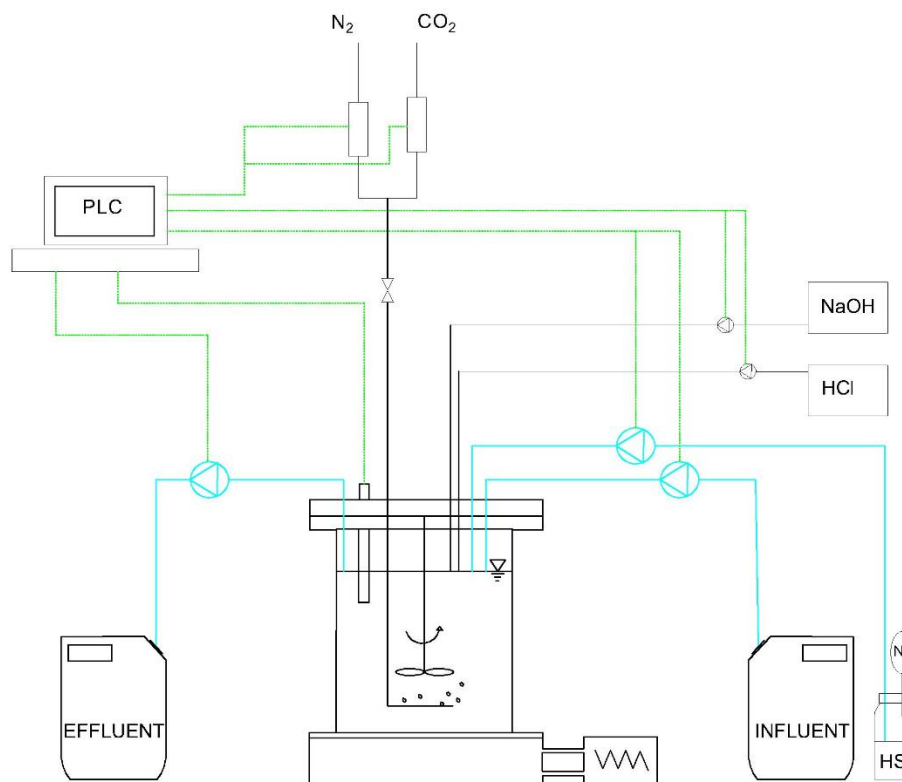


Figure 5.1 – Experimental set-up. Cyan, water line; green, probes and sensors.

The reactor was operated as an ideal chemostat, without biomass recirculation; thereby SRT was directly determined by dilution rates. Regular cleaning of reactor's internal wall and submersed mechanical stirrer and tubes was performed in order to remove any possible biofilm formation that could have altered the actual SRT. As a matter of fact, biofilm formations were never relevant but cleaning operations were done anyway as a precautionary measure.

After 115 days of operation, reactor R1 was emptied and a second reactor, R2, was inoculated with the sludge from reactor 1 and operated for ca 30 days, in continuity with reactor 1 (operational days 116-150)²⁷. The experimental set-up was the same apart from the following conditions: liquid volume was 3,5 litres; temperature was not controlled and ranged $22\pm 2^\circ C$; mixing was ensured by a magnetic stirrer and ORP was monitored continuously. Monitoring of the R2 performance was done two to four days per week.

²⁷ Reactor change was due to technical problems in reactor R1.

5.2.2 Experimental conditions

The strategy adopted to promote partial denitrification, with a concomitant complete oxidation of sulphide to sulphate, was based on the main evidences reported in literature regarding the paramount role of: influent S/N ratio, short HRT and nitrite inhibition on the NO_2^- - N_2 step. Specifically, e-donor limiting conditions are acknowledged to promote (temporary) nitrite accumulation (van den Bosch et al., 2007; Lin et al., 2018). Considering the following catabolic reactions:



S/N ratios values of 1,43 and 0,57 gS/gN are required for a complete oxidation of sulphide over a complete or partial reduction of nitrate, respectively. Thereby, we considered these two values as the upper and lower limits of the S/N range to be evaluated. Influent S/N was always kept below 1,43 gS/gN, in order to prevent complete denitrification, while a minimum of 0,57 gS/gN was ensured in order to provide sufficient e-donor to convert all the influent nitrate to nitrite. Catabolic ratios, rather than full-metabolic ones, were considered since full stoichiometry for SOBs is not straightforwardly defined as discussed elsewhere (see Chapter 6). Applied operational conditions are summarised in table 5.1. Phase 1, 2 and 3 were planned to test three SRT, starting from 40 h to 23 to 13 h and a range of S/N ratio, from strictly limiting to slightly limiting condition for the e-donor. SRT halving at each phase, was achieved by doubling influent flowrate; nitrate concentration in the mineral medium was kept at 200 mgN/l throughout the experimental period whereas sulphide concentration in the concentrated solution was set according to the required S/N. Therefore, each phase change implied a concomitant doubling in NLR (from 0,1 to 0,2 to 0,4 gN/l/d).

Table 5.1 Applied operation conditions in reactor R1.

	Operational days	SRT h	S/N g/g	NLR gN/l/d
Phase 1	1-51	40±2	0,73±0,06	0,11±0,01
Phase 2	52-93	23±1	0,65±0,12	0,20±0,01
Phase 3	94-115	13±1	0,96±0,20	0,38±0,05

Moreover, after nitrite accumulation was achieved, the role of high nitrite level in inhibiting the denitrification step was also addressed. Nitrite is a potential inhibitor of wide range of microorganism and there is general consensus on the fact that the actual cytotoxic role is played by its conjugated acid species, free nitrous acid

(FNA). Although the inhibition mechanisms on denitrifiers are still object of discussion, it is often reported that the major mechanism is due to enzymatic inhibition of nitrite reductase, as well as on N_2O reductase, the latter being responsible for possible N_2O emissions (Zhao et al., 2011). The denitrification step is reported not be hindered by high nitrite (or FNA) levels and, thereby, it is speculated that no enzymatic disturbance occurs for nitrate reductase (Mora et al., 2014a; Cui et al., 2019). FNA concentrations were calculated, either in the continuous experiment and in the respirometric tests, according to the following equation (Anthoniesen et al., 1976):

$$FNA = \frac{NO_2^-}{k_a * 10^{pH}} \quad \text{Eq. 5.3}$$

where $k_a = e^{\left(\frac{-2300}{273+T}\right)}$, FNA and NO_2^- are expressed as nitrogen and T as °C. Since nitrate concentration in the mineral medium was set and kept at 200 mgN/l, in case of total conversion to nitrite (i.e. 200 mgN- NO_2^- /l in the effluent at steady state conditions)²⁸, the corresponding FNA at slightly alkaline pH would fall in the reported inhibitory range 2-8 $\mu\text{gN/l}$ (Zhou et al., 2007; Qian et al., 2016; Cui et al., 2019). Higher influent nitrate concentrations were discarded in order to avoid excessive inhibitory conditions and possible collateral drawbacks. Figure 5.2 reports FNA concentration over the pH range 6-9, for three nitrite concentrations; red dotted lines define the upper and lower limits of the inhibitory range reported in literature.

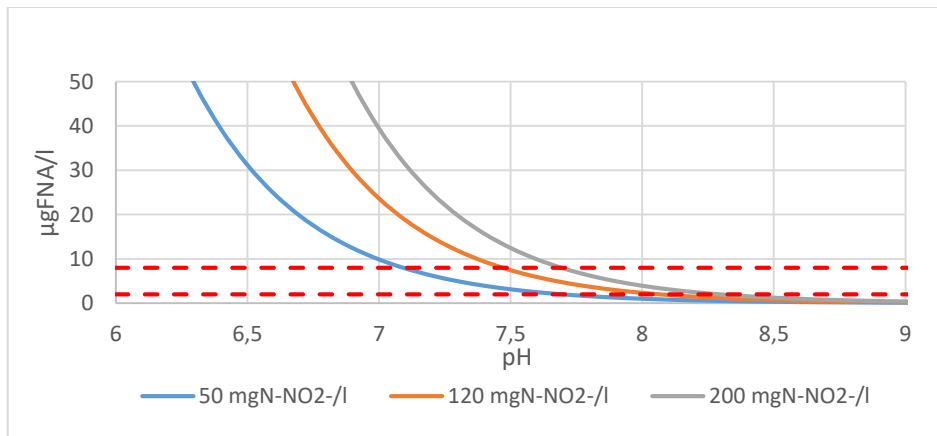


Figure 5.2 FNA concentration at 50, 120 and 200 mgN- NO_2^- /l as a function of pH (range 6-9), at $T=30^\circ\text{C}$. Red dotted lines indicate the inhibitory range reported in literature.

²⁸ The flowrate of the mineral medium was the far predominant contributor of the total influent flowrate. To be rigorous, the actual concentration in the reactor were diluted by a 5% compared to the concentration in the mineral medium due to the mixing with the sulphide concentrated solution flow, whose contribution in terms of influent flowrate was minor compared to the mineral medium. Mass balance and all the results are based on actual fluxes.

5.2.3 Process performance assessment

Nitrate removal efficiency (NRE) was expressed as the net nitrate removal between influent and effluent concentrations; nitrite conversion efficiency (NiCE) as the nitrite production over the removed nitrate; nitrite accumulation efficiency (NiAE) as the nitrite production over the influent nitrate and the dinitrogen gas production efficiency (dNPE) as the gaseous nitrogen produced over the influent nitrate. The mathematical formulations for efficiencies calculations are as follow (being a chemostat, all the efficiencies were calculated over influent and effluent concentrations, instead of loads):

$$NRE = \frac{NO_3^-{}_{in} - NO_3^-{}_{out}}{NO_3^-{}_{in}} \quad \text{Eq. 5.4}$$

$$NiCE = \frac{NO_2^-{}_{out}}{NO_3^-{}_{in} - NO_3^-{}_{out}} \quad \text{Eq. 5.5}$$

$$NiAE = \frac{NO_2^-{}_{out}}{NO_3^-{}_{in}} \quad \text{Eq. 5.6}$$

$$dNPE = \frac{N_{2out}}{NO_3^-{}_{in}} \quad \text{Eq. 5.7}$$

Where $NO_3^-{}_{in}$ is the nitrate concentration in the influent and $NO_3^-{}_{out}$ and $NO_2^-{}_{out}$ the nitrate and nitrite concentration in the effluent (all expressed as mgN/l).

From which it derives:

$$NRE = NiAE + dNPE$$

$$NiAE = NiCE * NRE$$

and $NiAE = NiCE$, in case of complete influent nitrate conversion to nitrite.

Considering the rate of the two denitrification steps, in case of unbalance between denitrification rate, r_{dNO_3} , and denitrification rate, r_{deNO_2} , the resulting nitrite accumulation rate, r_{NiA} can be calculated as follows:

$$r_{NiA} = r_{dNO_3} - r_{deNO_2} \quad \text{Eq. 5.8}$$

the rates expressed as gN/gVSS/h.

At steady state conditions, biomass yield was calculated according to equation 5.9.

$$Y_{X/S} = \frac{VSS_{out} - VSS_{in}}{HS^-_{in} - HS^-_{out}} \quad \text{Eq. 5.9}$$

Since the reactor was fed with synthetic wastewater for all the operation, VSS_{in} was zero and VSS_{out} was the concentration observed during reactor VSS monitoring.

5.2.4 Respirometric tests

Respirometric tests were conducted in a 300 ml glass vessel, sealed with a steel lid equipped with sensor and sampling ports. The vessel was placed in a thermostatic bath ensuring constant temperature of 30 ± 0.5 °C and monitored as described in section 2.2.3. Biomass was collected the same day or the day before the test, centrifuged at 10000 rpm and concentrated ca 4 times, by resuspension in a nutrient-free medium, except for test A, in which the reactor supernatant was used for biomass resuspension. Tests were run at day 54, 94 and 102 of R1 operation and at day 123 of R2 operation. Concentrated biomass was let overnight in a closed vessel, ensuring 10-20 mgNNO₃⁻/l, in order to allow endogenous conditions at the expenses of residual elemental sulphur and, thereby, limit possible disturbance in the targeted e-donor concentration and ratios in the tests. Each test was run according to the following procedure, similar to what reported in Mora (2014). The glass vessel was filled with concentrated and re-suspended biomass, sealed and placed in the pre-heated thermostatic bath. In order to achieve anoxic conditions, a nitrogen flow of 30 ml/min was sparged in the liquid until oxygen depletion; subsequently, the diffuser was placed at the headspace to discourage air inlet and limit sulphide stripping during the test, except for test A, in which it was maintained in the liquid phase. Once the DO, Temperature and pH reached the desired values, a bicarbonate concentrate solution was spiked in order to ensure sufficient inorganic carbon during the test. The bicarbonate solution was added after the pH was stable to limit CO₂ stripping during possible acid dosing. A wake-up spike of sulphide was provided (5-10 mgS/l, in the bulk liquid), once a minimum residual concentration of nitrate (ca 10-15 mgN-NO₃⁻/l) was ensured. After one hour, a sample was taken to characterize the initial concentration of sulphide, sulphate, thiosulfate, nitrite and nitrate. Then, pulses of concentrated solutions (1 M KNO₃, 0,5 M NaNO₂, 0,2-0,4 M Na₂S·9H₂O) were added, according to the concentrations targeted as initial conditions in the test. An undesired concentration of thiosulfate was detected following the HS⁻ pulse in tests B and C. Abiotic formation from sulphide is, in fact, often reported to occur even in the sulphide salt medium itself (Visser et al., 1997; van den Bosch et al., 2007 and references therein; see also section 1.1.3). In test D, a fresh sulphide solution prepared with a recently opened Na₂S·9H₂O salt bottle was prepared in order to limit thiosulfate concentration in the test. After each nutrient pulse, samples were taken regularly (every 10 to 40 minutes, depending on the test). A volume of 2 ml of raw sample were immediately analysed for sulphide concentration, and a further volume of 1,5 ml was filtered with a 0,22 µm disposable syringe filter for subsequent analysis of the other N and S species. The

concentration of elemental sulphur was not measured directly; rather, it was derived from sulphur balance (see sec. 5.2.4.1). Total inorganic carbon was analysed at the end and randomly during the tests, in order to check that the available concentration was sufficient for biomass uptake. In fact, it always exceeded 300 mgC/l. If deemed necessary, a second spike of e-donor or e-acceptor was added, during the test. TSS and VSS were analysed at the end of the test, by filtering the entire liquid volume. In case of evident sulphur accumulation at the end of the test (whitish turbidity of the liquid phase), the biomass was kept at ambient temperature overnight in order to limit sulphur interference in the VSS characterization, under the reasonable assumption that residual sulphur bias on VSS analysis would have been more significant than the possible increase in biomass concentration, due to the very low biomass yield over the S_0 uptake (see stoichiometry in Chapter 6). The initial concentrations of e-acceptor and e-donor, for each test, are reported in table 5.2. In general, tests were conducted in over stoichiometric conditions for the e- acceptor.

Table 5.2 Initial concentration of respirometric tests.

	NO_3^- mgN/l	NO_2^- mgN/l	HS^- mgS /l	Aim of the test
Test A	86	30	20	e-acceptor competition (preliminary)
Test B	35	5	40	Maximum NUR
Test C	-	55	11	Maximum NiUR
Test D	11	121	30	NiUR and NUR at high NO_2^- concentrations

5.2.4.1 Uptake rates, mass and electron balance calculations

Uptake rates were calculated for the N and S species by linear regression of concentrations trends observed in the test and, as a general rule, only value with $R^2 > 0,95$ were considered as reliable estimations (if not specified otherwise). For each test, two phases were distinguished: phase 1 referring to sulphide and thiosulfate consumption and phase 2, for S_0 consumption. Endogenous activity was neglected since it is reported to be less than 5% of the exogenous activity (Mora et al., 2014a), as expected according to the autotrophic nature of the biomass and the relatively low biomass concentration in the tests (ca 100-150 mgVSS/l). For each of the two phases, mass and electron balances were calculated. Elemental sulphur was used as pool for closing S balance, whereas dinitrogen gas for closing N balance as follows:

$$S_0 = HS^-_{in} + S_2O_3^{2-}_{in} + SO_4^{2-}_{in} - HS^-_{out} + S_2O_3^{2-}_{out} + SO_4^{2-}_{out}$$

$$N_2 = NO_3^-_{in} + NO_2^-_{in} - NO_3^-_{out} - NO_2^-_{out}$$

all the species being expressed as mgS/l and mgN/l, respectively.

Electron balance was calculated assuming the electron donated/acquired in each catabolic half reaction, as summarized in table 5.3.

Table 5.3 Released and acquired electrons in S oxidation and N reduction half reactions.

Half reaction	Electron transferred	
HS ⁻ -SO ₄ ²⁻	2	mole-/molS
S-SO ₄ ²⁻	6	mole-/molS
S ₂ O ₃ ²⁻ -SO ₄ ²⁻	4	mole-/molS
NO ₃ ⁻ -NO ₂ ⁻	2	mole-/molN
NO ₂ ⁻ -N ₂	3	mole-/molN

Proton production rate (HPR) was calculated at the net of the abiotic contribution. During respirometric tests B, C and D, a constant flow of nitrogen gas was flushed in the headspace, determining a constant abiotic stripping of CO₂, present in the medium as bicarbonate. An abiotic test was conducted in order to estimate acidity consumption related to CO₂ stripping so that a net biological HPR could be assessed. Specifically, it was assumed that the observed protons consumption/production, HPR_{obs}, derived from acid/base addition, comprised an abiotic and a biological contribution, HPR_{abiot} and HPR_{bio}, respectively (Mora et al., 2014b), resulting in the following equation:

$$\text{HPR}_{\text{obs}} = \text{HPR}_{\text{bio}} + \text{HPR}_{\text{abiot}}$$

Confidential intervals for uptake rates, balances and derived calculations were derived from the analytical accuracy for measuring N and S species as well as VSS, respectively: 5% for species analysed in IC, 10% for sulphide and VSS as well as error propagation.

5.2.5 Analytical methods

Samples were withdrawn from the bulk liquid, almost daily (except for the weekends), filtered with 0,22µm disposable syringe and either analysed in few hours or kept at 4°C and analysed within a couple of days. Filtered samples were analysed for nitrate, nitrite, sulphate and thiosulfate by ionic chromatography. Sulphide concentration in the reactor was checked randomly over the experimental period, since from the very first days of operation, sulphide was never detected in the reactor and its complete oxidation of sulphide was confirmed by sulphur mass balance (see section 5.3.1). VSS and TSS were analysed once or twice a week. Due to the very low concentration observed, 1 to 2 litres of fresh effluent were collected and then filtered for solid characterization. From day 1 to day 50, *regular* 0,7-µm glass fibre filter (Millipore AP4004705) were used;

from day 50 on, a highly retaining glass fibre filter (Millipore APFF04700) was used instead to ensure an almost complete retention of biomass. Complete biomass retention was checked by COD and TOC analysis on filtered samples using: regular 0,7- μm glass filters; highly retaining 0,7- μm glass filters; 0,45- μm and 0,22- μm nitrate cellulose filters (data not shown).

As a complementary monitoring of process performance, N_2O emissions were planned to be measured at each phase, provided steady state conditions were achieved. Nevertheless, in phase 3, more unstable conditions were obtained and it was decided not to take the measure during this last phase, due to the high sensitivity of the N_2O sensor to sulphide. Measurements were conducted on day 78 and 81 as representative for phase 1 and on day 93, for phase 2. The sensor Unisense N_2O microsensors (equipped with Unisense Microsensor multimeter, version 2.01) was placed in the headspace of the reactor and measurements recorded for 3 to 5 hours. No measurements in the liquid phase were conducted to prevent sensor damages from residual sulphide concentrations.

5.2.6 Microbial community analysis

Biomass samples were collected at day 0 (inoculum) and at the end of each phase (days 46, 79, 114). Samples were centrifuged and the concentrated pellets were kept in DNA-free Eppendorf vials, after supernatant removal; in case DNA extraction was not performed immediately after sample collection, concentrated biomass pellets were kept at -20°C until extraction. DNA was extracted with commercial kit (Norgen, Biofilm-kit), according to the manufacturer's instructions. More information on the 16s rRNA amplicon sequencing are presented in section 2.4.

5.3 Results

5.3.1 Successful NO_2^- accumulation

In figure 5.3, the results on R1 operation are reported. The first 15 days of operation (phase 1a) were characterized by highly variable influent S/N, due to technical problems mainly related to the fine tuning of the concentrated sulphide solution pump and of the consequent desired S/N ratio. Since inoculum biomass was not diluted nor washed prior to inoculation, initial concentrations of solids, nitrite, nitrate and sulphate were one order of magnitude higher than those achieved at steady state conditions due to higher loading conditions in the mother reactor. The main findings of reactor operation, at each phase are reported in table 5.4.

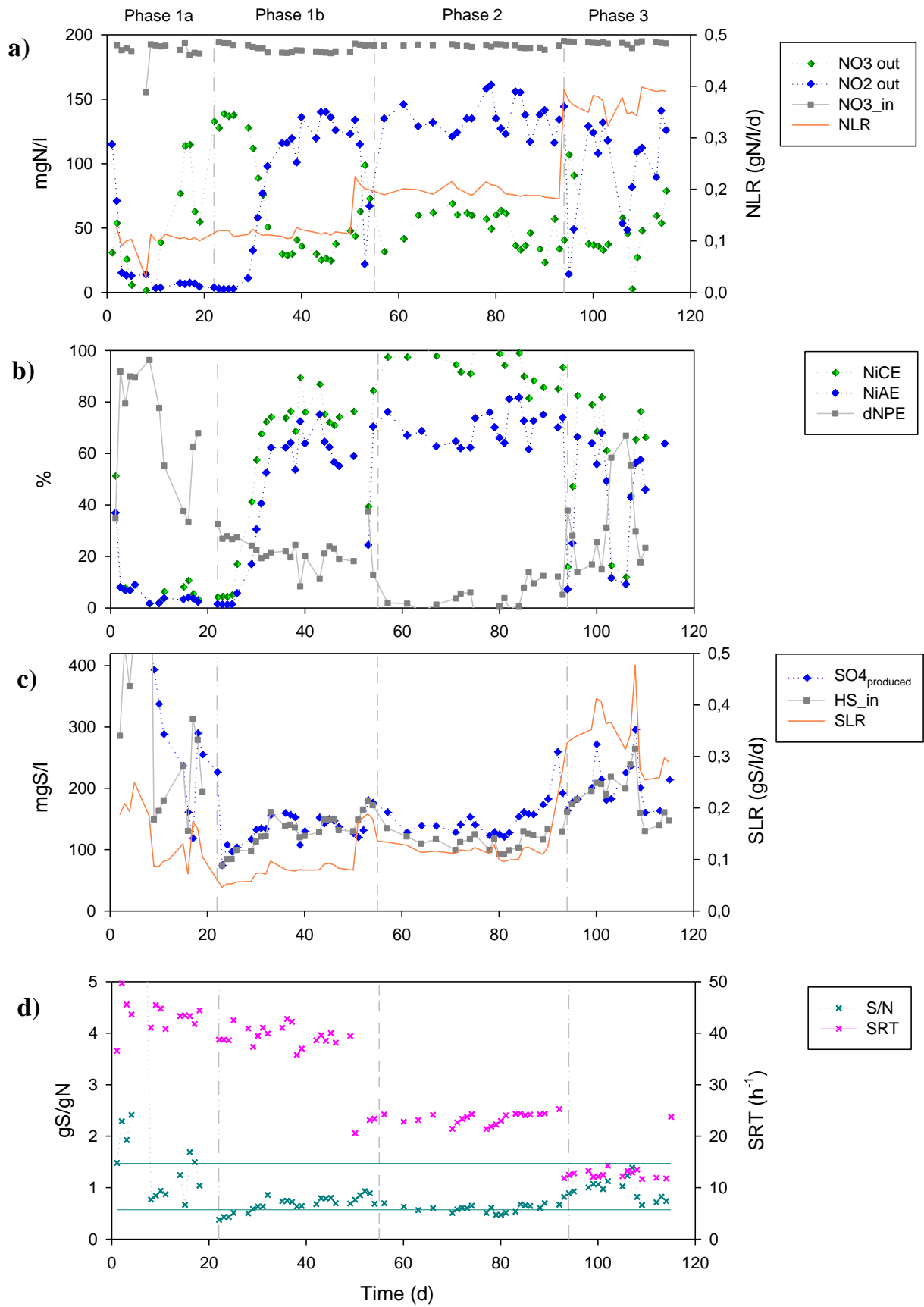


Figure 5.3 Experimental results on RI operation and performance: a) influent and effluent Nitrogen concentrations; b) Nitrogen conversion efficiencies; c) influent and effluent Sulphur concentration; d) applied SRT and S/N.

Table 5.4 Main results on nitrite conversion efficiencies at each phase of R1.

	NRE	NiCE	NiAE	dNPE
	$\frac{NO_{3_rem}}{NO_{3_in}}$	$\frac{NO_2}{NO_{3_rem}}$	$\frac{NO_2}{NO_{3_in}}$	$\frac{N_2}{NO_{3_in}}$
Phase 1b	83%	76%	63%	20%
Phase 2	74%	94%	70%	4%
Phase 3	82%	73%	57%	25%

In phase 1b, after day 21, influent S/N was set stably within the targeted range, ensuring sulphur-limited conditions at a dilution rate of $0,025 \text{ h}^{-1}$ (i.e. SRT of 40 h, fig.5.3). According to the catabolic stoichiometry, the sulphide provided in the first week of phase 1b was sufficient either to a full denitrification of 30% of the influent nitrate load or for an almost complete conversion to nitrite (assuming complete oxidation to sulphate). From day 22 to day 29, a 30% of nitrate removal efficiency (NRE) was, in fact, observed and accomplished by complete conversion of nitrate to dinitrogen gas (no nitrite was detected). After few days of stable and strict sulphide limiting conditions, a gradual nitrite accumulation was observed at a constant accumulation rate of 22 mgN/l/d , until a stable effluent concentration of $125 \pm 9 \text{ mgN-NO}_2^-/\text{l}$ was achieved and kept until day 50, resulting in a NiAE of $63 \pm 5\%$ and a NiCE of $76 \pm 6\%$ (table 5.4). In this phase, sulphate production closed sulphur balance within a 10% error, indicating that all the influent sulphide was converted to sulfate. At day 50, SRT was halved to 23 h (phase 2). The sudden increase of loading rates and dilution rate ($0,04 \text{ h}^{-1}$), determined a net drop in nitrite concentration down to $22 \text{ mgN-NO}_2^-/\text{l}$. Nevertheless, in three days, the concentration raised back to stable values of $136 \pm 13 \text{ mgNNO}_2^-/\text{l}$, kept throughout phase 2. A NiCE of $94 \pm 7\%$ was achieved with a concomitant NiAE of $70 \pm 6\%$, consequent nitrogen removal efficiency, NRE, was $74 \pm 7\%$. Specifically, on days 61-71, the lowest S/N of $0,58 \text{ gS/gN}$ was stably maintained and resulted in the maximum nitrite accumulation of NiAE $99 \pm 2\%$ ($1 \pm 1\%$ of dNPE) and NiCE of $69 \pm 6\%$, for a total NRE of $70 \pm 6\%$. Even though complete nitrate conversion was not achieved, an almost complete inhibition of dinitrogen gas production was obtained in this phase, as the remaining 30% of incoming nitrate was exiting the system as nitrate.

During phase 2, the reactor appeared as a whitish transparent liquid (see fig 5.4a), suggesting that no evident sulphur accumulation was occurring. Though, sulphate production was actually exceeding the influent sulphide by a 10 to 30%. It is assumed that an undesired presence of an additional reduced form of sulphur like thiosulfate or sulfate itself were present in the concentrated sulphide solution. Thiosulfate and sulfate can form chemically from sulphide oxidation, as already discussed. Since only 4 e- are donated per mole of $S-S_2O_3^{2-}$

oxidized to SO_4^- , compared to 8 e-mol per mol S-HS^- oxidized to SO_4^{2-} , the catabolic S/N ratio required for complete or partial denitrification over thiosulfate are 2,9 and 1,1 gS/gN, respectively, indeed the double than those of the correspondent sulphide-driven reactions. Thereby, even though the sulphur unbalance was significant, up to 30%, in the worst case of sole thiosulphate (and not sulphate) presence the ultimate effect on the nitrogen conversion is deemed as lower as 15% (according to the S/N ratios).

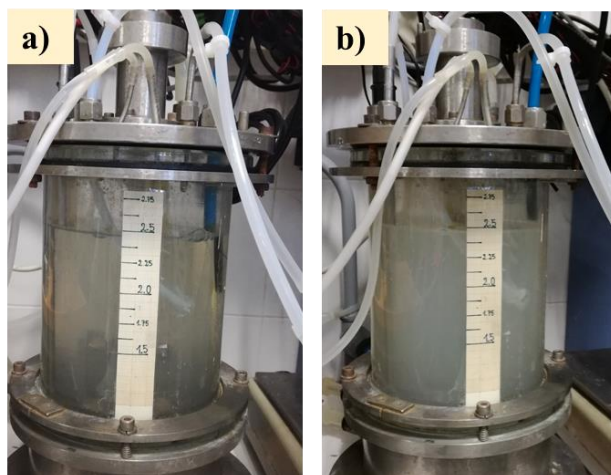


Figure 5.4 Pictures of reactor R1 during days with no S^0 accumulation and very transparent bulk liquid (a) and residual S^0 accumulation and more whitish and turbid bulk liquid.

In phase 3, the applied dilution rate was increased to $0,08 \text{ h}^{-1}$, resulting in NLR of $0,40 \pm 0,05 \text{ gN/l/d}$ and SRT of $12,6 \pm 0,7 \text{ h}$. As in the transition from phase 1 to phase 2, the sudden flowrate and load increase lead to a drop in nitrite concentration down to $49 \text{ mgN-NO}_2^-/\text{l}$, but nitrite accumulation recovered within three days. In phase 3, a S/N ratio of $0,96 \pm 0,2 \text{ gS/gN}$ was applied, in fact a value slightly higher than phase 2. This change was motivated by the fact that in phase 2 a residual concentration of nitrate was not removed and exited in the effluent, suggesting that the e-donor limitation might have been possibly excessive (i.e. not enough to convert all the influent nitrite to nitrate). Nevertheless, the moderately higher S supply resulted in the production of N_2 , successfully inhibited in phase 2. Despite that, a satisfactory nitrite concentration of $119 \pm 15 \text{ mgN-NO}_2^-/\text{l}$ was ensured. On day 108, a S/N ratio of 1,5 gS/gN was applied due to an excessive dosage of sulphide. As a consequence, nitrite concentration dropped again, but increased within one day, as the S/N returned S-limited. Phase 3 was characterised by more unstable operational conditions and resulting performance, also due to some technical problems in the mixing system. However, conversion efficiencies were maintained as high as $73 \pm 17\%$ and $57 \pm 9\%$ for NiCE and NiAE, respectively.

The three episodes of nitrite drop are deemed relevant as they allow assessing system resiliency against daily variation of S/N. Considering all the three episodes of nitrite drop, named D1, D2 and D3 hereafter, and subsequent restoration, nitrite accumulation rates have been estimated according to the linear increase and the correspondent solids concentrations in the reactor. Interestingly, the calculated rates for D1 and D2 result in

similar values of average $0,108 \pm 0,007$ gN-NO₂⁻/gVSS/h, whereas a lower value of $0,0304$ gN-NO₂⁻/gVSS/h results for D3. A discussion on such observed rates is presented in section 3.2 as a critical comparison with the rates observed in the respirometric tests.

Sulphate production in phase 3, closed sulphur balance with a 10% error, suggesting that almost all the inlet sulphide was completely oxidized to sulphate²⁹. Despite that, the reactor appeared more turbid than in phase 2, suggesting residual sulphur accumulation (Figure 5.4b). Elemental analysis conducted on day 106 and 107, when turbidity seemed significant revealed that only 2,9% and 1,7%, respectively, of the dry matter were actually accounted as sulphur. The resulting N/C ratio for the two samples was 0,27 (less than 0,2% deviation), in fact, in agreement with the general biomass composition of CH_{1,8}O_{0,5}N_{0,2} (Roels, 1983).

As it can be observed in table 5.4 and figure 5.3b, at all the tested conditions, high accumulation efficiencies (NiCE >70%) were achieved at all the conditions tested. Specifically, a NiCE close to 100% was achieved at SRT of 23 h and the lowest S/N ratio of 0,52 gS/gN (days 78-84), even though a residual concentration of nitrate was still present in the effluent with an average concentration of 50 mgN/L. Thereby, even though the complete conversion of influent nitrate was not achieved, an almost complete inhibition of dinitrogen gas production did occur, meaning that the nitrite conversion rate at this step was almost zero.

VSS concentration in the reactor kept at very low levels making their accurate analysis a challenging exercise, successfully accomplished through the precautions described in section 5.2.5. Specifically, the average VSS concentrations were 13 ± 5 , 13 ± 2 and 36 ± 10 mgVSS/l, in phase 1, 2 and 3, respectively. VSS/TSS ratio remained stable at $83 \pm 5\%$. The higher value observed in phase 3 was crossed with the elemental analysis and it did not seem to be related to significant elemental sulphur accumulation, as discussed above. Biomass yield estimated in phase 1, 2 and 3 are $0,11 \pm 0,05$, $0,12 \pm 0,04$ and $0,19 \pm 0,09$ gVSS/gS, respectively. Due to the higher instability of phase 3, the estimations from phase 2 and 3 are believed to be more reliable. A critical discussion on SOB biomass yield is reported in Chapter 6.

Reactor R2 was run for additional 30 days, after Reactor 1 operation. Results on R2 operation are not reported in figure 5.3 since the reactor was monitored only two to four times per week, differently from the careful monitoring of reactor R1. Still, when stable conditions were achieved, R2 performance showed comparable as reactor R1. At applied conditions of SRT of 23 h, temperature $22 \pm 2^\circ\text{C}$, S/N of 0,62 and NLR 0,14 gN/l, accumulation of nitrite was obtained and conversion efficiencies similar to R1 were achieved: 76% NRE, 84% NiCE, 62% NiAE and 19% dNPE.

The shortening of SRT down to 12 h in R1 did not cause any biomass washout, indicating a biomass growth rate higher than the applied dilution rate. Reactor R2 was also operated at SRT of 12 h but temperature was as low as $22 \pm 2^\circ\text{C}$. Again, no biomass washout was observed in R2, suggesting that the actual maximum specific

²⁹ In phase 3 more attention was dedicated on preparing fresh sulphide solution, prepared with a freshly opened bottle of sulphide salt, in order to limit as much as possible chemical oxidation by-products such as thiosulfate or sulfate.

growth rate is even higher than the applied dilution rate of $0,08 \text{ h}^{-1}$ ($1,9 \text{ d}^{-1}$). This is in line with the reported value of maximum specific growth rate of denitrifying SOB, ranging from $1,2$ to 3 d^{-1} (Claus and Kutzner, 1985, Oh et al., 2000; Mora et al., 2015).

5.3.2 N₂O emission

Nitrous oxide was measured in the headspace at the end of phase 1 (days 47 and 50) and phase 2. Measurements were intended to be performed at each phase, once steady-state was achieved, either in terms of applied conditions and resulting performance. Unfortunately, no measurements could be performed during phase 3, due to the higher instability that characterised this last phase. No measurements were conducted in the liquid phase nor estimates of the k_{La} of the system were available. Therefore, results on the N₂O emissions are not considered as exhaustive. Table 5.5 reports the average concentration of N₂O observed during the measurements on days 47, 50 and 93 (each measurement lasted 3 to 5 hours, average values are calculated over the measurement period, excluding less stable values registered in the very first minutes).

Table 5.5 N₂O concentration in the headspace and corresponding NO₂⁻ and FNA values in the bulk liquid (R1).

Measurements	N ₂ O_headspace	NO ₂ ⁻ _bulk	FNA_bulk
	µmol/l	mgN/l	µgN/l
Phase 1 (day 47)	2,5±0,1	111	5,5
Phase 1 (day 50)	1,7±0,1	109	5,3
Phase 2 (day 93)	3,7±0,2	134	6,6

An average concentration of $2,1±0,6 \text{ µmol/l}$ (as N₂O) could be estimated for phase 1, as average of the two measurements, whereas a higher value of $3,7±0,2 \text{ µmol/l}$ was observed in phase 2. Since no overpressure was observed in the system headspace despite the continuous supply of a moderate gas flux of N₂/CO₂ on the reactor's bottom, a rough estimation of the emission factor of the process has been conducted by assuming an effluent gas flow of 100 l/d (indeed, equal to the influent gas flow) holding the measured N₂O level. On a mass balance, it results that N₂O emissions are $2,0±0,5$ and $2,4\%$ of the influent N-NO₃⁻ load in phase 1 and phase 2, respectively. Thereby, despite the higher N₂O concentration registered in phase 2, the emission factor relative to the influent N load was comparable between the two phases. In the mini-review presented by Cui et al. (2019), S-based autotrophic (complete) denitrification systems often exhibit lower emissions factors than the heterotrophic ones, with values of $0,01-0,8\%$ vs $2,3-13\%$ of the influent N-NO₃⁻ load, respectively. In the present work higher emission values have been estimated. Since an electron limiting strategy was adopted for

achieving partial denitrification, denitrification intermediate other than nitrite are possible to be produced. From table 5.5, it can be observed that N_2O concentration increased with increasing FNA in the bulk. Disturbing effect of NO_2^- -FNA on N_2O reduction rate has been reported in literature either for heterotrophic and autotrophic denitrifiers (S or H_2 oxidizers), since the adverse effect is usually related to the N-reduction pathway (shared among denitrifying bacteria, with minor differences). From one side, among the proposed mechanisms, there is the interference of FNA on the activity of the N_2O reductase, specifically FNA might bind with the active site of the enzyme, competing with N_2O (Zhou et al., 2018). On the other side, also NO_2^- as such (not as FNA) can compete with N_2O for electrons' acquisition, since electrons are delivered to the enzymes corresponding to their reduction by the same electron carrier (typically periplasmic cytochrome) and thereby high level of NO_2^- might be undesirable even in case of high pH (low FNA), if electron supply is limited (Wang et al., 2018). Other inhibiting mechanisms range from increase in maintenance energy dissipation (due to an increase in proton permeability and alteration of electron transport chain and, ultimately, ATP synthesis) to transcriptional errors in enzymes production (Zhou et al., 2011). Yet, which mechanisms prevails under which conditions is still unclear and it likely depends on the peculiarity of the biomass system.

Yang et al. (2016) experienced N_2O accumulation during batch test when temporary nitrite accumulation lead to FNA values of 0,2-1,1 $\mu gN/l$, at pH 7. As reported by Wang et al. (2018), slightly alkaline pH can play an important role in relieving N_2O emissions. During the operation of a lab-scale hydrogenotrophic denitrifying system, the authors observed a remarkable attenuation of N_2O emissions at increasing pH and nitrite level of 40 $mgN-NO_2^-/l$, ranging pH values from 6,5 (maximum N_2O production) to 8,6 (no N_2O production). Strong pH effect on N_2O reduction rate has been also reported by Zhou et al. (2008) that indicated a 50% inhibition at FNA around 0,7-1 $\mu gN/l$, at pH 7 on denitrifying Enhanced Biological Phosphorous Removal (EBPR) sludge, ascribing to FNA rather than NO_2^- the actual inhibitory role.

In the present study, the observed FNA levels were higher than the one reported by Zhou et al. (2008) and Yang et al. (2015), but still within the inhibitory level reported by Cui et al. (2019) for an adverse effect on the denitrification step (see section 5.2.2). The operational pH maintained in the present study was 7,6; pH values of 8 or even 8,5 would lower FNA concentration below 2,7 and 1 $\mu gN/l$, respectively, possibly reducing the observed N_2O emissions.

It is believed that further studies are required in order to evaluate more accurate N_2O emissions from the sole PAD process and possible strategies for their mitigation. Moreover, such a drawback could be avoided in case of simultaneous PAD/A since the high affinity of anammox biomass for nitrite would lead to its fast consumption, preventing its further or incomplete reduction ($NO_2^- \rightarrow NO \rightarrow N_2O \rightarrow N_2$) as also reported by other authors (Qian et al., 2018).

5.3.3 Microbial diversity

Figure 5.5 reports the result on microbial diversity at class and genus level; OTUs showing a relative abundance lower than 1% were discarded for the present data elaboration. Samples were collected on the inoculum sludge, as well as at the end of each of the three operational phases in reactor R1 (day 49, 80 and 114 for phase 1, 2 and 3, respectively). As can be observed a clear shift in population was observed at class and genus level. At genus level, *Sulfurimonas* (belonging to the class of ϵ -proteobacteria) exhibited a relative abundance of 90% in the seeding sludge whereas its relative abundance dropped to 4% and 1% on days 49 and 80, respectively, and then raised back to 53% on day 114. On the contrary, the relative abundance of *Thiobacillus* genus (β -proteobacteria) was lower than the threshold level of 1% in the seeding sludge, but increased to 47% on day 49 and then reached 83% on day 80, prior to decrease to 38% on day 114. The high enrichment level observed on day 80 is in accordance with the very low SRT applied and feeding through organic-free synthetic medium, in fact conditions that do not favour microbial diversity.

Day 49 and 80 are representative of the stable and strict S-limiting conditions applied during phase 1b and 2, when the maximum NiCE and NAE were achieved, with complete or almost complete inhibition of the denitrification step at stably strict S-limiting conditions. Day 115, on the contrary was characterised by more unstable operation and slightly higher S/N, even though remarkable performance for the PAD process were ensured anyway.

Noteworthy, *Thiobacillus denitrificans* have been reported to have a higher efficiency in terms of cellular bioenergetics compared to *Sulfurimonas denitrificans* (Klatt and Polerecky, 2015). The proposed reasons are related to the fact that *T. denitrificans* adopt a membrane-bound nitrate reductase (Nar) whereas *S. denitrificans* a periplasmic nitrate reductase (Nap). As explained in section 1.1.4, on the opposite of Nap, the activity of Nar is directly linked to proton motive force generation and thereby energy is directly harvested during its activity. Moreover, the activity of Nar is less influenced by environmental conditions due to the fact that the reduction reaction occurs in the cytoplasm, differently from the Nap which operates in the periplasm, more susceptible to environmental conditions, such as pH, i.e. protons availability.

Moreover, regarding the S-oxidation metabolic pathways, *Thiobacillus* have been reported to encode both the enzyme pool required in the Sox-based pathway and those required in the branched pathway, this latter adopting the inverse action DSR and APS enzymes, whereas *Sulfurimonas* only rely on the Sox enzymatic system, resulting in a competitive advantage of the more versatile genus of *Thiobacillus* as it was speculated by Klatt and Polerecky (2015).

Thereby, it can be argued that strictly and stable energy limited conditions, resulting from electron donor limitation, lead to a competitive advantage of the genus with the higher energy efficiency. Behind its very interesting implications, it is believed that this finding can be a crucial aspect for achieving and controlling a stable PAD process at full-scale.

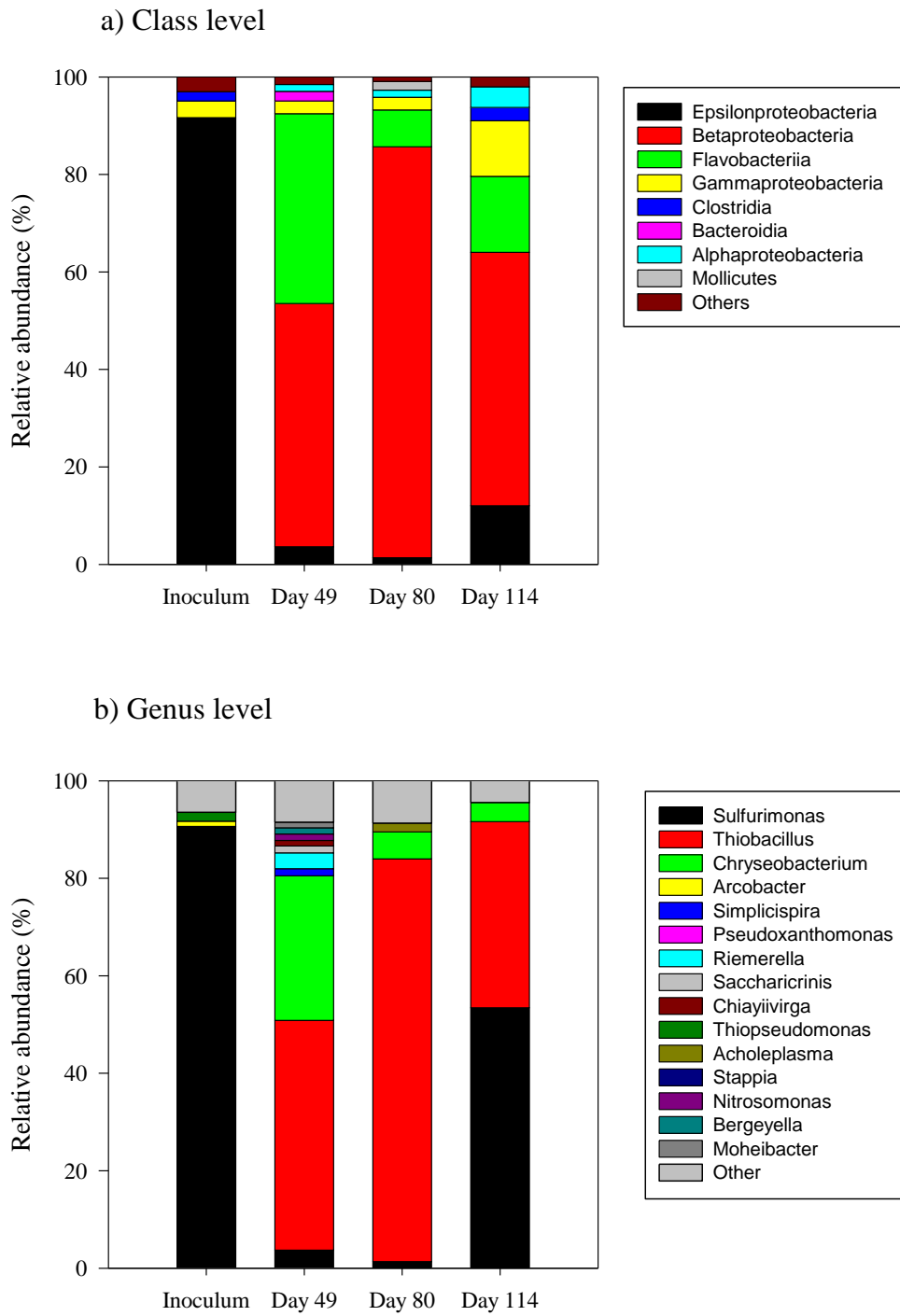


Figure 5.5 Microbial diversity in the inoculum and across the three operational phases of R1 (days 49, 80,114).

5.3.4 Respirometric test

Respirometric tests were conducted in order to assess specific biomass uptake rates for nitrate and nitrite, in order to gain insight on possible competition among the two as well as the role of nitrite inhibition in the successful nitrite accumulation observed in the reactor. The results of the respirometric and titrimetric tests are reported in figure 5.6.

In test A, only two points are available for sulphide uptake rates since the sulphide was removed very quickly due to concomitant biological uptake and significant stripping (nitrogen gas sparger was placed in the liquid phase). Since data are not sufficient to profile a clear uptake trend for sulphide, results were used only for NUR (Nitrate Uptake Rate) estimations as validations of the evidences from the subsequent tests and no e- balance nor HPR (H⁺ Production Rate) estimation were performed on this test. An aggregated value for NUR in step 1 and 2 was estimated to be 100 ± 35 mgN/gVSS/h, and confirmed in the other tests. In test B, C and D, phases 1 and 2 (referring to HS⁻ and S⁰ uptake) are clearly distinguished either in the Nitrogen uptake rates and in the proton production/consumption rates. The observed HPR, net of the abiotic contribution, were compared with the expected values, calculated as the observed S uptake rates (as mgS/l/h) multiplied by the stoichiometric H⁺/S ratio of the catabolic oxidation reaction.

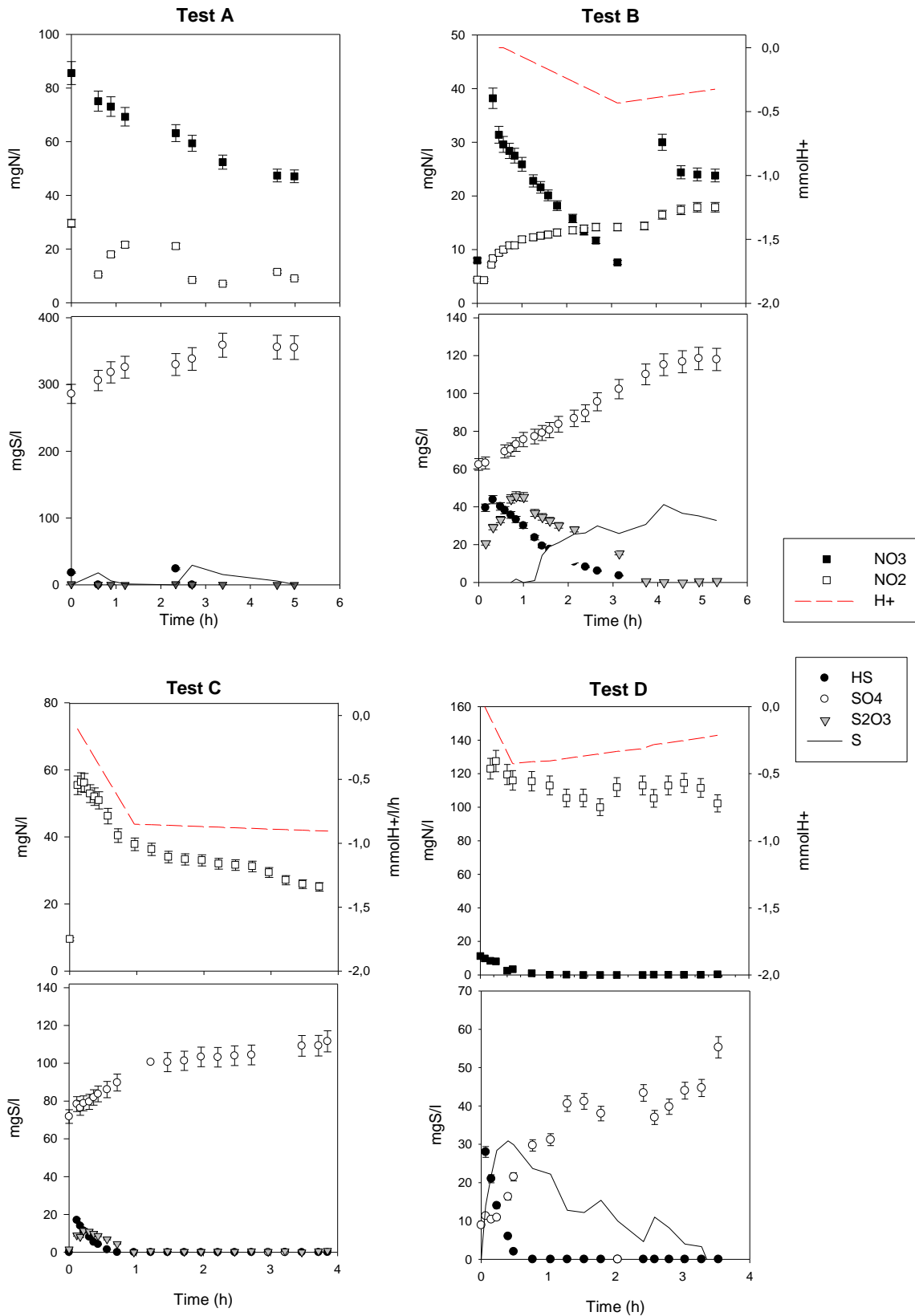


Figure 5.6 Results from respirometric and titrimetric tests A, B, C and D.

Test B presented a residual concentration of 10 mgN-NO₂⁻/l at the beginning of the test that resulted from partial nitrate reduction during the preliminary “wake-up” step. Thiosulfate formation was observed at the beginning of the test. Such a thiosulfate formation is believed to be the result of chemical interactions between dissolved sulphide, residual elemental sulphur from biomass withdrawn and residual polysulphide formation. Still, it owns to mention that sulphide bonded in polysulphide is later released and ultimately available for biomass uptake and that (van den Bosch et al., 2007; Lens, 2020) and thiosulfate is often used in S-denitrifying kinetic assessments, since it is considered interchangeable with sulphide for chemolithotrophic biomass (Mora et al., 2014c). A very straight linear depletion was observed for nitrate and sulphide, during phase 1, whereas certain delay was observed for thiosulfate uptake, compared to sulphide, according to the assumption explained above. A second pulse of nitrate was provided after sulphide and thiosulfate depletion, in order to ensure sufficient e-acceptor in phase 2. Yet, NUR uptake in the second phase is not clearly defined, since a sampling point was missed during the test. The uptake rates in phase 1 were 80±1 mgN-NO₃⁻/gVSS/h for nitrate, 200 mgS/gVSS/h for the sulphide and 125 mgS/gVSS/h for the thiosulfate. A small though constant accumulation of nitrite was also observed at an accumulation rate of 12 mgN-NO₂⁻/gVSS/h (R²=0,94). According to equation 5.8 (section 5.2.3), the nitrite consumption rate can be calculated and results in 65 mgN-NO₂⁻/gVSS/h. The observed HPR in phase 1 and phase 2 were -0,17 mmol/l/h (HPR<0, proton consumption, i.e. alkalinity production) and 0,05 mmolH⁺/l/h, in line with the expected behaviour, i.e. alkalinity production for step 1 and alkalinity depletion for step 2. Electron balance closed at 8% and 6%, in phase 1 and 2, respectively. In test C, a temporary delay in nitrite consumption was observed together with a slight thiosulfate formation at the expenses of sulphide. It can be speculated that it could result from an enzymatic response delay since the biomass was grown with nitrate as e- acceptor and, in the mother reactor, nitrite was predominantly accumulated rather than consumed. After the delay, consumption of e-acceptor and e-donor followed a linear trend and resulted in 190 mgN-NO₂⁻/gVSS/h; 140 mgS-HS⁻/gVSS/h and 90 mgS-S₂O₃²⁻/gVSS/h. NiUR in phase 2 was as low as 27 mgN-NO₂⁻/gVSS/h, 7 times lower than the value observed in phase 1. Electron balance in phase 1 closed with an 8% error and in phase 2 with a 17%; still, since the consumption and production of the N and S species were very low in phase 2, analytical accuracy is believed to be an important source of uncertainty in this case. HPR were -0,18 mmolH⁺/l/h and 0,02 mmolH⁺/l/h, in line with the alkalinity consumption and production, as a general trend. Test D was conducted at nitrite levels as high as those observed in the CSTR, in order to assess whether nitrite inhibition was playing a significant role in the reactor performance. When sulphide was present as sole e-donor, the test exhibited the following rates: 85 mgN-NO₃⁻/gVSS/h; 84 mgN-NO₂⁻/gVSS/h (R²=0,9) and 299 mgS-HS⁻/gVSS/h. No clear nitrite consumption could be gauged from phase 2. Electron balance in phase 1 closed at 10%, HPR was -1,02 mmolH⁺/l/h, confirming an alkalinity production behaviour, as expected.

Comparing the uptake rates observed in the respirometric tests along with the dynamic behaviour of the chemostat (R1) during the 3 nitrite drop episodes (D1, D2, D3) an interesting consistency is observed. A NUR of 88±10 gN/gVSS/h is considered as an average value gathered from test A, B and D. The nitrite accumulation

rate observed in D1 and D2, is 100 ± 20 mgN/gVSS/h; considering the confidential intervals of this latter value and that of the average NUR from respirometric tests, equation 5.8 can be applied for the estimation of the nitrite uptake rates in D1 and D2; NiUR results in fact null. This estimation is in line with the almost complete inhibition of the denitrification step observed in the reactor in the days right before and right after D1 and D2, i.e. dNPE was almost zero. In episodes D3, the nitrite accumulation rate was 35 ± 5 mgN/gVSS/h and according to equation 5.8, the nitrite uptake rate results in 65 mgN/gVSS/h; indeed, N₂ production was observed in that period.

Respirometric results highlighted some remarkable characteristics of S-driven autotrophic denitrification. Prior to the discussion, it owns to be mentioned that a straightforward comparison of reported specific uptake rates is not always exhaustive nor even possible, since many results are presented as uptake rates expressed as volumetric consumption rates, e.g. mgN/l/h or mgS/l/h, not related to the specific biomass content (VSS) of the test. Moreover, specific uptake rates (e.g. mgN/l/gVSS/h) are influenced by several factors, mainly related to the type of culture (mixed or enriched, suspended or aggregated, acclimated or not to specific exogenous/endogenous compounds), the prevailing microbial population as well as optimal or stressful operational conditions during the test (pH, salinity, e-donor/e-acceptor availability and balance). Besides that, a critical comparison can be carried out.

Table 5.6 Main results from activity tests.

	NUR	NiUR
	mgN/gVSS/h	mgN/gVSS/h
Test A	$100\pm 40^{1,2}$	
Test B	80^1	65^*
Test C	-	$190^1; 27^2$
Test D	85^1	84^1

¹ in step 1 (HS⁻ and S₂O₃²⁻, as e-donor)

² in step 2 (S₀, as e-donor)

* calculated from NO₂⁻ accumulation rate

Comparable nitrate uptake rates were observed in phase 1 of all tests, with an average NUR of 90 ± 10 mgN/gVSS/h, irrespective of the co-presence of nitrite, even at the high concentration of test D. Such a specific activity is in line with the values reported on pure or highly enriched SOB culture, like the one of the present work. Similar NUR were reported by Manconi et al. (2007) which observed a specific NUR of 85 mgN/gVSS/h for a pure culture of *Thiobacillus denitrificans*, in batch tests with thiosulfate as e-donor. Mora et al. (2014a) report 101 ± 28 and 55 ± 3 mgN/gVSS/h for a pure culture of *Thiobacillus denitrificans* and a mixed (enriched) culture, respectively, under not limiting conditions for thiosulfate at 30°C and pH of 7.5. Also, Campos et al.

(2008) obtained a comparable NUR value of 54 mgN/gVSS/h (at 30°C, pH 8) for enriched culture of denitrifying SOB fed by nitrate and sulphide³⁰.

On the contrary, nitrite uptake rate showed very different values according to the applied conditions: in test B, nitrite was rather produced than consumed, suggesting an out-competition of nitrate uptake, even at abundant availability of e-donors; in test C nitrite was the sole e-acceptor and the highest NUR of 190 mgN/gVSS/h was observed (during sulphide uptake). This evidence is in line with other studies reporting that, when sulphide is used as e-donor, nitrite may be consumed at higher rates than nitrate (Cui et al., 2019b), whereas the opposite is reported in case of sulphur as e-donor (Sahinkaya et al., 2011; Cui et al., 2019b). In test D, performed at a FNA concentration of 4-5 µg/l resulted in a lower uptake rate for nitrite, compared to test C, whereas nitrate uptake was observed as high as in test A and B. Indeed, the inhibitory effect of FNA is reported to affect the denitrification step only, which is consistently modelled in many works according to Haldane-like kinetic for nitrite (Fajardo et al., 2014; Mora et al., 2014c; Cui et al., 2019b). NiUR on elemental sulphur (phase 2) could be clearly estimated only for test C, resulting in a 7-fold lower value, which is in accordance with Cui et al., (2019b) reporting uptake values from 2 to 10 times lower in S⁰ uptake rather than HS⁻.

5.3.5 Discussion on nitrite accumulation strategies

According to the main outcomes obtained in the present study, successful and stable nitrite accumulation was achieved by ensuring strict sulphide-limiting conditions, i.e. under-stoichiometric S/N ratios (less than 0,8 gS/gN), whereas the SRT did not clearly affect process performance, at the tested values. Restated, S/N ratio appears to be a crucial and sufficient condition to conduct stable NO₂⁻ accumulation. These results are in line with Deng et al. (2019), achieved a stable nitrite accumulation, with a 50% of NiCE and 30% of NAE in a thiosulfate-based denitrification reactor, by maintaining S-limiting conditions in the influent at a HRT of 12-24 h, after one month of operation. Interestingly, two other studies (Chen et al., 2018 and Liu et al., 2017) report successful NO₂⁻ accumulation even though S/N is either not specified or significantly over stoichiometric for the e- donor. Chen et al. (2018), operated a suspended-culture SBR, fed by nitrate and with a weekly elemental sulphur supply in the reactor. Even though the exact S/N was not addressed in their study, increasing NLR conditions lead to nitrite accumulation, under the assumption that S⁰-driven denitrification step has lower kinetics than S⁰-driven denitrification. Thereby, NO₂⁻ accumulation was obtained through a kinetic out-competition between the two e-acceptors, i.e. NO₃⁻ was the preferred e-acceptor over NO₂⁻, at high NLR conditions and abundant S₀ as e-donor. Liu et al. (2017), operated a suspended-biomass UASB, fed by nitrate and sulphide, testing different S/N ratios, from S-limiting to N-limiting conditions, and a range of HRT (from 8 to 6 h). A stable nitrite accumulation, accounting for the 70% of converted nitrate (ca 50% of influent nitrate) was established together with 70% elemental sulphur production, at the highest S/N ratio of 3 gS/gN (1:0,76 molS/molN), while NLR and SLR were maintained at pretty sustained values of 1,2 gS/l/d and 0,4 gN/l/d. All

³⁰ In their work, Nitrate uptake rate was estimated in batch tests with thiosulfate as e-donor.

these evidences deserve a wider discussion, as presented below, including some parallelism with the control strategy operated in aerobic sulphide oxidation systems.

Autotrophic denitrification using HS^- as e- donor and NO_3^- as e-acceptor, is a multistep reaction with multiple possible combinations of e-donor/e-acceptor couples (fig. 5.7). As a general simplification HS^- oxidation to SO_4^{2-} is represented with the intermediate product of elemental sulphur. Analogously, NO_3^- reduction to N_2 , is represented with the intermediate product of NO_2^- . Many studies and real-scale applications have dealt with operational strategies to selectively favour SO_4^{2-} or S_0 as end-products of sulphide oxidation.

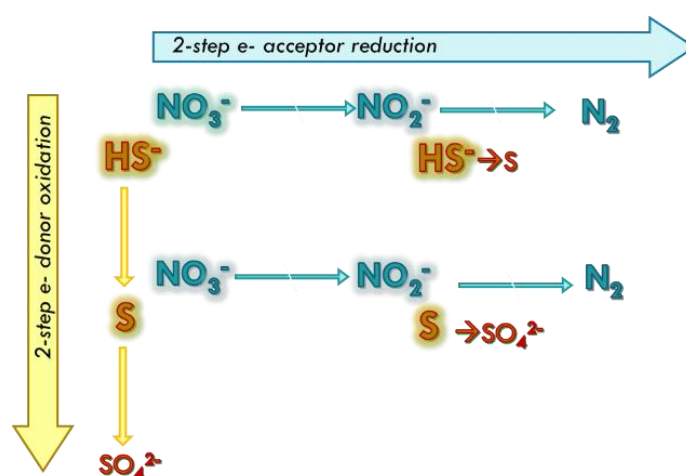


Figure 5.7 Main reaction step in sulphide oxidation and nitrate reduction.

Specifically, two main approaches can be distinguished: one based on supplying adequate e-acceptor over e-donor relying on influent S/N, ultimately on stoichiometry; the other one based on loading rate conditions relying on uptake rates, ultimately on kinetics. The stoichiometry-based approach indicates N-limiting conditions (i.e. S/N ratios higher than the stoichiometric ones) as a successful strategy to stop sulphide oxidation to elemental sulphur (Cardoso et al., 2006; An et al., 2010, Liu et al., 2017) whereas low S/N ratios favour sulphate as the finale end product. Similarly, also in aerobic sulphide oxidation DO limiting conditions are used when S^0 production is maximized (Cui et al., 2019 and all the reference therein; Lens, 2020). Other studies achieve selective S^0 production at high sulphide loading rate (kinetic-based approach), irrespective of the S/N, based on the evidence that HS^- uptake rates are generally higher than S uptake rates (Reyes-Avila 2004; An et al., 2010). Compared to the dissolved ionic state of HS^- (the prevalent species at pH 7-9), the bioavailability of S^0 is further hindered by its slowly soluble solid state, whose dissolution is often the actual bottleneck of oxidation kinetics.

Analogously to the sulphide-oxidation control strategies, it can be speculated that available results on nitrite accumulation (as end-product of partial nitrate reduction), can be also gathered in these two broad categories, even though very important differences between the two intermediates, sulphur and nitrite, have to be

mentioned first. Conversely to sulphide-sulphur competition as e-donors, nitrate-nitrite competition is not so straightforwardly addressed. In contrast to the intermediate sulphur, nitrite is a very good e-acceptor and, in general, a reactive compound also due to its highly unstable molecular structure, which is plane linear (O-N-O), compared with the more stable plane triangle of the nitrate molecule (Jing et al., 2010). Moreover, nitrite is a potential inhibitor, due to the high toxicity of its non-ionic form (FNA) whose effects on process performance have been discussed above.

In the reported applications of autotrophic denitrification, an interesting case is the utilization of nitrate injection in sea water oil reservoir treatments in order to limit biological sulfidogenesis (and consequent souring) from sulfate-reducing bacteria (SRB). Since nitrite is a strong SRB inhibitor (Fida et al., 2016), some studies are starting to pay attention on achieving and maintaining a residual nitrite concentration after nitrate injection. An et al. (2017) performed a study on sea-water samples taken from different off-shore oil reservoir testing different salinity levels and reports on nitrite accumulation (1-4 mM) only at salinity as high as 2,5M NaCl. The abovementioned authors refer on another study on nitrate injection for oil-field souring control where nitrite accumulation was favoured at temperature at or above 50°C (Fida et al., 2016). An et al. (2017) speculate that extremophilic conditions, either due to high salinity or high temperature, favour partial denitrification, i.e. nitrite accumulation.

According to our results and the available studies achieving nitrite accumulation, it is speculated that nitrite accumulation is somehow an energy optimizing mechanism, in response to different kind of “stress” conditions, possibly due to: (i) significant unbalance of e-donor/e-acceptor, specifically e-donor limiting conditions; (ii) high load conditions or (iii) extremophilic conditions. This hypothesis has been interestingly supported by the remarkable population shift observed in the present work. A thermodynamic insight on this issue is provided in Chapter 6.

5.4 Conclusions

In this chapter the successful results on stable nitrite accumulation under strictly S-limiting conditions have been presented and discussed. To the best of our knowledge, the obtained nitrite accumulation efficiencies are among the highest reported in literature and the present work is the first one in which partial autotrophic denitrification is obtained together with complete sulphide oxidation to sulphate, in and SRT-controlled system with a highly SOB-enriched culture.

Influent S/N ratio showed to be a sufficient control parameter in the chemostat reactor operated at low SRT (12 to 40 h), at 30°C and pH of 7,6. The SRT conditions tested during the three operational phases did not show a noticeable impact on the nitrite accumulation performance.

Nitrite Conversion Efficiency (NiCE) and Nitrite Accumulation Efficiencies (NiAE) achieved 73-94% and 60-70%, respectively, as average values over the three operational phases. The maximum NiCE of 100% was achieved at the lowest S/N ratio applied (0,58 gS/gN), at SRT of 13 h. This result implies that the denitrification step (N₂ production) was completely inhibited.

The limited measurements on N₂O emissions warn about a possible emission factor of 2-3% (over the influent N load), calling for further monitoring studies. Yet, operational conditions at slightly alkaline pH are believed to be a feasible solution to alleviate N₂O emissions, likely related to significant FNA concentrations.

Respirometric and titrimetric results confirmed that Nitrate Uptake Rate was not influenced by nitrite co-presence as additional electron acceptor, not even at the concentrations as high as 120 mgN-NO₂⁻/l, and an almost constant value of 88±10 gN/gVSS/h was observed. On the contrary, the values of Nitrite Uptake Rate exhibited values ranging from 27 to 190 mgN/gVSS/h depending on the applied conditions, suggesting the denitrification stability is more susceptible to the operational conditions applied. However, system response is strictly dependent on the biomass seed sludge, that in the present study was a highly enriched SOB biomass fed with sole nitrate and acclimated to high nitrite concentrations.

A clear population shift in microbial population from *Sulfurimonas* to *Thiobacillus* was observed after 80 days and under strict and stable S-limiting operational conditions. The higher metabolic versatility and energetic efficiency of *Thiobacillus* are believed to be key elements for explaining its out-competition over *Sulfurimonas*.

CHAPTER 6.

A thermodynamics insight on S-driven denitrification.

Focus on partial denitrification

6.1 Introduction

Sulphur Oxidizing-Nitrate Reducing process, SO-NR, is a complex process characterized by peculiar aspects such as: (i) multistep reactions involved both for e-acceptor reduction and e-donor oxidation; (ii) high chemical reactivity of reduced sulphur compounds, such as sulphide and thiosulphate; (iii) variety in microbial population able to mediate SO-NR reactions, from strictly to facultative anaerobic, from chemolithotrophic to mixotrophic (Madigan et al., 2019). Such a complexity is reflected in the highly different results that can be found in the literature in terms of biomass yields and substrate uptake rates, as well as favoured e- acceptor between nitrate and nitrite. Biomass cultivation mode and operational conditions also affect observed kinetics and stoichiometry. A direct comparison of reported results is often not possible and time-consuming result conversion needs to be carried out.

Due to the complexity of the possible reactions combination, solving the full stoichiometry is not a trivial exercise (Klatt and Polerecky, 2015). Indeed, while the catabolic reactions are straightforwardly derived from e- and mass balances, discrepancies are encountered in literature when full metabolic reactions are considered. Stoichiometries available in the literature, either empirically or theoretically-derived, slightly differ for the biomass yield reported.

In this chapter, a thermodynamic and stoichiometry-based study is presented to drive a critical discussion on the available stoichiometric information on the SO-NR process.

A first aim of this chapter is to provide aggregated and easily comparable information on the catabolic reactions in terms of S/N ratio and acidity production/consumption, as well as a brief study on free Gibbs energy change of the exergonic reactions in the operational range of pH and Temperature that can be found in real-scale applications.

Then, a study on biomass yields is presented, under different assumptions mainly related to overall biomass energy efficiency and biomass composition. Specifically, the Gibbs energy dissipation method formulated by Heijnen et al. (1992), and widely applied by Heijnen and Kleerebezem (2010) and Kleerebezem and van Loosdrecht (2014), was used to estimate theoretical biomass yields for the different reaction steps involved in autotrophic metabolism of sulphur oxidizing bacteria, using sulphide and elemental sulphur as e-donor and nitrate/nitrite as e-acceptor. A synthesis of the methods is provided in the introduction section, in order to better highlight the assumptions underlying the study.

A third objective of the chapter is to provide a thermodynamic-based insight to the experimental results obtained in Chapter 5. Free Gibbs energy yields at the studied conditions are calculated for the complete denitrification as well as for the complete denitritation (or partial denitrification, PD) reactions and a speculative discussion on the obtained results is presented.

6.1.1 Basics of Gibbs energy dissipation methods for overall growth estimation

A general model for microbial metabolism assuming catabolic and anabolic pathways is considered, as described in figure 6.1. Catabolism is the metabolic pathway that enables energy harvest in the form of ATP. Anabolism uses (some of) this energy to synthesize new biomass; maintenance accounts for all the energy-requiring processes not related to cellular synthesis.

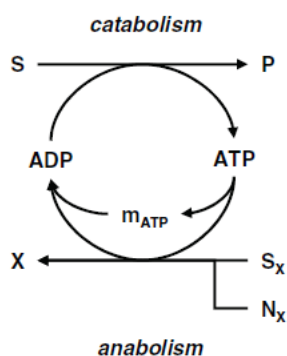


Figure 6. 1 Schematic of microbial metabolism from Kleerebezem and van Loosdrecht, 2010 (*S*, substrate; *P*, product; *S_x*, carbon source, *N_x*, nitrogen source, *m_{ATP}*, maintenance).

According to the method, overall growth stoichiometric reaction can be derived by combining the Gibbs energy of the anabolic and catabolic reactions. The first step of the method implies the definition of the catabolic and anabolic reactions.

Catabolic and anabolic reactions can be solved as follow:

- Catabolic reaction: select e-donor/e-acceptor couple and complete the equation according to mass/charge conservation balances or degree of reduction (γ) balance, referring the reaction to the consumption of 1 mol of e-donor.
- Anabolic reaction: select C and N source for biomass synthesis (as well as P, S, etc... for more thorough studies). Depending on the oxidation state of the C and N sources, an e-donor or acceptor is required for their reduction or oxidation into biomass. Usually the same e-donor/e-acceptor used in catabolism is used also in anabolism. Again, anabolic stoichiometry can be solved by mass/charge conservation balances or degree of reduction (γ) balance, referring the reaction to 1 C-mol of biomass formed.

Catabolic reactions are typically exergonic and the free Gibbs energy released depends on the e-acceptor/e-donor couple involved. In figure 6.2, the redox tower for some of the most common compounds involved in microbial systems is provided, together with their electronegative potential at standard conditions, E_0' . The electronegative potential E_0' is expressed in mV and indicates the tendency of a compound to donate or accept electrons, i.e. to be oxidized or reduced. The couples presented in the table indicate the oxidised state (on the

left) and the reduced state (on the right); electronegative potential is reported for each compound according to the corresponding reference compound.

At the top of the tower the couples with the more negative E_0' values indicate the high tendency of the reduced element to act as e-donor. On the contrary, at the bottom of the tower, couples with less negative (or even positive) E_0' values indicate a high tendency of the oxidized compound to act as e-acceptor. As it can be seen, Oxygen is the most electropositive compound, indeed, the best e-acceptor found in nature. Redox reactions mediated by microorganisms results from the combination of an electron donor (ED) and a terminal electron acceptor (TEA). As a general rule, the higher the distance of the e- donor and terminal e- acceptor in the tower, the higher the energy released by the redox reaction. Free Gibbs energy change in a reaction is proportional to the electronegativity gap and the number of electrons exchanged according to the Nerst equation³¹.

The complete metabolism or overall growth reaction (*Met*) can be considered as a function of the catabolic (*Cat*) and anabolic (*An*) reactions:

$$Met = \lambda_{Cat} \cdot Cat + \lambda_{An} An \quad \text{Eq. 6.1}$$

Being λ_{cat} and λ_{an} two multiplication factors indicating how many times the two reactions run. Overall growth stoichiometry is usually obtained through the link factor $Y_{X/S}^{Met}$, expressed as the inverse of e-donor required/consumed per C-mol biomass formed (usually referred as biomass yield), where X indicates the biomass and S the substrate (e-donor, in this case). Thereby, the biomass yield will result from the direct combination of the catabolic and anabolic reactions as follow:

$$Y_{X/S}^{Met} = \frac{\lambda_{Cat} Y_{Cat,X} + \lambda_{An} Y_{An,X}}{\lambda_{Cat} Y_{Cat,S} + \lambda_{An} Y_{An,S}}$$

Where: $Y_{Cat,X}$ and $Y_{An,X}$ are the stoichiometric coefficient for biomass in catabolism and anabolism, respectively, and $Y_{Cat,S}$ and $Y_{An,S}$ are the stoichiometric coefficients for the substrate in catabolism and anabolism, respectively. In general, all the energy-based estimations described herein are referred to the production of 1-C mol of biomass and therefore $\lambda_{an}=1$; moreover, biomass is not present in the catabolic reaction, $Y_{Cat,X}=0$, and λ_{cat} can be described as the number of times that the catabolic equation needs to run to deliver the energy requirement for the synthesis of 1 C-mol of biomass. Assuming that biomass is not involved in the catabolic reaction and that the same e-donor is used in catabolic and anabolic reaction, the biomass/e-donor yield, in the complete metabolism, can be expressed as:

$$Y_{X/S}^{Met} = \frac{1}{\lambda_{Cat} Y_{Cat,S} + Y_{An,S}} \quad \text{Eq. 6.2}$$

³¹ Derived from Nerst equation:

$$\Delta G = -zFE$$

Where: z is the number of e- donated/accepted, F is the Faraday constant and E is the Electronegative Potential

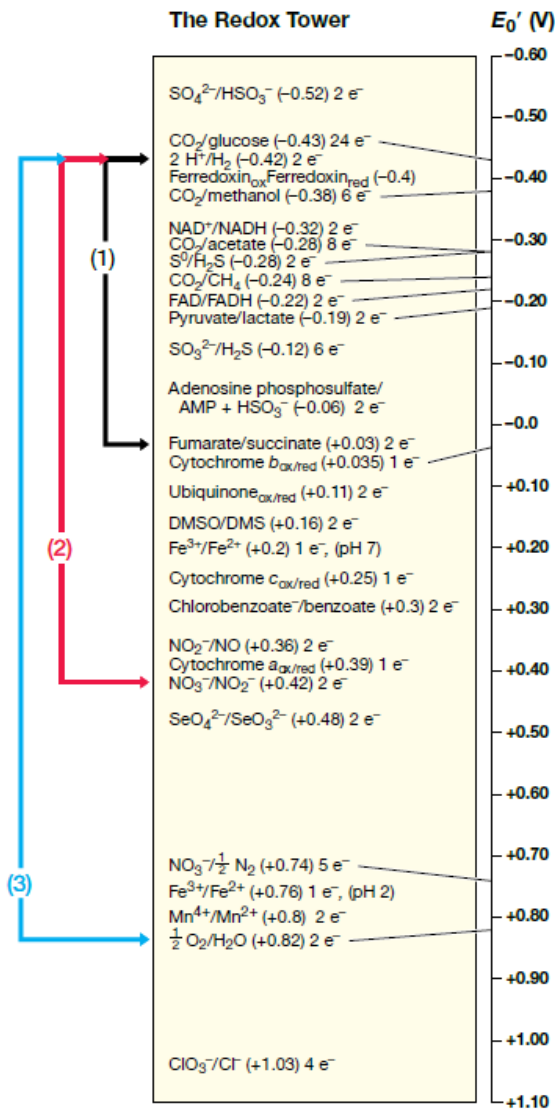


Figure 6.2 The redox tower (from Madigan et al., 2019).

If $Y_{\text{Met}/\text{S}}$ is available from experimental data, the complete metabolic reaction can be derived straightforwardly. Otherwise, semi-empirical methods have been proposed to provide a theoretical estimation of such a factor.

Among them, the Gibbs energy dissipation method by Heijnen et al. (1992) proposes that metabolic relations can also be expressed in terms of Gibbs energy change balances, between the catabolic and anabolic reactions:

$$\Delta G_{\text{Met}} = \lambda_{\text{Cat}} \cdot \Delta G_{\text{Cat}} + \Delta G_{\text{An}} \quad \text{Eq. 6.3}$$

The standard Gibbs energy change for a reaction is given by the following equation:

$$\Delta G_R^0 = \sum_i Y_i^R Gf_i^0 \quad \text{Eq. 6.4}$$

being Y_i^R the stoichiometric coefficient of component i ($Y_i^R < 0$ for substrates and $Y_i^R > 0$ for products) and Gf_i^0 the standard Gibbs energy of formation for each compound i , calculated on the basis of the correspondent reference compound. An extensive dataset of Gf^0 for the main inorganic and organic compounds involved in microbial metabolism is listed in Heijnen and Kleerebezem (2010) and has been used in the present work. Standard Gibbs energy of formation and, consequently, standard Gibbs energy change of a reaction are referred to the following standard conditions: (i) temperature of 298,15 K (25 °C); (ii) all aqueous (dissolved) diluted species are at 1 M concentration (assuming the *molar concentration* as equivalent to the *activity*); (iii) all gaseous species are at 1 bar partial pressure.

In order to calculate the actual Gibbs energy change, the correction for actual compounds' concentrations is given by the following expression:

$$\Delta G_R^1 = \Delta G_R^0 + RT_S * \ln Q_R = \Delta G_R^0 + RT * \ln \left\{ \frac{(C_{P1})^{Y_{P1}} (C_{P2})^{Y_{P2}} \dots (C_{Pn})^{Y_{Pn}}}{(C_{S1})^{Y_{S1}} (C_{S2})^{Y_{S2}} \dots (C_{Sn})^{Y_{Sn}}} \right\} \quad \text{Eq. 6.5}$$

Where R and T_S are the gas constant ($8,314 \cdot 10^{-3} \text{ kJmol}^{-1} \text{ K}^{-1}$) and the standard temperature (298,15 K), respectively, and Q_R is the reaction quotient, i.e. the mathematical products of the activities of each product at the power of its correspondent stoichiometric coefficient divided by the mathematical product of the activities of reactants at the power of its correspondent stoichiometric coefficient. In highly diluted solutions (ionic strength $< 0,01 \text{ M}$), activities are considered equal to molar concentrations and no corrections are required (Kleerebezem and van Loosdrecht, 2014).

The condition of standard concentration for all the dissolved species implies that also proton H^+ concentration is equal to 1 M, resulting in a solution pH of 0. Since such a condition is not reasonable when dealing with biological reactions, standard Gibbs energy changes are corrected to a pH value of 7. Such an assumption is in line with the fact that the intracellular pH, which is the environment where the majority of metabolic reactions takes place, is close to 7 (Heijnen and Kleerebezem, 2010). ΔG_R^{01} denotes the standard Gibbs energy of the reaction, at pH of 7. As a first estimation, all calculations in this work are referred to ΔG_R^{01} .

In an ideal closed system, equation 6.3 would equal zero as no energy dissipation would occur. Though, in real open systems, such as microorganism cells, energy dissipation does occur during catabolic and anabolic reaction steps as well as for material transport across the cell. Thereby, the catabolic reaction needs to provide anabolism-related energy, net of the different dissipation terms, here gathered together in the single term ΔG_{Dis} . The formulation, then becomes:

$$\lambda_{Cat} \cdot \Delta G_{Cat} + \lambda_{An} \cdot (\Delta G_{An} + \Delta G_{Dis}) = 0$$

or analogously, for 1 C-mol of biomass synthesized:

$$\Delta G_{Dis} = -\lambda_{Cat} \cdot \Delta G_{Cat} + \Delta G_{An} \quad \text{Eq. 6.6}$$

The term ΔG_{dis} has been also subject of discussion and theories have been proposed to offer mathematical formulation for its estimate.

Heijnen et al. (1992) proposed two different parametric approaches for heterotrophic and autotrophic biomass, according to an extensive dataset of empirical observed biomass yields ($Y^{met}_{X/S}$), for a variety of chemotrophic processes. The ultimate energy dissipation (somehow the inverse of energy efficiency) of microbial growth appeared in fact as a function of the C-source only and, in autotrophic growth, of the e-donor only (Kleerebezem and Van Loosdrecht, 2010).

More in details, for heterotrophic microorganisms, the dissipation energy turned to be a function of the organic compound used as C-source, specifically of its C-chain length (number of carbons in the chain, NoC) and the degree of reduction of the element C in the compound (γ). The abovementioned authors present an empirical equation to estimate ΔG_{dis} , based on this information on the organic source (equation 6.7). Cross validation with empirical reported value of $Y^{MET}_{X/S}$, showed that the calculated values allowed for estimation with an error within 13% with respect to experimental data.

$$\Delta G_{Dis} = 200 + 186 * (6 - NoC)^{1,8} + exp\{[(3.8 - \gamma)^2]^{0,16} * (3,6 + 0,4 * NoC)\} \quad \text{Eq. 6.7}$$

In case of autotrophic biomass, the dissipation energy is proposed as a function of the e-donor. As a general conclusion, the dissipation is mainly depending on whether the mechanism of reverse electron transport (RET) is involved in the metabolism or not. Reverse electron transport is a mechanism of inverse electron flow in the cellular electron chain. Electron flow is usually governed by redox potential gradients between e-donor intermediates and e- carriers (as cytochromes and quinones), the flow being driven from the more electronegative to the less electronegative compound and, ultimately, to the terminal electron acceptor. In the RET, electrons are transferred against the thermodynamic gradient and energy needs to be inverted to allow for the reaction to occur. In many autotrophic bacteria, thus using inorganic carbon as C-source for anabolic purposes, CO₂ fixation for cell synthesis implies RET mechanism for the production of the reducing power in the form of NADH (or FADH₂ or reduced Ferredoxin, depending on the CO₂ fixation pathways). Energy to act against the redox potential of the two compounds is usually provided by membrane gradients, i.e. proton motive force. Kleerebezem and Heijnen (2010) suggest that RET is needed when weak e- donors are involved in the catabolic reaction (such as NH₄⁺ or Fe²⁺), since the energy provided in the catabolic reaction is not sufficient to deliver anabolic-related energy, whereas metabolisms involving strong e-donor do not require RET. In this latter case, ΔG_{dis} can be calculated solving equation (7), assuming CO₂ as C-source. In case the

RET is involved, the resulting dissipation energy is very high and a standard value is assumed for all the anabolic reactions implying such a mechanism. As a conclusion:

1. $\Delta G_{\text{dis}} = 689 \text{ kJ/C-mol}$, if RET is not required.
2. $\Delta G_{\text{dis}} = 3500 \text{ kJ/C-mol}$, if RET is required.

As a general rule, the authors also suggest that for anabolic reaction with positive ΔG_{an} , RET is generally involved, and vice versa for negative ΔG_{an} .

Once the ΔG_{dis} is defined together with Gibbs energy changes in catabolism and anabolism, equation 6.6 can be solved for λ_{cat} and the $Y^{\text{MET}}_{\text{X/S}}$ derived from equation 6.2, i.e. the overall growth reaction can be completed.

6.26 Materials and Methods

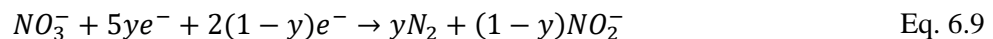
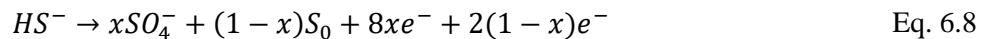
6.2.1 Catabolic reaction stoichiometry

Catabolic stoichiometry has been solved for all the possible intermediate steps of the SO-NR process, considering sulphide or elemental sulphur as e-donor and nitrate or nitrite as e-acceptor. Elemental sulphur and nitrite were considered either as reactant and end-products. Both oxidation and reduction reactions were simplified in a 2-step reactions and no other intermediary products were considered except sulphur and nitrite, respectively.

A focus study on the case of sulphide as e-donor and nitrate as terminal e-acceptor was conducted, being the process object of the present thesis work. Specifically, adopting a similar approach as Klatt and Polerecky (2015), a fraction x ($0 < x < 1$) has been introduced to account for the fraction of influent sulphide oxidized completely to sulphate. The remaining fraction $1-x$, accounted for the influent sulphide oxidized to elemental sulphur (Eq. 5.1).

Analogously, the fraction y ($0 < y < 1$) has been introduced to account for the fraction of influent nitrate completely reduced to dinitrogen gas; the remaining $1-y$ for the fraction reduced to nitrite.

In synthesis, a general formulation for the oxidation and reduction half reactions can be written as follows:



If $x=1$, all the influent sulphide is oxidised to sulphate; if $x=0$ all the influent sulphide is oxidized to sulphur. Analogously, if $y=1$, all the influent nitrate is reduced to dinitrogen gas; if $y=0$ all the influent nitrate is reduced to nitrite.

Also, a wider range of realistic conditions for pH and temperature has been evaluated, in order to assess any possible variations in free Gibbs energy change. As a starting point, free Gibbs energy change generated for each catabolic intermediate reaction, was calculated at standard conditions in terms of temperature (298,15 K), dissolved components (1 M concentration) and gaseous pressure (1 bar), and pH of 7. Then a range of pH and temperature values were considered and free Gibbs energy calculated according to equation 6.5. Specifically, the pH has been considered in the moderate alkaline range of 8-12 for three reasons: (i) alkaline environment are applied when dealing with dissolved forms of sulphide, in order to reduce its volatility; (ii) at pH of 8-12, HS⁻ is the dominant species and no changes accounting for a different speciation are required in free Gibbs energy calculations; (iii) moderate alkaline environments were the range of interest in this thesis, avoiding extreme alkaline conditions implying a shift in microbial population towards alkalophilic SOB. Moreover, the mesophilic temperature range of 25-35 °C was also studied, being a possible condition to be adopted in real-scale PAD/A implementations for industrial wastewaters (e.g. tannery wastewaters, see section 4.1).

6.2.2 Application of the free Gibbs energy method to study SOB biomass yield: hypotheses and simplifications

In the generalized method from Heijnen et al. (1992), the estimation of energy dissipation of autotrophic bacteria lays on the dualistic hypothesis that anabolism relies on RET mechanism or not, thereby lumping under this assumption the diverse metabolic mechanisms underlying the overall energetic efficiency of a cell (e.g. metabolic pathways, CO₂ fixation pathways, intermembrane transport). It owns to be mentioned that this specific aspect of anabolism (RET requirement) depends on the electron donor only and not on the e-donor/e-acceptor couple, as in the case of catabolism. Indeed, the e-donor oxidation pathway, in autotrophic metabolisms, drives the electron flow towards intermediate carriers, cytochromes or quinones, usually at a more positive E_0' value than NAD⁺. According to Kleerebezem and Van Loosdrecht (2010), when HS⁻ is then used as e-donor and oxidized to its final oxidation form SO₄²⁻, no RET would be required since HS⁻ is a strong e-donor. Despite that, Gibbs energy calculations for anabolic reaction in the present study resulted in positive values, suggesting the opposite. Moreover, sulphur-oxidizing chemolithotrophic bacteria are reported to adopt RET for C fixation (Klatt and Polerecky, 2015; Lin et al., 2018; Madigan et al., 2019) opening rooms for discussion. Defining if and how efficiently bacteria adopt RET is, in fact, not always straightforward since many metabolic mechanisms remain unclear. Three works from the literature have been selected to drive the present discussion.

1. Kleerebezem and Mendez (2002) have compared the biomass yield obtained in their SOB-based work with values reported in literature. A total of 8 studies were reviewed, adopting mainly thiosulphate as e-donor but also sulphide and elemental sulphur; literature biomass yields were then used to derive overall metabolic energy dissipation, by applying the free Gibbs energy method in a bottom-up approach. As a result, energy dissipation was estimated to be ca 1500±600 kJ/C-mol. Even though the

standard deviation was as high as the 40%, the confidential errors follows below the value of 3500 kJ/C-mol, suggesting a more efficient energy uptake.

2. Yavuz et al. (2007) have applied the free Gibbs energy method to estimate the theoretical biomass yield of SOB, under the assumption that a highly energy-requiring RET mechanism was required for biomass synthesis, i.e. $\Delta G_{\text{dis}} = 3500$ kJ/C-mol. Results from Yavuz et al. (2007) have been used by Can-Dogan et al. (2010) and Mora et al. (2014).
3. Klatt and Polerecky (2015) report an interesting study on SOB energetics proposing a new theoretical approach to estimate microbial bioenergetics efficiency, based on the factorization of the metabolic aspects involved in energy conversion and production. Specifically, for SOB bacteria, the energetic efficiency of the following aspects is considered: (i) energy production in the catabolic reaction, depending on the Sulphur metabolic pathway used by the microorganism (three main pathways are currently accepted, see section 1.1.3); (ii) CO₂ fixation cycles and (iii) e-donor consumption in RET for the reducing power to be produced (NADH, FADH₂ or reduced Ferredoxin). Even though, such a new method is not implemented in the present study, it is of interest to highlight the underlying assumptions and conclusions proposed by the authors. Concerning the issue on RET adoption by SOB biomass, authors do not question the use of RET by chemolithoautotrophic SOB, but they argue on the RET efficiency, instead.

Another aspect discussed in this section is the biomass formulation used in the stoichiometries available in literature. Some studies report a C-mol formulation of CH_{1,8}O_{0,5}N_{0,2} as reported in Roels (1983); some others a 5C-mol formulation of C₅H₇O₂N (Rittman and McCarty, 2001). Normalizing the second formulation to one C-mol, biomass stoichiometry results in CH_{1,4}O_{0,4}N_{0,2} slightly different for H and O fractions.

In the present work, full stoichiometry has been solved for all the possible reaction steps occurring in SO-NR, under the following scenarios:

1. Energy dissipation, EDiss
 - EDiss_1 $\Delta G_{\text{dis}} = 3500$ kJ/react;
 - EDiss_2 $\Delta G_{\text{dis}} = 1500$ kJ/C-mol (average value from Kleerebezem and Mendez, 2002)
2. Biomass composition, BC
 - BC_1: CH_{1,8}O_{0,5}N_{0,2} (Roels, 1983);
 - BC_2: CH_{1,4}O_{0,4}N_{0,2} (normalized to 1 C-mol from Rittman and McCarty, 2001)

As general assumptions, one single SO-NR biomass is assumed for all the possible reactions, CO₂ (as HCO₃⁻) and NH₄⁺ are considered as C and N source, respectively. A study on the derived theoretical biomass yield was conducted and compared with literature values.

6.2.3 Partial autotrophic denitrification: a thermodynamic insight on experimental outcomes

The experimental values reported in Chapter 5 were used to carry out a thermodynamic study on the specific system adopted. The underlying question of such a study was whether thermodynamics may somehow explain or provide a deeper insight to the catabolic shift observed in the experimental work, i.e. from complete denitrification to partial denitrification, under strictly S-limiting conditions. The approach described in the following paragraphs was used to address such an interrogative. As a brief synthesis of the experimental work, three different experimental phases were tested in the CSTR (Phase 1, 2 and 3), by varying the nitrate and sulphide load (mgN/h and mgS/h) as well as S/N_{applied} and SRT. In this chapter, SRT influence is not considered since it did not show a significant impact on nitrite accumulation performance at the low values tested. Catabolic equations and derived yields and free Gibbs energy change were taken from the results presented in section 6.3.1. Since the CSTR was fed with sulphide and nitrate, and the prevalent oxidation reaction was $\text{HS}^- \rightarrow \text{SO}_4^{2-}$, only the equation coupling this oxidation step and the two possible reduction of nitrate (to dinitrogen gas, namely R1 or to nitrite, namely R3) were considered. With reference of tab. 6.2, the first and third equations were considered.

Each reaction requires a minimum S/N ratio to be completed, which is 1,43gS/gN (S/N_{R1}) and 0,57 gS/gN (S/N_{R3}), respectively.

For each day of the experimental phase, the S/N_{applied} was compared with the S/N required for each of the two reactions. Two extreme conditions were considered:

1. the available electron donor is fully adopted for running reaction R1;
2. the available electron donor is fully adopted for running reaction R3.

For each of the two mutually exclusive conditions (only R1 or R3 takes place), the maximum nitrate removal (% of the inlet nitrate load) was calculated as described in table 6.1.

Table 6.1 Calculation of nitrate removal (%) under the assumed conditions.

R1	If $S/N_{applied} < S/N_{R1}$ →	$NO_3^-_{removal_{R1}} = \frac{S/N_{applied}}{S/N_{R1}} * 100$	Condition 1.a
	If $S/N_{applied} > S/N_{R1}$ →	$NO_3^-_{removal_{R1}} = 100\%$	Condition 1.b
R3	If $S/N_{applied} < S/N_{R3}$ →	$NO_3^-_{removal_{R3}} = \frac{S/N_{applied}}{S/N_{R3}} * 100$	Condition 2.a
	If $S/N_{applied} > S/N_{R3}^*$ →	$NO_3^-_{removal_{R3}} = 100\%$	Condition 2.b

* and lower than S/N_{R1}

For each day of the experimental work, free Gibbs energy delivery, expressed as kJ/h, was calculated for each conditions according to the following general formulation:

$$Energy\ delivery = NO_3^-_{removal} * \Delta G_{cat_R}^{01} * SLR \quad Eq. 6.10$$

Where $\Delta G_{cat_R}^{01}$ is the free Gibbs energy change of the catabolic reactions R1 or R3 (tab. 6.1) and SLR is the sulphide loading rate applied to the reactor and expressed as gS/h.

Conditions 1.b and 2.b imply that combinations of R1 and R3 were not considered in this chapter, i.e. the estimation of the energy delivery for the two reactions was calculated for R1 and R3 as they were mutually exclusive reactions (the available electron donor used only for running reaction R1 or reaction R3).

The aim of this approach was to estimate the theoretical energy supply from reaction R1 or R3, at given the limited electron donor availability.

6.3 Results

6.3.1 Study on the catabolic intermediate reactions

Catabolic reactions for the possible intermediate steps in SO-NR process have been solved and results are presented in table 6.2. The information on the S/N and H⁺/S presented in table 6.2 is presented in an aggregated form in figures 6.4 and 6.5.

Due to the complexity of the process, such an aggregated information is intended to provide a supporting tool for process implementation, design and optimization, as well as for a comprehensive and fast insight on process stoichiometry. It owns to be mentioned that catabolic stoichiometry instead of full-metabolic one is deemed sufficient for process design and optimization when dealing with autotrophic processes. As a matter of fact, considering the much more common autotrophic process of nitrification, titrimetric assessments are typically conducted considering the significant proton production occurring in the catabolic reaction only.

In section 4.1.1, a possible treatment scheme for PAD/A implementation has been presented. As already discussed, not only the layout scheme could be adopted to the specific conditions of a given wastewater treatment facility (e.g. one or two stage configuration, according to space availability and investment costs) but also, the end-product of the S-oxidation and N-reduction could be targeted according to the specific need. The aggregated information in terms of S/N and H^+/S provided in the present chapter are presented as support tool for the best combination of the N and S load in order to meet the requirement.

Table 6.2 Catabolic reactions in SO-NR process. For each reaction, required S/N ratio, acidity consumption/production and free Gibbs energy released are reported.

e- donor oxidation reaction	e- acceptor reduction reaction		HS ⁻	S	NO ₃ ⁻	NO ₂ ⁻	H ⁺	SO ₄ ⁻²	N ₂	H ₂ O	S/N		H ⁺ consumed/S _{oxidized}		ΔG ⁰¹	
											mol/mol	g/g	mol/mol	Acidity	kJ/S-mol	kJ/e-mol
HS ⁻ → SO ₄ ⁻²	NO ₃ ⁻ → N ₂	R1	-1	0	-1,6	0	-0,6	1	0,8	0,8	0,6	1,4	0,6	Consumption	-744,4	-93,1
	NO ₂ ⁻ → N ₂	R2	-1	0	0	-2,67	-1,67	1	1,33	1 3	0,4	0,9	1,7	Consumption	-920,6	-115,1
	NO ₃ ⁻ → NO ₂ ⁻	R3	-1	0	-4	4	1	1	0	0	0,3	0,6	-1,0	Production	-480,2	-60,0
HS ⁻ → S	NO ₃ ⁻ → N ₂	R4	-1	1	-0,4	0,0	-1,4	0	0,2	1,2	2,5	5,7	1,4	Consumption	-196,4	-98,2
	NO ₂ ⁻ → N ₂	R5	-1	1	0	-0,7	-1,7	0	0,3	1,3	1,5	3,4	1,7	Consumption	-240,4	-120,2
	NO ₃ ⁻ → NO ₂ ⁻	R6	-1	1	-1	1	-1	0	0	1	1,0	2,3	1,0	Consumption	-130,3	-65,2
S → SO ₄ ⁻²	NO ₃ ⁻ → N ₂	R7	0	-1	-1,2	0	0,8	1	0,6	-0,4	0,8	1,9	-0,8	Production	-548,1	-91,3
	NO ₂ ⁻ → N ₂	R8	0	-1	0	-2	0	1	1	0,00	0,5	1,1	0,0	Consumption	-680,2	-113,4
	NO ₃ ⁻ → NO ₂ ⁻	R9	0	-1	-3	3	2	1	0	-1	0,3	0,8	-2,0	Production	-349,9	-58,3

Acidity/alkalinity consumption

In pH-influencing processes, the assessment of alkalinity consumption or production is of prominent importance for the stability of the entire treatment line, in order to prevent problems such as severe pH drop (and quantify buffer/reagents requirements) or scaling/mineral precipitation problems (see Chapter 3). In case SO-NR is implemented for biogas desulphurization and wastewater denitrification, a typical bio-scrubber scheme is presented in figure 6.3. A chemical adsorption column is necessary prior to the biological unit in order to transfer sulphide from the gaseous to the liquid phase. Such a transfer is governed by pH according to the equilibrium reactions presented in chapter 1 (eq. 1.2 and 1.3, summarised in fig. 1.5). In order to obtain a good H₂S transfer, a minimum pH around 8-9 is usually maintained. In conventional chemical scrubbers, high pH and sufficient alkalinity is ensured by external supply of solutions based on CaOH or NaOH, thereby requiring chemicals addition. If recirculation from the biological SO-NR reactor is provided, such an alkalinity requirement could be entirely or partially fulfilled, depending on the prevailing catabolic step selected/occurring in the bioreactor. Assuming that at pH of 8-12, 1 mol H⁺ is consumed during the transfer of 1 mol of H₂S into the liquid (resulting in the production of 1 mol of HS⁻), an alkalinity neutral system would require a minimum supply of 1 mol H⁺ for each mol of HS⁻ oxidized in the biological reactor.

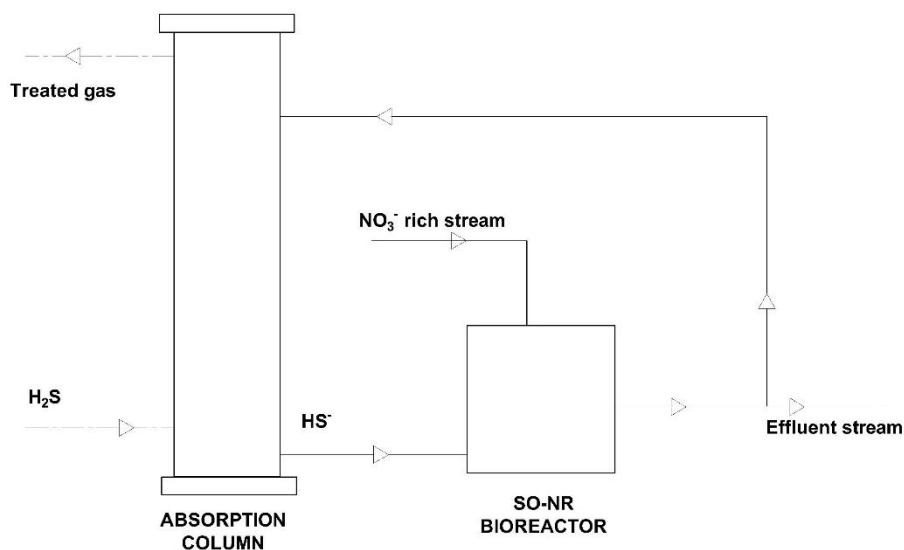


Figure 6.3 Schematic of an anoxic bioscrubber, coupling absorption column (for gas-liquid transfer) and SO-NR bioreactor (for the actual HS degradation). Dotted line, gas streams; solid line, liquid streams.

As presented in fig. 6.4, SO-NR can either be an alkalinity consuming or producing process, depending on the end-products of the redox reactions, since the proton consumption of the S oxidation is counteracted by the proton consumption of N reduction, in the different extent presented in the graph. The highest alkalinity recover is achieved when complete denitrification is coupled with 100% elemental sulphur production obtaining the highest acidity consumption of 1,4 molH⁺/S-mol (alkalinity production of 1,1 gCaCO_{3,eq}/gS). If

partial autotrophic denitrification (PAD, i.e. complete nitrite accumulation) is targeted, alkalinity recover corresponding to the proton consumption of 1 molH⁺/S-mol can be obtained if sulphide oxidation is driven towards elemental sulphur production. On the contrary, in case PAD is coupled with sulphate production (R3), which was the target process in the present thesis, an acidity production of 1 molH⁺/S-mol is obtained (alkalinity consumption of 0,8 gCaCO_{3,eq}/gS), thereby its implementation should be properly designed according to the alkalinity conditions of the treated wastewater stream. However, it should be noticed that the innovative PAD process, is intended to be coupled with the anammox process, an alkaline-producing process, consuming around 0,02-0,06 molH⁺/molN-NH₄⁺ (Lotti et al., 2014b), further increasing the net alkalinity production of the overall treatment. Thereby, the overall alkalinity assessment should be done over the coupled PAD/A process.

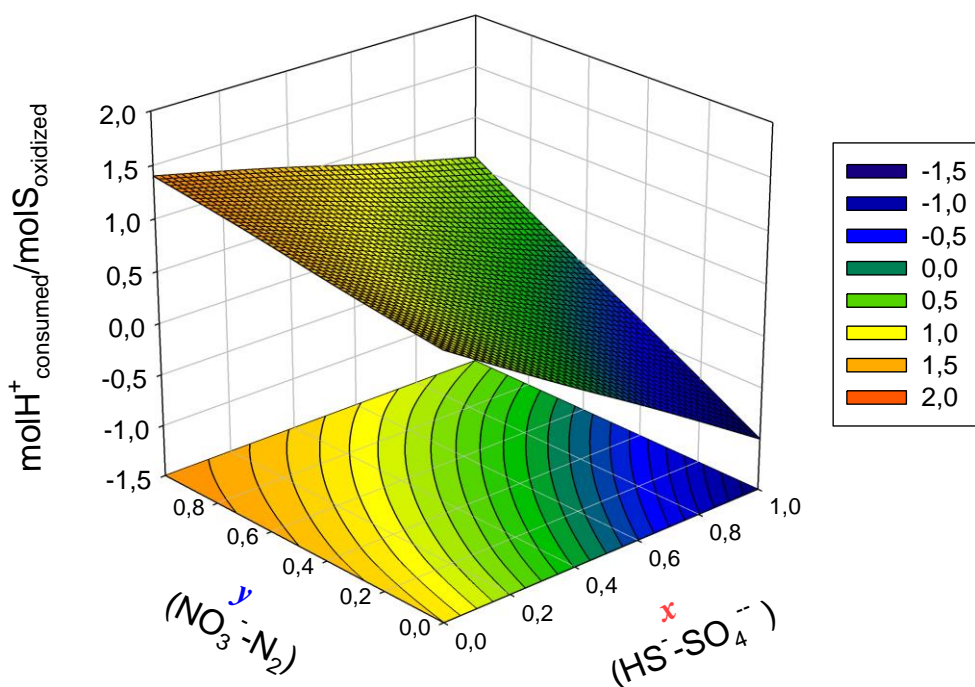


Figure 6.4 Proton consumption per mole of S oxidized in the studied range of possible intermediate reactions (positive values indicate proton consumption, i.e. alkalinity production; negative values indicate proton production, i.e. alkalinity consumption). If $x=0$ influent sulphide is completely oxidised to elemental sulphur, if $x=1$ influent sulphide is completely oxidised to sulfate. If $y=0$ influent nitrate is completely reduced to nitrite, if $y=1$ influent nitrate is completely reduced to dinitrogen gas.

S/N ratio

The information gathered in figure 6.5 shows that the S/N ratio, i.e. the amount of sulphide that can be removed per gram of nitrogen nitrate removed, varies in the wide range of 0,6-5,7 gS/gN.

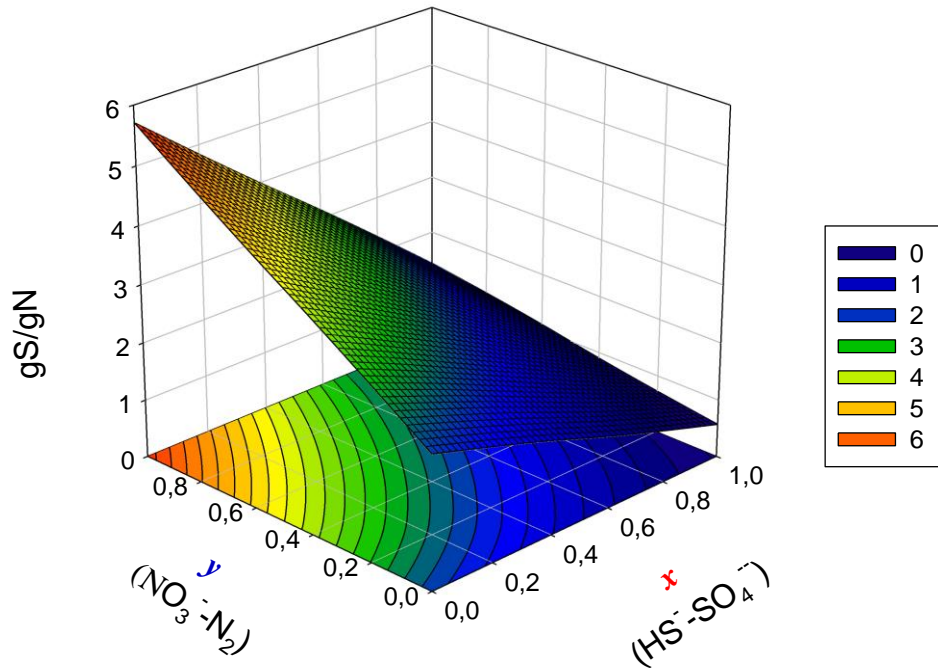


Figure 6.5 S/N ratio required in the studied range of possible intermediate reactions.

If $x=0$ influent sulphide is completely oxidised to elemental sulphur, if $x=1$ influent sulphide is completely oxidised to sulfate. If $y=0$ influent nitrate is completely reduced to nitrite, if $y=1$ influent nitrate is completely reduced to dinitrogen gas.

The graph clearly shows that the maximum S/N value is obtained when all the sulphide is oxidized to elemental sulphur and nitrate is fully reduced to dinitrogen gas. Vice versa, the minimum S/N ratio is obtained if PAD is coupled with sulphate production. Low S/N values correspond to high specific N removal per gram of sulphide removed. In the perspective of redesigning S and N cycles in WWTPs, the implementation of autotrophic S-driven denitrification allows for high flexibility in terms of S and N loads that can be combined. In case S- HS^- removal wants to be optimized, SO-NR process should be pushed towards reaction R4 (N_2 and S production). On the contrary, at a given sulphide load, N- NO_3^- removal is maximized when the process occurs according to reaction R3 (NO_2^- and SO_4^{2-} production). In the perspective of implementing the innovative process coupling PAD and AMX, both R6 and R3 would provide the required nitrite accumulation. In case of a one-stage configuration, the sulphur produced in R6 would remain available in the bulk liquid and would possibly accumulate in the reactor, altering the electron donor availability in case of an operational strategies based on strict S-limiting supply, as the one adopted in Chapter 5. Also an effective equilibrium among biomasses' affinity for nitrite as well as biomass growth in the system should be achieved and maintained stable. In a two-stage configuration, such problems could be overcome by introducing a S-recovery unit

between the SO-NR reactor and the AMX one (in case of S^0 as end product of sulphide oxidation, R6) and by favouring the optimum conditions for the two microbial population. On the other side, reaction R3 allows for the maximum N removal per gram of sulphide oxidized but special attention should be put on the resulting sulphate concentration, in order to comply with concentration limits for discharge.

Free Gibbs energy

As presented in table 6.2 catabolic reactions deriving from all the possible combination of e-acceptor/e-donor are strongly exergonic. Indeed, reduced sulphur compounds are very good electron donors (Kleerebezem and Van Loosdrecht, 2010).

Correction of $\Delta G_{\text{cat}}^{01}$ to the actual concentration of the species are reported to have a significant influence on the final λ_{cat} when the catabolic Gibbs energy change is low or close to zero. In the catabolic reactions considered in the present work, $\Delta G_{\text{cat}}^{01}$ are strongly negative, ranging from -130 to -920 kJ/react, depending on the e-donor/e-acceptor couple. Calculations of the actual Gibbs energy change, ΔG^1 , at 0,01 M concentration for the S and N substrates³² have been conducted only for the catabolic reactions involving partial oxidation of HS^- to S, being the ones with the lower absolute value of ΔG^{01} and therefore those potentially affected by errors if ΔG^{01} rather than ΔG^1 is considered. Yet, the calculated variations for Gibbs energy changes are in the order of 20-30 kJ/S-mol, confirming that calculations based on ΔG^{01} provide an exhaustive description of the process. Lin et al. (2018) report ΔG^{01} values of some of the catabolic reaction presented in table 6.2; literature values are in agreement with those calculated in the present work.

Figure 6.6 shows the results on ΔG^{01} variations at the different reaction steps. Neither pH nor temperature variations appear to have a significant influence in the studied range. Such a behaviour is in agreement with the fact that sulphide and elemental sulphur are strong electron donor and nitrate and nitrite are good electron acceptor, thereby the energy delivered by their oxidation/reduction remains high irrespective of the actual T and pH conditions of the process (at the considered parameters range).

An interesting evidence is that the denitritation step appears to be the most favourable in all the cases. Compared to the denitratation step, the higher energy potential of denitritation can be ascribed to the fact that 3 electrons are accepted when nitrite is reduced to dinitrogen gas whereas only 2 electrons are accepted when nitrate is reduced to nitrite. Still, ΔG^{01} related to denitritation are even more favourable than the complete nitrate denitrification to dinitrogen gas, where 5 electrons are involved. This is in line with the fact that nitrite is a highly reactive substance and nitrite accumulation are usually reported only in case of process disruption or unstable/unbalanced loads, denoting temporary process failures. From a first thermodynamic insight, intentionally preventing the denitritation step as desired in successful nitrite accumulation (i.e. PAD) seems to

³² Corresponding to 32 mgS/l and 14 mgN/l. These concentrations are more likely to occur in the bulk liquid of real CSTR reactors.

be a challenging task, since the nitrite reduction is the most favourable reaction step. Such an evidence is partially invalidated in section 6.3.3.

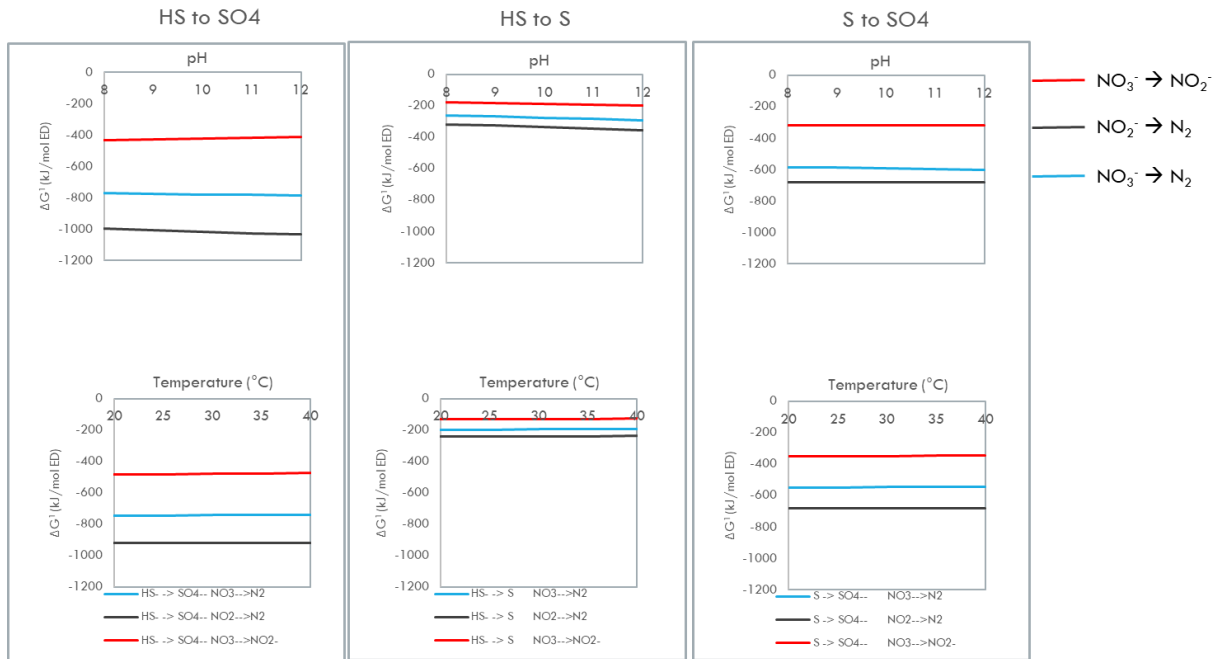


Figure 6.6 Results on free Gibbs energy change at mesophilic temperature and slightly alkaline pH.

6.3.2 Biomass yield: sensitivity study and literature review

The free Gibbs energy method has been applied for all the possible e-donor/e-acceptor couples, occurring in SO-NR. Table 6.3 reports the free Gibbs energy change of anabolic reactions, assuming the two biomass compositions available in literature. At each ED reduction step, all the possible TEA reduction combination are reported even though they do not affect $\Delta G_{01_anabolism}$ in order to stress out that anabolism energetics depends on the ED only. Table 6.4 reports a synthesis of the biomass yields derived for each catabolic step, under the assumptions on energy dissipation and biomass composition. Biomass yields (herein referred as Y) are reported both as C-mol/S-mol and C-mol/e-mol (i.e. C-mole production per electron mole released during the ED oxidation). First a general discussion on the TEA reaction impact on the biomass yield is offered. Then, the impact on the initial assumptions on overall energy dissipation and biomass composition is provided.

Table 6.3 Free Gibbs energy change in anabolic reactions, at the different ED/TEA couples and the two biomass composition reported in literature.

e- donor oxidation reaction	e- acceptor reduction reaction	$\Delta G_{01_anabolism}$ (kJ/C-mol)	
		CH _{1,8} O _{0,5} N _{0,2}	CH _{1,4} O _{0,4} N _{0,2}
1. HS ⁻ → SO ₄ ⁻²	NO ₃ ⁻ → N ₂	54,6	27,1
	NO ₂ ⁻ → N ₂		
	NO ₃ ⁻ → NO ₂ ⁻		
2. HS ⁻ → S	NO ₃ ⁻ → N ₂	33,1	6,6
	NO ₂ ⁻ → N ₂		
	NO ₃ ⁻ → NO ₂ ⁻		
3. S → SO ₄ ⁻²	NO ₃ ⁻ → N ₂	61,8	33,9
	NO ₂ ⁻ → N ₂		
	NO ₃ ⁻ → NO ₂ ⁻		

Table 6.4 Main results from biomass yield study.

	$\Delta G^{01}_{met} = 3500 \text{ kJ/Cmol}$				$\Delta G^{01}_{met} = 1500 \text{ kJ/Cmol}$			
	C-mol_biom/S-mol		C-mol_biom/e-mol		C-mol_biom/S-mol		C-mol_biom/e-mol	
	$\text{CH}_{1,8}\text{O}_{0,5}\text{N}_{0,2}$	$\text{CH}_{1,4}\text{O}_{0,4}\text{N}_{0,2}$	$\text{CH}_{1,8}\text{O}_{0,5}\text{N}_{0,2}$	$\text{CH}_{1,4}\text{O}_{0,4}\text{N}_{0,2}$	$\text{CH}_{1,8}\text{O}_{0,5}\text{N}_{0,2}$	$\text{CH}_{1,4}\text{O}_{0,4}\text{N}_{0,2}$	$\text{CH}_{1,8}\text{O}_{0,5}\text{N}_{0,2}$	$\text{CH}_{1,4}\text{O}_{0,4}\text{N}_{0,2}$
$\text{HS}^- \rightarrow \text{SO}_4^{2-}$ $\text{NO}_3^- \rightarrow \text{N}_2$	-0,189	-0,191	-0,024	-0,024	-0,383	-0,392	-0,048	-0,049
$\text{HS}^- \rightarrow \text{SO}_4^{2-}$ $\text{NO}_2^- \rightarrow \text{N}_2$	-0,228	-0,231	-0,028	-0,029	-0,452	-0,463	-0,056	-0,058
$\text{HS}^- \rightarrow \text{SO}_4^{2-}$ $\text{NO}_3^- \rightarrow \text{NO}_2^-$	-0,126	-0,128	-0,016	-0,016	-0,266	-0,272	-0,033	-0,034
$\text{HS}^- \rightarrow \text{S}$ $\text{NO}_3^- \rightarrow \text{N}_2$	-0,050	-0,050	-0,025	-0,025	-0,101	-0,103	-0,050	-0,052
$\text{HS}^- \rightarrow \text{S}$ $\text{NO}_2^- \rightarrow \text{N}_2$	-0,060	-0,060	-0,030	-0,030	-0,118	-0,121	-0,059	-0,060
$\text{HS}^- \rightarrow \text{S}$ $\text{NO}_3^- \rightarrow \text{NO}_2^-$	-0,034	-0,035	-0,017	-0,017	-0,072	-0,074	-0,036	-0,037
$\text{S} \rightarrow \text{SO}_4^{2-}$ $\text{NO}_3^- \rightarrow \text{N}_2$	-0,139	-0,141	-0,023	-0,023	-0,282	-0,289	-0,047	-0,048
$\text{S} \rightarrow \text{SO}_4^{2-}$ $\text{NO}_2^- \rightarrow \text{N}_2$	-0,168	-0,171	-0,028	-0,028	-0,334	-0,342	-0,056	-0,057
$\text{S} \rightarrow \text{SO}_4^{2-}$ $\text{NO}_3^- \rightarrow \text{NO}_2^-$	-0,092	-0,093	-0,015	-0,015	-0,194	-0,198	-0,032	-0,033
$\text{HS}^- \rightarrow \text{SO}_4^{2-}$	-0,181	-0,183	-0,023	-0,023	-0,367	-0,376	-0,046	-0,047
$\text{HS}^- \rightarrow \text{S}$	-0,048	-0,048	-0,024	-0,024	-0,097	-0,099	-0,049	-0,050
$\text{S} \rightarrow \text{SO}_4^{2-}$	-0,133	-0,135	-0,022	-0,022	-0,270	-0,276	-0,045	-0,046
$\text{HS}^- \rightarrow \text{SO}_4^{2-}$	-0,18±0,05		-0,023±0,006		-0,37±0,09		-0,046±0,012	
$\text{HS}^- \rightarrow \text{S}$	-0,05±0,01		-0,024±0,006		-0,10±0,02		-0,049±0,012	
$\text{S} \rightarrow \text{SO}_4^{2-}$	-0,13±0,04		-0,022±0,006		-0,27±0,07		-0,046±0,012	

At each ED oxidation reaction, biomass yield, either as C-mol/S-mol or C-mol/e-mol, varies by 27-29%, depending on the TEA reduction reaction that is used in catabolism. Such a wide range is to be ascribed to the fact that 2 to 5 electrons can be accepted in the TEA reduction steps, thereby affecting the free Gibbs energy available from catabolism and, ultimately, the λ_{Cat} determining the full metabolism stoichiometry. The last three rows of table 6.4 summarize the Y values for each ED oxidation step, reporting average value and

standard deviation, calculated over the three possible TEA reduction cases. Such aggregated values are used to facilitate the following discussion.

Considering biomass yields expressed as C-mol/S-mol, the values from the oxidation reaction $\text{HS}^- \rightarrow \text{S}$ is almost half of the one obtained from the reaction $\text{S} \rightarrow \text{SO}_4^-$ and almost one third of the one from reaction $\text{HS}^- \rightarrow \text{SO}_4^-$, consistently with the fact that 2, 4 and 6 electrons are released in each reaction, respectively. Such an evidence matches with the results of biomass yields normalized to the electron released at each corresponding ED oxidation step. All the yields as C-mol/e-mol, in fact, exhibit values of 0,23 and 0,47 C-mol/e-mol, for the assumption of 3500 and 1500 kJ/C-mol, respectively.

It can be easily observed that the hypothesis on the overall energy dissipation is much more relevant than the one on the biomass composition. Indeed, only 1 to 2% variation is observed comparing the results from the two biomass compositions. In the biomass composition from Roels (1983), $\text{CH}_{1,8}\text{O}_{0,5}\text{N}_{0,2}$, the reduction state of carbon is 0,2 and 4,2 e-mol/C-mol are required to the reduction of CO_2 to such a reduction state in biomass. In the biomass composition from Rittman and McCarty (2001), $\text{CH}_{1,4}\text{O}_{0,4}\text{N}_{0,2}$, the reduction state of carbon is zero and 4 e-mol/C-mol are required instead. Thereby, it is reasonable that such a minor difference in electron requirement (0,2 e-mol/C-mol) implies a slightly different requirement of electron donor in the anabolic stoichiometry. Still, considering $\Delta G_{01_anabolism}$ reported in tab. 6.3, a noticeable difference does occur when the different biomass formulations are used. Nevertheless, such a difference is far outweighed by the high values of free Gibbs energy of dissipation in the full metabolism. The assumption on the overall energy dissipation is, in fact, the one that influences the most the final results on biomass yields, resulting in 50% of variation, if the two values of 3500 or 1500 kJ/C-mol are considered.

Biomass yields available in literatures have been evaluated and gathered according to the corresponding catabolic reaction considered in each work. Only works where sulphide or sulphur were used as electron donor were considered and results are summarized in table 6.5. Nevertheless, the value reported by Kleerebezem and Mendez (2002) are considered as representative also of the experimental values using thiosulphate as electron donor, since the literature review presented by the authors encompasses works based on thiosulfate, sulphur and sulphide oxidation (coupled with denitrification) and anaerobic cellular yields on sulphide consumption are reported to be comparable with that on thiosulfate, for *T. denitrificans* (Timmer-ten Hoor, 1981). Biomass yield unit conversion has been calculated for each study, when the information reported were sufficient for calculations³³. Note that the use of granular or biofilm-based biomass in UASB-like reactors are often reported, but biomass concentration is rarely assessed. Thereby, many studies on denitrifying SOB could not be used in this literature review due to the lack of information on biomass growth.

³³ All the works with the sole exceptions of Kleerebezem and Mendez (2020) and Yavuz et al. (2007) use the biomass formulation of $\text{C}_5\text{H}_7\text{O}_2\text{N}$.

Table 6.5 Literature review on SOB biomass yield, from studies where sulphide or sulphur were used as electron donor and nitrate as electron acceptor.

	Y				Reference	Experimental method
	1C-mol/ S-mol	1C-mol/ e-mol	g_biom/gS	g_biom/gN		
HS⁻→SO₄²⁻ NO₃⁻→N₂	0,512	0,064	0,378	0,635	Sublette and Sylvester, 1987	Experimental
	0,333	0,042	0,256	0,451	Kleerebezem and Mendez, 2002	Review/Thermodynamic calculations
	0,511	0,064	0,361	0,694	Campos et al., 2008	-
	0,184	0,023	0,130	0,208	Can-Dogan et al., 2010	Thermodynamic calculations*** confirmed by experimental evidence
	0,465	0,058	0,328	0,610	Mora et al., 2014c	Experimental
	0,156	0,019	0,118	0,149	This study*	Experimental
	0,189-0,383	0,023-,046	0,145-0,294	0,230-0,526	This study**	Thermodynamic calculations
HS⁻→S NO₃⁻→N₂	0,159	0,08	0,562		Gadekar et al., 2006	Experimental and modelling
	0,046	0,023	0,032		Can-Dogan et al., 2010	Thermodynamic calculations*** confirmed by experimental evidence
	0,065	0,033	0,046	0,300	Mora et al., 2014c	Experimental
	0,050-0,1	0,025-0,05	0,038-0,077	0,244-0,563	This study**	Thermodynamic calculations
S→SO₄²⁻ NO₃⁻→N₂	0,364	0,061	0,257	0,646	Sahynkaya et al., 2011	-
	0,400	0,067	0,283	0,737	Mora et al., 2014c	Experimental
	0,364	0,061	0,257	0,646	Batchler and Lawrence, 1978	Experimental
	0,139-0,292	0,023-0,047	0,107-0,224	0,25-0,514	This study**	Thermodynamic calculations

* Experimental values estimated in Chapter 5. Note: the catabolic step combined HS⁻→SO₄²⁻ and NO₃⁻→NO₂⁻, i.e. denitrification only.

** Theoretical yield according to the free Gibbs energy change method, under the hypothesis of ΔG⁰¹_{met} of 3500 kJ/C-mol (lower limit) and 1500 kJ/C-mol (upper limit).

*** Free Gibbs energy change method, under the hypothesis of ΔG⁰¹_{met} of 3500 kJ/C-mol.

It can be observed that all the reported values – with the exception of Gadekar et al. (2006) – are comparable with the theoretical values calculated in the present study, but the values vary in a quite wide range (from 0,05 to 0,5 C-mol/S-mol), depending on the catabolic step considered. For the full oxidation of sulphide to sulphate the values reported by Campos et al. (2008) and Mora et al. (2014c) are higher than the one estimated by the free Gibbs energy method, under the assumption of ΔG⁰¹_{met} of 1500 kJ/C-mol. These evidences suggest an even higher energy efficiency of the SOB involved. It owns to recall that the assessment of sulphur oxidizing

biomass concentration is not an easy task and different methods are used in literature. Conventional VSS analysis may suffer from elemental sulphur interference (sulphur is volatile at $T < 550^{\circ}\text{C}$), unless it is applied when sulphate is the sole end-product and/or no significant residual sulphur is found in the bulk liquid. Organic nitrogen, protein content and optical density are also used (Sublette and Sylvester, 1987; van de Bosh 2006). Gadekar et al. (2006) used ATP measurement, assuming that 1 mg of ATP corresponds to 1 g of biomass (Shuler and Kargi, 2002). The biomass yield value reported in this latter study is much higher than the others, but *Thiomicrospira CVO* were used as pure culture whereas cultures enriched mainly in *Thiobacillus* and *Sulfurimonas* species are used in the other studies. Moreover, in case of suspended biomass with no or limited sludge retention system, low biomass concentrations are found at steady state conditions due to the low biomass yield of autotrophic denitrifying SOB. In these cases, special care should be taken during VSS analysis since the systematic error of the analytical procedure might turn relevant. Also, in case of sulphide as electron donor, both sulphate and sulphur may be formed, if no specific control is applied in the system, making the biomass yield estimation even more troubled.

The biomass yield estimated in Chapter 5 was calculated during the steady state condition of phase 1 and 2, during which sulphate and nitrite were the main end-products, and resulted in 0,11-0,12 gVSS/gS, i.e. ca 0,02 C-mol/e-mol, in line with the theoretical value calculated assuming the low energetic efficiency assumption ($\Delta G_{\text{met}}^{01} = 3500 \text{ kJ/C-mol}$, see table 6.4). During the considered experimental period, sulphate was the main end-product and the SRT was as low as 24 h resulting in a highly enriched *Thiobacillus* culture (>80% at genus level in phase 2, see section 5.3.3). Nevertheless, it should be considered that the prevailing catabolic reaction in the experimental work was based on nitrate reduction to nitrite, differently from the values reported in table 6.6 (on complete nitrate reduction to N_2), indeed the catabolic step delivering less energy and resulting in low theoretical biomass yields (tables 6.2 and 6.4).

As a conclusion, due to the complexity of the SO-NR systems and the related SOB population, it seems that a more consistent comparison is achieved when biomass yields are expressed as C-mol/e-mol, in line with what observed by Kleerebezem and Mendez (2002). Indeed all the reported values follow in the range of 0,02-0,07 C-mol/e-mol (st.dev.=37%) compared to the wider range of 0,03-0,4 gVSS/gS (st.dev=58%).

6.3.3 Thermodynamic study of experimental results on Partial Denitrification

Figure 6.7 reports the experimental data on the daily $\text{S}/\text{N}_{\text{applied}}$ (from Chapter 5), together with the calculated values for nitrate removal and energy delivery according to the assumptions described in section 6.2.4. During the first 20 days of the experimental work (Phase 1.a), the $\text{S}/\text{N}_{\text{applied}}$ was not stable and, in general, higher than $\text{S}/\text{N}_{\text{R3}}$. After day 20, $\text{S}/\text{N}_{\text{applied}}$ was stably lower than $\text{S}/\text{N}_{\text{R1}}$ and S-limiting conditions (with respect to R1 stoichiometry) were maintained for the rest of the experimentation, with few exceptions. Consequently, NO_3^- removal calculated for R1 never reaches 100%, but stays around 30 to 60%, whereas it is almost constant at 100% if calculated for R3. Stated in other words, the electron donor supply provided to the system was

theoretically sufficient to convert 30-60% of nitrate to dinitrogen gas or to convert 100% of nitrate to nitrite. In phase 1b and 2, S/N_{applied} was very close to S/N_{R3} . It can be observed that free Gibbs energy change (as kJ/h) delivered by R3 is more favourable than R1, when S/N is close to the value required by R3: up to 60% increase in free Gibbs energy change is observed in Phase 2 (days 60-80). R3 appears the reaction that allows for the maximum use of the very good electron donor of sulphide and the good electron acceptor of nitrate, somehow optimizing the energy potential present in the system.

At a first sight, such a result appears in contrast with the analysis on the free Gibbs energy change presented in section 6.3.2. ΔG^{cat} values of -744,4 and -480,2 kJ/S-mol are calculated for R1 and R3, respectively (table 6.2), which means that, under non-limiting conditions, R1 is thermodynamically more favourable than R3 and so it is in the studied pH and T range (slightly alkaline and mesophilic conditions). Still, in case of limiting conditions for the electron donor, as in the case of the experimental work presented in Chapter 5, all the energy potentially available from the full denitrification reaction is limited and ultimately comparable or lower than the energy delivered by the partial denitrification reaction.

In chapter 5, a speculative discussion on the possible mechanisms underlying a stable nitrite accumulation is presented. Enzymatic regulation/inhibition, kinetic limitation under high-loaded conditions and microbial population seem to be among the main factors. In this work, a further element is added to the speculative discussion. The result that denitrification is no more favourable under strict ED limitation might be somehow related to the enzymatic response and regulations, evolved and selected in order to better harvest energy according to a variety of environmental conditions. Also, considering the work presented by Klatt and Polerecky (2015), microbial population with an overall higher energy efficiency might be favoured in case of strict and stable ED limitation. The authors report that *Thiobacillus denitrificans* are more energetically efficient than *Sulfurimonas denitrificans*. Indeed, in the work described in chapter 5 we did observe a clear shift from *Sulfurimonas* to *Thiobacillus*.

As a conclusion, the thermodynamic study suggests that the shift in the catabolic reaction observed after one week of strict sulphide limitation might have been driven also by energy optimization mechanisms, either related to enzymatic regulation or microbial population shift.

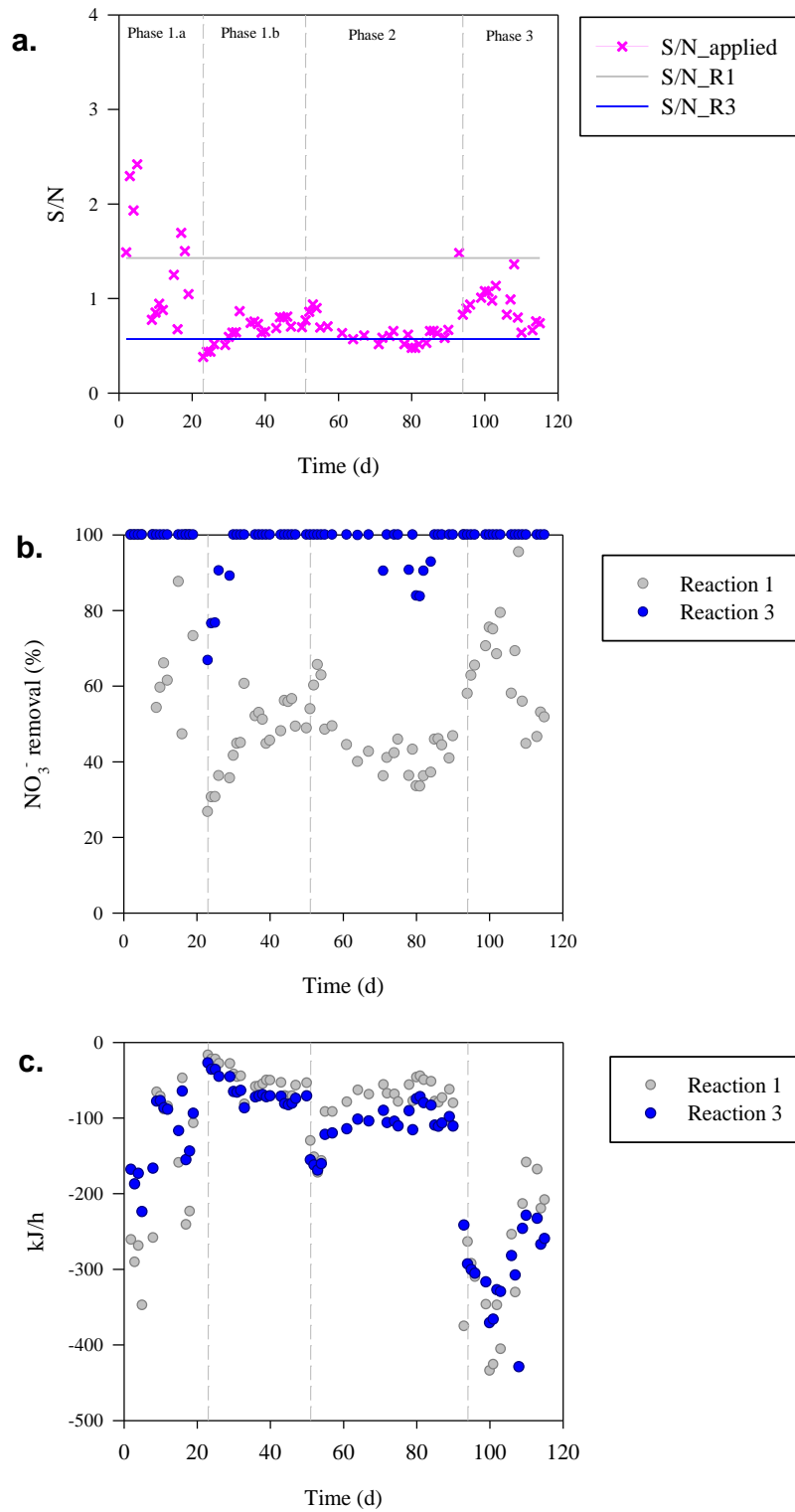


Figure 6.7 Experimental and reference values for S/N ratio (a); calculated NO₃⁻ removal, in R1 and R3 (b); energy delivered as kJ/h, in R1 and R3 (c).

6.4 Conclusions

In this study, aggregated information on some aspects of the numerous intermediate SO-NR steps are presented in order to provide a fast and comprehensive supporting tool for process design and optimization as well as for further research studies. Indeed, the proposed PAD/A treatment line allows for a remarkable flexibility and consequent N and S removal optimization according to the specific requirements.

The study on biomass yield allows for a critical discussion on the reported values as well as a more consistent comparison among values obtained from different intermediate steps and using different reduced forms of sulphur as electron donor. Yet, it is believed that comparison of literature values need to be completed with a critical understanding of the specific biomass and operational conditions adopted, due to the high complexity of the SO-NR process as well as the high metabolic diversity in SOB population.

The outcomes from the focus study on partial autotrophic denitrification remark that thermodynamics is a valuable tool to gain deeper insight in engineered microbial processes and to highlight aspects that are not obvious when non-limiting conditions are considered.

CHAPTER 7.

General conclusions

The main objective of the present thesis was to gain insight on the operational feasibility of the combined PAD/A process on tannery-like wastewaters. Such an objective was addressed through parallel lines of works aimed at studying in details the two processes, combining different experimental activities and chemical-physical analytical methods with molecular analysis techniques and theoretical knowledge. On the one hand, the results on the long-term operation of the anammox gas-lift reactor and the inhibition experiments with vegetable tannery wastewater are believed to have important implications for the future application of the anammox process to such an industrial stream. On the other hand, the results on the successful partial autotrophic denitrification are very promising and offer a comprehensive study encompassing operational conditions, microbial population and process flexibility.

As a general conclusion, the outcomes of the present thesis support and widen the state-of-the-art knowledge on the application of partial autotrophic denitrification as alternative nitrite supply process to be coupled with anammox, towards novel treatment lines for WRRFs achieving higher energy efficiencies as well as resource recovery and valorisation. More in details, the main conclusion for each line of work are presented in the following paragraphs.

In Chapter 3, results on the start-up and long-term stability of an anammox granular gas-lift reactor has been reported. A fast start-up and NLR increase was successfully achieved, provided that the reactor was inoculated with stored biomass after more than 1-year starving. A fast biomass reactivation was observed, witnessing that the storage procedure implemented was successful to keep residual anammox activity. This outcome is deemed relevant since the storage of active biomass is considered as an effective solution for fast reactor start-up or rescue in case of process failures. NLR of 0,48 gN-NO₂⁻/l/d and NO₂⁻ removal efficiency above 95% were obtained at a specific nitrogen load of 0,28 gN-NO₂⁻/gVSS/d. The observed mineral precipitation is an important warning for real-scale implementation; indeed, granular biomass mineralization and the consequent loss of biomass activity is an important factor often overlooked in real plants. The wide study on the composition of the precipitate mineral as well as the comprehensive analysis on the impact on the microbial composition, granular stability and biomass activity are believed to be valuable knowledge for addressing similar problems in real-scale granular systems and understand the possible mechanisms behind related systems' failures. Specifically, the integrated results from chemical analyses, simulated precipitation conditions and SEM-EDX analyses indicated that the inert formation was calcium and carbonate-based mineral, likely to be formed in waters with high calcium and carbonate-related alkalinity. The adopted rescue strategy proved effective for restoring good process performance and high biomass activity, even though around half of the active biomass present in the reactor was discarded due to severe precipitation. NLR of 0,23 gN-NO₂⁻/l/d and NO₂⁻ removal efficiency above 95% was stably achieved after re-inoculation and the maximum SAA of 0,387±0,027 gN-NO₂⁻/gVSS/d was observed in the last operational phase. The relative

abundance changes of *Ca. Brocadia* and *Ca. Kuenenia*, observed over the experimental work are in line with the reported k-based and r-based strategy adopted by the two microbial populations and support the assumption that substrate diffusion limitation was significant during the severe event of mineral precipitation. The k-strategist *Ca. Kuenenia* increased, in fact, its relative abundance after the most critical phase of mineral precipitation. Even though a scale-up of the applied strategy is not feasible, it is suggested that careful monitoring of the VSS/TSS ratio as well as the regular withdrawal of the denser granules from reactor's bottom (i.e. gravimetric selection) is a viable solution for controlling inert accumulation in real-scale granular systems.

The outcomes on the inhibition experiments, presented in Chapter 4, refer on the observed anammox response to the exposure to pre-treated vegetable tannery wastewaters (no readily biodegradable COD was present). Results indicate that no evident inhibitory effect can be ascribed to the industrial matrix. When the effect of the salinity and the bio-refractory organic fractions were studied separately, it was observed that salinity appeared to be the actual disturbing factor. Indeed, the saline control test showed a 28% reduction in SAA compared to the non-saline control test, whereas a 14% SAA reduction was observed for the tannery wastewater test (containing both salinity and recalcitrant COD). Even though it could not be excluded that heterotrophic denitrification also occurred during the manometric batch tests with tannery wastewater, its contribution is believed to be of minor extent compared to the anammox process as confirmed by the observed stoichiometry. The applied acclimation procedure was effective for preventing shock effect due to sharp salinity increase; nevertheless, a longer acclimation phase is recommended for real-scale implementation. The ability of anammox biomass to acclimate to saline conditions is widely reported in literature and it is believed that the SAA reduction observed in the inhibition experiment can be attenuated after proper biomass acclimation. It is concluded that there is no technical limitation in applying the anammox process to vegetable tannery wastewater.

The results on the PAD in Chapter 5 were very promising since high nitrite accumulation efficiencies were obtained at all the operational phases. The adopted experimental strategy was based on operating the chemostat at low SRT and e-donor limiting conditions. Moderate volumetric loading rate were applied as the NLR and SLR ranged 0,1-0,4 gN/l/d and 0,05-0,40 gS/l/d, respectively. The average values of Nitrite Conversion Efficiency (NiCE) and Nitrite Accumulation Efficiencies (NiAE), over the three operational phases were as high as 73-94% and 60-70%, respectively. A maximum 100% of NiAE was, in fact, observed at the lowest S/N value of 0,58 gS/gN; restated, the lower the influent S/N, the higher the observed nitrite accumulation efficiency. The system showed good resiliency against daily variations of S/N influent. Sudden variation due to loading rates or S/N ratio resulted in sharp drop in nitrite concentration, but high values were restored within a few days. This finding has an important operational implication in case of real-scale implementation, since system resilience and stability are important conditions for robust and highly performing treatment. Influent S/N ratio showed to be a sufficient control parameter in the chemostat reactor operated at low SRT (12 to 40 h), at 30°C and pH of 7,6. The observed clear shift in microbial population from *Sulfurimonas* to *Thiobacillus*

is believed to be a very interesting result, since the strict energy-deficient conditions promoted the genus that, among the two, is reported as the more efficient in terms of metabolic bioenergetics.

The respirometric tests showed that nitrate uptake rate was not affected by the co-presence of nitrite as additional electron donor, not even at level as high as 120 mgN-NO₂⁻/l, exhibiting an almost constant values of 88±10 gN/gVSS/h at the different applied conditions. On the contrary, nitrite uptake rate varied significantly according to the tested conditions, ranging from 27 to 190 mgN/gVSS/h and suggesting high resiliency for the denitratation step compared to the denitritation one. These results were in line with the behaviour observed in the continuous reactor but cannot be used for defining the favoured e-acceptor between nitrite and nitrate in absolute terms, since the actual uptake rates strongly depends on operational conditions and the biomass (in the present study, a highly enriched culture fed by nitrate and acclimated to high level of nitrite).

The thermodynamic-based study conducted in Chapter 6 addressed some of the critical aspects related to the complex process coupling sulphide-oxidation and nitrate-reduction. Specifically, the catabolic reactions of all the possible intermediate steps and the derived combinations of e-donor/e-acceptor were solved with the main objective of providing aggregated information on some characteristic yields of each catabolic reactions, i.e. the removed S/N and produced/consumed H⁺/S ratios, deemed crucial for successful process design and optimisation. In the perspective of integrating PAD/A process with biogas desulphurization, the proper combination of N and S loading and alkalinity requirements should be achieved. Thus, the complexity of the SO-NR system can be turned as a favourable feature, allowing for high system flexibility and thereby widening the range of possible applications. The thermodynamic insight on the partial denitrification vs complete denitrification, under non-limiting and limiting conditions for the electron donor, suggested that the PD pathway could actually be an energy optimization response in case of electron donor (and ultimately energy) deficiency conditions. Also, the discussion on the reported biomass yields and the theoretically derived values, confirms that yield values should be critically considered together with the specific conditions of the studied system, due to the high variety of the involved SOB population and the strong influence of the operational conditions. The study is intended to acknowledge the thermodynamic approach as a valuable support tool to be integrated with the experimental evidences.

7.1 Future work

The findings of the present thesis work are believed to be important pillars for future developments towards PAD/A implementation in tannery-like wastewaters, both for one-stage or two-stage configurations. In this section, possible study lines that are considered worthy of further investigation are presented.

Anammox implementation to vegetable tannery wastewater

A long-term operation of the anammox gas-lift reactor fed by pre-treated tannery wastewater is considered the natural follow-up of the presented work since it will increase the understanding on process stability. Specifically, due to the long-term salinity exposure, granular morphology, dimension and composition are suggested to be monitored. Indeed, as reported by recent studies, EPS composition can vary at high salinity conditions, promoting the hydrophilic water-retaining polysaccharide fraction instead of the hydrophobic protein fraction. Significant reduction in EPS hydrophobicity is suggested to lead to granules rupture and aggregate loosening. Also, the long-term effect of tannins (and salinity) on the microbial community would provide useful information on the selected microbial community. Adsorption phenomena of the colloidal tannins-related organic fraction onto the surface of the granules are also deemed interesting, as they could play a role in attenuating the concentration of the residual bio-refractory COD fraction, currently removed by chemical precipitation in tertiary treatments.

PAD process optimization

Interesting aspects that could be addressed in future investigations are: (i) the role of pH both in NO_2^- accumulation efficiency as well as its possible impact on N_2O emissions; (ii) maximisation of the influent nitrate conversion, indeed in the present work nitrite was the far predominant end-product of nitrate reduction but a fraction of the influent nitrate was not converted and it is believed that complete nitrate conversion should be addressed for further optimisation of the PAD system; (iii) the role of high SRT (from few days to almost complete biomass retention) on the successful S/N strategy, in order to answer the question “would the S/N strategy have worked also in case of high SRT systems promoting higher microbial diversity, instead of the highly enriched condition obtained in the present study?” (iii) in line with the previous point, a comparison on the robustness of strategies based on limiting S/N conditions (as the one reported in the present work) or high load conditions (as reported in other works in literature), in order to provide decision support tool for the best operational option to be chosen according to case-specific conditions.

One-stage PAD/A

In the perspective of one-stage PAD/A, an accurate kinetic characterisation of the two microbial community would be crucial for the operation and modelling of one-stage configuration, in order to optimise the synergy between the anammox and the SOB biomass. Mathematical modelling of the biofilm structure would shed light on redox and nutrient gradients across the novel biofilm, supporting process design optimisation. Technical options, such as granular system or mixed granular and suspended biomass systems, could be assessed in order to optimise the synergistic growth of the two biomass.

The implementation of effective and robust control strategy is deemed fundamental for stable PAD/A operation, primarily due to the fact the unbalanced $\text{HS}^-:\text{NO}_3^-:\text{NH}_4^+$ ratios could lead to insufficient nitrite supply or sulphide accumulation, with severe (if not irreversible) inhibition of the anammox biomass. The

redox potential (ORP) is believed to be a key control parameter, due to the high reducing tendency of sulphide. Buffer tanks with readily available nitrate supply or emergency oxygen supply systems could be necessary in order to face exceptional sulphide build-up and allow for system continuous operation and robustness. In case of a PAD/A implementation in a bioscrubber desulphurization unit, as the one proposed in the present thesis, proper attention should be paid on the alkalinity balance of the system. On-line and off-line titrimetric assays could be designed as collateral measurements in regular process monitoring. Off-gas measurements of N₂O emissions are also considered necessary in order to provide a comprehensive knowledge on the actual potential of the PAD/A technology in line with the emerging challenges in carbon footprint reduction of novel WWRRFs.

REFERENCES

- Abma, W R, W Driessen, R Haarhuis, and M C M Van Loosdrecht. 2010. "Upgrading of Sewage Treatment Plant by Sustainable and Cost-Effective Separate Treatment of Industrial Wastewater." *Water Science and Technology* 61 (7): 1715–22. <https://doi.org/10.2166/wst.2010.977>.
- Ali, Muhammad, Mamoru Oshiki, and Satoshi Okabe. 2014. "Simple, Rapid and Effective Preservation and Reactivation of Anaerobic Ammonium Oxidizing Bacterium ' Candidatus Brocadia Sinica .'" *Water Research* 57 (0): 215–22. <https://doi.org/10.1016/j.watres.2014.03.036>.
- An, Biwen A, Yin Shen, and Gerrit Voordouw. 2017. "Control of Sulfide Production in High Salinity Bakken Shale Oil Reservoirs by Halophilic Bacteria Reducing Nitrate to Nitrite." *Frontiers in Microbiology* 8 (June). <https://doi.org/10.3389/fmicb.2017.01164>.
- An, Shijie, Kimberley Tang, and Mehdi Nemati. 2010. "Simultaneous Biodesulphurization and Denitrification Using an Oil Reservoir Microbial Culture: Effects of Sulphide Loading Rate and Sulphide to Nitrate Loading Ratio." *Water Research* 44 (5): 1531–41. <https://doi.org/10.1016/j.watres.2009.10.037>.
- Anthonisen AC, Loehr RC, Prakasam TB, Srinath EG. Inhibition of nitrification by ammonia and nitrous acid. *Journal - Water Pollution Control Federation*. 1976 May;48(5):835-852.
- APHA-AWWA-WPCF. 2005. Standard methods for the examination of water and wastewater. American Publication Health Association, Washington.
- Arrojo, B, and J L Campos. 2006. "Effects of Mechanical Stress on Anammox Granules in a Sequencing Batch Reactor (SBR)" 123: 453–63. <https://doi.org/10.1016/j.jbiotec.2005.12.023>.
- Bao, P., Guo Li, J. Zhao, K. Wu, J. Wang, X. Jia, H. Zhang, Y. He, and H. Li. 2020. "Sulfur Reduction Coupled with Anaerobic Ammonium Oxidation Drove Prebiotic Proto-Anabolic Networks." *Preprint Version*. <https://doi.org/10.1101/461707>.
- Batchelor, Bill, and Alonzo W Lawrence. 1978. "Autotrophic Denitrification Using Elemental Sulfur." *Water Pollution Control Federation* 50 (8): 1986–2001.
- Batstone, D J, J Landelli, A Saunders, R I Webb, L L Blackall, and J Keller. 2018. "The Influence of Calcium on Granular Sludge in a Full-Scale UASB Treating Paper Mill Wastewater." *Water Science and Technology*, no. November: 187–94.
- Bell, Louise C, David J Richardson, and Stuart J Ferguson. 1990. "Periplasmic and Membrane-Bound Respiratory Nitrate Reductases in Thiosphaera Pantotropha The Periplasmic Enzyme Catalyzes the First Step in Aerobic Denitrification." *Febs Letters* 265 (1): 85–87.
- Beller, Harry R, Patrick S G Chain, Tracy E Letain, Anu Chakicherla, Frank W Larimer, Paul M Richardson, Matthew A Coleman, Ann P Wood, and Donovan P Kelly. 2006. "The Genome Sequence of the Obligately Chemolithoautotrophic, Facultatively Anaerobic Bacterium Thiobacillus Denitrificans." *JOURNAL OF BACTERIOLOGY* 188 (4): 1473–88. <https://doi.org/10.1128/JB.188.4.1473>.
- Cabello, P, M D Rolda, and F Castillo. 2009. "Nitrogen Cycle." 2009 Elsevier Inc.

- Campos, J L, S Carvalho, R Portela, and R Mendez. 2008. "Kinetics of Denitrification Using Sulphur Compounds: Effects of S / N Ratio, Endogenous and Exogenous Compounds." *Bioresource Technology* 99: 1293–99. <https://doi.org/10.1016/j.biortech.2007.02.007>.
- Can-dogan, Esra, Mustafa Turker, Levent Dagan, and Ayla Arslan. 2010. "Sulfide Removal from Industrial Wastewaters by Lithotrophic Denitrification Using Nitrate as an Electron Acceptor." *Water Resources and Industry*, 2286–93. <https://doi.org/10.2166/wst.2010.545>.
- Cardoso, Ricardo Beristain, Reyes Sierra-alvarez, Pieter Rowlette, Jim A Field, Elias Razo Flores, Jorge Gomez, and Jim A Field. 2006. "Sulfide Oxidation Under Chemolithoautotrophic Denitrifying Conditions." *Wiley InterScience*, no. 2. <https://doi.org/10.1002/bit>.
- Carucci, A., A. Chiavola, M. Majone, and E. Rolle. 1999. "Treatment of Tannery Wastewater in Sequencing Batch Reactor." *Water Science and Technology* 40 (1): 253–59.
- Carvajal-arroyo, José M, Wenjie Sun, Reyes Sierra-alvarez, and Jim A Field. 2013. "Chemosphere Inhibition of Anaerobic Ammonium Oxidizing (Anammox) Enrichment Cultures by Substrates, Metabolites and Common Wastewater Constituents." *Chemosphere* 91 (2): 22–27. <https://doi.org/10.1016/j.chemosphere.2012.11.025>.
- Chen, Jianwei, Qixing Ji, Ping Zheng, Tingting Chen, and Caihua Wang. 2010. "Floatation and Control of Granular Sludge in a High-Rate Anammox Reactor." *Water Research* 44 (11): 3321–28. <https://doi.org/10.1016/j.watres.2010.03.016>.
- Chen, Jianwei, and Marc Strous. 2013. "Biochimica et Biophysica Acta Denitri Fi Cation and Aerobic Respiration, Hybrid Electron Transport Chains and Co-Evolution ☆." *BBA - Bioenergetics* 1827 (2): 136–44. <https://doi.org/10.1016/j.bbabi.2012.10.002>.
- Chen, Hui, Chun Ma, Guang-feng Yang, Hui-zhong Wang, Zhi-ming Yu, and Ren-cun Jin. 2014. "Floatation of Flocculent and Granular Sludge in a High-Loaded Anammox Reactor." *Bioresource Technology* 169: 409–15. <https://doi.org/10.1016/j.biortech.2014.06.063>.
- Chen, Fangmin, Xiang Li, Chenwei Gu, Yong Huang, and Yan Yuan. 2018. "Bioresource Technology Selectivity Control of Nitrite and Nitrate with the Reaction of S₀ and Achieved Nitrite Accumulation in the Sulfur Autotrophic Denitri Fi Cation Process." *Bioresource Technology* 266 (June): 211–19. <https://doi.org/10.1016/j.biortech.2018.06.062>.
- Chen, Linlin, Hui Chen, Donghui Lu, Xiangyang Xu, and Liang Zhu. 2020. "Response of Methanogens in Calcified Anaerobic Granular Sludge: Effect of Different Calcium Levels." *Journal of Hazardous Materials*, no. December 2019: 122131. <https://doi.org/10.1016/j.jhazmat.2020.122131>.
- Claus, Giinter, and Hans Jiirgen Kutzner. 1985. "Physiology and Kinetics of Autotrophic Denitrification by *Thiobacillus Denitrificans*." *Appl Microbiol Biotechnol*, 283–88.
- Cristovao, Raquel, C. Botelho, R. Martins, J.M. Loureiro, and Rui A R Boaventura. 2015. "Fish Canning Industry Wastewater Treatment for Water Reuse e a Case Study." *Journal of Cleaner Production* 87. <https://doi.org/10.1016/j.jclepro.2014.10.076>.
- Cui, Yan-xiang, Basanta Kumar Biswal, Gang Guo, Yang-fan Deng, and Hao Huang. 2019. "Biological Nitrogen Removal from Wastewater Using Sulphur-Driven Autotrophic Denitrification." *Applied Microbiology and Biotechnology*, 6023–39.

- Cui, Yan-xiang, Gang Guo, George A Ekama, Yang-fan Deng, Ho-kwong Chui, Guang-hao Chen, and Di Wu. 2019. "Elucidating the Bio Fi Lm Properties and Biokinetics of a Sulfur-Oxidizing Moving-Bed Bio Fi Lm for Mainstream Nitrogen Removal." *Water Research* 162: 246–57. <https://doi.org/10.1016/j.watres.2019.02.061>.
- Cunha, Jorge Ricardo, Sara Morais, Joana C Silva, and Renata D Van Der Weijden. 2019. "Bulk PH and Carbon Source Are Key Factors for Calcium Phosphate Granulation." *Environ. Sci. Technol.* 53: 1334–43. <https://doi.org/10.1021/acs.est.8b06230>.
- D'Aniello, Mariachiara. 2010. Anammox process for livestock digestate treatment in a gas-lift pilot plant. Master thesis, Civil and Environmental Engineering Department University of Florence.
- Dapena-mora, A, J L Campos, A Mosquera-corrall, and R Mendez. 2004. "Stability of the ANAMMOX Process in a Gas-Lift Reactor and a SBR." *Journal of Biotechnology* 110: 159–70. <https://doi.org/10.1016/j.jbiotec.2004.02.005>.
- Dapena-mora, A, I Fern, J L Campos, A Mosquera-corrall, and M S M Jetten. 2007. "Evaluation of Activity and Inhibition Effects on Anammox Process by Batch Tests Based on the Nitrogen Gas Production." *Enzyme and Microbial Technology* 40 40: 859–65. <https://doi.org/10.1016/j.enzmictec.2006.06.018>.
- Dapena-mora, A, J R Vázquez-padín, J L Campos, A Mosquera-corrall, M S M Jetten, and R Méndez. 2010. "Monitoring the Stability of an Anammox Reactor under High Salinity Conditions." *Biochemical Engineering Journal* 51 (3): 167–71. <https://doi.org/10.1016/j.bej.2010.06.014>.
- Davidson, Eric A. 2009. "To Atmospheric Nitrous Oxide since 1860." *Nature Geoscience* 2 (9): 659–62. <https://doi.org/10.1038/ngeo608>.
- Deng, Yang-fan, George A Ekama, Yan-xiang Cui, Cong-jian Tang, Mark C M Van Loosdrecht, Guang-hao Chen, and Di Wu. 2019. "Coupling of Sulfur (Thiosulfate) -Driven Denitratation and Anammox Process to Treat Nitrate and Ammonium Contained Wastewater" 163 (3). <https://doi.org/10.1016/j.watres.2019.114854>.
- Fajardo, Carmen, Mabel Mora, Isaac Fernández, Anuska Mosquera-corrall, José Luis, and R Mendez. 2014. "Chemosphere Cross Effect of Temperature , PH and Free Ammonia on Autotrophic Denitrification Process with Sulphide as Electron Donor." *Chemosphere* 97: 10–15. <https://doi.org/10.1016/j.chemosphere.2013.10.028>.
- Falcioni, Serena. 2020. Coupling respirometric and titrimetric techniques for the characterisation of the biological activity of a Sulphide-Oxidizing Nitrate-Reducing (SO-NR) microbial community. Master thesis, Civil and Environmental Engineering Department, University of Florence.
- Fang, Fang, Ming-ming Yang, Han Wang, Peng Yan, You-peng Chen, and Jin-song Guo. 2018. "AC SC." *Chemosphere*. <https://doi.org/10.1016/j.chemosphere.2018.07.038>.
- Fida, Tekle Tafese, Chuan Chen, Gloria Okpala, and Gerrit Voordouw. 2016. "Implications of Limited Thermophilicity of Nitrite Reduction For." *Applied and Environmental Microbiology* 82 (14): 4190–99. <https://doi.org/10.1128/AEM.00599-16.Editor>.
- Frijters, C T M J, M Silvius, J Fischer, R Haarhuis, and R Mulder. 2007. "Full-Scale Applications for Both COD and Nutrient Removal in a CIRCOX w Airlift Reactor." *Water Science and Technology* 55: 107–14. <https://doi.org/10.2166/wst.2007.248>.

- Fuerst, John A. 2017. *Planctomycetes — New Models for Microbial Cells and Activities. Microbial Resources*. Elsevier Inc. <https://doi.org/10.1016/B978-0-12-804765-1/00001-1>.
- Gadekar, S, M A Nemati, and G A Hill. 2006. “Batch and Continuous Biooxidation of Sulphide by Thiomicrospira Sp . CVO : Reaction Kinetics and Stoichiometry.” *Water Research* 40: 2436–46. <https://doi.org/10.1016/j.watres.2006.04.007>.
- Galloway, James N, Alan R Townsend, Jan Willem Erisman, Mateete Bekunda, Zucong Cai, John R Freney, Luiz A Martinelli, Sybil P Seitzinger, and Mark A Sutton. 2008. “Transformation of the Nitrogen Cycle :” *Science* 320 (May): 889–93.
- Ghosh, Wriddhiman, and Bomba Dam. 2009. “Biochemistry and Molecular Biology of Lithotrophic Sulfur Oxidation by Taxonomically and Ecologically Diverse Bacteria and Archaea.” *FEMS Microbiol Rev.* <https://doi.org/10.1111/j.1574-6976.2009.00187.x>.
- Graaf, Astrid A Van De, Peter De Bruijn, Lesley A Robertson, Mike M Jetten, and J Gijs Kuenen. 1996. “Autotrophic Growth of Anaerobic Am Mon i u M-Oxi d Izi Ng m i Cro-Org a n Isms in a Fluidized Bed Reactor.” *Microbiology* 142: 2187–96.
- Guest, Jeremy S, Steven J Skerlos, James L Barnard, M Bruce Beck, C H M Hill, North Carolina, Steven J Jackson, Linda Macpherson, and C H M Hill. 2009. “A New Planning and Design Paradigm to Achieve Sustainable Resource Recovery From.” *Environ. Sci. Technol.* 43 (16): 6126–30. <https://doi.org/10.1021/es803001r>.
- Gustafsson, Jon Petter. 2014. “Visual MINTEQ 3.1 User Guide,” 1–73.
- Haron, Mohammad, Veeriah Jegatheesan, and Dimuth Navaratna. 2019. “The Potential of Adopting Struvite Precipitation as a Strategy for the Removal of Nutrients from Pre-AnMBR Treated Abattoir Wastewater.” *Journal of Environmental Management*, no. October: 109783. <https://doi.org/10.1016/j.jenvman.2019.109783>.
- Heijnen, J.J., Vanloosdrecht, M.C.M., and Tijhuis, L. (1992). A black-box mathematical-model to calculate autotrophic and heterotrophic biomass yields based on Gibbs energy-dissipation. *Biotechnology and Bioengineering*, 40(10),1139–1154.
- Heijnen, Joseph & Kleerebezem, Robbert. (2010). Bioenergetics of Microbial Growth. 10.1002/9780470054581.eib084.
- Hu, Qian-yi, Da Kang, Ru Wang, A-qiang Ding, Ghulam Abbas, and Meng Zhang. 2018. “Characterization of Oligotrophic AnAOB Culture : Morphological , Physiological , and Ecological Features.” *ENVIRONMENTAL BIOTECHNOLOGY*, 995–1003. <https://doi.org/https://doi.org/10.1007/s00253-017-8587-8>.
- Hu, Ziyi, Hans J C T Wessels, Theo Alen, Mike S M Jetten, and Boran Kartal. 2019. “Oxidation.” *NATURE COMMUNICATIONS*. <https://doi.org/10.1038/s41467-019-09268-w>.
- Jain, Mahak, Abhradeep Majumder, Partha Sarathi, and Ashok Kumar. 2020. “A Review on Treatment of Petroleum Refinery and Petrochemical Plant Wastewater : A Special Emphasis on Constructed Wetlands.” *Journal of Environmental Management* 272 (July): 111057. <https://doi.org/10.1016/j.jenvman.2020.111057>.

- Jia, Mingsheng, Celia M Castro-barros, Mari K H Winkler, and Eveline I P Volcke. 2018. "Environmental Science." *Environmental Science: Water Research & Technology*, no. May 2020. <https://doi.org/10.1039/C8EW00125A>.
- Jetten, Mike S M, Laura Van Niftrik, Marc Strous, Boran Kartal, Jan T Keltjens, and Huub J M Op Den Camp. 2009. "Biochemistry and Molecular Biology of Anammox Bacteria." *Critical Reviews in Biochemistry and Molecular Biology* 44 (December 2008): 65–84. <https://doi.org/10.1080/10409230902722783>.
- Jin, Ren-cun, Chun Ma, Qaisar Mahmood, Guang-feng Yang, and Ping Zheng. 2011. "Anammox in a UASB Reactor Treating Saline Wastewater." *Process Safety and Environmental Protection* 89 (5): 342–48. <https://doi.org/10.1016/j.psep.2011.05.001>.
- Jin, Ren-cun, Guang-feng Yang, Jin-jin Yu, and Ping Zheng. 2012. "The Inhibition of the Anammox Process: A Review." *Chemical Engineering Journal* 197: 67–79. <https://doi.org/10.1016/j.cej.2012.05.014>.
- Jin, Ren-cun, Bao-shan Xing, Qiong Guo, Guang-feng Yang, Zheng-zhe Zhang, Peng Li, and Li-xin Guo. 2015. "Granules: Roles of Ambient Temperature, Salinity and Calcium Department of Environmental Science and Engineering , Hangzhou Normal Key Laboratory of Hangzhou City for Ecosystem Protection and Restoration , Corresponding Author : Ren-Cun Jin." *SEPARATION AND PURIFICATION TECHNOLOGY*. <https://doi.org/10.1016/j.seppur.2015.04.035>.
- Jing, Cai, Zheng Ping, and Qaisar Mahmood. 2010. "Bioresource Technology Influence of Various Nitrogenous Electron Acceptors on the Anaerobic Sulfide Oxidation." *Bioresource Technology Journal* 101: 2931–37. <https://doi.org/10.1016/j.biortech.2009.11.047>.
- Johansson, Sara, Maël Ruscalleda, and Jesús Colprim. 2017. "Phosphorus Recovery through Biologically Induced Precipitation by Partial Nitritation-Anammox Granular Biomass." *Chemical Engineering Journal* 327: 881–88. <https://doi.org/10.1016/j.cej.2017.06.129>.
- Justin, Pauline, and Donovan P Kelly. 1978. "Growth Kinetics of Thiobacillus Denitrificans in Anaerobic and Aerobic Chemostat Culture ByPAULINE." *Journal of General Microbiology* 107: 123–30.
- Kalyuzhnyi, Sergey, Marina Gladchenko, Arnold Mulder, and Bram Versprille. 2006. "DEAMOX — New Biological Nitrogen Removal Process Based on Anaerobic Ammonia Oxidation Coupled to Sulphide-Driven Conversion of Nitrate into Nitrite." *Water Research* 40: 3637–45. <https://doi.org/10.1016/j.watres.2006.06.010>.
- Kalyuzhnyi, S V, M A Gladchenko, Ho Kang, A Mulder, and A Versprille. 2008. "Development and Optimisation of VFA Driven DEAMOX Process for Treatment of Strong Nitrogenous Anaerobic Effluents." *Water Science and Technology*, no. 2: 323–28. <https://doi.org/10.2166/wst.2008.044>.
- Kalyuzhnyi, Sergey, and Marina Gladchenko. 2009. "DEAMOX – New Microbiological Process of Nitrogen Removal from Strong Nitrogenous Wastewater." *DES* 248 (1–3): 783–93. <https://doi.org/10.1016/j.desal.2009.02.054>.
- Kampschreur, MJ, Robbert Kleerebezem, Picorena Christian, Lars Bakken, Linda Bergaust, Simon De Vries, Mike S M Jetten, and Mark C M Van Loosdrecht. 2012. "Metabolic Modeling of Denitrification in Agrobacterium Tumefaciens : A Tool to Study Inhibiting and Activating Compounds for the Denitrification Pathway." *Frontiers in Microbiology* 3 (October): 1–19. <https://doi.org/10.3389/fmicb.2012.00370>.

- Kang, Da, Leiyan Guo, Qianyi Hu, Dongdong Xu, Tao Yu, Yiyu Li, Zhuo Zeng, and Wenji Li. 2019. "Surface Convexity of Anammox Granular Sludge: Digital Characterization , State Indication and Formation Mechanism." *Environment International* 131 (April): 105017. <https://doi.org/10.1016/j.envint.2019.105017>.
- Kartal, Boran, Mariana Koleva, Roumen Arsov, Wouter Van Der Star, Mike S M Jetten, and Marc Strous. 2006. "Adaptation of a Freshwater Anammox Population to High Salinity Wastewater." *Journal of Biotechnology* 126: 546–53. <https://doi.org/10.1016/j.jbiotec.2006.05.012>.
- Kartal, Boran, Laura Van Niftrik, Jan T Keltjens, J M Huub, Op Den Camp, and Mike S M Jetten. 2012. *Anammox — Growth Physiology , Cell Biology , and Metabolism*. Vol. 60. Elsevier Ltd. <https://doi.org/10.1016/B978-0-12-398264-3.00003-6>.
- Kelly, Donovan P, and Ann P Wood. 2000. "Confirmation of Thiobacillus Denitrificans as a Species of the Genus Thiobacillus, in the β - Subclass of the Proteobacteria, with Strain NCIMB 9548 as the Type Strain." *International Journal of Systematic and Evolutionary Microbiology* 50: 547–50.
- Klatt, Judith M, and Lubos Polerecky. 2015. "Assessment of the Stoichiometry and Efficiency of CO₂ Fixation Coupled to Reduced Sulfur Oxidation." *Frontiers in Microbiology* 6 (May). <https://doi.org/10.3389/fmicb.2015.00484>.
- Kleerebezem, R, and R Mendez. 2002. "Autotrophic Denitrification for Combined Hydrogen Sulfide Removal from Biogas and Post-Denitrification." *Water Science and Technology* 45 (October): 349–56.
- Kleerebezem, Robbert, and Mark C M van Loosdrecht. 2010. "A Generalized Method for Thermodynamic State Analysis of Environmental Systems" no. September 2014: 37–41. <https://doi.org/10.1080/10643380802000974>.
- Kleinjan, Wilfred E, Arie De Keizer, and Albert J H Janssen. 2005. "Kinetics of the Chemical Oxidation of Polysulfide Anions in Aqueous Solution." *Water Research* 39: 4093–4100. <https://doi.org/10.1016/j.watres.2005.08.006>.
- Kraft, Beate, Marc Strous, and Halina E Tegetmeyer. 2011. "Microbial Nitrate Respiration – Genes, Enzymes and Environmental Distribution." *Journal of Biotechnology* 155 (1): 104–17. <https://doi.org/10.1016/j.jbiotec.2010.12.025>.
- Kuenen, J Gijs. 2020. "How We Did It! Anammox and Beyond." *Environmental Microbiology* 22: 525–36. <https://doi.org/10.1111/1462-2920.14904>.
- Kumar, Murugan, Mohammad Tarique Zeyad, Prassan Choudhary, Surinder Paul, Hillol Chakdar, and Mahendra V. S. Rajawat. 2020. "Murugan Kumar, Mohammad Tarique Zeyad, Prassan Choudhary, Surinder Paul, Hillol Chakdar, Mahendra Vikram Singh Rajawat." *Beneficial Microbes in Agro-Ecology*, 545–57. <https://doi.org/10.1016/B978-0-12-823414-3.00026-5>.
- Kuypers, Marcel M M, Hannah K Marchant, and Boran Kartal. 2018. "The Microbial Nitrogen-Cycling Network." *Nature Publishing Group*. <https://doi.org/10.1038/nrmicro.2018.9>.
- Lackner, Susanne, Eva M Gilbert, Siegfried E Vlaeminck, Adriano Joss, Harald Horn, and Mark C M Van Loosdrecht. 2014. "ScienceDirect Full-Scale Partial Nitritation / Anammox Experiences e An Application Survey." *Water Research* 55 (0): 292–303. <https://doi.org/10.1016/j.watres.2014.02.032>.
- Langelier, W.F. 1936. The analytical control of anti-corrosion water treatment. *Journal of the American Water Works Association*, vol. 28, no. 10. pp. 1500–1521.

- Langerak, E P A V A N, H Ramaekers, J Wiechers, H V M Hamelers, and G Lettinga. 2000. “impact of location of CaCO₃ precipitation on the development of intact anaerobic SLUDGE.” *Water Research* 34 (2): 437–46.
- Lens, Piet N L. 2020. *Environmental Technologies to Treat Sulfur Pollution Environmental Technologies to Treat Sulfur Pollution Principles and Engineering – 2nd Edition*. 1st ed. IWA Publishing.
- Li, Wei, Ping Zheng, Junyuan Ji, Meng Zhang, Jun Guo, Jiqiang Zhang, and Ghulam Abbas. 2014. “Floation of Granular Sludge and Its Mechanism: A Key Approach for High-Rate Denitrifying Reactor.” *Bioresource Technology Journal* 152: 414–19. <https://doi.org/10.1016/j.biortech.2013.11.056>.
- Li, Jin, Panqing Qi, Zhimin Qiang, Huiyu Dong, Dawen Gao, and Dan Wang. 2018. “Is Anammox a Promising Treatment Process for Nitrogen Removal from Nitrogen-Rich Saline Wastewater? Bioresource Technology Is Anammox a Promising Treatment Process for Nitrogen Removal from Nitrogen-Rich Saline Wastewater?” *Bioresource Technology*, no. October: 0–1. <https://doi.org/10.1016/j.biortech.2018.08.115>.
- Lin, Y M, T Lotti, P K Sharma, and M C M Van Loosdrecht. 2013. “Apatite Accumulation Enhances the Mechanical Property of Anammox Granules.” *Water Research* 47 (13): 4556–66. <https://doi.org/10.1016/j.watres.2013.04.061>.
- Lin, Ximao, and Yayi Wang. 2017. “Microstructure of Anammox Granules and Mechanisms Endowing Their Intensity Revealed by Microscopic Inspection and Rheometry.” *Water Research*. <https://doi.org/10.1016/j.watres.2017.04.053>.
- Lin, Sen, Hamish R Mackey, Tianwei Hao, Gang Guo, Mark C M Van Loosdrecht, and Guanghao Chen. 2018. “Biological Sulfur Oxidation in Wastewater Treatment: A Review of Emerging Opportunities.” *Water Research*. <https://doi.org/10.1016/j.watres.2018.06.051>.
- Lin, Lan, Yanlong Zhang, Markus Beckman, Wenzhi Cao, Tong Ouyang, and Shaopo Wang. 2019. “Process Optimization of Anammox-Driven Hydroxyapatite Crystallization for Simultaneous Nitrogen Removal and Phosphorus Recovery.” *Bioresource Technology* 290 (May): 121779. <https://doi.org/10.1016/j.biortech.2019.121779>.
- Lisa, Jessica A, Bongkeun Song, Craig R Tobias, and Kimberley A Duernberger. 2014. “Impacts of Freshwater Flushing on Anammox Community Structure and Activities in the New River Estuary , USA.” *AQUATIC MICROBIAL ECOLOGY* 72: 17–31. <https://doi.org/10.3354/ame01682>.
- Liu, Chunshuang, Wenfei Li, Xuechen Li, Dongfeng Zhao, Bin Ma, Yongqiang Wang, Fang Liu, and Duu-jong Lee. 2017. “Nitrite Accumulation in Continuous-Flow Partial Autotrophic Denitrification Reactor Using Sulfide as Electron Donor.” *Bioresource Technology* 243: 1237–40. <https://doi.org/10.1016/j.biortech.2017.07.030>.
- Lotti, T, W R L Van Der Star, R Kleerebezem, C Lubello, M C M Van Loosdrecht, W R L van der Star, R Kleerebezem, C Lubello, and M C M van Loosdrecht. 2012. “The Effect of Nitrite Inhibition on the Anammox Process.” *Water Research* 46 (8): 2559–69. <https://doi.org/http://dx.doi.org/10.1016/j.watres.2012.02.011>.
- Lotti, T, R Kleerebezem, Z Hu, B Kartal, M S M Jetten, and M C M Van Loosdrecht. 2014. “Simultaneous Partial Nitritation and Anammox at Low Temperature with Granular Sludge.” *Water Research* 66: 111–21. <https://doi.org/10.1016/j.watres.2014.07.047>.

- Lotti, Tommaso, Robbert Kleerebezem, Claudio Lubello, and Mark C.M. van Loosdrecht. 2014b. "Physiological and Kinetic Characterization of a Suspended Cell Anammox Culture." *Water Research* 60: 1–14. <https://doi.org/10.1016/j.watres.2014.04.017>.
- Lotti, T, R Kleerebezem, J M Abelleira-pereira, B Abbas, and M C M Van Loosdrecht. 2015. "Faster through Training: The Anammox Case." *Water Research* 81: 261–68. <https://doi.org/10.1016/j.watres.2015.06.001>.
- Lu, Hui, Di Wu, Feng Jiang, George A Ekama, Mark C M Van Loosdrecht, and Guang-hao Chen. 2012. "The Demonstration of a Novel Sulfur Cycle-Based Wastewater Treatment Process : Sulfate Reduction , Autotrophic Denitrification , and Nitrification Integrated (SANI 1) Biological Nitrogen Removal Process." *Biotechnology and Bioengineering* 109 (11): 2778–89. <https://doi.org/10.1002/bit.24540>.
- Lu, Hui-feng, Ping Zheng, Qi-xing Ji, Hong-tao Zhang, Jun-yuan Ji, Lan Wang, Shuang Ding, et al. 2012. "The Structure, Density and Settability of Anammox Granular Sludge in High-Rate Reactors." *Bioresource Technology* 123: 312–17. <https://doi.org/10.1016/j.biortech.2012.07.003>.
- Ma, Chun, Ren-cun Jin, Guang-feng Yang, Jin-jin Yu, Bao-shan Xing, and Qian-qian Zhang. 2012. "Impacts of Transient Salinity Shock Loads on Anammox Process Performance." *Bioresource Technology* 112: 124–30. <https://doi.org/10.1016/j.biortech.2012.02.122>.
- Ma, Haiyuan, Yi Xue, Yuanfan Zhang, Takuro Kobayashi, Kengo Kubota, and Yu-you Li. 2020. "Simultaneous Nitrogen Removal and Phosphorus Recovery Using an Anammox Expanded Reactor Operated at 25 °C." *Water Research*, 115510. <https://doi.org/10.1016/j.watres.2020.115510>.
- Madigan, Michael T., Kelly S. Bender, Daniel H. Buckley, W. Matthew Sattley, and David A. Stail. 2019. *Brock Biology of Microorganisms*. Edited by Pearson. 15th ed. Pearson Education Limited.
- Mañas, Angela, Beatrice Biscans, and M. Sperandio. 2011. "Biologically Induced Phosphorus Precipitation in Aerobic Granular Sludge Process." *Water Research* 5: 0–10. <https://doi.org/10.1016/j.watres.2011.04.031>.
- Manconi, I, A Carucci, and P Lens. 2007. "Combined Removal of Sulfur Compounds and Nitrate by Autotrophic Denitrification in Bioaugmented Activated Sludge System." *Biotechnology and Bioengineering* 98 (3): 551–60. <https://doi.org/10.1002/bit>.
- Mannucci, Alberto, Giulio Munz, Gualtiero Mori, and Claudio Lubello. 2010. "Anaerobic Treatment of Vegetable Tannery Wastewaters: A Review." *DES* 264 (1–2): 1–8. <https://doi.org/10.1016/j.desal.2010.07.021>.
- Marin Leal, Julio, Carlos A. Chinga Panta, Pierre Velasquez Ferrin, Abrahm I. Gonzales Cabo, and Luz Maria Zambrano Rodriguez. 2015. "Tratamiento de Aguas Residuales de Una Industria Procesadora de Pescado En Reactores Anaeróbicos Discontinuos. Ciencia e Ingeniería Neogranadina, 25 (1), Pp. 27 - 42," no. Dci: 27–42.
- Mazzoli, Lorenzo, Giulio Munz, Tommaso Lotti, and Matteo Ramazzotti. 2020. "OPEN A Novel Universal Primer Pair for Prokaryotes with Improved Performances for Anammox Containing Communities." *Scientific RepoRtS*, no. 0123456789: 1–7. <https://doi.org/https://doi.org/10.1038/s41598-020-72577-4>.
- Mora, Mabel, Albert Guisasola, Xavier Gamisans, and David Gabriel. 2014. "Chemosphere Examining Thiosulfate-Driven Autotrophic Denitrification through Respirometry." *CHEMOSPHERE* 113: 1–8. <https://doi.org/10.1016/j.chemosphere.2014.03.083>.

- Mora, Mabel, Luis R López, Xavier Gamisans, and David Gabriel. 2014b. "Coupling Respirometry and Titrimetry for the Characterization of the Biological Activity of a SO-NR Consortium." *CHEMICAL ENGINEERING JOURNAL* 251: 111–15. <https://doi.org/10.1016/j.cej.2014.04.024>.
- Mora, Mabel. 2014c. Characterization of S-oxidizing biomass through respirometric techniques under anoxic and aerobic conditions. PhD thesis. Universitat Autònoma de Barcelona.
- Mora, Mabel, Maikel Fernández, José Manuel Gómez, Domingo Cantero, Javier Lafuente, Xavier Gamisans, and David Gabriel. 2015. "Kinetic and Stoichiometric Characterization of Anoxic Sulfide Oxidation by SO-NR Mixed Cultures from Anoxic Biotrickling Filters." *Appl Microbiol Biotechnol*, 77–87. <https://doi.org/10.1007/s00253-014-5688-5>.
- Moussa, M S, D U Sumanasekera, S H Ibrahim, H J Lubberding, and C M Hooijmans. 2006. "Long Term Effects of Salt on Activity, Population Structure and Floc Characteristics in Enriched Bacterial Cultures of Nitrifiers R2 R3." *Water Research* 40: 1377–88. <https://doi.org/10.1016/j.watres.2006.01.029>.
- Mulder, A, A A Van De Graaf, L A Robertson, and J G Kuenen. 1995. "Anaerobic Ammonium Oxidation Discovered in a Denitrifying Fluidized Bed Reactor." *FEMS Microbiology Ecology* 16: 177–84.
- Munz, G, D De Angelis, R Gori, G Mori, M Casarci, and C Lubello. 2009. "The Role of Tannins in Conventional and Membrane Treatment of Tannery Wastewater." *Journal of Hazardous Materials* 164: 733–39. <https://doi.org/10.1016/j.jhazmat.2008.08.070>.
- Munz G., Mori G., Vannini C. & Lubello C. (2010) Kinetic parameters and inhibition response of ammonia- and nitrite-oxidizing bacteria in membrane bioreactors and conventional activated sludge processes, *Environmental Technology*, 31:14, 1557-1564, DOI: 10.1080/09593331003793828
- Nelson, K E, A N Pell, P H Doane, and P Schofield. 1997. "CHEMICAL AND BIOLOGICAL ASSAYS TO EVALUATE BACTERIAL INHIBITION BY TANNINS." *Journal of Chemical Ecology*, 23 (4): 1175–94.
- Niccolai, E., E. Russo, S. Baldi, F. Ricci, G. Nannini, M. Pedone, F.C. Stingo, et al. 2020. "Significant and Conflicting Correlation of IL-9 with Prevotella and Bacteroides in Human 2 Colorectal Cancer." *Preprint Version*. <https://doi.org/https://doi.org/10.1101/2020.04.28.066001>.
- Nsenga, Mathieu, Tommaso Lotti, and S Engin. 2020. "Chemosphere Anammox-Based Processes: How Far Have We Come and What Work Remains ? A Review by Bibliometric Analysis." *Chemosphere* 238. <https://doi.org/10.1016/j.chemosphere.2019.124627>.
- Oh, S, K Kim, H Choi, J Cho, and I S Kim. 2000. "Kinetics and Physiological Characteristics of Autotrophic Denitrification by Denitrifying Sulfur Bacteria." *Water Science and Technology*, 59–68.
- Oshiki, Mamoru, Muhammad Ali, Kaori Shinyako-hata, Hisashi Satoh, and Satoshi Okabe. n.d. "Hydroxylamine-Dependent Anaerobic Ammonium Oxidation (Anammox) by 'Candidatus Brocadia Sinica.'" *Environmental Microbiology* 18: 3133–43. <https://doi.org/10.1111/1462-2920.13355>.
- Oshiki, Mamoru, Hisashi Satoh, and Satoshi Okabe. 2016. "Minireview Ecology and Physiology of Anaerobic Ammonium Oxidizing Bacteria." *Environmental Microbiology*. <https://doi.org/10.1111/1462-2920.13134>.
- Peeters, Stijn H, and Laura Van Niftrik. 2019. "Trending Topics and Open Questions in Anaerobic Ammonium Oxidation." *Current Opinion in Chemical Biology* 49: 45–52. <https://doi.org/10.1016/j.cbpa.2018.09.022>.

- Pishgar, Roya, John Albino Dominic, Joo Hwa Tay, and Angus Chu. 2020. "Pilot-Scale Investigation on Nutrient Removal Characteristics of Mineral-Rich Aerobic Granular Sludge: Identification of Uncommon Mechanisms." *Water Research* 168: 115151. <https://doi.org/10.1016/j.watres.2019.115151>.
- Prokopenko, M G, D E Hammond, W M Berelson, J M Bernhard, L Stott, and R Douglas. 2006. "Nitrogen Cycling in the Sediments of Santa Barbara Basin and Eastern Subtropical North Pacific: Nitrogen Isotopes, Diagenesis and Possible Chemosymbiosis between Two Lithotrophs (Thioploca and Anammox)— Riding on a Glider Q." *Earth and Planetary Science Letters* 242: 186–204. <https://doi.org/10.1016/j.epsl.2005.11.044>.
- Qian, Jin, Mingkuan Zhang, Yaoguo Wu, Juntao Niu, Xing Chang, and Hairui Yao. 2018. "A Feasibility Study on Biological Nitrogen Removal (BNR) via Integrated Thiosulfate-Driven Denitrification with Anammox." *Chemosphere* 208: 793–99. <https://doi.org/10.1016/j.chemosphere.2018.06.060>.
- Qian, Jin, Junmei Zhou, Zhen Zhang, Rulong Liu, and Qilin Wang. 2016. "Biological Nitrogen Removal through Nitritation Coupled with Thiosulfate-Driven Denitrification." *Nature Publishing Group*, no. June: 1–10. <https://doi.org/10.1038/srep27502>.
- Qin, Yujie, Chenglong Wu, Buqing Chen, Junyi Ren, and Linyi Chen. 2019. "Short Term Performance and Microbial Community of a Sulfide-Based Denitrification and Anammox Coupling System at Different N / S Ratios." *Bioresourcetechnology* 294 (September): 122130. <https://doi.org/10.1016/j.biortech.2019.122130>.
- Queiroz, Leila, Adriana Gonc, Maria Isabel, Silva Manetti, and Eduardo Jacob-lopes. 2013. "Fish Processing Wastewater as a Platform of the Microalgal Biorefineries." *Biosystem Engineering* 5. <https://doi.org/10.1016/j.biosystemseng.2012.12.013>.
- Reyes-Avila, Jesus, Elías Razo-Flores, and Jorge Gomez. 2004. "Reyes J . Razo and Gomez J (2004). Simultaneous Biological Removal of Simultaneous Biological Removal of Nitrogen , Carbon and Sulfur by Denitrification." *Water Research* 38 (October 2004): 3313–21. <https://doi.org/10.1016/j.watres.2004.04.035>.
- Richardson, David, Heather Felgate, Nick Watmough, Andrew Thomson, and Elizabeth Baggs. 2009. "Mitigating Release of the Potent Greenhouse Gas N₂O from the Nitrogen Cycle – Could Enzymic Regulation Hold the Key ?" *Trends in Biotechnology* 27 (June). <https://doi.org/10.1016/j.tibtech.2009.03.009>.
- Rios-Del Toro, E. Emilia, and Francisco J. Cervantes. 2016. "Coupling between Anammox and Autotrophic Denitrification for Simultaneous Removal of Ammonium and Sulfide by Enriched Marine Sediments." *Biodegradation* 27 (2–3): 107–18. <https://doi.org/10.1007/s10532-016-9759-4>.
- Rittmann B, McCarty P. 2001. *Environmental Biotechnology Principles and Applications*. Columbus, Ohio McGraw-Hill.
- Robertson, Lesley A, and J Gijss Kuenen. 2006. "The Colorless Sulfur Bacterium." *Prokaryotes*, 985–1011. https://doi.org/10.1007/0-387-30742-7_31.
- Roels, 1983. J.A. Roels *Energetics and Kinetics in Biotechnology*. Elsevier Biomedical Press, Amsterdam (1983).
- Russ, Lina, Daan R Speth, Mike S M Jetten, Huub J M Op Den Camp, and Boran Kartal. 2014. "Interactions between Anaerobic Ammonium and Sulfur-Oxidizing Bacteria in a Laboratory Scale Model System." *Environmental Microbiology* 16: 3487–98. <https://doi.org/10.1111/1462-2920.12487>.

- Sahinkaya, Erkan, Nesrin Dursun, Adem Kilic, Sevgi Demirel, Sinan Uyanik, and Ozer Cinar. 2011. "Simultaneous Heterotrophic and Sulfur-Oxidizing Autotrophic Denitrification Process for Drinking Water Treatment : Control of Sulfate Production." *Water Research* 45 (20): 6661–67. <https://doi.org/10.1016/j.watres.2011.09.056>.
- Saxena, Gaurav, Ram Chandra, and Ram Naresh Bharagava. 2016. "Environmental Pollution , Toxicity Profile and Treatment Approaches for Tannery Wastewater and Its Chemical Pollutants." *Reviews of Environmental Contamination and Toxicology*. <https://doi.org/10.1007/398>.
- Scaglione, D, S Caffaz, E Bettazzi, and C Lubello. 2009. "Experimental Determination of Anammox Decay Coefficient." *J Chem Technol Biotechnol*, no. January: 1250–54. <https://doi.org/10.1002/jctb.2149>.
- Shuler, M.L., Kargi, F., 2002. *Bioprocess Engineering, Basic Concepts*, second ed. Prentice-Hall Inc., Englewood Cliffs, NJ, pp. 158–160.
- Sievert, Stefan M, Kathleen M Scott, Martin G Klotz, Patrick S G Chain, Loren J Hauser, James Hemp, Michael Hu, et al. 2008. "Genome of the Epsilonproteobacterial Chemolithoautotroph." *Applied and Environmental Microbiology* 74 (4): 1145–56. <https://doi.org/10.1128/AEM.01844-07>.
- Soler-jofra, Aina, Julio Pérez, and Mark C M Van Loosdrecht. 2021. "Hydroxylamine and the Nitrogen Cycle : A Review." *Water Research* 190. <https://doi.org/10.1016/j.watres.2020.116723>.
- Song, Xiaoye, Wenhai Luo, Faisal I Hai, William E Price, Wenshan Guo, and Hao H Ngo. 2018. "Resource Recovery from Wastewater by Anaerobic Membrane Bioreactors : Opportunities and Challenges." *Bioresource Technology* 270 (June): 669–77. <https://doi.org/10.1016/j.biortech.2018.09.001>.
- Sparacino-Watkins, Courtney Stolzb, John F., and Basu. 2014. "Nitrate and Periplasmic Nitrate Reductases." *Chem. Soc. Rev.*, 676–706. <https://doi.org/10.1039/c3cs60249d>.
- Stuedel, Ralf. 1996. "Mechanism for the Formation of Elemental Sulfur from Aqueous Sulfide in Chemical and Microbiological Desulfurization Processes." *Ind. Eng. Chem. Res.* 35 (4): 1417–23.
- Strous, M, J.J. Heijnen, Kuenen J. G., and M S M Jetten. 1998. "The Sequencing Batch Reactor as a Powerful Tool for the Study of Slowly Growing Anaerobic Ammonium-Oxidizing Microorganisms." *Appl Microbiol Biotechnol* 50: 589–96.
- Strous, Marc, Eric Pelletier, Sophie Mangenot, Thomas Rattei, Angelika Lehner, Michael W Taylor, Nuria Fonknechten, et al. 2006. "Deciphering the Evolution and Metabolism of an Anammox Bacterium from a Community Genome." *Nature Letters* 440 (April): 790–94. <https://doi.org/10.1038/nature04647>.
- Sublette, Kerry L, and Nicholas D Sylvester. 1987. "Of Natural Gas." *Biotechnology and Bioengineering* XXIX: 249–57.
- Szpyrkowicz, Lidia, and Santosh N Kaul. 2004. "Biochemical Removal of Nitrogen from Tannery Wastewater: Performance and Stability of a Full-Scale Plant." *Journal Of Chemical Technology and Biotechnology* 888 (October 2003): 879–88. <https://doi.org/10.1002/jctb.1064>.
- Takahashi, Shunsuke, Junko Tomita, Kaori Nishioka, Takayoshi Hisada, and Miyuki Nishijima. 2014. "Development of a Prokaryotic Universal Primer for Simultaneous Analysis of Bacteria and Archaea Using Next-Generation Sequencing." *PLoS ONE* 9 (8). <https://doi.org/10.1371/journal.pone.0105592>.
- Takai, Ken, Masae Suzuki, Satoshi Nakagawa, Masayuki Miyazaki, Yohey Suzuki, Fumio Inagaki, and Koki Horikoshi. 2006. "Chemolithoautotroph within the Epsilonproteo- Bacteria Isolated from a Deep-Sea

- Hydrothermal Vent Polychaete Nest , Reclassification of Thiomicrospira Denitrificans as Sulfurimonas Denitrificans Comb . Nov . and Emended Description of the Genus Sulfurimon.” *International Journal of Systematic and Evolutionary Microbiology* 56: 1725–33. <https://doi.org/10.1099/ijs.0.64255-0>.
- Tavares, P, A S Pereira, J J G Moura, and I Moura. 2006. “Metalloenzymes of the Denitrification Pathway.” *Journal of Inorganic Biochemistry* 100: 2087–2100. <https://doi.org/10.1016/j.jinorgbio.2006.09.003>.
- Tervahauta, Taina, Renata D Van Der Weijden, Roberta L Flemming, and Cees J N Buisman. 2013. “Calcium Phosphate Granulation in Anaerobic Treatment of Black Water : A New Approach to Phosphorus Recovery.” *Water Research* 8 (0): 0–10. <https://doi.org/10.1016/j.watres.2013.10.012>.
- Tiessen, H, TL Roberts, and JWB Stewart. 1983. “Carbonate Analysis in Soils and Minerals by Acid Digestion and Two End-Point Titration.” *Comm. in Soil Sci.Plant Anal.* 14 (2): 161–66.
- Tijhuis, L., Loosdrecht, M.C.M. Van, 1994. Solids Retention Time in Spherical Biofilms in a Biofilm Airlift Suspension Reactor 44, 867–879. Timmer-ten Hoor, Anjie. 1981. “Cell Yield and Bioenergetics of Thiomicrospira Denitrificans Compared with Thiobacillus Denitrificans.” *Antonie van Leeuwenhoek* 47: 231–43.
- Trigo, C, J L Campos, J M Garrido, and R Mendez. 2006. “Start-up of the Anammox Process in a Membrane Bioreactor.” *Journal of Biotechnology* 126: 475–87. <https://doi.org/10.1016/j.jbiotec.2006.05.008>.
- Trukhina, A I, M A Gladchenko, and S V Kaluzhnyi. 2011. “Reactivation of Biocatalysts after Long Term Storage and Startup of the DEAMOX Process.” *Applied Biochemistry and Microbiology* 47 (7): 688–94. <https://doi.org/10.1134/S0003683811070106>.
- Van, Pim L F Den Bosch, Otto C Van Beusekom, Cees J N Buisman, and Albert J H Janssen. 2007. “Sulfide Oxidation at Halo-Alkaline Conditions in a Fed-Batch Bioreactor.” *Biotechnology and Bioengineering* 97 (5): 1053–63. <https://doi.org/10.1002/bit>.
- Van Loosdrecht, M. C., Nielsen, P. H., Lopez-Vazquez, C. M., & Brdjanovic, D., 2016. *Experimental Methods in Wastewater Treatment* | IWA Publishing.
- Villarín, María C, and Sylvain Merel. 2020. “Paradigm Shifts and Current Challenges in Wastewater Management.” *Journal of Hazardous Materials* 390 (September 2019): 122139. <https://doi.org/10.1016/j.jhazmat.2020.122139>.
- Visser, J A N M, Lesley A Robertson, Henk W V A N Verseveld, and J Gijs Kuenen. 1997. “Sulfur Production by Obligately Chemolithoautotrophic Thiobacillus Species.” *APPLIED AND ENVIRONMENTAL MICROBIOLOGY* 63 (6): 2300–2305.
- Vitousek, Peter, Johon Aber, Robert Howarth, Gene Likens, Pamela Matson, D Avid W Schindler, W Illiam H Schlesinger, and D Avid G Tilman. 1997. “HUMAN ALTERATION OF THE GLOBAL NITROGEN CYCLE: SOURCES AND CONSEQUENCES.” *Ecological Applications* 7 (November 1996): 737–50.
- Wang, Jin, Hui Lu, Guang-hao Chen, G Ngai Lau, W L Tsang, and Mark C M Van Loosdrecht. 2009. “A Novel Sulfate Reduction, Autotrophic Denitrification , Nitrification Integrated (SANI) Process for Saline Wastewater Treatment.” *Water Research* 43 (9): 2363–72. <https://doi.org/10.1016/j.watres.2009.02.037>.
- Wang, Yajiao, Peng Li, Jiame Zuo, Yutao Gong, Sike Wang, and Xuchuan Shi. 2018. “Inhibition by Free Nitrous Acid (FNA) and the Electron Competition of Nitrite in Nitrous Oxide (N 2 O) Reduction

- during Hydrogenotrophic Denitri Fi Cation.” *Chemosphere* 213: 1–10.
<https://doi.org/10.1016/j.chemosphere.2018.08.135>.
- Xing, Bao-shan, Qiong Guo, Guang-feng Yang, Jue Zhang, Tian-yue Qin, Peng Li, Wei-min Ni, and Ren-cun Jin. 2015. “The Influences of Temperature, Salt and Calcium Concentration on the Performance of Anaerobic Ammonium Oxidation (Anammox) Process.” *CHEMICAL ENGINEERING JOURNAL* 265: 58–66. <https://doi.org/10.1016/j.cej.2014.12.007>.
- Xue, Yi, Haiyuan Ma, Zhe Kong, Yan Guo, and Yu-you Li. 2020. “Bulking and Floation of the Anammox-HAP Granule Caused by Low Phosphate Concentration in the Anammox Reactor of Expanded Granular Sludge Bed (EGSB).” *Bioresource Technology* 310 (April): 123421.
<https://doi.org/10.1016/j.biortech.2020.123421>.
- Yan, Jia, Huijun Wen, Qingqing Li, Siji Wang, Jiehui Xie, Meiping Chen, Jiayi Li, Xiangyang Chang, Hongguo Zhang, and Yiguo Hong. 2020. “Enhanced Elemental Sulfur Recovery and Nitrogen Removal through Coupling of Sulfide-Dependent Denitrification and Anammox Processes during Ammonium- and Sulfide-Laden Waste Stream Treatment.” *International Biodeterioration & Biodegradation* 155 (September): 105086. <https://doi.org/10.1016/j.ibiod.2020.105086>.
- Yang, Weiming, Qing Zhao, Hui Lu, Zhi Ding, Liao Meng, and Guang-hao Chen. 2016. “Sulfide-Driven Autotrophic Denitri Fi Cation Signi Fi Cantly Reduces N2O Emissions.” *Water Research* 90: 176–84.
<https://doi.org/10.1016/j.watres.2015.12.032>.
- Yavuz, Berna, Mustafa Türker, and Güleda Önköl Engin. 2007. “Autotrophic Removal of Sulphide from Industrial Wastewaters Using Oxygen and Nitrate as Electron Acceptors.” *Environmental Engineering Science* 24 (4). <https://doi.org/10.1089/ees.2006.0068>.
- Yu, Lintang, Shengdong Chen, Wenjing Chen, and Jun Wu. 2020. “Science of the Total Environment Experimental Investigation and Mathematical Modeling of the Competition among the Fast-Growing “ r-Strategists ” and the Slow- Growing “ K-Strategists ” Ammonium-Oxidizing Bacteria and Nitrite-Oxidizing Bacteria in Nitrification.” *Science of the Total Environment* 702: 135049.
<https://doi.org/10.1016/j.scitotenv.2019.135049>.
- Zhang, Aiyu, Shuai Wang, Mingming Yang, Hanxiang Li, Han Wang, and Fang Fang. 2020. “Journal of Water Process Engineering Influence of NaCl Salinity on the Aggregation Performance of Anammox Granules.” *Journal of Water Process Engineering*, no. July.
<https://doi.org/https://doi.org/10.1016/j.jwpe.2020.101687>.
- Zhang, Wenjie, Dunqiu Wang, and Yue Jin. 2017. “Effects of Inorganic Carbon on the Nitrous Oxide Emissions and Microbial Diversity of an Anaerobic Ammonia Oxidation Reactor.” *Bioresource Technology*. <https://doi.org/10.1016/j.biortech.2017.11.027>.
- Zhang, Zhengzhe, Yu Zhang, and Yinguang Chen. 2019. “Recent Advances in Partial Denitrification in Biological Nitrogen Removal: From Enrichment to Application.” *Bioresource Technology*, 122444.
<https://doi.org/10.1016/j.biortech.2019.122444>.
- Zhou, Yan, Adrian Oehmen, Melvin Lim, Vel Vadivelu, and Wun Jern Ng. 2011. “The Role of Nitrite and Free Nitrous Acid (FNA) in Wastewater Treatment Plants.” *Water Research* 5 (2): 4672–82.
<https://doi.org/10.1016/j.watres.2011.06.025>.
- Zhou, Yan, Maite Pijuan, and Zhiguo Yuan. 2007. “Free Nitrous Acid Inhibition on Anoxic Phosphorus Uptake and Denitrification by Poly-Phosphate Accumulating Organisms.” *Biotechnology and Bioengineering* 98 (4): 903–12. <https://doi.org/10.1002/bit>.

Zumft, Walter G. 1997. "Enzyme Diversity and Mosaic Gene Organization in Denitrification." *Kluwer Academic Publishers*. 14405: 43–58.

APPENDIX

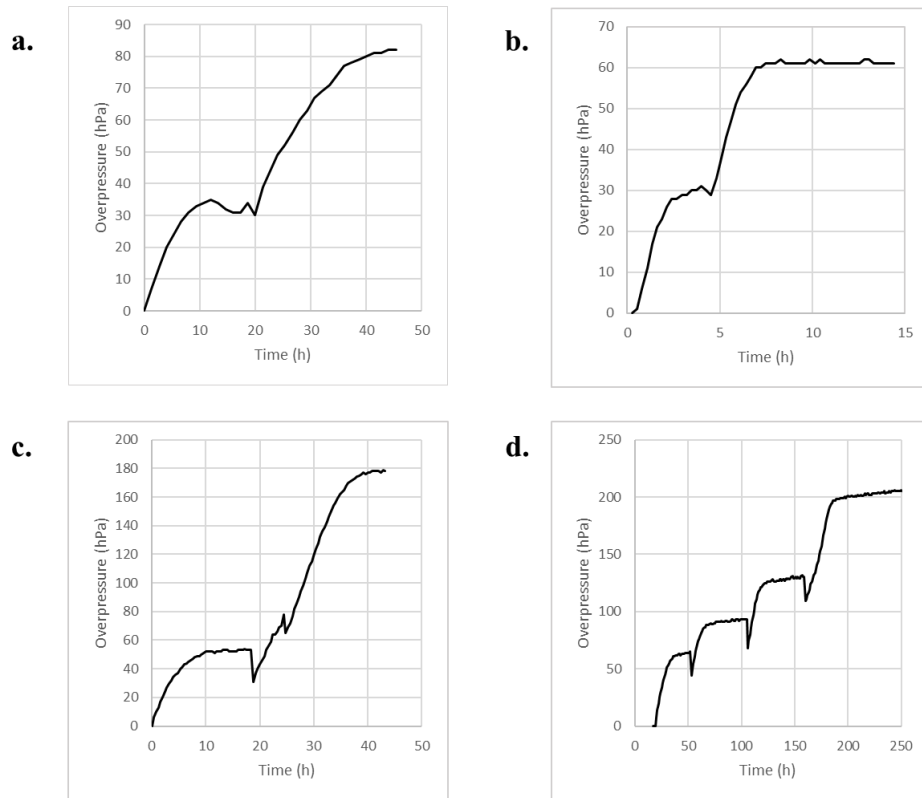
Pressure profiles during the activity tests on the anammox biomass (Chapter 3).

Figure A.1 Manometric tests (Oxitop system) on the anammox biomass conducted on days: 47 (a), 83 (b), 117 (c), 218 (d).

Results from in-situ activity tests, presented in Chapter 3.

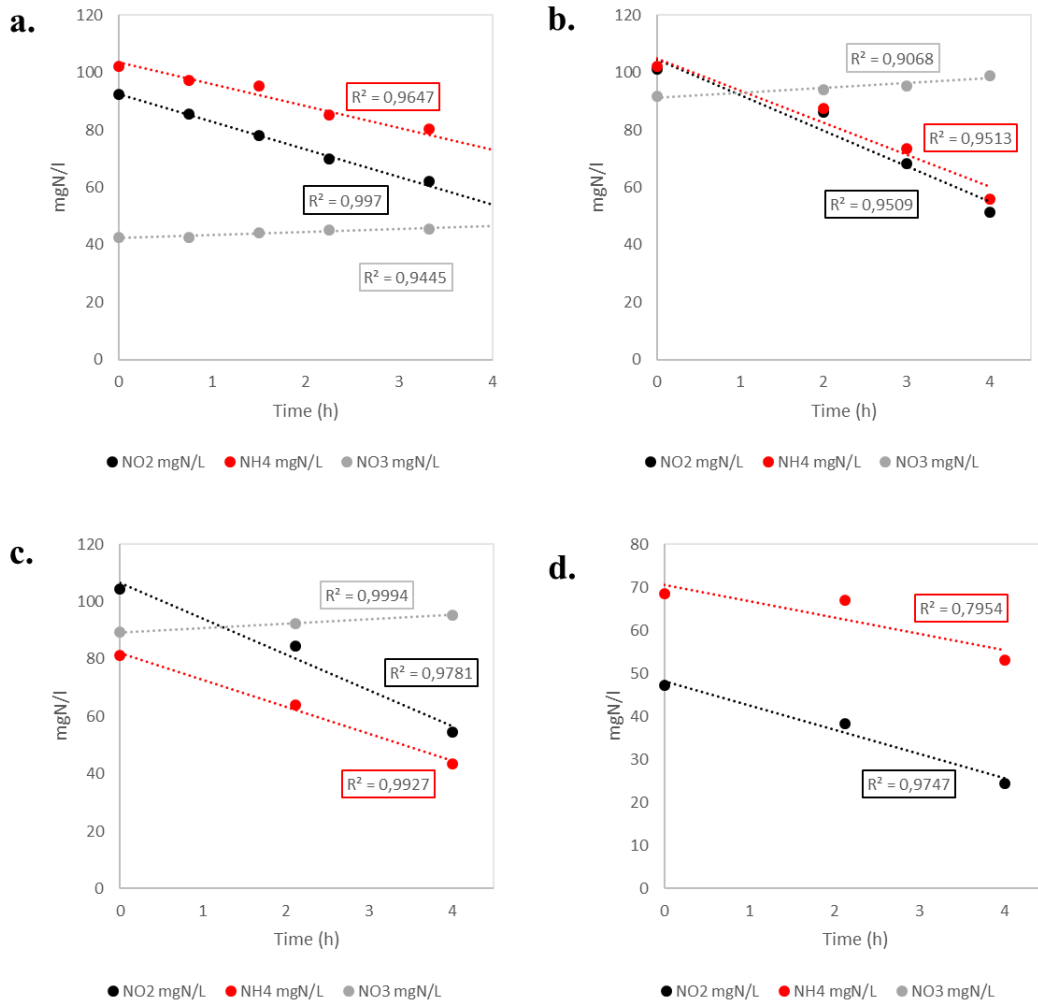


Figure A.2 In-situ batch tests for the anammox biomass, conducted on days: 36 (a), 117 (b), 135 (c), 218 (d).

Picture for image elaboration for granule size distribution, presented in Chapter 3.

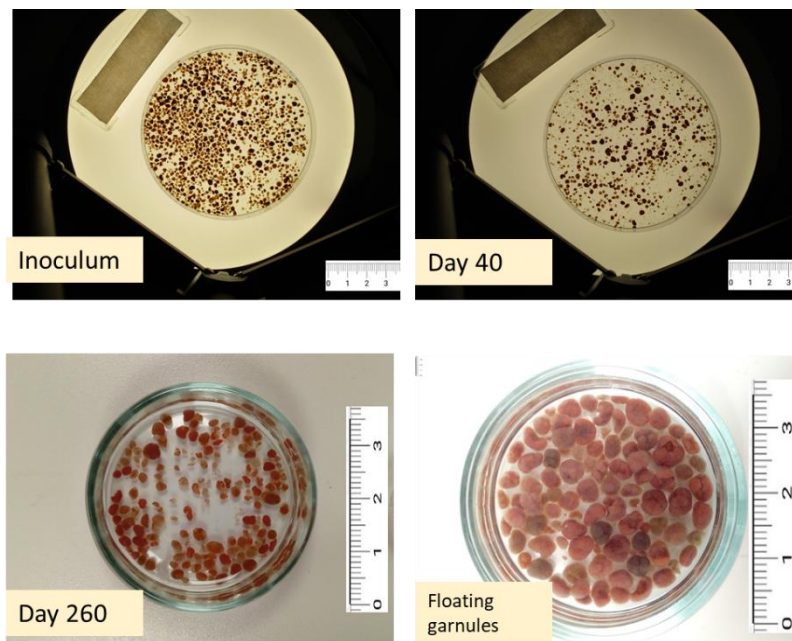


Figure A.3 Pictures of anammox granules withdrawn throughout the experimental period.

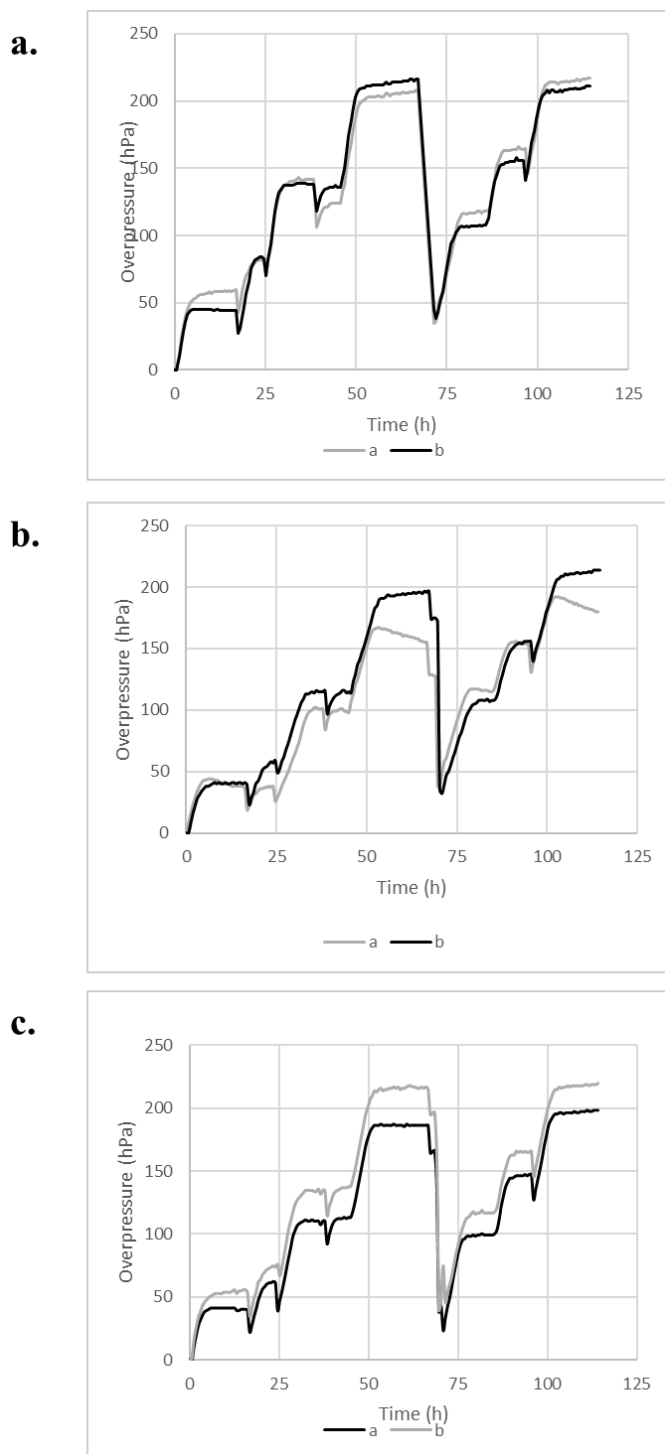
Pressure profiles of the second inhibition tests, presented in Chapter 4.

Figure A.4 Manometric tests (conducted in duplicate, a and b) on the second inhibition experiment: Control Test, CT (a); Saline Control Test, SCT (b) and Tannery WW Test, TWT (c). Pressure drop around minute 70 is due to re-equilibration of the headspace pressure with atmospheric pressure. Results from the CT were also used for the assessment of the biomass activity test on day 245 in Chapter 3.





